5-3-2022 10:00 AM

Exploring Valuable and Potentially Harmful By-Products Formed and/or Released from Smouldering Treatment of Sewage Sludge

Taryn Ashley Fournie, *The University of Western Ontario*

Supervisor: Gerhard, Jason I., *The University of Western Ontario*
Co-Supervisor: Switzer, Christine, *University of Strathclyde*
A thesis submitted in partial fulfillment of the requirements for the Doctor of Philosophy degree in Civil and Environmental Engineering

Abstract

The presence of potentially toxic elements (PTEs) and emerging contaminants (e.g., per- and polyfluoroalkyl substances (PFAS)) makes sewage sludge management challenging. Due to their hazards, there is significant interest in thermal treatment technologies that can destroy these compounds, like incineration. However, incineration still poses several risks due to forming and/or releasing hazardous emissions (e.g., polychlorinated dibenzo-*p*-dioxins and dibenzofurans (PCDD/Fs) and PTEs). More recently, the use of smouldering has been introduced as a potential treatment technique for managing sewage sludge. Smouldering presents several advantages over traditional incineration due to its lower energy and pre-treatment requirements and potential for beneficial by-products; however, little is known about the process by-products.

This question was investigated during smouldering tests conducted at the laboratory reactor scale and oil drum reactor scale. Tests were evaluated for key compounds of interest – PCDD/Fs, PTEs, and PFAS – before and after treatment as well as in process emissions. For the PFAS experiments, adjustments were made to the tests to improve PFAS degradation. The USEPA Leaching Environmental Assessment Framework (LEAF) was then used on the post-treatment ash to evaluate phosphorus and PTE release and extraction potential. This study found negligible PCDD/Fs in process emissions during robust smouldering and low levels of PCDD/Fs during weak smouldering. Overall, smouldering acts as a sink for PCDD/Fs. In addition, 94-100% of all the PTEs analyzed were retained in the post-treatment ash following smouldering treatment, not released in the emissions. Smouldering completely removed all PFAS from 3C-8C from the sludge under all

laboratory conditions, where much of the PFAS was likely volatilized into the emissions requiring further treatment. Supplementing the sewage sludge with granular activated carbon increased the energy of the system and improved PFAS degradation for high moisture content sludge. When a calcium amendment was added, the PFAS content in the emissions was 97 – 99% lower than all other conditions. Smouldered sewage sludge ash contains higher quantities of inorganic phosphorus than the parent sludge and releases lower initial and total PTEs. Furthermore, 72% of the phosphorus is recoverable. With low emissions risks, high potential for PFAS treatment, and phosphorus reuse opportunities for land application and direct recovery, smouldering has significant potential as a valuable waste management technique.

Keywords

Sewage sludge, Smouldering combustion, Phosphorus, Potentially toxic elements, Incinerated ash, Availability, Leachability, Leaching Environmental Assessment Framework, PCDD/Fs, Phosphorus, Smouldering, Land application, Recovery, Circular economy, PFAS,

Summary for Lay Audience

The foods we eat contain many vitamins and minerals, which, if broken down to their most basic forms, consists of nutrients like phosphorus, and metals like cobalt and zinc. These nutrients and metals are present in small amounts in our faeces, however, during treatment at wastewater treatment plants, they become concentrated in sewage sludge. This is important because most of our phosphorus for fertilizers comes from mines which are being quickly depleted. Therefore, we need to recycle phosphorus and other valuable elements from other sources, including sewage sludge. However, just as valuable elements end up concentrated in sewage sludge, so can harmful compounds, such as PFAS, a group of human-made chemicals used for waterproof coatings and food containers. Therefore, before useful compounds in sewage sludge can be recycled (including phosphorus), the sewage sludge needs to be treated to remove harmful compounds. Incineration is a typical method for treating sewage sludge which consists of very high temperatures to burn the material. While effective, incineration is very expensive and requires a lot of energy.

An alternative method for treating sewage sludge is smouldering. Smouldering is a flameless, more energy efficient form of burning that is commonly seen in a barbecue. However, using smouldering to treat sewage sludge is relatively new so little is known about how well it removes harmful compounds, and if new ones are formed during the process, such as dioxins, a group of hazardous compounds formed during waste burning. This research looked at the types of harmful compounds present in and released during sewage sludge smouldering and tried to minimize them. Additionally, methods of recycling valuable compounds, especially phosphorus, were explored. Smouldering was able to treat

the sewage sludge, forming an ash that contained almost no PFAS. Additionally, it is unlikely that smouldering sewage sludge produces any dioxins. In terms of element recycling, smouldering retained nearly all the valuable elements in the ash, making recycling simpler. This research demonstrated that smouldering is an effective treatment method for sewage sludge, removing most harmful compounds (while not forming any additional), and creating an ash that is rich in valuable elements, especially phosphorus.

Co-Authorship Statement

The thesis was written in accordance with the guidelines and regulations for an integrated-article format stipulated by the School of Graduate and Postdoctoral Studies at The University of Western Ontario, Canada. The candidate conducted all laboratory experiments presented in this thesis, analyzed all data, and formed the conclusions presented. The work was conducted under the supervision of Dr. Jason I. Gerhard and co-supervision of Dr. Christine Switzer. The candidate wrote the thesis and was the lead author on the manuscripts of the following chapters:

Chapter 3: USEPA LEAF methods for characterizing phosphorus and potentially toxic elements in raw and thermally treated sewage sludge

A version of this chapter has been published: Fournie, T., Switzer, C., & Gerhard, J. I. (2021). USEPA LEAF methods for characterizing phosphorus and potentially toxic elements in raw and thermally treated sewage sludge. *Chemosphere*, *275*, 130081. DOI: https://doi.org/10.1016/j.chemosphere.2021.130081

Chapter 4: Phosphorus Recovery and Reuse Potential from Smouldered Sewage Sludge Ash

A version of this chapter has been published: Fournie, T., Rashwan, T. L., Switzer, C., & Gerhard, J. I. (2022). Phosphorus recovery and reuse potential from smouldered sewage sludge ash. *Waste Management*, *137*, 241-252. DOI: 10.1016/j.wasman.2021.11.001

Chapter 5: Behaviour of PCDD/Fs and potentially toxic elements in sewage sludge during smouldering treatment

A version of this chapter has been submitted to a peer-reviewed journal: Fournie, T., Rashwan, T. L., Switzer, C., Grant, G., & Gerhard, J. I. (2022). Behaviour of PCDD/Fs and potentially toxic elements in sewage sludge during smouldering treatment.

Chapter 6: Smouldering to treat PFAS in sewage sludge

A version of this chapter will be submitted to a peer-reviewed journal: Fournie, T., Rashwan, T. L., Switzer, C., & Gerhard, J. I. (2022). Smouldering to treat PFAS in sewage sludge.

Contributions:

Taryn A. Fournie:	Initiated the research topic for Chapter 6, conceptualized, designed, and performed all experiments, collected and analyzed most emissions and solids samples, completed analysis and interpretation of all results, wrote the original draft for all chapters.
Christine Switzer:	Initiated the research topic for Chapters 3 and 4, helped design and supervise the project, assisted in data interpretation, reviewed and revised all chapters.

Jason I. Gerhard:	Initiated the research topic for Chapters 4 and 5, funded the research, helped design and supervise the project, assisted in data interpretation, reviewed and revised all chapters.
Tarek L. Rashwan:	Initiated the research topic for Chapter 5, assisted with all smouldering experiments in Chapters 4 and 5, and the larger scale smouldering experiments in Chapter 6, assisted with data interpretation, and reviewed all chapters.
Gavin Grant:	Supported and advised on the larger scale smouldering experiments in Chapters 4, 5, and 6, reviewed Chapter 5 draft.

Acknowledgments

Funding was provided by the Ontario Ministry of Research, Innovation and Science; the Government of Canada through the Federal Economic Development Agency for Southern Ontario through the Ontario Water Consortium's Advancing Water Technologies Program (Grant SUB02392) with in-kind support from: 1) the Ontario Ministry of the Environment, Conservation and Parks and 2) Savron, a wholly owned subdivision of Geosyntec Consultants Ltd; and the Natural Sciences and Engineering Research Council of Canada (Postgraduate Scholarship-Doctoral [PGS D 3 - 535379 – 2019 and PGSD 3 - 489978 – 2016] and Grant Nos. CREATE 449311-14, RGPIN 2018-06464, and RGPAS-2018-522602), the Government of Ontario (Ontario Graduate Scholarship 2018), and the Water Environment Association of Ontario's Residuals and Biosolids Research Fund Award (2018 and 2019).

I want to express my gratitude to my supervisor, Dr. Jason Gerhard. I first got involved in research and RESTORE when I saw a presentation on STAR in Jason's 2nd year Introduction to Environmental Engineering course. I went up to Jason at the end of the lecture and asked how I could get involved and I have been a part of the RESTORE family ever since. Jason inspires greatness through his mentorship, support, and kindness. Jason often says that he has the best graduate students, but I believe that it is our deep respect and appreciation for Jason that makes us want to work hard. Jason also introduced me to Dr. Christine Switzer which gave me the opportunity to fulfill a lifelong dream of studying in Scotland.

I want to thank Dr. Christine Switzer for all her support and guidance for both all this research and generally. Christine is one of my biggest inspirations. She is hands on with her research, incredibly curious, and has achieved a balance between work and outdoor adventuring that I aspire to. From the beginning, Christine has pushed all my research projects to be better than I ever expected. I am extremely grateful for her hospitality, hosting me at her home university in Scotland.

I want to acknowledge Dr. Tarek Rashwan. I couldn't have completed this PhD without him; he had the original idea to smoulder sewage sludge and obtained all the funding to take me on as an additional graduate student on the project. My long research discussions with Tarek led to many of my research plans and hypotheses. Tarek was always a joy to work with. He is a phenomenal leader, mentor, researcher, and friend. I'm thankful for the opportunity to have worked so closely with him and am excited to see what he does in the future.

The identification and quantification of the PCDD/Fs were performed in collaboration with the Ontario Ministry of the Environment, Conservation and Parks mass spectrometry laboratory in Toronto, Ontario, with PCDD/F extraction and analysis performed by Dr. Liad Haimovici. The identification and quantification of the PFAS were performed in collaboration with the Royal Military College, Environmental Science Group in Kingston, Ontario, with analyses performed by David Patch.

We gratefully acknowledge the assistance of all summer students. Especially Kia Barrow for help in performing elemental analyses, column percolation tests, pH-dependent leaching tests, sieve and elemental analyses. This project would not have been possible

without assistance from Brendan Evers, Thomas Mathias, Dillon McIntyre, Jordan Teeple, Jad Choujaa, Maxwell Servos, Nick Rogowski, and Christopher Kwan, who all helped set-up our industrial space and ran numerous laboratory-, intermediate-, and large-scale smouldering experiments. I also acknowledge and appreciate the help of Anna Duong, Madeleine Hooper, and Natalie Connors, running the PFAS smouldering experiments.

Thank you to the entire RESTORE group which has been my extended family for the past 8 years. Specifically, I gratefully acknowledge the assistance and valuable input of Alex Duchesne and Brian Harrison in creating the PFAS and HF glass sampling train, experimental set-up and procedure, the assistance and valuable input of Joshua Brown in creating the PCDD/F glass sampling train and overall smouldering and lab assistance, and additional project support from Jiahao Wang, and Gillian Wilton. I want to thank Dr. Clare Robinson; she has been a major role model to me ever since I joined RESTORE in 2014. I was inspired by her ability to balance academia and athleticism. Clare supervised me when I first got into research and I'm thankful for her support and all the skills I learned under her supervision to help me succeed in grad school. I also want to thank Dr. Christopher Power. Chris exemplifies what it means to be a 'RESTORE' member. I'm thankful to have had the opportunity to TA for and work with Chris.

I also want to acknowledge additional project support from Gudgeon Thermfire International (particularly from Justin Barfett and Randy Adamski), London Ontario's Greenway Wastewater Treatment Centre (especially from Randy Bartholomew, Michael Wemyss, and Anthony Van Rossum, Chris McKenzie).

I want to thank the entire Civil and Engineering Department at Western. They have been my family and supported me through both undergrad and grad school. Especially, Caitlin Corcoran, Stephanie Laurence, Sandra McKay, and Kristen Edwards.

I want to acknowledge my family and friends who have supported me throughout this journey. Jaeleah and Alex, I'm thankful to have experienced both undergrad and grad school with them, they made the experience happier and more fun. Lauren, who was there with me through both the best and most challenging parts of undergrad and grad school. Benedict, who helped me enjoy my time outside of research and also who patiently listened to me discuss my research on a regular basis.

Finally, and perhaps most importantly, I want to thank my dad. I have spent my life looking up to him as my biggest role model and only ever wanted to be like him. He is the reason I love problem solving and how I got into engineering at Western in the first place.

Table of Contents

List of Tables

List of Figures

List of Abbreviations and Symbols

BDL	Below detection limit
CaF_2	Calcium fluoride
CaO	Calcium oxide
$Ca(OH)_2$	Calcium hydroxide
$C_nF_{(2n+1)}$-R	Chemical structure of PFAS
CH_4	Methane
$CHCl_3$	Chloroform
CM1	More stringent metal concentration limits for applied NASM under Ontario Regulation 338/09
CO_2	Carbon dioxide
CO	Carbon monoxide
DI	Deionized
DM	Dry matter
DS	Dry sludge
$FeCl_3$	Iron (III) chloride
GAC	Granular activated carbon
GC-MS	Gas chromatography – mass spectrometry
H1	Step 1 of the Hedley procedure representing immediately available
H2	Step 2 of the Hedley procedure representing labile phosphorus
H3	Step 3 of the Hedley procedure representing loosely bound phosphorus
H4	Step 4 of the Hedley procedure representing moderately bound phosphorus
H5	Step 5 of the Hedley procedure representing non-labile phosphorus
H6	Step 6 of the Hedley procedure representing residual phosphorus
HCl	Hydrochloric acid
HDPE	High density polyethylene
HF	Hydrofluoric acid
HpCDD	Heptachlorodibenzo-*p*-dioxin
HpCDF	Heptachlorodibenzofuran
HPLC	High performance liquid chromatography
HNO_3	Nitric acid
H_2SO_4	Sulfuric acid
HxCDD	Hexachlorodibenzo-*p*-dioxin
HxCDF	Hexachlorodibenzofuran
ICP-OES	Inductive Coupled Plasma Optical Emission Spectrometer
ISSA	Incinerated sewage sludge ash
KOH	Potassium hydroxide
LC-MS/MS	Liquid chromatography with tandem mass spectrometry
LEAF	Leaching Environmental Assessment Framework
L/S	Liquid-to-solid ratio
MC	Moisture content
$MgCl_2$	Magnesium chloride
MSW	Municipal solid waste
mV	Millivolts

$Na_3C_3H_6O_7$	Sodium citrate
NaCl	Sodium chloride
$NaHCO_3$	Sodium bicarbonate
NaOH	Sodium hydroxide
NASM	Non-Agricultural Source Material from Ontario Regulation 338/09
$Na_2S_2O_4$	Sodium dithionite
NATO	North Atlantic Treaty Organization
NDIR	Non-Dispersive Infrared Gas Analyzer
NH_4Cl	Ammonium chloride
NH_4F	Ammonium fluoride
OCDD	Octachlorodibenzo-*p*-dioxin
OCDF	Octachlorodibenzofuran
PAH	Polyaromatic hydrocarbon
PCDD	Polychlorinated dibenzo-*p*-dioxins
PCDF	Polychlorinated dibenzofurans
PeCDD	Pentachlorodibenzo-*p*-dioxin
PeCDF	Pentachlorodibenzofuran
PFAA	Perfluoroalkyl acids
PFAS	Per- and polyfluoroalkyl substance
PFBA	Perfluorobutanoic acid
PFBS	Perfluorobutanesulfonic acid
PFHpA	Perfluoroheptanoic acid
PFHpS	Perfluoroheptanesulfonic acid
PFHxA	Perfluorohexanoic acid
PFHxS	Perfluorohexanesulfonic acid
PFPA	Perfluoropropanoic acid
PFPeA	Perfluoropentanoic acid
PFPeS	Perfluoropentanesulfonic acid
PFOA	Perfluorooctanoic acid
PFOS	Perfluorooctanesulfonic acid
PO_4^{3-}	Orthophosphate
ppb	Parts per billion
PTE	Potentially toxic element
R	Functional group
RPM	Revolutions per minute
SO_2	Sulfur dioxide
SO_3	Sulfur trioxide
SO_x	Sulfur oxides
STAR	Self-Sustaining Treatment for Active Remediation
STARx	Self-Sustaining Treatment for Active Remediation applied ex-situ
T01	USEPA LEAF Method 1313 sample 1 at pH 13 ± 0.5
T02	USEPA LEAF Method 1313 sample 2 at pH 12 ± 0.5
T03	USEPA LEAF Method 1313 sample 3 at pH 10.5 ± 0.5
T04	USEPA LEAF Method 1313 sample 4 at pH 9 ± 0.5
T05	USEPA LEAF Method 1313 sample 5 at pH 8 ± 0.5
T06	USEPA LEAF Method 1313 sample 6 at pH 7 ± 0.5

T07	USEPA LEAF Method 1313 sample 7 at pH 5.5 ± 0.5
T08	USEPA LEAF Method 1313 sample 8 at pH 4 ± 0.5
T09	USEPA LEAF Method 1313 sample 9 at pH 2 ± 0.5
TC	Thermocouple
TCDD	Tetrachlorodibenzo-*p*-dioxin
TCDF	Tetrachlorodibenzofuran
TEF	Toxic equivalency factor
TEQ	Toxic equivalent quantity
TFA	Trifluoroethylene
TISAB	Total Ionic Strength Adjustment Buffer
USEPA	United States Environmental Protection Agency
VOC	Volatile organic compound
WHO	World Health Organization
WWTP	Wastewater treatment plant
XAD	Non-ionic macroreticular resin

Chapter 1

1 Introduction

1.1 Background

Increases in the proportion of waste components being recycled and reused compared to landfilled are evidence of societal shifts towards more sustainable practices. Recent research and regulations have demonstrated growing interest in circular economies, with significant focus on making waste disposal processes more cyclic (Canadian Municipal Water Consortium, 2015; Donatello and Cheeseman, 2013a; Fang et al., 2020; Gorazda et al., 2017; Mayer et al., 2016; Mulchandani and Westerhoff, 2016). Resource recovery, in particular, for nutrients and metals, not only relieves the depletion of essential elements but can also have environmental and economic benefits for wastewater treatment plants (WWTPs) (Neczaj and Grosser, 2018).

However, recovery and reuse of nutrients and metals from sludge remains a challenge for numerous reasons. For example, several concerns arise when considering the direct application of sewage sludge as a fertilizer. Sewage sludge contains high quantities of potentially toxic elements (PTEs; especially metals), legacy contaminants (e.g., pesticides), and many emerging contaminants, e.g., per- and polyfluorinated substances (PFAS) (Clarke and Smith, 2011; Jiwan and Ajah, 2011; Zhou et al., 2019) which have been shown to cause adverse health and environmental impacts (Lindstrom et al., 2011; Miralles-Marco and Harrad, 2015; Zhang et al., 2017b). Therefore, there is strong interest in thermal treatment methods that remove these compounds from the sludge and limit their environmental release (Pudasainee et al., 2013; Werther and Ogada, 1999;

Zabaniotou and Theofilou, 2008). For example, incineration is an attractive option for treating sewage sludge due to its ability to destroy organic contaminants and significantly reduce the waste volume (Adam et al., 2009; Werther and Ogada, 1999). However, the pre-drying required to facilitate sludge incineration makes the treatment process energy intensive and expensive (Khiari et al., 2004; Werther and Ogada, 1999). Furthermore, the by-product emissions from sewage sludge incineration often contains hazardous compounds that require additional treatment, e.g., PTEs (especially metals), and polychlorinated dibenzo-*p*-dioxins (PCDDs) and polychlorinated dibenzofurans (PCDFs) (Fullana et al., 2004; Pudasainee et al., 2013; Shao et al., 2008; Werther and Ogada, 1999).

Another emerging thermal option is 'STAR' (Self-Sustaining Treatment for Active Remediation). Now a fully commercial technology, STAR is applied regularly to remediate soil contaminated with hydrocarbons, tars, and emerging contaminants such as PFAS (Duchesne et al., 2020; Scholes et al., 2015; Switzer et al., 2009). STAR utilizes smouldering combustion, a flameless form of burning that occurs on the surface of a fuel within a porous media, for example, glowing red charcoal in a barbecue (Rein, 2016). Recently, smouldering combustion has been demonstrated as a novel sludge treatment technology to reduce energy and carbon demand in WWTPs (Rashwan et al., 2016). Smouldering can manage high moisture content (MC) sludge (80-85% MC) with minimal pre-processing (Rashwan et al., 2016). This is an important advantage compared to flaming combustion systems – such as incinerators – because pre-drying sewage sludge is an energy intensive and expensive process at WWTPs (Werther and Ogada, 1999; Khiari et al., 2004). While smouldering has many advantages as a low-energy thermal treatment option, the

lack of information regarding potential formation and/or release of by-products and treatments required to manage them is a barrier to widespread application.

A recent study identified that smouldered sewage sludge ash is likely safe for landfilling (Feng et al., 2020). However, landfilling ignores the recovery and reuse potential of limited resources such as phosphorus (Donatello and Cheeseman, 2013a; Fang et al., 2020). Moreover, recovering PTEs from sewage sludge ash has a twofold benefit of removing these PTEs from a pathway into the environment and providing value-added recovery (Westerhoff et al., 2015). While several studies have assessed the recovery and reuse potential from incinerated sewage sludge ash (Biswas et al., 2009; Fang et al., 2020, 2018; Gorazda et al., 2017, 2016; Krüger and Adam, 2014; Mattenberger et al., 2008; Petzet et al., 2012; Schaum et al., 2007; Takahashi et al., 2001; Wzorek et al., 2006), these opportunities have not been fully explored for smouldering.

1.2 Research Objectives

The overall objective of this research is to advance the scientific understanding of sewage sludge smouldering in an environmental engineering context. A detailed literature review (summarized in Section 2.0) raises the key question: what are the beneficial and potentially hazardous by-products from smouldering combustion of sewage sludge?

To answer this question, this research proposal focuses on these specific objectives:

1. Establish a reliable method of assessing the bioavailability of phosphorus from sewage sludge before and after thermal treatment.
2. Use the method established during Objective 1 to assess the bioavailability of phosphorus within post-treatment smouldered sewage sludge ash to determine the

feasibility for reuse and recovery potential. Furthermore, explore the impacts of bulking with sand compared to particulate organic waste on reuse and recovery potential.

3. Explore the fate of PTEs during sewage sludge smouldering, including their retention in the post-treatment material and subsequent susceptibility to leaching.
4. Evaluate the formation and/or release of PCDD/Fs and VOCs from treating sewage sludge via smouldering.
5. Evaluate the use of smouldering to treat PFAS in sewage sludge.
    a. Evaluate PFAS removal under typical sewage sludge smouldering conditions.
    b. Assess methods of improving the mineralization of PFAS and process conditions.
    c. Explore the impact of scaling on PFAS removal.

Overall, this work progresses smouldering towards a more sustainable and cyclic process that produces beneficial by-products and helps preserve the environment. Furthermore, this work will help improve our understanding of risks associated with smouldering treatment which can be applied to other wastes. Moreover, the insights on potential by-product formation and/or release can inform treatments required to manage these risks. These results will ultimately help eliminate barriers for widespread application of smouldering treatment.

1.3 Thesis Outline

This thesis is written in "Integrated Article Format". A brief description of each chapter is presented below.

Chapter 1 provides a brief introduction into smouldering combustion and the beneficial and harmful by-products formed and/or released during the smouldering treatment of sewage sludge. This chapter also delineates the objectives of this thesis.

Chapter 2 provides a literature review of smouldering combustion, focusing on the process and application for treating sewage sludge. Phosphorus was explored as a beneficial element to recover or reuse from the post-treatment ash. Harmful compounds originally present in sewage sludge were also explored, including PTEs, PCDD/Fs, and PFAS, along with current methods of treating these compounds. Emphasis was placed on thermal treatment methods and the impacts of temperature on these compounds. Finally, knowledge gaps in literature were discussed.

Chapter 3 titled "USEPA LEAF methods for characterizing phosphorus and potentially toxic elements in raw and thermally treated sewage sludge" is a manuscript that compared two methods for analyzing phosphorus in sewage sludge, the widely used Hedley et al. (1982) fractionation method and USEPA Leaching Environmental Assessment Framework (LEAF). In addition to comparing the two methods on their performance for evaluating available phosphorus in sewage sludge and incinerated ash, this study also demonstrated the ability of the LEAF methods to provide valuable additional quantification on PTEs that may be present in these materials with no further analytical steps required.

This chapter was published in July 2021 in Chemosphere. DOI: https://doi.org/10.1016/j.chemosphere.2021.130081

Chapter 4 titled "Phosphorus Recovery and Reuse Potential from Smouldered Sewage Sludge Ash" is a manuscript that examined opportunities for reusing and recycling smouldered sewage sludge ash. In this work, smouldered sewage sludge ash was collected from two experiments, (1) sludge mixed with coarse silica sand, and (2) co-treatment of sludge and organic waste (i.e., woodchips). Total elemental contents of ashes from both systems were determined and compared to Canadian land application guidelines to explore the suitability of each for direct land application. Additionally, a combination of pH-dependent leaching tests and column percolation experiments were used to explore the land application potential and extraction potential of the post-treatment ashes. This chapter was published in January 2022 in Waste Management. DOI: https://doi.org/10.1016/j.wasman.2021.11.001

Chapter 5 titled "Behaviour of PCDD/Fs and potentially toxic elements in sewage sludge during smouldering treatment" is a manuscript that evaluated the formation and/or release of PTEs, PCDD/Fs, and VOCs from treating sewage sludge via smouldering. The behaviour of PTEs post smouldering treatment was examined by developing a mass balance of the smouldering reactor system. Additionally, PCDD/Fs samples were collected from the combustion gases during four oil-drum scale reactor and two laboratory column scale experiments to explore the potential formation and/or release of these compounds during smouldering. This chapter has been submitted to the Journal of Environmental Management.

Chapter 6 titled “Smouldering to treat PFAS in sewage sludge” is a manuscript that explored the removal of PFAS from sewage sludge under base case smouldering experiments at the laboratory scale. Changes were then made to the base case tests, including treating high moisture content sludge (what is typically observed at WWTPs) supplemented with granular activated carbon to increase the treatment temperature. Additionally, the use of a calcium amendment to improve fluorine mineralization at lower treatment temperatures was explored. Finally, PFAS was measured at the oil-drum reactor scale pre- and post-smouldering treatment to understand the impacts of scaling on removal. This chapter will be submitted to a leading international journal.

Chapter 7 summarizes the key contributions and conclusions from this thesis and presents recommendations for future work.

Appendix A presents Supplementary Material for “USEPA LEAF methods for characterizing phosphorus and potentially toxic elements in raw and thermally treated sewage sludge”, presents additional USEPA LEAF Method 1313 and 1314 results.

Appendix B provides Supplementary Material for “Phosphorus Recovery and Reuse Potential from Smouldered Sewage Sludge Ash”, presents temperature profiles, elemental mass balance calculations, additional USEPA LEAF Method 1313 and 1314 results, and recovery potential calculations.

Appendix C provides Supplementary Material for “Behaviour of PCDD/Fs and potentially toxic elements in sewage sludge during smouldering treatment”, presents temperature profiles, sampling information, stack emissions data, PCDD/F data for pre- and post-treatment materials, and normalization calculations.

Appendix D provides Supplementary Material for "Smouldering to treat PFAS in sewage sludge", presents preliminary PFAS results, temperature profiles, heating rates, additional PFAS results, normalization calculations, and mineral analysis results.

1.4 References

Adam, C., Peplinski, B., Michaelis, M., Kley, G., Simon, F.G., 2009. Thermochemical treatment of sewage sludge ashes for phosphorus recovery. Waste Manag. 29, 1122–1128. https://doi.org/10.1016/j.wasman.2008.09.011

Biswas, B.K., Inoue, K., Harada, H., Ohto, K., Kawakita, H., 2009. Leaching of phosphorus from incinerated sewage sludge ash by means of acid extraction followed by adsorption on orange waste gel. J. Environ. Sci. 21, 1753–1760. https://doi.org/10.1016/S1001-0742(08)62484-5

Clarke, B.O., Smith, S.R., 2011. Review of 'emerging' organic contaminants in biosolids and assessment of international research priorities for the agricultural use of biosolids. Environ. Int. 37, 226–247. https://doi.org/10.1016/J.ENVINT.2010.06.004

Donatello, S., Cheeseman, C.R., 2013. Recycling and recovery routes for incinerated sewage sludge ash (ISSA): A review. Waste Manag. 33, 2328–2340. https://doi.org/10.1016/j.wasman.2013.05.024

Duchesne, A.L., Brown, J.K., Patch, D.J., Major, D., Weber, K.P., Gerhard, J.I., 2020. Remediation of PFAS-Contaminated Soil and Granular Activated Carbon by Smoldering Combustion. Environ. Sci. Technol. 54, 12631–12640. https://doi.org/10.1021/acs.est.0c03058

Fang, L., Li, J. shan, Guo, M.Z., Cheeseman, C.R., Tsang, D.C.W., Donatello, S., Poon, C.S., 2018. Phosphorus recovery and leaching of trace elements from incinerated sewage sludge ash (ISSA). Chemosphere 193, 278–287. https://doi.org/10.1016/j.chemosphere.2017.11.023

Fang, L., Wang, Q., Li, J.-S., Poon, C.S., Cheeseman, C.R., Donatello, S., Tsang, D.C.W., 2020. Feasibility of wet-extraction of phosphorus from incinerated sewage sludge ash (ISSA) for phosphate fertilizer production: A critical review. Crit. Rev. Environ. Sci. Technol. 1–33. https://doi.org/10.1080/10643389.2020.1740545

Feng, C., Cheng, M., Gao, X., Qiao, Y., Xu, M., 2020. Occurrence forms and leachability of inorganic species in ash residues from self-sustaining smouldering combustion of sewage sludge. Proc. Combust. Inst. 000, 1–8. https://doi.org/10.1016/j.proci.2020.06.008

Fullana, A., Conesa, J.A., Font, R., Sidhu, S., 2004. Formation and destruction of

chlorinated pollutants during sewage sludge incineration. Environ. Sci. Technol. 38, 2953–2958. https://doi.org/10.1021/es034896u

Gorazda, K., Tarko, B., Wzorek, Z., Kominko, H., Nowak, A.K., Kulczycka, J., Henclik, A., Smol, M., 2017. Fertilisers production from ashes after sewage sludge combustion – A strategy towards sustainable development. Environ. Res. 154, 171–180. https://doi.org/10.1016/j.envres.2017.01.002

Gorazda, K., Tarko, B., Wzorek, Z., Nowak, A.K., Kulczycka, J., Henclik, A., 2016. Characteristic of wet method of phosphorus recovery from polish sewage sludge ash with. Open Chem. 14, 37–45. https://doi.org/10.1515/chem-2016-0006

Jiwan, S., Ajah, K.S., 2011. Effects of Heavy Metals on Soil, Plants, Human Health and Aquatic Life. Int. J. Res. Chem. Environ. 1, 15–21.

Khiari, B., Marias, F., Zagrouba, F., Vaxelaire, J., 2004. Analytical study of the pyrolysis process in a wastewater treatment pilot station. Desalination 167, 39–47. https://doi.org/10.1016/j.desal.2004.06.111

Krüger, O., Adam, C., 2014. Recovery potential of German sewage sludge ash. Waste Manag. 45, 400–406. https://doi.org/10.1016/j.wasman.2015.01.025

Lindstrom, A.B., Strynar, M.J., Libelo, E.L., 2011. Polyfluorinated compounds: Past, present, and future. Environ. Sci. Technol. 45, 7954–7961. https://doi.org/10.1021/es2011622

Mattenberger, H., Fraissler, G., Brunner, T., Herk, P., Hermann, L., Obernberger, I., 2008. Sewage sludge ash to phosphorus fertiliser: Variables influencing heavy metal removal during thermochemical treatment. Waste Manag. 28, 2709–2722. https://doi.org/10.1016/j.wasman.2008.01.005

Miralles-Marco, A., Harrad, S., 2015. Perfluorooctane sulfonate: A review of human exposure, biomonitoring and the environmental forensics utility of its chirality and isomer distribution. Environ. Int. 77, 148–159. https://doi.org/10.1016/J.ENVINT.2015.02.002

Petzet, S., Peplinski, B., Cornel, P., 2012. On wet chemical phosphorus recovery from sewage sludge ash by acidic or alkaline leaching and an optimized combination of both. Water Res. 46, 3769–3780. https://doi.org/10.1016/j.watres.2012.03.068

Pudasainee, D., Seo, Y.C., Kim, J.H., Jang, H.N., 2013. Fate and behavior of selected heavy metals with mercury mass distribution in a fluidized bed sewage sludge incinerator. J. Mater. Cycles Waste Manag. 15, 202–209. https://doi.org/10.1007/s10163-013-0115-z

Rashwan, T.L., Gerhard, J.I., Grant, G.P., 2016. Application of self-sustaining smouldering combustion for the destruction of wastewater biosolids. Waste Manag. 50, 201–212. https://doi.org/10.1016/j.wasman.2016.01.037

Rein, G., 2016. Smoldering Combustion, in: Hurley, M.J., Gottuk, D.T., Hall Jr., J.R., Harada, K., Kuligowski, E.D., Puchovsky, M., Torero, J.L., Watts Jr., J.M., Wieczorek, C.J. (Ed.), SFPE Handbook of Fire Protection Engineering. Springer New York, New York, pp. 581–603.

Schaum, C., Cornel, P., Jardin, N., 2007. Phosphorus recovery from sewage sludge ash–a wet chemical approach, in: Proceeding of the IWA Conference on Biosolids, Moving Forward Wastewater Biosolids Sustainability: Technical, Managerial, and Public Synergy.

Scholes, G.C., Gerhard, J.I., Grant, G.P., Major, D.W., Vidumsky, J.E., Switzer, C., Torero, J.L., 2015. Smoldering Remediation of Coal-Tar-Contaminated Soil: Pilot Field Tests of STAR. Environ. Sci. Technol. 49, 14334–14342. https://doi.org/10.1021/ACS.EST.5B03177

Shao, J., Yan, R., Chen, H., Yang, H., Lee, D.H., Liang, D.T., 2008. Emission characteristics of heavy metals and organic pollutants from the combustion of sewage sludge in a fluidized bed combustor. Energy and Fuels 22, 2278–2283. https://doi.org/10.1021/ef800002y

Switzer, C., Pironi, P., Gerhard, J.I., Rein, G., Torero, J.R., 2009. Self-sustaining smoldering combustion: A novel remediation process for non-aqueous-phase liquids in porous media. Environ. Sci. Technol. 43, 5871–5877. https://doi.org/10.1021/es803483s

Takahashi, M., Kato, S., Shima, H., Sarai, E., Ichioka, T., Hatyakawa, S., Miyajiri, H., 2001. Technology for recovering phosphorus from incinerated wastewater treatment sludge, in: Chemosphere. Pergamon, pp. 23–29. https://doi.org/10.1016/S0045-6535(00)00380-5

Werther, J., Ogada, T., 1999. Sewage sludge combustion. Prog. Energy Combust. Sci. https://doi.org/10.1016/S0360-1285(98)00020-3

Westerhoff, P., Lee, S., Yang, Y., Gordon, G.W., Hristovski, K., Halden, R.U., Herckes, P., 2015. Characterization, Recovery Opportunities, and Valuation of Metals in Municipal Sludges from U.S. Wastewater Treatment Plants Nationwide. Environ. Sci. Technol. 49, 9479–9488. https://doi.org/10.1021/es505329q

Wzorek, Z., Jodko, M., Gorazda, K., Rzepecki, T., 2006. Extraction of phosphorus compounds from ashes from thermal processing of sewage sludge. J. Loss Prev. Process Ind. 19, 39–50. https://doi.org/10.1016/j.jlp.2005.05.014

Zabaniotou, A., Theofilou, C., 2008. Green energy at cement kiln in Cyprus-Use of sewage sludge as a conventional fuel substitute. Renew. Sustain. Energy Rev. https://doi.org/10.1016/j.rser.2006.07.017

Zhang, M., Shi, Y., Lu, Y., Johnson, A.C., Sarvajayakesavalu, S., Liu, Z., Su, C., Zhang, Y., Juergens, M.D., Jin, X., 2017. The relative risk and its distribution of endocrine

disrupting chemicals, pharmaceuticals and personal care products to freshwater organisms in the Bohai Rim, China. Sci. Total Environ. 590–591, 633–642. https://doi.org/10.1016/j.scitotenv.2017.03.011

Zhou, Y., Meng, J., Zhang, M., Chen, S., He, B., Zhao, H., Li, Q., Zhang, S., Wang, T., 2019. Which type of pollutants need to be controlled with priority in wastewater treatment plants: Traditional or emerging pollutants? Environ. Int. 131. https://doi.org/10.1016/j.envint.2019.104982

Chapter 2

2 Literature Review

2.1 Introduction

Approximately 82% of Canadians are serviced by municipal wastewater treatment plants (WWTPs) (Statistics Canada, 2019). More than 20% of municipalities' energy consumption is from WWTPs (Means, 2004).

Disposal methods of sewage sludge including land application, incineration, and landfilling possess benefits and pose challenges (Fytili and Zabaniotou, 2008). For example, land application of sludge allows reuse of valuable nutrients and minerals to depleted soils (Neczaj and Grosser, 2018); however, transportation can be expensive, and concentrations of potentially toxic elements (PTEs) and organic pollutants may exceed regulations (McBride, 1995). Landfilling the sludge is not sustainable due to increasing volumes of waste and losses of valuable elements (Fytili and Zabaniotou, 2008; Westerhoff et al., 2015).

Thermal processes for managing sewage sludge are now common in the industry. For example, incinerating allows for volume reduction and contaminant destruction (Adam et al., 2009). However, the pre-drying required to facilitate sludge incineration makes the treatment process energy intensive and expensive (Khiari et al., 2004; Werther and Ogada, 1999).

Self-sustaining smouldering combustion has been shown to be a simple, energy efficient method for treating sewage sludge (Rashwan et al., 2016). While smouldering has been demonstrated to be a promising method of treating sewage sludge, studies to date

have focused on process optimization (Rashwan et al., 2016), scaling (Rashwan et al., 2021a), landfilling safety (Feng et al., 2020), and some emissions analysis of common combustion gases (Feng et al., 2021). There is limited understanding of the by-products from smouldering sewage sludge. Most of the literature focuses on more common methods of sewage sludge combustion (primarily incineration). Therefore, this chapter will provide relevant background on smouldering, with a focus of its ability to treat sewage sludge, and then use literature from common combustion methods to explore both the beneficial and potentially harmful by-products from thermal treatment of sewage sludge. Finally, this review will highlight some of the major knowledge gaps in these areas and use previous research to draw implications for smouldering.

2.2 Smouldering Combustion

Smouldering combustion is a flameless form of burning that occurs on the surface of a condensed fuel (i.e., liquid or solid) within a porous medium (Ohlemiller, 1985; Rein, 2016, 2009). The two reactions involved in smouldering combustion are (1) pyrolysis, and (2) oxidation (Rein, 2016). The same two reactions are present in typical flaming combustion (Figure 2.1); however, they are characteristically different (Wyn et al., 2020). Pyrolysis is a generally endothermic reaction that occurs in the absence of oxygen (Mahinpey and Gomez, 2016; Susastriawan et al., 2017). Temperatures above 200°C initiate the breakdown of the fuel (Rein, 2009). The by-products of this reaction are gaseous emissions, including volatiles, water vapour, polyaromatic hydrocarbons, carbon monoxide (CO), and carbon dioxide (CO_2), and solid char and ash (Mahinpey and Gomez, 2016; Rein, 2016). The secondary exothermic reaction produces heat from the heterogenous oxidation (i.e., oxygen directly attacks the condensed fuel surface) of the

remaining fuel and char (Ohlemiller, 1985; Rein, 2016, 2009). The by-products from this oxidation reaction are heat, CO_2, water vapour, ash, and other gases (Rein, 2016).

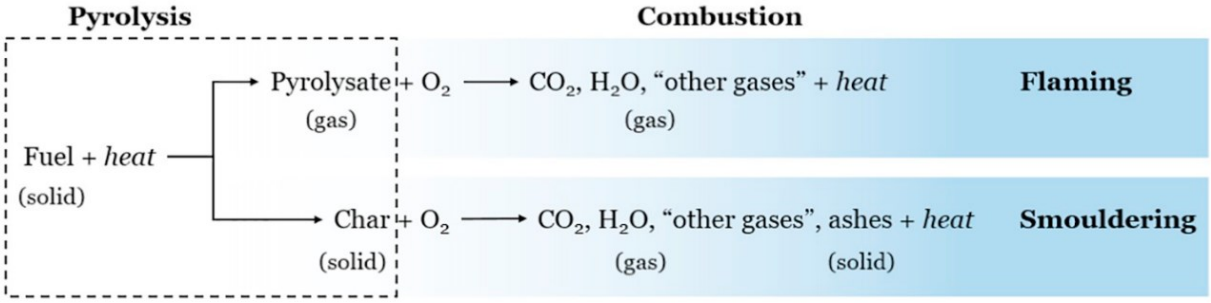

Figure 2.1: Pyrolysis and oxidation reaction pathways in smouldering versus flaming combustion (Wyn et al., 2020).

Smouldering is limited by both oxygen supply and energy losses (Ohlemiller, 1985; Rein, 2016; Switzer et al., 2009; Yermán, 2016; Zanoni et al., 2019). There is a strong relationship (mostly linear) between the rate of smouldering propagation (and fuel consumption) and the applied airflow rate (Ohlemiller, 1985; Pironi et al., 2009; Torero and Fernandez-Pello, 1996; Yermán et al., 2017, 2015). Furthermore, a positive local energy balance around the smouldering front is required for propagation with a steady velocity and in a 'self-sustaining' manner (i.e., without additional, external energy input) (Switzer et al., 2009; Zanoni et al., 2019). This occurs when energy generation by fuel oxidation exceeds energy lost to endothermic process (e.g., water evaporation and pyrolysis) and lateral heat losses (Zanoni et al., 2019).

Smouldering can only occur within a porous fuel or fuels embedded in a porous medium. The porous matrix (1) increases the surface area for reaction, (2) creates pathways for oxygen to flow to the reaction, (3) insulates the reaction thereby reducing heat losses, and (4) creates a more uniform smouldering front (Gianfelice et al., 2019; Ohlemiller, 1985; Torero et al., 2020; Yermán, 2016).

2.2.1 Applied Smouldering Systems for Waste Management

Smouldering combustion has been demonstrated to be an effective, energy efficient remediation strategy for both soil treatment (Grant et al., 2016; Pironi et al., 2009; Scholes et al., 2015; Switzer et al., 2009) and management of wastewater sludges (Rashwan et al., 2016) and faeces (Yermán et al., 2015). In this context, the organic contaminants and/or wastes are the fuel, and self-sustained smouldering destroys virtually all of it by oxidation (Rashwan et al., 2016; Switzer et al., 2009). After smouldering, typically only inert soil grains (e.g., quartz sand) and ash composed of inorganic compounds remains (Yermán et al., 2015). 'STAR' (Self-Sustaining Treatment for Active Remediation) is the commercially available technology used for smouldering treatment by Savron Ltd., Guelph, ON. This technology is applied regularly to remediate soil contaminated with non-aqueous phase liquids (Pironi et al., 2011; Switzer et al., 2009), coal tar (Pironi et al., 2009; Scholes et al., 2015), and emerging contaminants such as PFAS (Duchesne et al., 2020). STAR has been applied for in-situ (Grant et al., 2016; Pironi et al., 2009; Scholes et al., 2015; Switzer et al., 2009; Torero et al., 2018) and ex-situ (known as 'STARx') (Sabadell et al., 2019; Solinger et al., 2020) applications. STARx involves mixing wastes with sand (to produce a smoulderable mixture) above ground (Sabadell et al., 2019).

Smouldering involves three key zones: inert heating, reaction, and cooling (Torero et al., 2020). In an applied smouldering system, smouldering is initiated by applying an external heat source to the fuel to provide a short term, localized energy input to the system (Yermán, 2016). For wet fuels, the initial input of energy from the heater vaporizes a small, localized region of fuel to support ignition, known as the inert heating zone (Pironi et al., 2011; Rashwan et al., 2021a; Torero et al., 2020). The inert heating zone consists of

endothermic processes (i.e., water boiling and evaporation) (Torero et al., 2020; Yermán, 2016). As the inert heating zone lengthens, the dry fuel continues to heat (Rashwan et al., 2016). Ignition of the fuel is confirmed when the first thermocouple in the fuel bed peaks (Pironi et al., 2009). Heat from ignition supports pyrolysis reactions (Yermán, 2016). Forced air injection (supplying oxygen) supports oxidation and convective heat transfer to propagate the smouldering front through the waste bed (Torero et al., 2020; Yermán, 2016). In forward smouldering (i.e., in the direction of air flow), heterogenous oxidation supplies heat to the adjacent condensed fuel, supporting pyrolysis reactions (Torero and Fernandez-Pello, 1996). Both pyrolysis and oxidation reactions compete in the reaction zone (Zanoni et al., 2020). As long as the fuel oxidation produces sufficient energy to support the endothermic processes and overcome losses, smouldering will propagate in a self-sustaining manner until all the fuel is consumed (Yermán, 2016). This feature means that smouldering treatment ranks highly for energy efficiency metrics and sustainability rankings (Gerhard et al., 2020; Torero et al., 2020). After the fuel is consumed, the inert, post-treatment materials are cooled via the injected air (Yermán, 2016).

2.2.2 Smouldering Sewage Sludge

Compared to incineration, smouldering is able to ignite much lower calorific value fuels (e.g., sludges) with much higher MCs (Hadden and Rein, 2011; Rashwan et al., 2016; Torero et al., 2020; Yermán et al., 2015). Smouldering has been shown to effectively treat sewage sludge at both the laboratory-scale (0.0080 – 0.012 m^3) (Feng et al., 2020; Rashwan et al., 2021a, 2016), and drum-scale (0.28 – 0.79 m^3) (Feng et al., 2021; Rashwan et al., 2021a). When treating high moisture content and low permeability fuels, silica sand is usually added to create higher permeability porous medium (Rashwan et al., 2016; Yermán

et al., 2015). The proof-of-concept study by Rashwan et al. (2016), developed the parameter space for smouldering sewage sludge mixed with sand at the laboratory scale, based on the MC, sand-to-sludge ratio, and lower heating value (Figure 2.2). Up to 80% MC (by mass) sewage sludge could be smouldered using a sand-to-sludge ratio of 3.5:1 (g/g), and a sand-to-sludge ratio as low as 1.5:1 (g/g) is feasible (Rashwan et al., 2016).

An alternative to adding an inert matrix involves adding granular biomass (e.g., woodchips, waste crushed carbon, nut shells) to sewage sludge prior to thermal treatment to supplement low calorific values and improve treatment (Feng et al., 2021; Gorazda et al., 2017; Kijo-Kleczkowska et al., 2016). One study explored the use of sawdust in combination with sand to create the porous matrix and supplement the sewage sludge during smouldering (Feng et al., 2021), however, a completely organic matrix has not been used. The use of biomass for smouldering treatment of sewage sludge is promising, however, it is not well studied (Torero et al., 2020; Wyn et al., 2020).

Treating these high moisture content fuels introduces some challenges. The pre-heating procedure vaporizes water from the fuel in a small, localized region adjacent to the heater (Yermán et al., 2017). This water then recondenses further up the reactor and could result in extinction if insufficient energy is provided by the fuel oxidation to overcome heat losses (e.g., from excessive amounts of water boiling) (Rashwan et al., 2016; Torero et al., 2020; Yermán, 2016; Yermán et al., 2017). Furthermore, the size of reactor may also influence the smouldering performance of these systems (Rashwan et al., 2021b, 2021a). Smaller laboratory scale smouldering experiments have been shown to be more significantly influenced by heat losses and less efficient than at larger scales (65 ± 3% efficiency in the lab versus 86 ± 5% in the drum reactor) (Rashwan et al., 2021b).

Comparatively, larger, drum-scale experiments may in some circumstances be subjected to more severe non-uniform air flux and non-uniform reactions, which, in combination can significantly decrease smouldering performance (Rashwan et al., 2021a), which are also potential concerns at full-scale operation. This variable smouldering performance could pose challenges for managing other hazardous compounds in the sludge (e.g., endocrine disrupting compounds), due to a greater potential for weaker smouldering conditions.

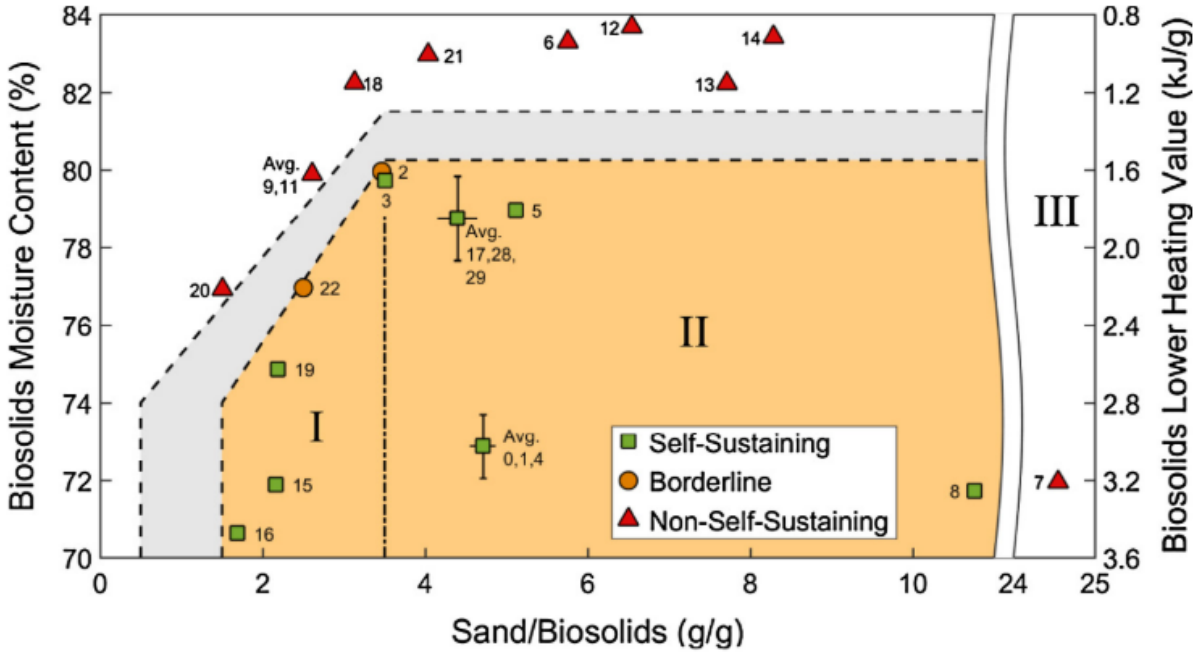

Figure 2.2: Parameter space delineating conditions for self-sustaining smouldering of biosolids based on moisture content, sand-to-biosolids ratio, and the lower heating value of the biosolids (Rashwan et al., 2016).

2.3 Potential Benefits from the Thermal Treatment of Sewage Sludge

Increases in the proportion of waste components being recycled and reused compared to landfilled are evidence of societal shifts towards more sustainable practices. Recent research and regulations have demonstrated growing interest in circular economies, with significant focus on making waste disposal processes more cyclic (Canadian Municipal Water Consortium, 2015; Donatello and Cheeseman, 2013b; Fang et al., 2020; Gorazda et al., 2017; Mayer et al., 2016; Mulchandani and Westerhoff, 2016).

2.3.1 Element Recovery

Resource recovery, in particular, for nutrients and metals, not only relieves the depletion of essential elements but can also have environmental and economic benefits for WWTPs (Neczaj and Grosser, 2018). Phosphorus is a key opportunity. For modern agriculture to meet future global food demands, large quantities of phosphorus rich fertilizer will be required (Mayer et al., 2016). Almost all phosphorus for fertilizers comes from mined phosphate rock, where current global phosphate reserves are declining and may be depleted in the upcoming decades (Fang et al., 2020; Li et al., 2016). Therefore, there is significant interest in exploring recovery methods to extract phosphorus and other limited resources from human waste streams (Mayer et al., 2016). The phosphorus present in sewage sludge from WWTPs has similar concentrations of phosphorus found in phosphate rock (Mayer et al., 2016). For an average Canadian WWTP servicing 200,000 people, approximately 1300 tonnes of phosphorus is present in the sewage sludge annually (London, 2019a), making it an important reservoir and promising source of phosphorus recovery. Moreover, recovering PTEs – such as chromium and zinc – from sewage sludge

ash has a twofold benefit of removing these PTEs from a pathway into the environment and providing value-added recovery (Westerhoff et al., 2015).

2.3.1.1 Methods of Phosphorus Extraction

More than 90% of phosphorus can be leached from incinerated sewage sludge ash through an acid extraction at a pH < 2 (Krüger and Adam, 2014; Petzet et al., 2012; Schaum et al., 2007). This pH may maximize phosphorus recovery; however, highly acidic extraction solutions produce hazardous waste that are difficult and costly to dispose of (Mulchandani and Westerhoff, 2016). During acidic extraction procedures, PTEs are also dissolved into solutions (Donatello and Cheeseman, 2013a). Therefore, additional processing is required to separate the recovered phosphorus from PTEs (Takahashi et al., 2001). However, the high dissolution of both phosphorus and other PTEs at low pH could be beneficial by creating a synergistic recovery opportunity whereby harmful elements are removed, and the value-added recovery is increased (Krüger and Adam, 2014; Westerhoff et al., 2015). Several studies have developed innovative separation methods including a sequential dissolution (Takahashi et al., 2001), Al-P dissolution and Ca-P precipitation (SESAL) (Petzet et al., 2012), ion exchange and sulphide treatment (Franz, 2008), and nanofiltration (Schaum et al., 2007).

An alternative to the typical acidic recovery procedures uses an alkaline extractant (Petzet et al., 2012). The differences in extraction efficiency from incinerated sewage sludge ash at different pH values was explored by Schaum et al. (2007). Additionally, the study showed the relationship between the total phosphorus and calcium content of the incinerated sewage sludge ash and the phosphorus recovery potential using alkaline extractants. Schaum et al., (2007) observed that lower calcium content relative to

phosphorus content resulted in the maximum recovery at high pH, while a ratio of total phosphorus-to-calcium between 0.75-1 resulted in a mere 0-30% phosphorus recovery. Numerous studies have shown that sewage sludge incineration results in a significant portion of the phosphorus being mineralized as calcium phosphate compounds (Adam et al., 2009; Petzet et al., 2012; Schaum et al., 2007). Since calcium phosphate is only soluble in acids (Stumm and Morgan, 2012), the formation of calcium phosphates during the thermal treatment of the sludge is binding phosphorus in a form that can only be recovered using acidic extractants.

2.3.1.2 Methods of Extraction for Elements other than Phosphorus

Several studies have assessed methods of recovering PTEs from the incineration of municipal solid waste (MSW) (Karlfeldt Fedje et al., 2010; Wu and Ting, 2006; Zhang and Itoh, 2006) and biosolids (J. Deng et al., 2009; Gheju et al., 2011). PTEs present in post-treatment incinerator ash in high concentrations may permit economic recovery and reuse (Bosshard et al., 1996). Leaching methods are often applied to recover PTEs from post-treatment ashes (Bosshard et al., 1996; Wang et al., 2001; Wu and Ting, 2006; Yang et al., 2009). Typical methods used for PTE extraction from treated waste ashes include chemical leaching (Gorazda et al., 2017; Petzet et al., 2012; Stark et al., 2006; Wu and Ting, 2006), bioleaching (Bosshard et al., 1996; Wu and Ting, 2006; Xu et al., 2014; Yang et al., 2009), and water-washing (Wang et al., 2001). Chemicals (e.g., organic acids) added to the ash can form complexes with the PTEs that are more readily leached and subsequently removed from the ash (Karlfeldt Fedje et al., 2010). Bioleaching uses microorganisms to oxidize PTEs during the production of organic and inorganic acids (Xu et al., 2014). Alternatively, washing the post-treatment ash with water has also been shown as an effective method of

PTE removal (Wang et al., 2001). While chemical leaching may be highly effective at extracting PTEs, it produces large quantities of waste that is difficult to dispose of (Donatello and Cheeseman, 2013a). Therefore, bioleaching and water washing are typically considered to be more environmentally favourable methods (Rhee and Mishra, 2010; Wang et al., 2001).

Previous research on PTE recovery from incinerated sewage sludge ash has shown that using an acidic extractant results in the highest recovery of zinc and nickel (J. Deng et al., 2009; Gheju et al., 2011). High removal of zinc and nickel has been associated with weak adsorption of these PTEs to sludge biomass or presence as inorganic precipitates, both of which are easily soluble in strong acid (Gheju et al., 2011). Chromium has been shown to be one of the most difficult elements to extract from both virgin sludge and the post-treatment materials under all pH conditions (Gheju et al., 2011; Wozniak and Huang, 1982). High organic contents of sewage sludge tend to strongly adsorb with chromium and lead (Gheju et al., 2011). For soil organic matter, release of chromium is only possible under pH conditions significantly less than 2 where the solids matrix is also dissolved (Pichtel and Pichtel, 1997), the same is likely true for sewage sludge. Additionally, copper has been shown to strongly bind to the sewage sludge biomass resulting in lower recovery (J. Deng et al., 2009). Molybdenum has been shown to be more available under neutral to alkaline conditions than acidic (Lahann, 1976).

It is difficult to directly compare between extraction efficiencies observed in literature due to significant procedural variabilities (Krüger & Adam, 2015) including differences in extraction times (e.g., 2 hours versus 24 hours), liquid-to-solids ratios (e.g., 10:1 versus 50:1), and the strength and type of the chemical extractants (e.g., 0.5 M versus

2 M acid solution) (J. Deng et al., 2009; Fang et al., 2018; Gheju et al., 2011; Krüger and Adam, 2014).

2.3.2 Land Application and Associated Considerations

An alternative to element recovery from sewage sludge and treated ashes is direct land application (Donatello and Cheeseman, 2013b). However, several concerns arise when considering the direct application of sewage sludge as a fertilizer. High water and organic matter content, pathogens, and numerous compounds of concern in the sludge can require sludge processing prior to such use (Hossain et al., 2011; McBride, 1995). Thermal processes for managing sewage sludge are now common in the industry. For example, incineration allows for volume reduction and contaminant destruction (Adam et al., 2009). However, these thermal treatment methods may impact the efficacy of the ash as a soil amendment (Gorazda et al., 2017; Hossain et al., 2011; Mattenberger et al., 2008).

2.3.2.1 Bioavailable Phosphorus

One of the considerations that should be included when assessing viability of a material as a phosphorus rich fertilizer is the biological availability of phosphorus containing macro-nutrients i.e., phosphorus bioavailability (Johnston and Steen, 2002). This is particularly true when high temperatures, such as those experienced in sewage sludge incineration, are involved since they can affect phosphorus bioavailability (Pape et al., 2015) as well as bioavailability of elements of potential concern.

Bioavailable phosphorus is typically divided into three pools based on the timeframe of availability for uptake by plants, namely, the short-term or immediately available pool, the medium-term pool, and the long-term or unavailable pool (Pansu and

Gautheyrou, 2007). Each of these pools consists of different phosphorus containing compounds. The short-term pool contains mainly orthophosphate (PO_4^{3-}), the most reactive form of inorganic phosphorus, which is readily soluble and therefore easily utilized by plants (Johnston et al., 2014). The medium-term phosphorus pool is associated with phosphorus bound to aluminum and iron oxides and hydroxides (Cross and Schlesinger, 1995; Li et al., 2015; Pansu and Gautheyrou, 2007). Finally, the long-term pool or unavailable phosphorus is considered to consist primarily of calcium bound apatite mineral compounds (Li et al., 2015; Pansu and Gautheyrou, 2007).

Some studies have shown that heating affects phosphorus in environmental matrices. For example, the burning process during forest fires resulted in changes in the forms of phosphorus compounds present in the soil (Galang et al., 2010). Since certain phosphorus compounds are more readily available for uptake by plants than others, changes to the various fractions of phosphorus containing compounds during combustion may alter the bioavailability. Several studies have observed that incinerating sewage sludge at temperatures at or above approximately 600°C results in a decrease in phosphorus bioavailability by at least 50% due to the phosphorus being transformed into forms in the long-term phosphorus pool (Möller et al., 2007; Qian and Jiang, 2014; Thygesen et al., 2011). Alternatively, lower treatment temperatures around 400°C have been shown to have similar quantities of plant available phosphorus as raw sewage sludge (Thygesen et al., 2011) and increased phosphorus in the medium-term pool (Qian and Jiang, 2014). Previous research has primarily focused on investigating how incineration (Franz, 2008; Nanzer et al., 2014) and pyrolysis (Müller-Stöver et al., 2018; Qian and Jiang, 2014) of sewage sludge affects the quantity and bioavailability of phosphorus.

Understanding the bioavailable fractions of phosphorus compounds within the smouldered ash is important to develop best practices for land application as a phosphorus rich fertilizer. Although high bioavailable phosphorus fractions are favourable to promote plant growth, this fraction has the potential to contribute to water contamination if improperly distributed (Gerdes and Kunst, 1998). When fertilizers are land applied, there is the potential for some of the nutrients to leach into the subsurface or be transported via runoff and enter surface waters (Johnston and Steen, 2002). Bioavailable phosphorus within freshwater bodies can contribute to early eutrophication by promoting rapid algal growth and ultimate consumption of dissolved oxygen (Gerdes and Kunst, 1998).

2.3.2.2 Methods for Understanding Phosphorus Bioavailability: Sequential Extraction

Numerous methods have been developed to quantify phosphorus, especially bioavailable phosphorus, in a wide range of solids. Most literature and analytical methods focus on soils and the Hedley sequential fractionation method (Hedley et al., 1982) dominates the field (Chen and Ma, 2001; Condron et al., 1990; Cross and Schlesinger, 1995). Hedley forms the basis for many related sequential fractionation methods (Huang et al., 2008; Iyamuremye et al., 1996; Tiessen and Moir, 1993; Zhang and Kovar, 2009). Common modifications to the Hedley method include (i) an initial deionized water step prior to anion exchange resin (Huang et al., 2008), (ii) excluding quantification of microbial phosphorus (Iyamuremye et al., 1996), (iii) eliminating sonication during the extraction of moderately-bound phosphorus (Tiessen and Moir, 1993), and (iv) using heated digestion to quantify residual (unavailable) phosphorus (Zhang and Kovar, 2009). The purpose of the Hedley method is to quantify the inorganic and organic phosphorus

present in the various soil fractions. During the extraction procedure, progressively stronger chemical extractants are used to extract the more recalcitrant forms of phosphorus (Linquist et al., 1997). Inferences are then drawn between the quantity of phosphorus within the fractions and the potential sources and sinks of available phosphorus over time (Verma et al., 2005).

Despite sequential phosphorus extraction procedures being extensively used in research to quantify bioavailable phosphorus, numerous studies have been conducted that identify and address issues with fractionation procedures (e.g., (Guggenberger et al., 1996; Neyroud and Lischer, 2003; Soinne, 2009)). The chemical extractant and molarity used to quantify the phosphorus present in each pool is highly variable depending on the extraction procedure followed. Table 2.1 summarizes the significant variability among studies.

Since phosphorus dissolution and release is highly dependent on pH (Bolan and Hedley, 1990), extraction methods are likely to yield different results for available phosphorus depending on chosen extractants and procedure order (Neyroud and Lischer, 2003; Soinne, 2009). Soinne (2009) compared the sequential phosphorus extraction procedures outlined by Chang and Jackson (1957) and Hedley et al. (1982) and found that each step influenced the solubility of the proceeding extraction. The same results were reached in a study by Neyroud and Lischer (2003) which concluded that it can be difficult to draw correlations between laboratory extractions and natural bioavailability due to the significant variability in the quantity of available phosphorus measured depending on the extraction procedure followed.

The third and fourth steps of the Hedley method utilize sodium hydroxide (NaOH) as the chemical extractant which have been shown to overestimate the inorganic phosphorus fraction within this pool due to the hydrolyzation of the organic phosphorus (Guggenberger et al., 1996). Since the Hedley method is a sequential extraction, erroneous results in a single step will impact the proceeding extractions. Extractions with strong bases (e.g., NaOH) and strong acids (e.g., HCl) produce results with limited applicability since the pH at each step of the extraction is significantly different than the sediment (Golterman, 1996). Furthermore, strong extractants can change the chemical structure of phosphorus species (Cade-Menun and Preston, 1996; Gikonyo et al., 2011; Guggenberger et al., 1996; Hartikainen and Yli-Halla, 1996). As a consequence, conclusions on phosphorus availability from studies using fractionation methods are inconsistent (Hartmann et al., 2019; Neyroud and Lischer, 2003) and sometimes contradictory (Johnson et al., 2003).

Studies assessing phosphorus availability in other solids including animal manure and sewage sludge have used modified versions of Hedley and soil phosphorus test procedures (González Medeiros et al., 2005; Huang et al., 2008; Qian and Jiang, 2014; Self-Davis and Moore Jr, 2000; Xu et al., 2012b). Only a few studies have attempted to fractionate phosphorus in sewage sludge (Han et al., 2019; Huang et al., 2008; Qian and Jiang, 2014; Xu et al., 2012a). Such evaluations are anticipated to suffer from the same problems identified for sequential fractionation of phosphorus in soils and may well be amplified because of the higher organic matter content of sludge.

Table 2.1: Summary of the Chemical Extractants Utilized by Sequential Extraction Studies to Quantify Bioavailable Phosphorus in Soils

P-pools	Bioavailability	Extractant	Method
Soluble-P	Readily	0.03 N NH_4F + 0.025 N HCl	Bray & Kurtz (1945)
		0.5 M $NaHCO_3$	Olsen (1954)
		1 M NH_4Cl	Chang & Jackson (1957)
		Resin	**Hedley et al. (1982)**
		1 M NH_4Cl	Olsen & Sommers (1982)
		$FeCl_3$ strips	Menon et al. (1989)
		Resin	Tiessen & Moir (1993)
		Water [a]	H. Zhang & Kovar (2009)
Loosely bound-P/ Labile	Readily	0.5 M $NaHCO_3$	Bowman & Cole (1978)
		0.5 M $NaHCO_3$	**Hedley et al. (1982)**
		0.1 N NaOH + 1 M NaCl	Olsen & Sommers (1982)
		$MgCl_2$	Ruttenberg (1992)
		0.5 M $NaHCO_3$	Tiessen & Moir (1993)
		1 M NH_4Cl [a] / 0.5 M $NaHCO_3$ [b]	H. Zhang & Kovar (2009)
Al-P	Potentially soluble under anoxic and reducing conditions	0.5 M NH_4F	Chang & Jackson (1957)
		0.5 M NH_4F + NaCl [a]	H. Zhang & Kovar (2009)
Fe-P	Potentially soluble under anoxic and reducing conditions	0.1 M NaOH	Chang & Jackson (1957)
		CDB + $MgCl_2$	Ruttenberg (1992)
		0.1 M NaOH [a]	H. Zhang & Kovar (2009)
Reductant soluble-P/ Moderately labile	Phosphorus from the matrices of aggregates and minerals	0.5 M NaOH	Bowman & Cole (1978)
		0.1 M NaOH	**Hedley et al. (1982)**
		1 M NaCl + 0.3 M $Na_3C_3H_6O_7$	Olsen & Sommers (1982)
		0.1 M NaOH	Tiessen & Moir (1993)
		0.3 M $Na_3C_3H_6O_7$ + 1 M $NaHCO_3$ + 0.5 g $Na_2S_2O_4$ [a] / 1 M HCl [b]	H. Zhang & Kovar (2009)
Ca-P	Inorganic phosphorus from apatite or octocalcium phosphate	0.25 M H_2SO_4	Chang & Jackson (1957)
		1 N HCl	Olsen & Sommers (1982)
		Acetate buffer + $MgCl_2$	Ruttenberg (1992)
		0.25 M H_2SO_4 [a]	H. Zhang & Kovar (2009)
Occluded-P	Resistant inorganic phosphorus	0.1 M NaOH	Chang & Jackson (1957)
		1 M HCl	**Hedley et al. (1982)**
		1 g $Na_2S_2O_4$	Olsen & Sommers (1982)
		1 M HCl	Ruttenberg (1992)
		1 M HCl	Tiessen & Moir (1993)
		0.5 M NaOH [b]	H. Zhang & Kovar (2009)
Residual	Slowly or non-exchangeable from mineral surface	Ashing [c]	Bowman & Cole (1978)
		Conc. H_2SO_4	**Hedley et al. (1982)**
		Ashing [c] + 1 M HCl + Conc. H_2SO_4	Ruttenberg (1992)
		Conc. H_2SO_4 + H_2O_2	Tiessen & Moir (1993)
		Ashing [c] + 1 M H_2SO_4 [b]	H. Zhang & Kovar (2009)

[a] Sequential extraction scheme for inorganic-P by Zhang and Kovar (2008)
[b] Sequential extraction scheme for organic-P by Zhang and Kovar (2008)
[c] Ashing performed at 550°C

2.3.2.3 Leaching and Assessment Methods

Accumulation of phosphorus within soils can increase the risk of phosphorus leaching (Abdala et al., 2015; Maguire and Sims, 2002). Several studies have demonstrated that phosphorus leaching may occur from soils that have been applied with manures (Abdala et al., 2015; Jalali and Ostovarzadeh, 2009) and inorganic fertilizers (Maguire and Sims, 2002; Turner and Haygarth, 2000). In addition to supplying nutrients to soil, the application of fertilizers may also impact PTE mobility by increasing the solubility of certain PTEs (del Castilho et al., 1993; Japenga et al., 2006).

PTEs exist naturally in soils in trace concentrations (Kabata-Pendias, 2000). Contamination of PTEs in the environment has primarily been due to anthropogenic influences including mine tailings, improper waste disposal, and fertilizer application (Khan et al., 2008). Several studies have shown that the application of sewage sludge as a fertilizer can increase the concentrations of toxic metals in both the soil and groundwater, potentially resulting in safe level exceedances (Keller et al., 2002; Wierzbowska et al., 2016). Therefore, when evaluating a material for use as a fertilizer, it is essential to understand elemental availability and release.

Phosphorus retention and transport in the subsurface depends on both chemical (e.g., pH) and hydrological (e.g., soil permeability) properties (Maguire and Sims, 2002). Common methods for assessing the potential for phosphorus losses from soils include column leaching experiments and phosphorus tests (Kumaragamage et al., 2011). Column leaching experiments are beneficial because they can mimic subsurface hydrological conditions and provide an indication of leaching potential under various rainfall conditions (Banzhaf and Hebig, 2016). Most commonly, column experiments are performed at the

native pH of the sediment which does not demonstrate how leaching is influenced by pH changes. Historically, phosphorus test methods in both Canada and the U.S. have been divided into agronomic and environmental phosphorus tests (Kumaragamage et al., 2011). The purpose of agronomic phosphorus tests (including Bray and Kurtz P-1, Mehlich P-1, Mehlich P-3, and Olsen-P) is to maximize economic gain from fertilizers, while environmental phosphorus testing (including water-extractable and Fe-impregnated strips) is aimed at assessing the potential implications and fate of soil phosphorus (Kumaragamage et al., 2011; Y. T. Wang et al., 2015). Agronomic and environmental phosphorus tests are commonly performed as batch experiments and can provide insights into leaching behaviour under various chemical conditions; however, they are limited in their ability to account for hydrological properties (Y. T. Wang et al., 2015). Most leaching tests are meant to simulate the release of constituents under a pre-defined release scenario restricting their relevance (Kosson et al., 2017).

Following decades of development, the USEPA released the Leaching Environmental Assessment Framework (LEAF) in 2010. LEAF is a characterization-based leaching framework combining experimental data on relevant intrinsic leaching behaviour with scenario-specific information for environmental assessments (Kosson et al., 2017). LEAF includes method 1313 which consists of a series of parallel batch experiments to produce a liquid-solid partitioning curve of the sediment of interest as a function of pH (USEPA, 2012a). The complementary USEPA Method 1314 involves a column percolation experiment to obtain eluate concentrations and/or cumulative release as a function of the liquid-to-solids ratio (USEPA, 2012b). Previously, LEAF has been used to assess leaching behaviour of PTEs from coal fly ash (Garrabrants et al., 2014; Tiwari et

al., 2015), MSW incinerator ash (Zhang et al., 2016), concrete waste (Garrabrants et al., 2014; Kosson et al., 2014), and sewage sludge compost (Fang et al., 2016). Using LEAF to assess phosphorus is less common and has been used for inorganic phosphorus from mining waste (L. Jiang et al., 2016; L. G. Jiang et al., 2016). The methodology seems promising to evaluate bioavailable phosphorus for a wide range of organic and inorganic matrices.

2.4 Potential Harmful By-Products from the Thermal Treatment of Sewage Sludge

Sewage sludge contains high quantities of PTEs and many emerging contaminants such as antibiotic resistant bacteria, polychlorinated dibenzo-*p*-dioxins (PCDDs) and polychlorinated dibenzofurans (PCDFs), and perfluorinated compounds (Jiwan and Ajah, 2011; Zhou et al., 2019), which have been shown to cause adverse human health and environmental impacts (Zhang et al., 2017b). Therefore, there is strong interest in thermal conversion techniques that limit the environmental release of these harmful substances (Pudasainee et al., 2013; Werther and Ogada, 1999; Zabaniotou and Theofilou, 2008). In particular, incineration is an attractive option for treating sewage sludge due to its ability to destroy organic contaminants (Werther and Ogada, 1999). However, the by-product emissions from sewage sludge incineration often contains hazardous compounds that require additional treatment, e.g., PTEs (especially metals), volatile organic compounds (VOCs), polyaromatic hydrocarbons (PAHs), and PCDD/Fs (Fullana et al., 2004; Pudasainee et al., 2013; Shao et al., 2008; Werther and Ogada, 1999). Similar by-products may be formed and/or released during sewage sludge smouldering; however, research in

this area is limited and focuses on common combustion gases (e.g., O_2, CO, CO_2, CH_4) (Feng et al., 2021; Rashwan, 2020; Rashwan et al., 2021a).

2.4.1 Potentially Toxic Elements (PTEs)

The by-products from the incineration of sewage sludge (Han et al., 2006; Marani et al., 2003; Pudasainee et al., 2013) and MSW (R. G. Barton et al., 1988; Karlfeldt Fedje et al., 2010; Łach et al., 2016) have been studied extensively in literature. The primary PTEs of concern during the combustion of both municipal solid waste and sewage sludge are Cd, Pb, Hg, Cr, As, and Be (Fullana et al., 2004; Shao et al., 2008). PTEs emitted during the incineration process pose a serious risk to human health and the environment which is why their atmospheric release is heavily regulated and emissions treatment is an essential component of the waste treatment process (Senior et al., 2000).

Several factors have been identified to influence the distribution of PTEs during incineration including properties and type of waste; physicochemical properties of specific elements; reactor type; residence time; and incineration conditions, such as temperature and airflow rate (Nowak et al., 2013; Zhang et al., 2008). For example, metallic elements with high vapour pressures are more likely to be vaporized and adsorb onto particles within the exhaust gas (Senior et al., 2000). The high temperatures associated with incineration can result in an increase in the vaporization of certain metallic elements by providing conditions which alter chemical forms, producing compounds with higher vapour pressures (R. Barton et al., 1988; Council, 2000). When toxic metals are volatilized, they either adsorb onto particulate matter present in the combustion emissions, or they recondense back into the ash (Pudasainee et al., 2013).

2.4.1.1 PTEs in Smouldering Systems

Recently, smouldered sewage sludge ash has been shown as likely safe for landfilling (Feng et al., 2020), but more work is still needed to understand compounds being formed and/or released from sewage sludge smouldering, especially within the emissions.

There are several reasons why metal emissions may be reduced in smouldering applications relative to incineration: (i) the lower air flow rates and use of fixed beds, compared to the fluidized bed incinerators, may result in less mobilization of particulate matter; (ii) the lower operating temperatures may result in lower quantities of metals being volatilized, and (iii) the fact that smouldering produces negligible soot, reducing the potential for sorbed metal transport in the emissions (Torero et al., 2020; Wyn et al., 2020). With potentially lower quantities of metals being released in the emissions; these elements are likely to be retained within the sand and ash of the reactor which may simplify and increase the potential for recovery and reuse of these compounds.

2.4.2 Dioxins and Furans (PCDD/Fs)

Similar to PTEs, the release of PCDD/Fs during sewage sludge incineration is a major concern because these compounds are highly toxic and persistent (Fiedler, 2003; Reiner, 2016; Van Den Berg et al., 2006). PCDD/Fs may enter WWTPs from a variety of sources such as via runoff containing pesticides. Within WWTPs, PCDD/Fs have been shown to behave quite conservatively, being retained and concentrated in sewage sludge (Jones and Sewart, 1997).

PCDD/Fs are planar molecules whose structure includes two benzene rings connected by two oxygen bridges (PCDD), or an oxygen bridge and chlorine atom (PCDF) (Reiner, 2016). PCDD/Fs can contain one to eight chlorine atoms that can be attached in multiple locations, forming 75 different PCDDs and 135 different PCDFs (Reiner, 2016). The seventeen PCDD/Fs containing chlorine atoms in the 2,3,7,8 positions on the benzene ring are considered the most toxic and are used to approximate the toxic equivalent quantity (TEQ) of a compound (Reiner, 2016). The TEQ considers both the toxicity of the congener, and typical concentrations (Van Den Berg et al., 2006). The toxicity is determined by multiplying the concentrations of the 2,3,7,8 – positional congeners (i.e., the most toxic) by their respective toxic equivalency factors (TEFs) (Van Den Berg et al., 2006). As our understanding of PCDD/Fs evolve, the TEFs are being updated (NATO/CCMS, 1988; USEPA, 2003; Van Den Berg et al., 2006). Progressions of the TEFs are presented in Table 2.2.

Although typically produced in low concentrations, PCDD/Fs are extremely harmful – even at low concentrations – due to their persistence, lipophilicity, mutagenicity, and bioaccumulation (McKay, 2002; Zhang et al., 2017a). Therefore, there is no safe limit for these compounds (Schecter and Gasiewicz, 2005). Dioxins and furans are known carcinogens, and exposure to these compounds has also been associated with reproductive and developmental issues, and immune system damage (Schecter and Gasiewicz, 2005).

Table 2.2: Common internationally accepted Toxic Equivalency Factors (TEFs) for PCDD/Fs

Congener	EPA (1987)	NATO (1988)	WHO (1998)	WHO (2005)
PCDDs				
2378-TCDD	1	1	1	1
12378-PeCDD	0.5	0.5	1	1
123478-HxCDD	0.04	0.1	0.1	0.1
123678-HxCDD	0.04	0.1	0.1	0.1
123789-HxCDD	0.04	0.1	0.1	0.1
1234678-HpCDD	0.001	0.01	0.01	0.01
OCDD	0	0.001	0.0001	0.0003
PCDFs				
2378-TCDF	0.1	0.1	0.1	0.1
12378-PeCDF	0.1	0.05	0.05	0.03
23478-PeCDF	0.1	0.5	0.5	0.3
123478-HxCDF	0.01	0.1	0.1	0.1
123678-HxCDF	0.01	0.1	0.1	0.1
234678-HxCDF	0.01	0.1	0.1	0.1
123789-HxCDF	0.01	0.1	0.1	0.1
1234678-HpCDF	0.001	0.01	0.01	0.01
1234789-HpCDF	0.001	0.01	0.01	0.01
OCDF	0	0.0001	0.0001	0.0003

2.4.2.1 PCDD/Fs in Combustion Systems

Any thermal process proceeding in the presence of carbon, chlorine, oxygen, and metal catalyst has the potential to produce PCDD/Fs (Stanmore, 2004; Zhang et al., 2017a). The most common sources for PCDD/F production from combustion processes include incineration (e.g., of sewage sludge or MSW) (Aurell, 2008; W. Deng et al., 2009; Fullana et al., 2004), fossil fuel combustion (Lin et al., 2007), wood combustion (Gullett and Touati, 2003; Schatowitz et al., 1994), and sintering plants (Lin et al., 2007; Ooi and Lu, 2011).

Two temperature windows have been reported for PCDD/F formation, 500-800°C where 'homogenous' pyrogenic routes proceed in the gas phase, and 200-400°C with 'heterogenous' catalytic gas/solid reactions (McKay, 2002; Stanmore, 2004; Zhang et al., 2017a). Homogenous formation accounts for much less production than heterogenous

mechanisms (Altarawneh et al., 2009; Stanmore, 2004). Heterogenous pathways can be further divided into (a) *de novo* synthesis, and (b) precursor pathways (Stanmore, 2004). Several studies have explored the mechanisms of PCDD/F formation during combustion processes (mostly incineration), and it is generally agreed that the major formation pathways are: (*i*) incomplete combustion of existing PCDD/Fs fed to the combustor; (*ii*) reactions from precursor compounds; and (*iii*) *de novo* synthesis from carbon and chlorine (McKay, 2002; Stanmore, 2004; Zhang et al., 2017a).

2.4.2.2 Fate of PCDD/Fs during Incineration

Elevated temperatures, such as those typically observed during incineration, typically support complete combustion and therefore the degradation of PCDD/Fs (Zhang et al., 2017a). The residence time is an important consideration in combination with the treatment temperature. For example, PCDD/Fs can be destroyed when exposed to slightly lower temperatures and longer residence times (e.g., 2s at 800 – 900°C), or slightly higher temperatures and shorter residence times (e.g., 1s at >1000°C) (Aurell, 2008; McKay, 2002).

Fluidized bed incinerators immediately subject sludge to high temperatures 750 – 925°C for 2 – 5 seconds (USEPA, 1995). Since these conditions have been shown to be sufficient for complete destruction of PCDD/Fs originally present in the sludge, most PCDD/Fs in incinerator emissions are thought to be produced through heterogeneous production pathways in the post-combustion chamber (Altwicker et al., 1992; Lavric et al., 2004).

2.4.2.3 Heterogeneous Pathways of Formation

Volatile matter released during the pyrolysis and oxidation reactions of combustion systems tend to form cyclic compounds in the emissions, e.g., aromatics, PAHs, and soot (Zhang et al., 2017a). Insufficient oxygen supply, temperature, or residence time may not fully degrade volatile matter into typical combustion by-products, i.e., carbon dioxide and water (Caillat and Vakkilainen, 2013). The result is the formation of products of incomplete combustion (PICs) (Zhang et al., 2017a). PICs may then be converted into PCDD/Fs via precursor and *de novo* synthesis pathways, or through direct chlorination of dibenzofuran and dibenzo-*p*-dioxin (Addink and Olie, 1995; Altarawneh et al., 2009; Tame et al., 2007).

Precursors to PCDD/Fs are compounds that are structurally similar to dioxins (Stanmore, 2004). The most common precursor compounds include chlorophenols (e.g., from herbicides), chlorobenzenes (e.g., from pharmaceuticals), polychlorinated biphenyls (e.g., from dyes), and polycyclic aromatic hydrocarbons (Addink and Olie, 1995; Tuppurainen et al., 1998). These precursors may form PCDD/Fs by relatively straightforward reactions and are thermodynamically favoured at low temperature due to the strong structural similarities between the compounds (Huang and Buekens, 1995; Stanmore, 2004). For example, the condensation of chlorophenols is a documented mechanism of formation (Figure 2.3) (Tame et al., 2007). Precursors that are more structurally similar to PCDD/Fs and have a faster reaction rate than simpler cyclic aromatics. For example, the reaction rate for chlorophenols is two orders of magnitude faster than chlorobenzene (Altwicker et al., 1992). Certain metals present in the sewage sludge (especially copper) may act as catalysts and further promote the formation of PCDD/Fs during combustion (Olie et al., 2011; Tame et al., 2007).

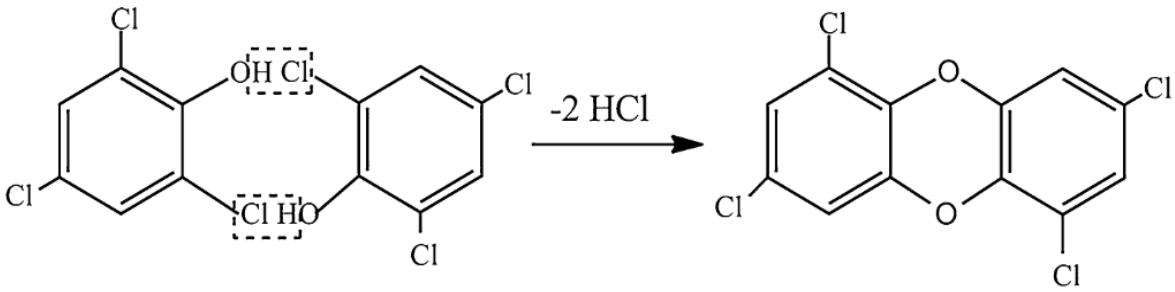

Figure 2.3: Condensation of chlorophenols, forming 1,3,6,8-PCDD (Zhang et al., 2017a)

Similar to the precursor compounds, *de novo* synthesis reactions occur on the surface of carbonaceous solids (e.g., soot) with additional volatilized chlorine (Altarawneh et al., 2009; Stanmore, 2004; Zhang et al., 2017a). During *de novo* synthesis, the combined chlorine-carbon matrix experiences oxidative degradation (Figure 2.4) (Zhang et al., 2017a). These reactions are also catalyzed by metals in the emissions which can lower the temperatures required for the oxidative degradation (Addink and Olie, 1995; Stieglitz et al., 1993). Relative to precursor formation, *de novo* synthesis has slower reaction rates (Altwicker and Milligan, 1993; Dickson et al., 1992). Furthermore, for fuels containing minute quantities of chlorinated compounds (especially $CuCl_2$), formation of PCDD/Fs via *de novo* synthesis are likely minimal (Tame et al., 2007). The presence of chlorinated compounds in sewage sludge has been shown to increase PCDD/F formation during incineration, however, the extent of this increase is dependent on the initial content in the sludge and will therefore vary (Fullana et al., 2004).

The high sulfur to chlorine ratio typically observed in sewage sludge may inhibit the formation of PCDD/Fs via *de novo* pathways (W. Deng et al., 2009; Werther and Ogada, 1999). The presence of sulfur promotes the formation of sulfur dioxide (SO_2) since it is more thermochemically favourable for the sulfur to react with oxygen instead of the

chlorine (Fullana et al., 2004; Werther and Ogada, 1999). The chlorine will then react with the hydrogen, forming hydrochloric acid (HCl) following the Deacon reaction (Equation 2.1)(Griffin, 1986). Since chlorination is less favourable by HCl than Cl_2, chlorination reactions will be reduced (Griffin, 1986).

$$SO_2 + Cl + H_2O \leftrightarrow SO_3 + HCl \tag{2.1}$$

Similar to PCDD/F formation via precursor transformation, *de novo* synthesis is catalyzed by metals that are emitted during incineration (Olie et al., 2011). The sulfates and HCl compete for these metals which helps reduce the formation of chlorinated pollutants (Ke et al., 2010; Ryan et al., 2006). However, this method results in the production of SO_x and HCl, both of which are hazardous emissions and would need to be treated (Syed-Hassan et al., 2017).

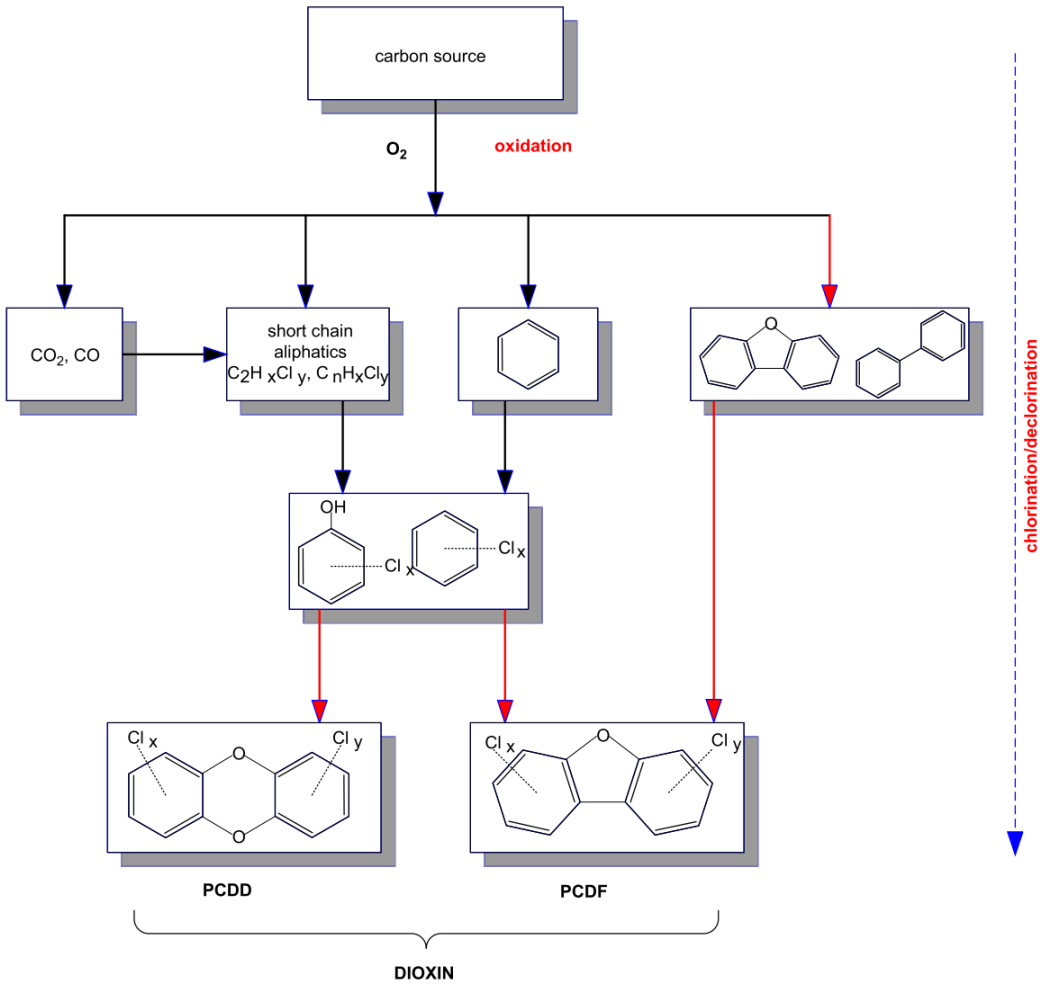

Figure 2.4: Potential reaction pathways for *de novo* synthesis of PCDD/Fs, where the red arrows represent the most likely pathways (Tame et al., 2007).

2.4.2.4 PCDD/Fs in Smouldering Systems

While heterogeneous reactions at the gas – solids interface are generally the dominant PCDD/F formation mechanisms in incinerators (Fullana et al., 2004; Stanmore, 2004; Zhang et al., 2017a), the same may not be true for smouldering systems. Smouldering systems often exhibit lower treatment temperatures (~400-550°C) that may promote PCDD/F release/formation instead of destruction (W. Deng et al., 2009). Furthermore, since smouldering is generally limited by oxygen transport to the fuel surface, it often results in incomplete combustion (Grant et al., 2016; Torero et al., 2020; Wyn et al., 2020).

The extent of combustion completeness in incinerators has been shown to affect the release PCDD/Fs in incinerator emissions, where more incomplete combustion generally corresponds to higher amounts of PCDD/Fs in the emissions (Fiedler, 2003; McKay, 2002).

A metric that may be important for evaluating the behaviour of PCDD/Fs in smouldering systems is combustion performance, which may be more sensitive, and therefore, variable than incinerators (Rashwan et al., 2021c, 2021b, 2021a). With smouldering, the sludge is treated in a fixed bed where the combustion performance may be variable and influenced by both radial heat losses and reaction uniformity (Rashwan et al., 2021d, 2021c). Radial heat losses in the cooling zone behind the smouldering front can lead to non-uniform air flux (Rashwan et al., 2021d). Non-uniform reactions have been shown to result in an unburned crust around the edges of the reactor (Rashwan et al., 2021a). Combined, non-uniform reactions and non-uniform air flux may reduce overall smouldering performance enough to cause extinction (Rashwan et al., 2021c). The lower peak temperatures and significant unburned edges that result from reduced smouldering performance could limit the destruction of PCDD/Fs originally present in the waste material which has been demonstrated with other combustion systems (Aurell, 2008). Therefore, smouldering performance is an important factor that needs to be considered when evaluating PCDD/F behaviour during sewage sludge smouldering.

Filtration by the inert porous media ahead of the smouldering front has been observed in applied smouldering systems (Kinsman, 2015). This filtration results in less particulate matter in the emissions from smouldering reactors compared to typical incinerators (Torero et al., 2020). Since particulate matter in the post-combustion region is

required for *de novo* synthesis of PCDD/Fs to occur (McKay, 2002; Zhang et al., 2017a), smouldering systems seem less likely to produce PCDD/Fs via this pathway.

2.4.3 Per- and Poly-Fluorinated Substances (PFAS)

Per- and poly-fluoroalkyl substances (PFAS) are a group of thousands of chemicals with the chemical structure $C_nF_{(2n+1)} - R$ (where R is the attached functional group) (Buck et al., 2011). The properties of PFAS, including chemical and thermal stability (due partially to the C – F bond), have made them useful in many applications including firefighting foams, aerospace, medical use, and household use (e.g., non-stick cookware) (Kissa, 2001). However, these compounds pose serious health risks, including neurotoxicity, reproductive issues, and increased cancer risk (Lindstrom et al., 2011; Miralles-Marco and Harrad, 2015). The PFAS of highest concern include perfluorooctane sulfonate (PFOS; containing a sulfonic acid functional head group) and perfluorooctanoic acid (PFOA; containing a carboxylic acid functional head group), both of which are also the most common PFAS (Buck et al., 2011). Due to their toxicity and persistence in the environment, both PFOS and PFOA production have been restricted around the world (UNEP, 2019; USEPA, 2020). Furthermore, regulations on PFOS and PFOA have also been implemented for drinking water (Pontius, 2019; USEPA, 2021) and soil (Environment and Climate Change Canada, 2017), and others have been suggested (Bhavsar et al., 2016). However, due to high stability and resistance to degradation, these compounds are challenging to remediate and continue to persist and accumulate in the environment (Kissa, 2001). Therefore, there is significant interest in developing methods to effectively treat PFAS (Mahinroosta and Senevirathna, 2020; Ross et al., 2018).

2.4.3.1 PFAS at WWTPs

PFAS are becoming ubiquitous in the environment, including at WWTPs (Arvaniti et al., 2014, 2012; Gómez-Canela et al., 2012; Moodie et al., 2021; Sindiku et al., 2013; Sun et al., 2011; Venkatesan and Halden, 2013; Yan et al., 2012). Figure 2.5 shows PFAS concentrations at different WWTPs across the world. It should be noted, however, that since no standardized methods for PFAS extraction and quantification were used across these studies, the values may not be completely accurate. Extraction methods are evolving in efficiency and quantification methods are evolving to include lower concentrations and a wider variety of compounds (Guo et al., 2008; Higgins et al., 2005; Hutchinson et al., 2020; Zhang et al., 2010). Furthermore, the concentrations may not be fully representative of the concentrations observed at the plants today since changes in regulations over time will result in changes in compounds observed (Houtz et al., 2016). Sources of PFAS to WWTPs include industrial discharge (Kunacheva et al., 2011; Washington et al., 2010), landfill leachate (Gallen et al., 2016), and domestic sources (Pan et al., 2010). Since conventional wastewater treatment methods are ineffective at treating PFAS, WWTPs tend to be a sink for these compounds (Ahrens et al., 2009). Additionally, WWTPs are potential sources of PFAS since they can be formed via precursor degradation under a variety of treatment conditions (Houtz et al., 2018; Lakshminarasimman et al., 2021; Pan et al., 2010; Sepulvado et al., 2011).

With increasing concerns regarding health and environmental impacts of PFAS, there has been significant interest in studying the behaviour of PFAS at WWTPs (Lenka et al., 2021). Due to the higher distribution coefficients (K_d) of longer chain PFAS (e.g., PFOS and PFOA), these compounds have a greater tendency to become concentrated in

sewage sludge compared to shorter chain PFAS (Arvaniti et al., 2014; Clarke and Smith, 2011; Milinovic et al., 2016; Zhang et al., 2013). Therefore, sewage sludge management needs to consider the fate of these compounds. Landfilling sewage sludge may result in PFAS entering the environment via leachate (Ahrens et al., 2011; Gallen et al., 2016). A common alternative to landfilling sewage sludge is direct land application as a soil amendment. Land applied sludges can be a significant source of PFAS contamination to the environment through surface runoff or infiltration (Johnson, 2022; Sepulvado et al., 2011). PFAS from land applied sludges may also circulate in the environment via plant uptake (Blaine et al., 2013; Ghisi et al., 2019).

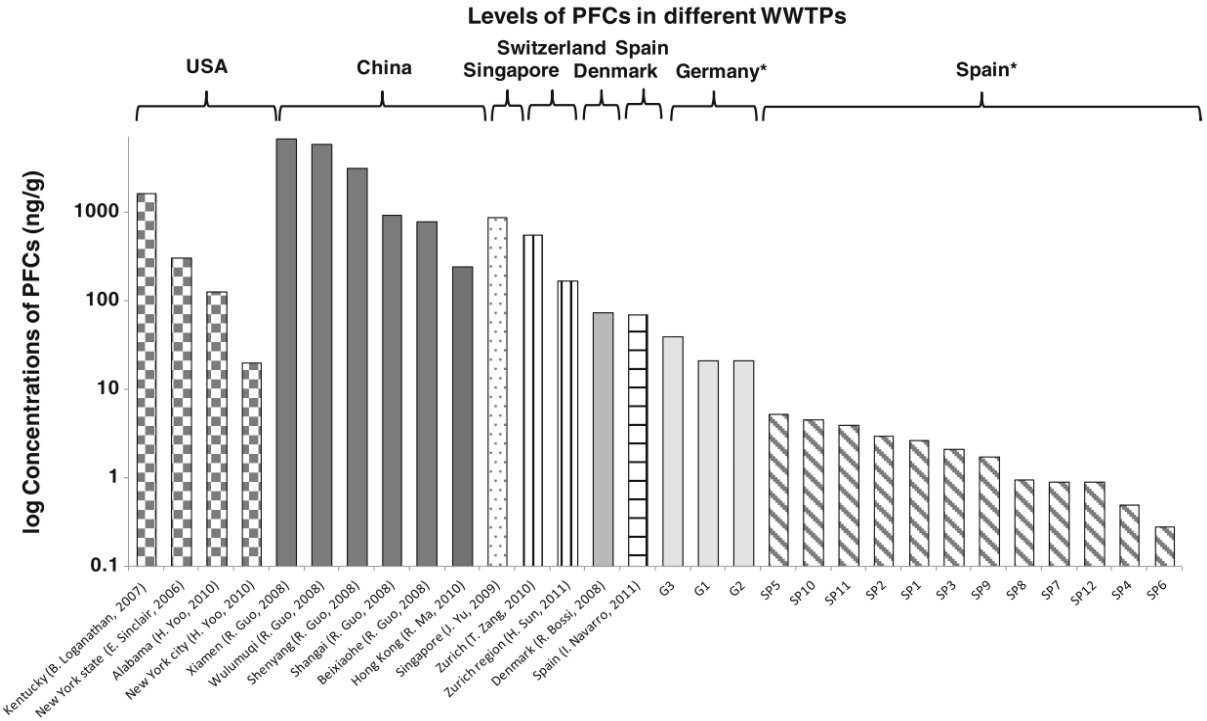

Figure 2.5: Concentrations of perfluorochemicals (PFCs) at WWTPs around the world (Gómez-Canela et al., 2012).

2.4.3.2 Potential Treatment Methods for PFAS in Sewage Sludge

With increasing regulations, especially for PFOS and PFOA (USEPA, 2021), there is significant interest in developing methods of removing and degrading PFAS from sewage sludge. The use of thermal treatment methods to remove PFAS from sewage sludge is relatively limited. Current thermal methods being explored include incineration (Wang et al., 2013), pyrolysis (Kim et al., 2015; Kundu et al., 2021), and hydrothermal treatments (Yu et al., 2020a; Zhang and Liang, 2021).

Incineration of dried sludge amended with hydrated lime ($Ca(OH)_2$) has been shown to effectively mineralize >70% of fluorine at treatment temperatures >600°C (Wang et al., 2013). While demonstrating a highly effective method of treating PFAS contaminated sludge, the long residence times (up to 15 minutes), and the high sludge/$Ca(OH)_2$ ratio required (0.7 g/0.3 g) may make scaling this treatment method challenging and expensive. However, the effectiveness of the process should be noted, and this study provides valuable information that can help advance treatment technologies, but more work is needed. While incineration may be an effective method of destroying contaminants present in sewage sludge (Ross et al., 2018), it is also an energy intensive and expensive process (Werther and Ogada, 1999). Therefore, alternative treatment methods are being explored.

Pyrolysis has shown mixed results in its ability to remove PFAS from sewage sludge. Kim et al., (2015) was the first study assessing the use of pyrolysis to treat PFAS in sewage sludge. Pyrolysis of virgin sewage sludge (i.e., no PFAS spiking or drying) was shown to have little influence on the PFOA or PFOS content, irrespective of the temperature (300°C or 700°C treatments). In comparison, another study showed effective

removal (>90%) of PFOS and PFOA using pyrolysis at 500°C, including no detection in the biochar or water scrubber (Kundu et al., 2021).

Hydrothermal treatments have also shown mixed results for PFAS treatment. One study reported reductions of 35 – 45% PFOS and ~100% PFOA from sludge at temperatures between 260 – 350°C (Yu et al., 2020b). It should be noted, however, that emissions/gaseous by-products were not measured during this study. Therefore, the degradation of the PFAS assessed in this study cannot be fully understood since the concentrations and types of compounds leaving the system with the emissions is unknown. Another study on hydrothermal treatment of sewage sludge showed that reductions in perfluoroalkyl acids (PFAAs) were often coupled with increases in PFAA precursors (Zhang and Liang, 2021).

Other methods that have been explored and found to be ineffective at removing PFAS from sewage sludge include ultrasound (Zhang et al., 2022), and acid-microwave assisted persulfate digestion (Hamid and Li, 2018). Long ultrasonic treatment of sewage sludge was shown to release PFAS, rather than degrade it (Zhang et al., 2022). While slightly more effective than ultrasound, microwave-assisted persulfate oxidation of sewage sludge was only able to remove ~42% of PFOA following 4 hours of treatment at 70°C (Hamid and Li, 2018), making it infeasible at larger scales.

2.4.3.3 Smouldering for PFAS Treatment

In 2020, smouldering combustion was shown to be an effective method of treating PFAS contaminated soils (Duchesne et al., 2020). To achieve thermal destruction of PFAS, GAC was added to the soil as a supplemental fuel (Duchesne et al., 2020). Adding greater

than 35 g GAC/kg soil resulted in treatment temperatures >900°C which have been shown to support PFAS degradation (Duchesne et al., 2020; Mahinroosta and Senevirathna, 2020).

Smouldering sewage sludge generates temperatures between 400 – 550°C (Rashwan et al., 2021a, 2016). At these relatively low treatment temperatures, PFAS present in the sewage sludge would likely volatilize rather than degrade (Crownover et al., 2019; Winchell et al., 2021). Therefore, to achieve thermal degradation of PFAS in sewage sludge via smouldering, a supplemental fuel, e.g., GAC would need to be added.

Alternatively, when a calcium amendment is added to the fuel, 50 – 70% transformation of PFAS to solid CaF_2 in the bottom ash is possible at incineration temperatures as low as 400°C (F. Wang et al., 2015; Wang et al., 2013). The presence of calcium to mineralize fluorine from PFAS has been shown to prevent the release of short and longer-chained PFAS (>3C) (Wang et al., 2013) and reduces the production of secondary fluorinated compounds (Riedel et al., 2021). In particular, the use of $Ca(OH)_2$ as a calcium amendment has been shown to more effectively mineralize fluorine at lower temperatures and in the presence of water (F. Wang et al., 2015). This presents a unique opportunity for using smouldering to treat PFAS in sewage sludge which has not previously been explored.

2.5 Summary of Key Findings

Smouldering sewage sludge has been explored in the context of process optimization (Rashwan et al., 2016), scaling (Feng et al., 2021; Rashwan et al., 2021a), and landfilling potential (Feng et al., 2020). However, the by-products of the smouldering treatment of wastes such as sewage sludge have not been well studied. Understanding the fate of key elements and compounds as well as potential by-product formation from smouldering combustion of sewage sludge will help to maximize value recovery and minimize risks associated with this process and subsequent uses of the treated material.

Recovery potential from incinerated sewage sludge ash has been well studied, especially recently, due to shifts towards more circular economies. Numerous extraction methods have been developed and optimized for incinerator ash. While reviews of smouldering have expressed the significant potential for exploring value-added products from the process, the recovery opportunities from smouldered sewage sludge, in particular, of phosphorus are largely unknown.

As an alternative to direct recovery, land application of sewage sludge and ashes following thermal treatment have been widely utilized to recycle nutrients. While treatment is important for making sewage sludge safe for land application, the elevated temperatures associated with incineration and pyrolysis have been shown to decrease the bioavailability of phosphorus. With relatively lower peak temperatures, smouldering sewage sludge may avoid this problem.

To evaluate phosphorus bioavailability, fractionation methods are commonly used. Despite fractionation methods being extensively used in research to quantify phosphorus

bioavailability, numerous studies also identified inconsistencies and other problems with fractionation procedures. Moreover, there is significant discrepancy among literature drawing correlations between chemical extractants and plant availability. An alternative method that is promising for assessing the suitability of a fertilizer source and developing application guidelines is the USEPA Leaching Environmental Assessment Framework (LEAF). This study will be the first to assess the suitability of LEAF for analyzing the leaching behaviour of both phosphorus and other constituents from smouldered sewage sludge ash.

The high quantities of PTEs and other emerging contaminants within sewage sludge have necessitated the use of thermal treatment methods for managing this waste. The by-products from common thermal treatment methods (especially incineration) have been extensively studied to mitigate any associated risks. The same is not well-known for smouldering sewage sludge. One such hazard is PCDD/Fs which have been shown to form during incineration processes and during biomass smouldering (i.e., during forest fires). Although these PCDD/Fs risks from sewage sludge incineration are well-characterized, they are not well-understood from smouldering systems. Research has shown that there are significant differences between smouldering systems and incinerators. Since these differences are expected to govern the behaviour of PCDD/F formation and/or release, it is challenging to extrapolate findings across these systems. Therefore, there is a strong need for direct experiments to evaluate the PCDD/Fs formed and/or released from smouldering sewage sludge. Another emerging contaminant in sewage sludge is PFAS. PFAS is ubiquitous in the environment and at WWTPs where longer chain compounds are concentrated in the sewage sludge. Due to significant health and environmental hazards

associated with these compounds, there is a need for developing methods of treating PFAS in sewage sludge. The use of thermal treatment methods to remove PFAS from sewage sludge is relatively limited and show variable results. While current treatment studies demonstrate the limited understanding and complexities of treating PFAS in sewage sludge, they also provide valuable information that can help advance treatment technologies. Overall, more work is needed in this area. Previously demonstrated to effectively treat PFAS contaminated soil, smouldering has potential as an alternative thermal treatment method for PFAS in sewage sludge. Therefore, this study will explore – for the first time – how PFAS originally present in sewage sludge behaves during smouldering treatment. Understanding the formation and/or release of hazardous by-products during the smouldering treatment of sewage sludge is important to provide insight into potential emissions treatment required to meet air quality regulations, and additional processing needed ahead of land application.

2.6 References

Abdala, D.B., da Silva, I.R., Vergütz, L., Sparks, D.L., 2015. Long-term manure application effects on phosphorus speciation, kinetics and distribution in highly weathered agricultural soils. Chemosphere 119, 504–514. https://doi.org/10.1016/j.chemosphere.2014.07.029

Adam, C., Peplinski, B., Michaelis, M., Kley, G., Simon, F.G., 2009. Thermochemical treatment of sewage sludge ashes for phosphorus recovery. Waste Manag. 29, 1122–1128. https://doi.org/10.1016/j.wasman.2008.09.011

Addink, R., Olie, K., 1995. Mechanisms of Formation and Destruction of Polychlorinated Dibenzo-p-dioxins and Dibenzofurans in Heterogeneous Systems. Environ. Sci. Technol. 29, 1425–1435. https://doi.org/10.1021/ES00006A002

Ahrens, L., Felizeter, S., Sturm, R., Xie, Z., Ebinghaus, R., 2009. Polyfluorinated compounds in waste water treatment plant effluents and surface waters along the River Elbe, Germany. Mar. Pollut. Bull. 58, 1326–1333. https://doi.org/10.1016/j.marpolbul.2009.04.028

Ahrens, L., Shoeib, M., Harner, T., Lee, S.C., Guo, R., Reiner, E.J., 2011. Wastewater treatment plant and landfills as sources of polyfluoroalkyl compounds to the atmosphere. Environ. Sci. Technol. 45, 8098–8105. https://doi.org/10.1021/es1036173

Altarawneh, M., Dlugogorski, B.Z., Kennedy, E.M., Mackie, J.C., 2009. Mechanisms for formation, chlorination, dechlorination and destruction of polychlorinated dibenzo-p-dioxins and dibenzofurans (PCDD/Fs). Prog. Energy Combust. Sci. 35, 245–274. https://doi.org/10.1016/J.PECS.2008.12.001

Altwicker, E.R., Konduri, R.K.N.V., Lin, C., Milligan, M.S., 1992. Rapid formation of polychlorinated dioxins/furans in the post combustion region during heterogeneous combustion. Chemosphere 25, 1935–1944. https://doi.org/10.1016/0045-6535(92)90032-M

Altwicker, E.R., Milligan, M.S., 1993. Formation of dioxins: Competing rates between chemically similar precursors and de novo reactions. Chemosphere 27, 301–307. https://doi.org/10.1016/0045-6535(93)90306-P

Arvaniti, O.S., Andersen, H.R., Thomaidis, N.S., Stasinakis, A.S., 2014. Sorption of Perfluorinated Compounds onto different types of sewage sludge and assessment of its importance during wastewater treatment. Chemosphere 111, 405–411. https://doi.org/10.1016/j.chemosphere.2014.03.087

Arvaniti, O.S., Ventouri, E.I., Stasinakis, A.S., Thomaidis, N.S., 2012. Occurrence of different classes of perfluorinated compounds in Greek wastewater treatment plants and determination of their solid-water distribution coefficients. J. Hazard. Mater. 239–240, 24–31. https://doi.org/10.1016/j.jhazmat.2012.02.015

Aurell, J., 2008. Effects of Varying Combustion Conditions on PCDD/F Formation. Umeå University, Umeå, Sweden.

Banzhaf, S., Hebig, K.H., 2016. Use of column experiments to investigate the fate of organic micropollutants - A review. Hydrol. Earth Syst. Sci. 20, 3719–3737. https://doi.org/10.5194/HESS-20-3719-2016

Barton, R., Maly, P., Clark, W., Seeker, W., 1988. Prediction of the fate of toxic metals in waste incinerators, in: ASME 13th National Waste Processing Conference.

Barton, R.G., Maly, P.M., Clark, W.D., Seeker, W.R., 1988. Prediction of the fate of toxic metals in waste incinerators, in: ASME 13th National Waste Processing Conference. pp. 379–386.

Bhavsar, S.P., Fowler, C., Day, S., Petro, S., Gandhi, N., Gewurtz, S.B., Hao, C., Zhao, X., Drouillard, K.G., Morse, D., 2016. High levels, partitioning and fish consumption based water guidelines of perfluoroalkyl acids downstream of a former firefighting training facility in Canada. Environ. Int. 94, 415–423. https://doi.org/10.1016/J.ENVINT.2016.05.023

Blaine, A.C., Rich, C.D., Hundal, L.S., Lau, C., Mills, M.A., Harris, K.M., Higgins, C.P., 2013. Uptake of perfluoroalkyl acids into edible crops via land applied biosolids: Field and greenhouse studies. Environ. Sci. Technol. 47, 14062–14069. https://doi.org/10.1021/es403094q

Bolan, N.S., Hedley, M.J., 1990. Dissolution of phosphate rocks in soils. 2. Effect of pH on the dissolution and plant availability of phosphate rock in soil with pH dependent charge. Fertil. Res. 24, 125–134. https://doi.org/10.1007/BF01073580

Bosshard, P.P., Bachofen, R., Brandl, H., 1996. Metal leaching of fly ash from municipal waste incineration by Aspergillus niger. Environ. Sci. Technol. 30, 3066–3070. https://doi.org/10.1021/es960151v

Bowman, R.A., Cole, C. V., 1978. Transformations of organic phosphorus substrates in soils as evaluated by NaHCO3extraction. Soil Sci. 125, 49–54. https://doi.org/10.1097/00010694-197801000-00008

Bray, R.H., Kurtz, L.T., 1945. Determination of total, organic, and available forms of phosphorus in soils. Soil Sci. 59, 39–45. https://doi.org/10.1097/00010694-194501000-00006

Buck, R.C., Franklin, J., Berger, U., Conder, J.M., Cousins, I.T., Voogt, P. De, Jensen, A.A., Kannan, K., Mabury, S.A., van Leeuwen, S.P.J., 2011. Perfluoroalkyl and polyfluoroalkyl substances in the environment: Terminology, classification, and origins. Integr. Environ. Assess. Manag. 7, 513–541. https://doi.org/10.1002/IEAM.258

Cade-Menun, B.J., Preston, C.M., 1996. A comparison of soil extraction procedures for 31P NMR spectroscopy. Soil Sci. 161, 770–785. https://doi.org/10.1097/00010694-199611000-00006

Caillat, S., Vakkilainen, E., 2013. Large-scale biomass combustion plants: an overview. Biomass Combust. Sci. Technol. Eng. 189–224. https://doi.org/10.1533/9780857097439.3.189

Canadian Municipal Water Consortium, 2015. Canadian Municipal Water Priorities Report- Towards Sustainable and Resilient Water Management.

Chang, S., Jackson, M., 1957. Fractionation of soil phosphorus. Soil Sci. 84, 133–144.

Chen, M., Ma, L.Q., 2001. Taxonomic and Geographic Distribution of Total Phosphorus in Florida Surface Soils. Soil Sci. Soc. Am. J. 65, 1539–1547. https://doi.org/10.2136/sssaj2001.6551539x

Clarke, B.O., Smith, S.R., 2011. Review of 'emerging' organic contaminants in biosolids and assessment of international research priorities for the agricultural use of biosolids. Environ. Int. 37, 226–247. https://doi.org/10.1016/J.ENVINT.2010.06.004

Condron, L.M., Frossard, E., Tiessen, H., Newmans, R.H., Stewart, J.W.B., 1990. Chemical nature of organic phosphorus in cultivated and uncultivated soils under different environmental conditions. J. Soil Sci. 41, 41–50. https://doi.org/10.1111/j.1365-2389.1990.tb00043.x

Council, N.R., 2000. Waste incineration and public health. National Academies Press.

Cross, A.F., Schlesinger, W.H., 1995. A literature review and evaluation of the. Hedley fractionation: Applications to the biogeochemical cycle of soil phosphorus in natural ecosystems. Geoderma 64, 197–214. https://doi.org/10.1016/0016-7061(94)00023-4

Crownover, E., Oberle, D., Kluger, M., Heron, G., 2019. Perfluoroalkyl and polyfluoroalkyl substances thermal desorption evaluation. Remediat. J. 29, 77–81. https://doi.org/10.1002/REM.21623

del Castilho, P., Chardon, W.J., Salomons, W., 1993. Influence of Cattle-Manure Slurry Application on the Solubility of Cadmium, Copper, and Zinc in a Manured Acidic, Loamy-Sand Soil. J. Environ. Qual. 22, 689–697. https://doi.org/10.2134/jeq1993.00472425002200040009x

Deng, J., Feng, X., Qiu, X., 2009. Extraction of heavy metal from sewage sludge using ultrasound-assisted nitric acid. Chem. Eng. J. 152, 177–182. https://doi.org/10.1016/j.cej.2009.04.031

Deng, W., Jianhua, Y., Xiaodong, L.I., Fei, W., Yong, C., Shengyong, L.U., 2009. Emission characteristics of dioxins, furans and polycyclic aromatic hydrocarbons during fluidized-bed combustion of sewage sludge. J. Environ. Sci. 21, 1747–1752. https://doi.org/10.1016/S1001-0742(08)62483-3

Dickson, L.C., Lenoir, D., Hutzinger, O., 1992. Quantitative comparison of de novo and precursor formation of polychlorinated dibenzo-p-dioxins under simulated municipal solid waste incinerator postcombustion conditions. Environ. Sci. Technol. 26, 1822–1828. https://doi.org/10.1021/ES00033A017

Donatello, S., Cheeseman, C.R., 2013a. Recycling and recovery routes for incinerated sewage sludge ash (ISSA): A review. Waste Manag. https://doi.org/10.1016/j.wasman.2013.05.024

Donatello, S., Cheeseman, C.R., 2013b. Recycling and recovery routes for incinerated sewage sludge ash (ISSA): A review. Waste Manag. 33, 2328–2340. https://doi.org/10.1016/j.wasman.2013.05.024

Duchesne, A.L., Brown, J.K., Patch, D.J., Major, D., Weber, K.P., Gerhard, J.I., 2020. Remediation of PFAS-Contaminated Soil and Granular Activated Carbon by Smoldering Combustion. Environ. Sci. Technol. 54, 12631–12640. https://doi.org/10.1021/acs.est.0c03058

Environment and Climate Change Canada, 2017. Canadian Environmental Protection

Act, 1999 Federal Environmental Quality Guidelines Perfluorooctane Sulfonate (PFOS).

Fang, L., Li, J. shan, Guo, M.Z., Cheeseman, C.R., Tsang, D.C.W., Donatello, S., Poon, C.S., 2018. Phosphorus recovery and leaching of trace elements from incinerated sewage sludge ash (ISSA). Chemosphere 193, 278–287. https://doi.org/10.1016/j.chemosphere.2017.11.023

Fang, L., Wang, Q., Li, J.-S., Poon, C.S., Cheeseman, C.R., Donatello, S., Tsang, D.C.W., 2020. Feasibility of wet-extraction of phosphorus from incinerated sewage sludge ash (ISSA) for phosphate fertilizer production: A critical review. Crit. Rev. Environ. Sci. Technol. 1–33. https://doi.org/10.1080/10643389.2020.1740545

Fang, W., Wei, Y., Liu, J., 2016. Comparative characterization of sewage sludge compost and soil: Heavy metal leaching characteristics. J. Hazard. Mater. 310, 1–10. https://doi.org/10.1016/j.jhazmat.2016.02.025

Feng, C., Cheng, M., Gao, X., Qiao, Y., Xu, M., 2020. Occurrence forms and leachability of inorganic species in ash residues from self-sustaining smouldering combustion of sewage sludge. Proc. Combust. Inst. 000, 1–8. https://doi.org/10.1016/j.proci.2020.06.008

Feng, C., Huang, J., Yang, C., Li, C., Luo, X., Gao, X., Qiao, Y., 2021. Smouldering combustion of sewage sludge: Volumetric scale-up, product characterization, and economic analysis. Fuel 305, 121485. https://doi.org/10.1016/J.FUEL.2021.121485

Fiedler, H., 2003. Dioxins and Furans (PCDD/PCDF), in: Persistent Organic Pollutants. Springer-Verlag, pp. 123–201. https://doi.org/10.1007/10751132_6

Franz, M., 2008. Phosphate fertilizer from sewage sludge ash (SSA). Waste Manag. 28, 1809–1818. https://doi.org/10.1016/j.wasman.2007.08.011

Fullana, A., Conesa, J.A., Font, R., Sidhu, S., 2004. Formation and destruction of chlorinated pollutants during sewage sludge incineration. Environ. Sci. Technol. 38, 2953–2958. https://doi.org/10.1021/es034896u

Fytili, D., Zabaniotou, A., 2008. Utilization of sewage sludge in EU application of old and new methods--A review. Renew. Sustain. Energy Rev. 12, 116–140.

Galang, M.A., Markewitz, D., Morris, L.A., 2010. Soil phosphorus transformations under forest burning and laboratory heat treatments. Geoderma 155, 401–408. https://doi.org/10.1016/J.GEODERMA.2009.12.026

Gallen, C., Drage, D., Kaserzon, S., Baduel, C., Gallen, M., Banks, A., Broomhall, S., Mueller, J.F., 2016. Occurrence and distribution of brominated flame retardants and perfluoroalkyl substances in Australian landfill leachate and biosolids. J. Hazard. Mater. 312, 55–64. https://doi.org/10.1016/J.JHAZMAT.2016.03.031

Garrabrants, A.C., Kosson, D.S., DeLapp, R., van der Sloot, H.A., 2014. Effect of coal combustion fly ash use in concrete on the mass transport release of constituents of potential concern. Chemosphere 103, 131–139. https://doi.org/10.1016/J.CHEMOSPHERE.2013.11.048

Gerdes, P., Kunst, S., 1998. Bioavailability of phosphorus as a tool for efficient P reduction schemes, in: Water Science and Technology. Elsevier Sci Ltd, pp. 241–247. https://doi.org/10.1016/S0273-1223(98)00076-6

Gerhard, J.., Grant, G.P., Torero, J.L., 2020. STAR: A Uniquely Sustainable In Situ and Ex Situ Remediation Process, in: Sustainable Remediation of Contaminated Soil and Groundwater: Materials, Processes, and Assessment. Butterworth-Heinemann, pp. 221–245.

Gheju, M., Pode, R., Manea, F., 2011. Comparative heavy metal chemical extraction from anaerobically digested biosolids. Hydrometallurgy 108, 115–121. https://doi.org/10.1016/j.hydromet.2011.03.006

Ghisi, R., Vamerali, T., Manzetti, S., 2019. Accumulation of perfluorinated alkyl substances (PFAS) in agricultural plants: A review. Environ. Res. 169, 326–341. https://doi.org/10.1016/J.ENVRES.2018.10.023

Gianfelice, G., Della Zassa, M., Biasin, A., Canu, P., 2019. Onset and propagation of smouldering in pine bark controlled by addition of inert solids. Renew. Energy 132, 596–614. https://doi.org/10.1016/J.RENENE.2018.08.028

Gikonyo, E.W., Zaharah, A.R., Hanafi, M.M., Anuar, A.R., 2011. Degree of phosphorus saturation and soil phosphorus thresholds in an ultisol amended with triple superphosphate and phosphate rocks. ScientificWorldJournal. 11, 1421–1441. https://doi.org/10.1100/tsw.2011.131

Golterman, H.L., 1996. Fractionation of sediment phosphate with chelating compounds: A simplification, and comparison with other methods. Hydrobiologia. https://doi.org/10.1007/BF00013687

Gómez-Canela, C., Barth, J.A.C., Lacorte, S., 2012. Occurrence and fate of perfluorinated compounds in sewage sludge from Spain and Germany. Environ. Sci. Pollut. Res. 19, 4109–4119. https://doi.org/10.1007/s11356-012-1078-7

González Medeiros, J.J., Pérez Cid, B., Fernández Gómez, E., 2005. Analytical phosphorus fractionation in sewage sludge and sediment samples. Anal. Bioanal. Chem. 381, 873–878. https://doi.org/10.1007/s00216-004-2989-z

Gorazda, K., Tarko, B., Wzorek, Z., Kominko, H., Nowak, A.K., Kulczycka, J., Henclik, A., Smol, M., 2017. Fertilisers production from ashes after sewage sludge combustion – A strategy towards sustainable development. Environ. Res. 154, 171–180. https://doi.org/10.1016/j.envres.2017.01.002

Grant, G.P., Major, D., Scholes, G.C., Horst, J., Hill, S., Klemmer, M.R., Couch, J.N., 2016. Smoldering Combustion (STAR) for the Treatment of Contaminated Soils: Examining Limitations and Defining Success. Remediat. J. 26, 27–51. https://doi.org/10.1002/rem.21468

Griffin, R.D., 1986. A new theory of dioxin formation in municipal solid waste combustion. Chemosphere 15, 1987–1990. https://doi.org/10.1016/0045-6535(86)90498-4

Guggenberger, G., Christensen, B.T., Rubaek, G., Zech, W., 1996. Land-use and fertilization effects on P forms in two European soils: resin extraction and 31P-NMR analysis. Eur. J. Soil Sci. 47, 605–614. https://doi.org/10.1111/j.1365-2389.1996.tb01859.x

Gullett, B.K., Touati, A., 2003. PCDD/F emissions from forest fire simulations. Atmos. Environ. 37, 803–813. https://doi.org/10.1016/S1352-2310(02)00951-2

Guo, R., Zhou, Q., Cai, Y., Jiang, G., 2008. Determination of perfluorooctanesulfonate and perfluorooctanoic acid in sewage sludge samples using liquid chromatography/quadrupole time-of-flight mass spectrometry. Talanta 75, 1394–1399. https://doi.org/10.1016/j.talanta.2008.01.052

Hadden, R., Rein, G., 2011. Burning and Water Suppression of Smoldering Coal Fires in Small-Scale Laboratory Experiments. Coal Peat Fires A Glob. Perspect. 317–326. https://doi.org/10.1016/B978-0-444-52858-2.00018-9

Hamid, H., Li, L.Y., 2018. Fate of perfluorooctanoic acid (PFOA) in sewage sludge during microwave-assisted persulfate oxidation treatment. Environ. Sci. Pollut. Res. 25, 10126–10134. https://doi.org/10.1007/s11356-018-1576-3

Han, J., Xu, M., Yao, H., Furuuchi, M., Sakano, T., Kanchanapiya, P., Kanaoka, C., 2006. Partition of heavy and alkali metals during sewage sludge incineration. Energy and Fuels 20, 583–590. https://doi.org/10.1021/ef0501602

Han, X., Wang, F., Zhou, B., Chen, H., Yuan, R., Liu, S., Zhou, X., Gao, L., Lu, Y., Zhang, R., 2019. Phosphorus complexation of sewage sludge during thermal hydrolysis with different reaction temperature and reaction time by P K-edge XANES and 31P NMR. Sci. Total Environ. 688, 1–9. https://doi.org/10.1016/j.scitotenv.2019.06.017

Hartikainen, H., Yli-Halla, M., 1996. Solubility of soil phosphorus as influenced by urea. Zeitschrift für Pflanzenernährung und Bodenkd. 159, 327–332. https://doi.org/10.1002/jpln.1996.3581590403

Hartmann, T., Wollmann, I., You, Y., Müller, T., 2019. Sensitivity of Three Phosphate Extraction Methods to the Application of Phosphate Species Differing in Immediate Plant Availability. Agronomy 9, 29. https://doi.org/10.3390/agronomy9010029

Hedley, M.J., Stewart, J.W.B., Chauhan, B.S., 1982. Changes in Inorganic and Organic Soil Phosphorus Fractions Induced by Cultivation Practices and by Laboratory Incubations. Soil Sci. Soc. Am. J. 46, 970–976. https://doi.org/10.2136/sssaj1982.03615995004600050017x

Higgins, C.P., Field, J.A., Criddle, C.S., Luthy, R.G., 2005. Quantitative determination of perfluorochemicals in sediments and domestic sludge. Environ. Sci. Technol. 39, 3946–3956. https://doi.org/10.1021/es048245p

Hossain, M.K., Strezov Vladimir, V., Chan, K.Y., Ziolkowski, A., Nelson, P.F., 2011. Influence of pyrolysis temperature on production and nutrient properties of wastewater sludge biochar. J. Environ. Manage. 92, 223–228. https://doi.org/10.1016/j.jenvman.2010.09.008

Houtz, E., Wang, M., Park, J.S., 2018. Identification and Fate of Aqueous Film Forming Foam Derived Per- and Polyfluoroalkyl Substances in a Wastewater Treatment Plant. Environ. Sci. Technol. 52, 13212–13221. https://doi.org/10.1021/acs.est.8b04028

Houtz, E.F., Sutton, R., Park, J.S., Sedlak, M., 2016. Poly- and perfluoroalkyl substances in wastewater: Significance of unknown precursors, manufacturing shifts, and likely AFFF impacts. Water Res. 95, 142–149. https://doi.org/10.1016/J.WATRES.2016.02.055

Huang, H., Buekens, A., 1995. On the mechanisms of dioxin formation in combustion processes. Chemosphere 31, 4099–4117. https://doi.org/10.1016/0045-6535(95)80011-9

Huang, X.-L., Chen, Y., Shenker, M., 2008. Chemical Fractionation of Phosphorus in Stabilized Biosolids. J. Environ. Qual. 37, 1949–1958. https://doi.org/10.2134/jeq2007.0220

Hutchinson, S., Rieck, T., Wu, X., Hutchinson, S., Rieck, T., Wu, X., 2020. Advanced PFAS precursor digestion methods for biosolids. Environ. Chem. 17, 558–567. https://doi.org/10.1071/EN20008

Iyamuremye, F., Dick, R.P., Baham, J., 1996. Organic amendments and phosphorus dynamics: II. distribution of soil phosphorus fractions. Soil Sci. 161, 436–443. https://doi.org/10.1097/00010694-199607000-00003

Jalali, M., Ostovarzadeh, H., 2009. Evaluation of phosphorus leaching from contaminated calcareous soils due to the application of sheep manure and ethylenediamine tetraacetic acid. Environ. Earth Sci. 59, 441–448. https://doi.org/10.1007/s12665-009-0042-4

Japenga, J., Dalenberg, J.W., Wiersma, D., Scheltens, S.D., Hesterberg, D., Salomons, W., 2006. Effect of Liquid Animal Manure Application on the Solubilization of Heavy Metals from Soil. http://dx.doi.org/10.1080/03067319208026994 46, 25–39.

https://doi.org/10.1080/03067319208026994

Jiang, L., Yin, C., Liang, B., 2016. Effects of environmental pH on phosphorus leaching characteristics of phosphate waste rock deposited within Xiangxi River watershed. Chinese J. Environ. Eng. 10, 2674–2680. https://doi.org/10.12030/j.cjee.201511004

Jiang, L.G., Liang, B., Xue, Q., Yin, C.W., 2016. Characterization of phosphorus leaching from phosphate waste rock in the Xiangxi River watershed, Three Gorges Reservoir, China. Chemosphere 150, 130–138. https://doi.org/10.1016/j.chemosphere.2016.02.008

Jiwan, S., Ajah, K.S., 2011. Effects of Heavy Metals on Soil, Plants, Human Health and Aquatic Life. Int. J. Res. Chem. Environ. 1, 15–21.

Johnson, A.H., Frizano, J., Vann, D.R., 2003. Review: Biogeochemical implications of labile phosphorus in forest soils determined by the Hedley fractionation procedure. Oecologia 135, 487–499. https://doi.org/10.1007/s00442-002-1164-5

Johnson, G.R., 2022. PFAS in soil and groundwater following historical land application of biosolids. Water Res. 211, 118035. https://doi.org/10.1016/J.WATRES.2021.118035

Johnston, A., Steen, I., 2002. Understanding phosphorus and its use in agriculture. European Fertilizer Manufacturers Association, Brussels.

Johnston, A.E., Poulton, P.R., Fixen, P.E., Curtin, D., 2014. Phosphorus: Its Efficient Use in Agriculture. Adv. Agron. 123, 177–228. https://doi.org/10.1016/B978-0-12-420225-2.00005-4

Jones, K.C., Sewart, A.P., 1997. Dioxins and furans in sewage sludges: A review of their occurrence and sources in sludge and of their environmental fate, behavior, and significance in sludge-amended agricultural systems. Crit. Rev. Environ. Sci. Technol. https://doi.org/10.1080/10643389709388497

Kabata-Pendias, A., 2000. Trace Elements in Soils and Plants. Trace Elem. Soils Plants. https://doi.org/10.1201/9781420039900

Karlfeldt Fedje, K., Ekberg, C., Skarnemark, G., Steenari, B.-M., 2010. Removal of hazardous metals from MSW fly ash—An evaluation of ash leaching methods. J. Hazard. Mater. 173, 310–317. https://doi.org/10.1016/j.jhazmat.2009.08.094

Ke, S., Jianhua, Y., Xiaodong, L., Shengyong, L., Yinglei, W., Muxing, F., 2010. Inhibition of de novo synthesis of PCDD/Fs by SO2 in a model system. Chemosphere 78, 1230–1235. https://doi.org/10.1016/J.CHEMOSPHERE.2009.12.043

Keller, C., McGrath, S.P., Dunham, S.J., 2002. Trace Metal Leaching through a Soil–Grassland System after Sewage Sludge Application. J. Environ. Qual. 31, 1550–

1560. https://doi.org/10.2134/JEQ2002.1550A

Khiari, B., Marias, F., Zagrouba, F., Vaxelaire, J., 2004. Analytical study of the pyrolysis process in a wastewater treatment pilot station. Desalination 167, 39–47. https://doi.org/10.1016/j.desal.2004.06.111

Kijo-Kleczkowska, A., Środa, K., Kosowska-Golachowska, M., Musiał, T., Wolski, K., 2016. Experimental research of sewage sludge with coal and biomass co-combustion, in pellet form. Waste Manag. 53, 165–181. https://doi.org/10.1016/j.wasman.2016.04.021

Kim, J.H., Ok, Y.S., Choi, G.H., Park, B.J., 2015. Residual perfluorochemicals in the biochar from sewage sludge. Chemosphere 134, 435–437. https://doi.org/10.1016/j.chemosphere.2015.05.012

Kinsman, L.L., 2015. Smouldering Remediation: Transient Effects of Front Propogation. Western University.

Kissa, E., 2001. Fluorinated surfactants and repellents, Vol. 97. ed. CRC Press.

Kosson, D.S., Garrabrants, A., Thorneloe, S., Fagnant, D., Helms, G., Connolly, K., Rodgers, M., 2017. Leaching Environmental Assessment Framework (LEAF) How-To Guide: Understanding the LEAF Approach and How and When to Use It. Nashville, TN.

Kosson, D.S., Garrabrants, A.C., DeLapp, R., van der Sloot, H.A., 2014. PH-dependent leaching of constituents of potential concern from concrete materials containing coal combustion fly ash. Chemosphere 103, 140–147. https://doi.org/10.1016/j.chemosphere.2013.11.049

Krüger, O., Adam, C., 2014. Recovery potential of German sewage sludge ash. Waste Manag. 45, 400–406. https://doi.org/10.1016/j.wasman.2015.01.025

Kumaragamage, D., Akinremi, O.O., Flaten, D., Heard, J., 2011. Agronomic and environmental soil test phosphorus in manured and non-manured Manitoba soils. https://doi.org/10.4141/S06-030 87, 73–83. https://doi.org/10.4141/S06-030

Kunacheva, C., Tanaka, S., Fujii, S., Boontanon, S.K., Musirat, C., Wongwattana, T., Shivakoti, B.R., 2011. Mass flows of perfluorinated compounds (PFCs) in central wastewater treatment plants of industrial zones in Thailand. Chemosphere 83, 737–744. https://doi.org/10.1016/J.CHEMOSPHERE.2011.02.059

Kundu, S., Patel, S., Halder, P., Patel, T., Hedayati Marzbali, M., Pramanik, B.K., Paz-Ferreiro, J., De Figueiredo, C.C., Bergmann, D., Surapaneni, A., Megharaj, M., Shah, K., 2021. Removal of PFASs from biosolids using a semi-pilot scale pyrolysis reactor and the application of biosolids derived biochar for the removal of PFASs from contaminated water. Environ. Sci. Water Res. Technol. 7, 638–649. https://doi.org/10.1039/d0ew00763c

Łach, M., Mikuła, J., Hebda, M., 2016. Thermal analysis of the by-products of waste combustion. J. Therm. Anal. Calorim. 125, 1035–1045. https://doi.org/10.1007/S10973-016-5512-9/TABLES/7

Lahann, R.W., 1976. Molybdenum hazard in land disposal of sewage sludge. Water, Air, Soil Pollut. 1976 61 6, 3–8. https://doi.org/10.1007/BF00158710

Lakshminarasimman, N., Gewurtz, S.B., Parker, W.J., Smyth, S.A., 2021. Removal and formation of perfluoroalkyl substances in Canadian sludge treatment systems – A mass balance approach. Sci. Total Environ. 754. https://doi.org/10.1016/j.scitotenv.2020.142431

Lavric, E.D., Konnov, A.A., De Ruyck, J., 2004. Dioxin levels in wood combustion—a review. Biomass and Bioenergy 26, 115–145. https://doi.org/10.1016/S0961-9534(03)00104-1

Lenka, S.P., Kah, M., Padhye, L.P., 2021. A review of the occurrence, transformation, and removal of poly- and perfluoroalkyl substances (PFAS) in wastewater treatment plants. Water Res. 199, 117187. https://doi.org/10.1016/J.WATRES.2021.117187

Li, R., Zhang, Z., Li, Y., Teng, W., Wang, W., Yang, T., 2015. Transformation of apatite phosphorus and non-apatite inorganic phosphorus during incineration of sewage sludge. Chemosphere 141, 57–61. https://doi.org/10.1016/j.chemosphere.2015.05.094

Li, X., Zhang, D., Yang, T., Bryden, W., 2016. Phosphorus Bioavailability: A Key Aspect for Conserving this Critical Animal Feed Resource with Reference to Broiler Nutrition. Agriculture 6, 25. https://doi.org/10.3390/agriculture6020025

Lin, L.F., Lee, W.J., Li, H.W., Wang, M.S., Chang-Chien, G.P., 2007. Characterization and inventory of PCDD/F emissions from coal-fired power plants and other sources in Taiwan. Chemosphere 68, 1642–1649. https://doi.org/10.1016/J.CHEMOSPHERE.2007.04.002

Lindstrom, A.B., Strynar, M.J., Libelo, E.L., 2011. Polyfluorinated compounds: Past, present, and future. Environ. Sci. Technol. 45, 7954–7961. https://doi.org/10.1021/es2011622

Linquist, B.A., Singleton, P.W., Cassman, K.G., 1997. Inorganic and organic phosphorus dynamics during a build-up and decline of available phosphorus in an ultisol. Soil Sci. 162, 254–264. https://doi.org/10.1097/00010694-199704000-00003

London, C. of, 2019. Greenway Wastewater Treatment Centre 2018 Annual Report.

Maguire, R.O., Sims, J.T., 2002. Soil Testing to Predict Phosphorus Leaching. J. Environ. Qual. 31, 1601–1609. https://doi.org/10.2134/jeq2002.1601

Mahinpey, N., Gomez, A., 2016. Review of gasification fundamentals and new findings:

Reactors, feedstock, and kinetic studies. Chem. Eng. Sci. 148, 14–31. https://doi.org/10.1016/J.CES.2016.03.037

Mahinroosta, R., Senevirathna, L., 2020. A review of the emerging treatment technologies for PFAS contaminated soils. J. Environ. Manage. https://doi.org/10.1016/j.jenvman.2019.109896

Marani, D., Braguglia, C.M., Mininni, G., Maccioni, F., 2003. Behaviour of Cd, Cr, Mn, Ni, Pb, and Zn in sewage sludge incineration by fluidised bed furnace. Waste Manag. 23, 117–124.

Mattenberger, H., Fraissler, G., Brunner, T., Herk, P., Hermann, L., Obernberger, I., 2008. Sewage sludge ash to phosphorus fertiliser: Variables influencing heavy metal removal during thermochemical treatment. Waste Manag. 28, 2709–2722. https://doi.org/10.1016/j.wasman.2008.01.005

Mayer, B.K., Baker, L.A., Boyer, T.H., Drechsel, P., Gifford, M., Hanjra, M.A., Parameswaran, P., Stoltzfus, J., Westerhoff, P., Rittmann, B.E., 2016. Total Value of Phosphorus Recovery. Environ. Sci. Technol. 50, 6606–6620. https://doi.org/10.1021/acs.est.6b01239

McBride, M.B., 1995. Toxic Metal Accumulation from Agricultural Use of Sludge: Are USEPA Regulations Protective? J. Environ. Qual. 24, 5–18. https://doi.org/10.2134/JEQ1995.00472425002400010002X

McKay, G., 2002. Dioxin characterisation, formation and minimisation during municipal solid waste (MSW) incineration: Review. Chem. Eng. J. 86, 343–368. https://doi.org/10.1016/S1385-8947(01)00228-5

Menon, R.G., Chien, S.H., Hammond, L.L., Henao, J., 1989. Modified techniques for preparing paper strips for the new Pi soil test for phosphorus. Fertil. Res. 19, 85–91. https://doi.org/10.1007/BF01054679

Milinovic, J., Lacorte, S., Rigol, A., Vidal, M., 2016. Sorption of perfluoroalkyl substances in sewage sludge. Environ. Sci. Pollut. Res. 23, 8339–8348. https://doi.org/10.1007/s11356-015-6019-9

Miralles-Marco, A., Harrad, S., 2015. Perfluorooctane sulfonate: A review of human exposure, biomonitoring and the environmental forensics utility of its chirality and isomer distribution. Environ. Int. 77, 148–159. https://doi.org/10.1016/J.ENVINT.2015.02.002

Möller, H.B., Jensen, H.S., Tobiasen, L., Hansen, M.N., 2007. Heavy metal and phosphorus content of fractions from manure treatment and incineration. Environ. Technol. 28, 1403–1418. https://doi.org/10.1080/09593332808618900

Moodie, D., Coggan, T., Berry, K., Kolobaric, A., Fernandes, M., Lee, E., Reichman, S., Nugegoda, D., Clarke, B.O., 2021. Legacy and emerging per- and polyfluoroalkyl

substances (PFASs) in Australian biosolids. Chemosphere 270, 129143. https://doi.org/10.1016/J.CHEMOSPHERE.2020.129143

Mulchandani, A., Westerhoff, P., 2016. Recovery opportunities for metals and energy from sewage sludges. Bioresour. Technol. https://doi.org/10.1016/j.biortech.2016.03.075

Müller-Stöver, D.S., Jakobsen, I., Grønlund, M., Rolsted, M.M.M., Magid, J., Hauggaard-Nielsen, H., 2018. Phosphorus bioavailability in ash from straw and sewage sludge processed by low-temperature biomass gasification. Soil Use Manag. 34, 9–17. https://doi.org/10.1111/SUM.12399

Nanzer, S., Oberson, A., Huthwelker, T., Eggenberger, U., Frossard, E., 2014. The molecular environment of phosphorus in sewage sludge ash: implications for bioavailability. J. Environ. Qual. 43, 1050–1060. https://doi.org/10.2134/JEQ2013.05.0202

NATO/CCMS, 1988. International Toxicity Equivalency Factor (I-TEF) Method of Risk Assessment for Complex Mixtures of Dioxins and Related Compounds, Report No. 178.

Neczaj, E., Grosser, A., 2018. Circular Economy in Wastewater Treatment Plant–Challenges and Barriers. Proceedings 2, 614. https://doi.org/10.3390/proceedings2110614

Neyroud, J.-A., Lischer, P., 2003. Do different methods used to estimate soil phosphorus availability across Europe give comparable results? J. Plant Nutr. Soil Sci. 166, 422–431. https://doi.org/10.1002/jpln.200321152

Nowak, B., Aschenbrenner, P., Winter, F., 2013. Heavy metal removal from sewage sludge ash and municipal solid waste fly ash - A comparison. Fuel Process. Technol. 105, 195–201. https://doi.org/10.1016/j.fuproc.2011.06.027

Ohlemiller, T.J., 1985. Modeling of smoldering combustion propagation. Prog. Energy Combust. Sci. 11, 277–310. https://doi.org/10.1016/0360-1285(85)90004-8

Olie, K., Addink, R., Schoonenboom, M., 2011. Metals as Catalysts during the Formation and Decomposition of Chlorinated Dioxins and Furans in Incineration Processes. https://doi.org/10.1080/10473289.1998.10463656 48, 101–105. https://doi.org/10.1080/10473289.1998.10463656

Olsen, S.R., 1954. Estimation of available phosphorus in soils by extraction with sodium bicarbonate. US Department of Agriculture.

Olsen, S.R., Sommers, L.E., 1982. Phosphorus, in: Methods of Soil Analysis. Madison, WI., pp. 403–430.

Ooi, T.C., Lu, L., 2011. Formation and mitigation of PCDD/Fs in iron ore sintering.

Chemosphere 85, 291–299. https://doi.org/10.1016/J.CHEMOSPHERE.2011.08.020

Pan, Y., Shi, Y., Wang, J., Cai, Y., 2010. Evaluation of perfluorinated compounds in seven wastewater treatment plants in Beijing urban areas. Sci. China Chem. 2011 543 54, 552–558. https://doi.org/10.1007/S11426-010-4093-X

Pansu, M., Gautheyrou, J., 2007. Handbook of soil analysis: mineralogical, organic and inorganic methods. Springer Science & Business Media.

Pape, A., Switzer, C., McCosh, N., Knapp, C.W., 2015. Impacts of thermal and smouldering remediation on plant growth and soil ecology. Geoderma 243–244, 1–9. https://doi.org/10.1016/J.GEODERMA.2014.12.004

Petzet, S., Peplinski, B., Cornel, P., 2012. On wet chemical phosphorus recovery from sewage sludge ash by acidic or alkaline leaching and an optimized combination of both. Water Res. 46, 3769–3780. https://doi.org/10.1016/j.watres.2012.03.068

Pichtel, J., Pichtel, T.M., 1997. Comparison of solvents for ex situ removal of chromium and lead from contaminated soil. Environ. Eng. Sci. 14, 97–104. https://doi.org/10.1089/ees.1997.14.97

Pironi, P., Switzer, C., Gerhard, J.I., Rein, G., Torero, J.L., 2011. Self-sustaining smoldering combustion for NAPL remediation: Laboratory evaluation of process sensitivity to key parameters. Environ. Sci. Technol. 45, 2980–2986. https://doi.org/10.1021/ES102969Z/SUPPL_FILE/ES102969Z_SI_001.PDF

Pironi, P., Switzer, C., Rein, G., Fuentes, A., Gerhard, J.I., Torero, J.L., 2009. Small-scale forward smouldering experiments for remediation of coal tar in inert media. Proc. Combust. Inst. 32 II, 1957–1964. https://doi.org/10.1016/j.proci.2008.06.184

Pontius, F., 2019. Regulation of Perfluorooctanoic Acid (PFOA) and Perfluorooctane Sulfonic Acid (PFOS) in Drinking Water: A Comprehensive Review. Water 2019, Vol. 11, Page 2003 11, 2003. https://doi.org/10.3390/W11102003

Pudasainee, D., Seo, Y.C., Kim, J.H., Jang, H.N., 2013. Fate and behavior of selected heavy metals with mercury mass distribution in a fluidized bed sewage sludge incinerator. J. Mater. Cycles Waste Manag. 15, 202–209. https://doi.org/10.1007/s10163-013-0115-z

Qian, T.T., Jiang, H., 2014. Migration of phosphorus in sewage sludge during different thermal treatment processes. ACS Sustain. Chem. Eng. 2, 1411–1419. https://doi.org/10.1021/sc400476j

Rashwan, T., 2020. Sustainable Smouldering for Waste-to-Energy: Scale, Heat Losses, and Energy Efficiency. Electron. Thesis Diss. Repos.

Rashwan, T.L., Fournie, T., Torero, J.L., Grant, G.P., Gerhard, J.I., 2021a. Scaling up self-sustained smouldering of sewage sludge for waste-to-energy. Waste Manag.

135, 298–308. https://doi.org/10.1016/J.WASMAN.2021.09.004

Rashwan, T.L., Gerhard, J.I., Grant, G.P., 2016. Application of self-sustaining smouldering combustion for the destruction of wastewater biosolids. Waste Manag. 50, 201–212. https://doi.org/10.1016/j.wasman.2016.01.037

Rashwan, T.L., Torero, J.L., Gerhard, J.I., 2021b. The improved energy efficiency of applied smouldering systems with increasing scale. Int. J. Heat Mass Transf. 177, 121548. https://doi.org/10.1016/J.IJHEATMASSTRANSFER.2021.121548

Rashwan, T.L., Torero, J.L., Gerhard, J.I., 2021c. Heat losses in a smouldering system: The key role of non-uniform air flux. Combust. Flame 227, 309–321. https://doi.org/10.1016/j.combustflame.2020.12.050

Rashwan, T.L., Torero, J.L., Gerhard, J.I., 2021d. Heat losses in applied smouldering systems: Sensitivity analysis via analytical modelling. Int. J. Heat Mass Transf. 172, 121150. https://doi.org/10.1016/j.ijheatmasstransfer.2021.121150

Rein, G., 2016. Smoldering Combustion, in: Hurley, M.J., Gottuk, D.T., Hall Jr., J.R., Harada, K., Kuligowski, E.D., Puchovsky, M., Torero, J.L., Watts Jr., J.M., Wieczorek, C.J. (Ed.), SFPE Handbook of Fire Protection Engineering. Springer New York, New York, pp. 581–603.

Rein, G., 2009. Smouldering Combustion Phenomena in Science and Technology. Int. Rev. Chem. Eng. 1, 3–18.

Reiner, E.J., 2016. Analysis of Dioxin and Dioxin-Like Compounds, in: Dioxin and Related Compounds: Special Volume in Honor of Otto Hutzinger. Springer International Publishing, pp. 51–94.

Rhee, Y.H., Mishra, D., 2010. Current Research Trends of Microbiological Leaching for Metal Recovery from Industrial Wastes. Curr. Res. Technol. Educ. Top. Appl. Microbiol. Microb. Biotechnol. 1289–1296.

Riedel, T.P., Wallace, M.A.G., Shields, E.P., Ryan, J. V., Lee, C.W., Linak, W.P., 2021. Low temperature thermal treatment of gas-phase fluorotelomer alcohols by calcium oxide. Chemosphere 272, 129859. https://doi.org/10.1016/J.CHEMOSPHERE.2021.129859

Ross, I., Mcdonough, J., Miles, J., Storch, P., Kochunarayanan, P.T., Kalve, E., Hurst, J., Dasgupta, S.S., Burdick, J., 2018. A review of emerging technologies for remediation of PFASs. Remediation 28, 101–126. https://doi.org/10.1002/rem.21553

Ruttenberg, K.C., 1992. Development of a sequential extraction method for different forms of phosphorus in marine sediments. Limnol. Oceanogr. 37, 1460–1482. https://doi.org/10.4319/lo.1992.37.7.1460

Ryan, S.P., Li, X.D., Gullett, B.K., Lee, C.W., Clayton, M., Touati, A., 2006.

Experimental Study on the Effect of SO2 on PCDD/F Emissions: Determination of the Importance of Gas-Phase versus Solid-Phase Reactions in PCDD/F Formation. Environ. Sci. Technol. 40, 7040–7047. https://doi.org/10.1021/ES0615369

Sabadell, G., Scholes, G., Thomas, D., Murray, C., Bireta, P., Grant, G., Major, D., 2019. EX SITU TREATMENT OF ORGANIC WASTES OR OIL-IMPACTED SOIL USING A SMOLDERING PROCESS. WIT Trans. Ecol. Environ. 231, 367–376. https://doi.org/10.2495/WM180341

Schatowitz, B., Brandt, G., Gafner, F., Schlumpf, E., Bühler, R., Hasler, P., Nussbaumer, T., 1994. Dioxin emissions from wood combustion. Chemosphere 29, 2005–2013. https://doi.org/10.1016/0045-6535(94)90367-0

Schaum, C., Cornel, P., Jardin, N., 2007. Phosphorus recovery from sewage sludge ash–a wet chemical approach, in: Proceeding of the IWA Conference on Biosolids, Moving Forward Wastewater Biosolids Sustainability: Technical, Managerial, and Public Synergy.

Schecter, A., Gasiewicz, T.A., 2005. Dioxins and Health. Dioxins Heal. https://doi.org/10.1002/0471722014

Scholes, G.C., Gerhard, J.I., Grant, G.P., Major, D.W., Vidumsky, J.E., Switzer, C., Torero, J.L., 2015. Smoldering Remediation of Coal-Tar-Contaminated Soil: Pilot Field Tests of STAR. Environ. Sci. Technol. 49, 14334–14342. https://doi.org/10.1021/ACS.EST.5B03177

Self-Davis, M., Moore Jr, P., 2000. Determining water-soluble phosphorus in animal manure, in: Soil Sampling and Methods of Analysis. Raleigh, NC, pp. 74–76.

Senior, C.L., Helble, J.J., Sarofim, A.F., 2000. Emissions of mercury, trace elements, and fine particles from stationary combustion sources. Fuel Process. Technol. 65, 263–288. https://doi.org/10.1016/S0378-3820(00)00082-5

Sepulvado, J.G., Blaine, A.C., Hundal, L.S., Higgins, C.P., 2011. Occurrence and fate of perfluorochemicals in soil following the land application of municipal biosolids. Environ. Sci. Technol. 45, 8106–8112. https://doi.org/10.1021/es103903d

Shao, J., Yan, R., Chen, H., Yang, H., Lee, D.H., Liang, D.T., 2008. Emission characteristics of heavy metals and organic pollutants from the combustion of sewage sludge in a fluidized bed combustor. Energy and Fuels 22, 2278–2283. https://doi.org/10.1021/ef800002y

Sindiku, O., Orata, F., Weber, R., Osibanjo, O., 2013. Per- and polyfluoroalkyl substances in selected sewage sludge in Nigeria. Chemosphere 92, 329–335. https://doi.org/10.1016/j.chemosphere.2013.04.010

Soinne, H., 2009. Extraction methods in soil phophorus characterisation- Limitations and applications. University of Helsinki, Helsinki, Finland.

Solinger, R., Grant, G.P., Scholes, G.C., Murray, C., Gerhard, J.I., 2020. STARx Hottpad for smoldering treatment of waste oil sludge: Proof of concept and sensitivity to key design parameters: https://doi.org/10.1177/0734242X20904430 38, 554–566. https://doi.org/10.1177/0734242X20904430

Spinosa, L., Vesilind, P.A., 2007. Sludge into Biosolids - Processing, Disposal, Utilization. Water Intell. Online 6, 9781780402215–9781780402215. https://doi.org/10.2166/9781780402215

Stanmore, B.R., 2004. The formation of dioxins in combustion systems. Combust. Flame 136, 398–427. https://doi.org/10.1016/j.combustflame.2003.11.004

Stark, K., Plaza, E., Hultman, B., 2006. Phosphorus release from ash, dried sludge and sludge residue from supercritical water oxidation by acid or base. Chemosphere 62, 827–832. https://doi.org/10.1016/j.chemosphere.2005.04.069

Statistics Canada, 2019. Municipal wastewater systems in Canada, 2013 to 2017. Ottawa.

Stieglitz, L., Eichberger, M., Schleihauf, J., Beck, J., Zwick, G., Will, R., 1993. The oxidative degradation of carbon and its role in the de-novo-synthesis of organohalogen compounds in fly ash. Chemosphere 27, 343–350. https://doi.org/10.1016/0045-6535(93)90311-R

Stumm, W., Morgan, J.J., 2012. Aquatic Chemistry: Chemical Equilibria and Rates in Natural Waters - Werner Stumm, James J. Morgan - Google Books.

Sun, H., Gerecke, A.C., Giger, W., Alder, A.C., 2011. Long-chain perfluorinated chemicals in digested sewage sludges in Switzerland. Environ. Pollut. 159, 654–662. https://doi.org/10.1016/j.envpol.2010.09.020

Susastriawan, A.A.P., Saptoadi, H., Purnomo, 2017. Small-scale downdraft gasifiers for biomass gasification: A review. Renew. Sustain. Energy Rev. 76, 989–1003. https://doi.org/10.1016/J.RSER.2017.03.112

Switzer, C., Pironi, P., Gerhard, J.I., Rein, G., Torero, J.R., 2009. Self-sustaining smoldering combustion: A novel remediation process for non-aqueous-phase liquids in porous media. Environ. Sci. Technol. 43, 5871–5877. https://doi.org/10.1021/es803483s

Syed-Hassan, S.S.A., Wang, Y., Hu, S., Su, S., Xiang, J., 2017. Thermochemical processing of sewage sludge to energy and fuel: Fundamentals, challenges and considerations. Renew. Sustain. Energy Rev. 80, 888–913. https://doi.org/10.1016/J.RSER.2017.05.262

Takahashi, M., Kato, S., Shima, H., Sarai, E., Ichioka, T., Hatyakawa, S., Miyajiri, H., 2001. Technology for recovering phosphorus from incinerated wastewater treatment sludge, in: Chemosphere. Pergamon, pp. 23–29. https://doi.org/10.1016/S0045-6535(00)00380-5

Tame, N.W., Dlugogorski, B.Z., Kennedy, E.M., 2007. Formation of dioxins and furans during combustion of treated wood. Prog. Energy Combust. Sci. 33, 384–408. https://doi.org/10.1016/J.PECS.2007.01.001

Thygesen, A.M., Wernberg, O., Skou, E., Sommer, S.G., 2011. Effect of incineration temperature on phosphorus availability in bio-ash from manure. Environ. Technol. 32, 633–638. https://doi.org/10.1080/09593330.2010.509355

Tiessen, H., Moir, J., 1993. Characterization of available P by sequential extraction, in: Soil Sampling and Methods of Analysis. pp. 5–229.

Tiwari, M.K., Bajpai, S., Dewangan, U.K., Tamrakar, R.K., 2015. Suitability of leaching test methods for fly ash and slag: A review. J. Radiat. Res. Appl. Sci. 8, 523–537. https://doi.org/10.1016/j.jrras.2015.06.003

Torero, J.L., Fernandez-Pello, A.C., 1996. Forward smolder of polyurethane foam in a forced air flow. Combust. Flame 106, 89–109. https://doi.org/10.1016/0010-2180(95)00245-6

Torero, J.L., Gerhard, J.I., Kinsman, L.L., Yermán, L., 2018. Using fire to remediate contaminated soils. Undergr. Coal Gasif. Combust. 601–625. https://doi.org/10.1016/B978-0-08-100313-8.00019-0

Torero, J.L., Gerhard, J.I., Martins, M.F., Zanoni, M.A.B., Rashwan, T.L., Brown, J.K., 2020. Processes defining smouldering combustion: Integrated review and synthesis. Prog. Energy Combust. Sci. https://doi.org/10.1016/j.pecs.2020.100869

Tuppurainen, K., Halonen, I., Ruokojärvi, P., Tarhanen, J., Ruuskanen, J., 1998. Formation of PCDDs and PCDFs in municipal waste incineration and its inhibition mechanisms: A review. Chemosphere. https://doi.org/10.1016/S0045-6535(97)10048-0

Turner, B.L., Haygarth, P.M., 2000. Phosphorus Forms and Concentrations in Leachate under Four Grassland Soil Types. Soil Sci. Soc. Am. J. 64, 1090–1099. https://doi.org/10.2136/sssaj2000.6431090x

UNEP, 2019. SC-9/12: Listing of perfluorooctanoic acid (PFOA), its salts and PFOA-related compounds. Geneva.

USEPA, 2021. Contaminants on the Fourth Drinking Water Contaminant Candidate List. Environmental Protection Agency.

USEPA, 2020. Significant New Use Rule: Long-Chain Perfluoroalkyl Carboxylate and Perfluoroalkyl Sulfonate Chemical Substances. Environmental Protection Agency.

USEPA, 2012a. Method 1313: Liquid-Solid Partitioning as a Function of pH for Constituents in Solid Materials Using a Parallel Batch Extraction Procedure. Nashville, TN.

USEPA, 2012b. Method 1314: Liquid-Solid Partitioning as a Function of Liquid-to-Solid Ratio for Constituents in Solid Materials Using a Percolation Column Procedure. Nashville, TN.

USEPA, 2003. Toxic Equivalency Factors (TEF) for Dioxin and Related Compounds Exposure and Human Health Reassessment of 2,3,7,8-Tetrachlorodibenzo-p-Dioxin (TCDD) and Related Compounds Part II: Health Assessment for 2,3,7,8-Tetrachlorodibenzo-p-dioxin (TCDD. Washington, D.C.

USEPA, 1995. Solid Waste Disposal 2.2-1 2.2: Sewage Sludge Incineration.

Van Den Berg, M., Birnbaum, L.S., Denison, M., De Vito, M., Farland, W., Feeley, M., Fiedler, H., Hakansson, H., Hanberg, A., Haws, L., Rose, M., Safe, S., Schrenk, D., Tohyama, C., Tritscher, A., Tuomisto, J., Tysklind, M., Walker, N., Peterson, R.E., 2006. The 2005 World Health Organization Reevaluation of Human and Mammalian Toxic Equivalency Factors for Dioxins and Dioxin-Like Compounds Downloaded from. Toxicol. Sci. 93, 223–241. https://doi.org/10.1093/toxsci/kfl055

Venkatesan, A.K., Halden, R.U., 2013. National inventory of perfluoroalkyl substances in archived U.S. biosolids from the 2001 EPA National Sewage Sludge Survey. J. Hazard. Mater. 252–253, 413–418. https://doi.org/10.1016/j.jhazmat.2013.03.016

Verma, S., Subehia, S.K., Sharma, S.P., 2005. Phosphorus fractions in an acid soil continuously fertilized with mineral and organic fertilizers. Biol. Fertil. Soils 41, 295–300. https://doi.org/10.1007/S00374-004-0810-Y

Wang, F., Lu, X., Li, X.Y., Shih, K., 2015. Effectiveness and mechanisms of defluorination of perfluorinated alkyl substances by calcium compounds during waste thermal treatment. Environ. Sci. Technol. 49, 5672–5680. https://doi.org/10.1021/es506234b

Wang, F., Shih, K., Lu, X., Liu, C., 2013. Mineralization Behavior of Fluorine in Perfluorooctanesulfonate (PFOS) during Thermal Treatment of Lime-Conditioned Sludge. Environ. Sci. Technol. 47, 2621–2627. https://doi.org/10.1021/es305352p

Wang, K.S., Chiang, K.Y., Lin, K.L., Sun, C.J., 2001. Effects of a water-extraction process on heavy metal behavior in municipal solid waste incinerator fly ash. Hydrometallurgy 62, 73–81. https://doi.org/10.1016/S0304-386X(01)00186-4

Wang, Y.T., Zhang, T.Q., O'Halloran, I.P., Hu, Q.C., Tan, C.S., Speranzini, D., Macdonald, I., Patterson, G., 2015. Agronomic and environmental soil phosphorus tests for predicting potential phosphorus loss from Ontario soils. Geoderma 241–242, 51–58. https://doi.org/10.1016/J.GEODERMA.2014.11.001

Washington, J.W., Yoo, H., Ellington, J.J., Jenkins, T.M., Libelo, E.L., 2010. Concentrations, distribution, and persistence of perfluoroalkylates in sludge-applied soils near Decatur, Alabama, USA. Environ. Sci. Technol. 44, 8390–8396. https://doi.org/10.1021/ES1003846/SUPPL_FILE/ES1003846_SI_001.PDF

Werther, J., Ogada, T., 1999. Sewage sludge combustion. Prog. Energy Combust. Sci. https://doi.org/10.1016/S0360-1285(98)00020-3

Westerhoff, P., Lee, S., Yang, Y., Gordon, G.W., Hristovski, K., Halden, R.U., Herckes, P., 2015. Characterization, Recovery Opportunities, and Valuation of Metals in Municipal Sludges from U.S. Wastewater Treatment Plants Nationwide. Environ. Sci. Technol. 49, 9479–9488. https://doi.org/10.1021/es505329q

Wierzbowska, J., Sienkiewicz, S., Krzebietke, S., Bowszys, T., 2016. Heavy Metals in Water Percolating Through Soil Fertilized with Biodegradable Waste Materials. Water. Air. Soil Pollut. 227. https://doi.org/10.1007/S11270-016-3147-X

Winchell, L.J., Ross, J.J., Wells, M.J.M., Fonoll, X., Norton, J.W., Bell, K.Y., 2021. Per- and polyfluoroalkyl substances thermal destruction at water resource recovery facilities: A state of the science review. Water Environ. Res. 93, 826–843. https://doi.org/10.1002/WER.1483

Wozniak, D.J., Huang, J.Y., 1982. Variables Affecting Metal Removal from Sludge . Water Pollut. Control Fed.

Wu, H.Y., Ting, Y.P., 2006. Metal extraction from municipal solid waste (MSW) incinerator fly ash - Chemical leaching and fungal bioleaching. Enzyme Microb. Technol. 38, 839–847. https://doi.org/10.1016/j.enzmictec.2005.08.012

Wyn, H.K., Konarova, M., Beltramini, J., Perkins, G., Yermán, L., 2020. Self-sustaining smouldering combustion of waste: A review on applications, key parameters and potential resource recovery. Fuel Process. Technol. 205, 106425. https://doi.org/10.1016/J.FUPROC.2020.106425

Xu, H., He, P., Gu, W., Wang, G., Shao, L., 2012a. Recovery of phosphorus as struvite from sewage sludge ash. J. Environ. Sci. (China) 24, 1533–1538. https://doi.org/10.1016/S1001-0742(11)60969-8

Xu, H., Zhang, H., Shao, L., He, P., 2012b. Fraction distributions of phosphorus in sewage sludge and sludge ash. Waste and Biomass Valorization 3, 355–361. https://doi.org/10.1007/s12649-011-9103-5

Xu, T.J., Ramanathan, T., Ting, Y.P., 2014. Bioleaching of incineration fly ash by Aspergillus niger - Precipitation of metallic salt crystals and morphological alteration of the fungus. Biotechnol. Reports 3, 8–14. https://doi.org/10.1016/j.btre.2014.05.009

Yan, H., Zhang, C.J., Zhou, Q., Chen, L., Meng, X.Z., 2012. Short- and long-chain perfluorinated acids in sewage sludge from Shanghai, China. Chemosphere 88, 1300–1305. https://doi.org/10.1016/j.chemosphere.2012.03.105

Yang, J., Wang, Qunhui, Wang, Qi, Wu, T., 2009. Heavy metals extraction from municipal solid waste incineration fly ash using adapted metal tolerant Aspergillus

niger. Bioresour. Technol. 100, 254–260. https://doi.org/10.1016/j.biortech.2008.05.026

Yermán, L., 2016. Self-sustaining Smouldering Combustion as a Waste Treatment Process, in: Developments in Combustion Technology. InTech. https://doi.org/10.5772/64451

Yermán, L., Hadden, R.M., Carrascal, J., Fabris, I., Cormier, D., Torero, J.L., Gerhard, J.I., Krajcovic, M., Pironi, P., Cheng, Y.L., 2015. Smouldering combustion as a treatment technology for faeces: Exploring the parameter space. Fuel 147, 108–116. https://doi.org/10.1016/j.fuel.2015.01.055

Yermán, L., Wall, H., Torero, J.L., 2017. Experimental investigation on the destruction rates of organic waste with high moisture content by means of self-sustained smoldering combustion. Proc. Combust. Inst. 36, 4419–4426. https://doi.org/10.1016/J.PROCI.2016.07.052

Yu, J., Nickerson, A., Li, Y., Fang, Y., Strathmann, T.J., 2020a. Fate of per- and polyfluoroalkyl substances (PFAS) during hydrothermal liquefaction of municipal wastewater treatment sludge. Environ. Sci. Water Res. Technol. 6, 1388–1399. https://doi.org/10.1039/c9ew01139k

Yu, J., Nickerson, A., Li, Y., Fang, Y., Strathmann, T.J., 2020b. Fate of per- and polyfluoroalkyl substances (PFAS) during hydrothermal liquefaction of municipal wastewater treatment sludge. Environ. Sci. Water Res. Technol. 6, 1388–1399. https://doi.org/10.1039/c9ew01139k

Zabaniotou, A., Theofilou, C., 2008. Green energy at cement kiln in Cyprus-Use of sewage sludge as a conventional fuel substitute. Renew. Sustain. Energy Rev. https://doi.org/10.1016/j.rser.2006.07.017

Zanoni, M.A.B., Rein, G., Yermán, L., Gerhard, J.I., 2020. Thermal and oxidative decomposition of bitumen at the Microscale: Kinetic inverse modelling. Fuel 264, 116704. https://doi.org/10.1016/J.FUEL.2019.116704

Zanoni, M.A.B., Torero, J.L., Gerhard, J.I., 2019. Determining the conditions that lead to self-sustained smouldering combustion by means of numerical modelling. Proc. Combust. Inst. 37, 4043–4051. https://doi.org/10.1016/J.PROCI.2018.07.108

Zhang, C., Yan, H., Li, F., Hu, X., Zhou, Q., 2013. Sorption of short- and long-chain perfluoroalkyl surfactants on sewage sludges. J. Hazard. Mater. 260, 689–699. https://doi.org/10.1016/j.jhazmat.2013.06.022

Zhang, F.S., Itoh, H., 2006. Extraction of metals from municipal solid waste incinerator fly ash by hydrothermal process. J. Hazard. Mater. 136, 663–670. https://doi.org/10.1016/j.jhazmat.2005.12.052

Zhang, H., He, P.-J., Shao, L.-M., 2008. Fate of heavy metals during municipal solid

waste incineration in Shanghai. J. Hazard. Mater. 156, 365–373. https://doi.org/10.1016/j.jhazmat.2007.12.025

Zhang, H., Kovar, J., 2009. Fractionation of soil phosphorus, in: Methods of Phosphorus Analysis for Soils, Sediments, Residuals, and Waters. pp. 50–60.

Zhang, Mengmei, Buekens, A., Li, • Xiaodong, 2017. Dioxins from Biomass Combustion: An Overview. Waste and Biomass Valorization. https://doi.org/10.1007/s12649-016-9744-5

Zhang, Meng, Shi, Y., Lu, Y., Johnson, A.C., Sarvajayakesavalu, S., Liu, Z., Su, C., Zhang, Y., Juergens, M.D., Jin, X., 2017. The relative risk and its distribution of endocrine disrupting chemicals, pharmaceuticals and personal care products to freshwater organisms in the Bohai Rim, China. Sci. Total Environ. 590–591, 633–642. https://doi.org/10.1016/j.scitotenv.2017.03.011

Zhang, T., Sun, H., Gerecke, A.C., Kannan, K., Müller, C.E., Alder, A.C., 2010. Comparison of two extraction methods for the analysis of per- and polyfluorinated chemicals in digested sewage sludge. J. Chromatogr. A 1217, 5026–5034. https://doi.org/10.1016/j.chroma.2010.05.061

Zhang, W., Liang, Y., 2021. Effects of hydrothermal treatments on destruction of per- and polyfluoroalkyl substances in sewage sludge. Environ. Pollut. 285, 117276. https://doi.org/10.1016/J.ENVPOL.2021.117276

Zhang, W., Zhang, Q., Liang, Y., 2022. Ineffectiveness of ultrasound at low frequency for treating per- and polyfluoroalkyl substances in sewage sludge. Chemosphere 286, 131748. https://doi.org/10.1016/J.CHEMOSPHERE.2021.131748

Zhang, Y., Chen, J., Likos, W.J., Edil, T.B., 2016. Leaching Characteristics of Trace Elements from Municipal Solid Waste Incineration Fly Ash, in: Geo-Chicago 2016. American Society of Civil Engineers, Reston, VA, pp. 168–178. https://doi.org/10.1061/9780784480168.018

Zhou, Y., Meng, J., Zhang, M., Chen, S., He, B., Zhao, H., Li, Q., Zhang, S., Wang, T., 2019. Which type of pollutants need to be controlled with priority in wastewater treatment plants: Traditional or emerging pollutants? Environ. Int. 131. https://doi.org/10.1016/j.envint.2019.104982

Chapter 3

3 USEPA LEAF methods for characterizing phosphorus and potentially toxic elements in raw and thermally treated sewage sludge

3.1 Introduction

Land application of solids, such as manure, inorganic fertilizers, and wastewater treatment plant (WWTPs) sludge, are valuable sources of phosphorus and other nutrients. However, accumulation of phosphorus within soils can increase leaching (Maguire and Sims, 2002) as previously studied with applied manures (Abdala et al., 2015; Jalali and Ostovarzadeh, 2009) and inorganic fertilizers (Maguire and Sims, 2002; Turner and Haygarth, 2000). Released phosphorus is transported through the subsurface or via runoff to surface waters (Johnston and Steen, 2002); contributing to eventual eutrophication (Gerdes and Kunst, 1998). Determining the biologically available (i.e., bioavailable) phosphorus in land applied solids is important for developing application guidelines, maximizing beneficial use, and establishing regulatory compliance.

Numerous methods have been developed to quantify phosphorus, especially bioavailable phosphorus, in a wide range of solids. Most literature and analytical methods focus on soils and the Hedley sequential fractionation method (Hedley et al., 1982) dominates the field (Chen and Ma, 2001; Condron et al., 1990; Cross and Schlesinger, 1995). Hedley uses progressively stronger chemical extractants to recover increasingly recalcitrant forms of phosphorus (Linquist et al., 1997), inferring potential sources and sinks of phosphorus based on phosphorus quantity within various fractions. Bioavailable

phosphorus is typically divided into several “pools” ranging from highly available to unavailable (Pansu and Gautheyrou, 2007).

Hedley forms the basis for many related sequential fractionation methods (Huang et al., 2008; Iyamuremye et al., 1996; Tiessen and Moir, 1993; Zhang and Kovar, 2009). Common modifications to the Hedley method include (i) an initial deionized water step prior to anion exchange resin (Huang et al., 2008), (ii) excluding quantification of microbial phosphorus (Iyamuremye et al., 1996), (iii) eliminating sonication during the extraction of moderately-bound phosphorus (Tiessen and Moir, 1993), and (iv) using heated digestion to quantify residual (unavailable) phosphorus (Zhang and Kovar, 2009). Sequential phosphorus fractionation methods vary significantly in the type of chemical extractant and molarity used to quantify each pool (a summary of published methods can be found in Chapter 2). Since phosphorus dissolution is highly pH dependent (Bolan and Hedley, 1990), extraction methods are likely to yield different results for available phosphorus depending on chosen extractants and procedure order (Neyroud and Lischer, 2003; Soinne, 2009). Furthermore, strong extractants can change the chemical structure of phosphorus species (Cade-Menun and Preston, 1996; Gikonyo et al., 2011; Guggenberger et al., 1996; Hartikainen and Yli-Halla, 1996). As a consequence, conclusions on phosphorus availability from studies using fractionation methods are inconsistent (Hartmann et al., 2019; Neyroud and Lischer, 2003) and sometimes contradictory (Johnson et al., 2003).

Studies assessing phosphorus availability in other solids including animal manure and sewage sludge have used modified versions of Hedley and soil phosphorus test procedures (González Medeiros et al., 2005; Huang et al., 2008; Qian and Jiang, 2014;

Self-Davis and Moore Jr, 2000; Xu et al., 2012b). Only a few studies have attempted to fractionate phosphorus in sewage sludge (Han et al., 2019; Huang et al., 2008; Qian and Jiang, 2014; Xu et al., 2012a). Such evaluations are anticipated to suffer from the same problems identified for sequential fractionation of phosphorus in soils.

Following decades of development, the USEPA released the Leaching Environmental Assessment Framework (LEAF) in 2010. LEAF is a characterization-based leaching framework combining experimental data on relevant intrinsic leaching behaviour with scenario-specific information for environmental assessments (Kosson et al., 2017). USEPA Method 1313 from LEAF consists of a series of parallel batch experiments to produce a liquid-solid partitioning curve of the material of interest as a function of pH (USEPA, 2012a). The complementary USEPA Method 1314 involves a column percolation experiment to obtain eluate concentrations and/or cumulative release as a function of the liquid-to-solids ratio (USEPA, 2012b). LEAF has been used to assess leaching behaviour of potentially toxic elements (PTEs) from coal fly ash (e.g., (Garrabrants et al., 2014; Tiwari et al., 2015)); municipal solid waste (MSW) incinerator ash (e.g., (Zhang et al., 2016)); concrete waste (Kosson et al., 2014); and sewage sludge compost (Fang et al., 2016). Using LEAF to assess phosphorus is less common and has been used for inorganic phosphorus from mining waste (L. Jiang et al., 2016; L. G. Jiang et al., 2016). The methodology seems promising to evaluate bioavailable phosphorus for a wide range of organic/inorganic matrices.

The aim of this research was to evaluate analytical procedures for assessing bioavailable phosphorus from sewage sludge before and after thermal treatment. The two procedures chosen for comparison were the widely used Hedley fractionation method and

USEPA LEAF. This study demonstrates that the LEAF provides a more consistent method for analyzing phosphorus bioavailability in sludges and suggests that it may be more widely applicable to soils and other solids under consideration for land application. This study also illustrates how the LEAF methods provide valuable quantification of PTEs that may be present in these materials with no further analytical steps required.

3.2 Materials and Methods

The sludge utilized in this study was collected from Greenway Wastewater Treatment Plant (Greenway), London, Ontario, Canada. At Greenway, sludge is produced as a by-product of primary and secondary treatment. Primary clarification removes settleable solids (i.e., primary sludge). Following aerobic digestion and thickening, secondary clarification settles out waste activated sludge via dissolved air flotation units and rotating drums. Centrifugation with polymer addition is used to dewater a combined slurry of primary and waste activated sludge to produce a cake sludge. All sludge was collected as cake sludge in a single batch on July 26th, 2018, to minimize compositional variability.

3.2.1 Sample Preparation and Storage

Sludge was oven-dried to prevent decomposition and moulding. Prior to subsequent analyses, the oven-dried sludge was pulverized into a homogenous powder using an immersion blender and mortar and pestle. Batches of ~100 g of dried sludge were placed in large crucibles and heated in a muffle furnace at 950°C for 2 hours to produce incinerated sewage sludge ash (herein referred to as 'incinerated ash'). The ash appeared to be a

relatively homogenous powder; no further grinding was done. All materials were stored in sealed 20 L pails at 5°C prior to use.

3.2.2 Preliminary Analysis

Moisture content, volatile matter, ash content, and fixed carbon of the sludge were determined following EPA Method 1684 (Telliard, 2001), with three replicates analyzed for each. The sludge had an average moisture content of 73 ± 0.2%, volatile matter content of 18 ± 0.3%, ash content of 7 ± 0.1%, and fixed carbon content of 2 ± 0.4%, all on a wet-mass basis. Laboratory incineration at 950°C resulted in mass loss of ~93%.

Pseudo-total elemental concentrations (herein referred to as total concentrations) were determined for aluminum, cadmium, cobalt, chromium, copper, iron, manganese, molybdenum, nickel, phosphorus, lead, and zinc within sludge and ash. Elements were extracted from the solid phase through microwave assisted acid digestion following USEPA Method 3051A (Element, 2007). Acid digestions were performed in triplicate.

3.2.3 Hedley Method

In the Hedley method, inorganic and organic phosphorus fractions are extracted using progressively stronger chemical reagents. Figure 3.1a illustrates the series of 6 extracts (H1 – H6). In each extraction, 1 g dried sample was added to a 250 mL polyethylene bottle. An anion exchange resin bag (Dowex™ resin, Sigma-Aldrich Canada Co., within 41 μm nylon mesh, Fisher Scientific Co Ltd.) and 30 mL deionized water were added and shaken at 170 RPM on a rotary shaker for 16 hours. Phosphorus was removed from the resin with 20 mL 0.5 M hydrochloric acid (HCl) (H1). The supernatant was decanted and disposed of followed by the addition of 30 mL 0.5 M sodium bicarbonate

($NaHCO_3$). The bottle was shaken for 16 hours, then the supernatant was collected (H2). This process was repeated, adding 30 mL 0.1 M sodium hydroxide (NaOH) (H3), 20 mL 0.1 M NaOH with 2 min sonication (H4), and 30 mL 1 M HCl (H5). Following the resin extraction procedure, a repeat sample was used to determine the microbial biomass phosphorus by spiking the solid material with 1 mL concentrated chloroform ($CHCl_3$), leaving the sample to fumigate for 16 hours, then extracting the phosphorus with 30 mL 0.5 M $NaHCO_3$. The microbial biomass phosphorus is calculated as the difference between the total labile phosphorus extracted with only $NaHCO_3$ and pretreated with $CHCl_3$ (Hedley and Stewart, 1982). The residual phosphorus is determined by digesting (H5) in 10 M sulfuric acid (H_2SO_4) (H6). Importantly, pH is not dictated in this method. Instead, following each procedure step, eluate samples were analyzed for pH and conductivity using a Fisher Scientific accumet™ AB200 pH/mV/Conductivity meter (Waltham, MA, USA), then preserved for further analysis of inorganic and total phosphorus. Concentrations of organic phosphorus were calculated as the difference between total and inorganic phosphorus in each extract. All extractions were performed in triplicate with results presented as averages including standard error.

Each extract is associated with a phosphorus pool and mechanism of phosphorus binding to solid surfaces, as illustrated in Figure 3.1a. Whether each of the chemical extractants can accurately dissociate the target phosphorus compounds from the solids is not fully understood, and it is likely that each pool contains a combination of compounds (Turner et al., 2005).

3.2.4 USEPA LEAF Methods 1313 and 1314

USEPA LEAF Method 1313 consists of 9 parallel batch extractions (Figure 3.1b) to produce a liquid-solid partitioning curve of the material of interest over eluate pH range $2 \leq pH \leq 13$. For each extraction, 10 g of material was combined with 100 mL of extraction solution consisting of deionized water with either 2 N nitric acid (HNO_3) or 1 N potassium hydroxide (KOH) to achieve 9 target pH values ± 0.5 for each (Figure 3.1b). The liquid-to-solids ratio was 10 mL/g-dry. Quantities of HNO_3 or KOH were determined after measuring the native pH of the material using deionized water. Mixtures were prepared in 125 mL HDPE bottles, sealed, and shaken end-over-end at 170 RPM for 24 hours. Following shaking, bottles were centrifuged. pH was measured to confirm the final solution remained within target ranges; electrical conductivity was also measured. Eluate samples were filtered, preserved, and analyzed for total and inorganic phosphorus. Additionally, cadmium, cobalt, chromium, copper, molybdenum, nickel, lead, and zinc were analyzed because they are typically monitored and/or regulated at WWTPs.

USEPA LEAF Method 1314 uses a percolation column experiment to evaluate constituent release from the material of interest as a function of the liquid-to-solid ratio (L/S). The L/S is computed as the quantity of solution (mL) passed through the fixed quantity of solid material (g) within the column. A glass column (DWK Life Sciences, KIMBLE®) of 5 cm outer diameter and 30 cm height was used for each test. A 5 cm layer of acid-washed, air-dried sand (Number 12, Bell & Mackenzie) was packed into the base of the column. Dried material (sludge or incinerated ash) was added to the column in successive layers (~60 g), tamping each using a glass rod, until 300 g of sample was added. A second 5 cm layer of acid-washed sand was added to the top of the material pack to

minimize material loss from the column. Deionized water (neutral pH) was pumped using a Masterflex® L/S® digital peristaltic pump (Cole-Parmer Instrument Company, IL, USA) upwards at a L/S of 1.0 mL/g/day until breakthrough occurred. The pump was stopped, letting the saturated column rest for 24 hours. After resting, water flow was reintroduced and maintained at rate of 0.75 ± 0.5 mL/g/day to collect the nine eluate samples (T01-T09) at specified L/S of 0.2, 0.5, 1.0 ± 0.1, and 1.5, 2.0, 4.5, 5.0, 9.5, and 10.0 ± 0.2 mL/g-dry matter. The pH and electrical conductivity of each eluate sample were measured within an hour of collection. Eluate samples were filtered through 0.45 μm filters (Whatman 0.45 μm celluacetate filters, VWR International) via a vacuum pump. Filtered samples were preserved with concentrated HNO_3 and analyzed for total and inorganic phosphorus as well as cadmium, cobalt, chromium, copper, molybdenum, nickel, lead, and zinc.

3.2.5 Analytical Methods

Total elemental concentrations in the microwave extracts, Hedley method extracts, and LEAF Method 1313 and 1314 samples, were analyzed using an Agilent 720 Inductive Coupled Plasma Optical Emission Spectrometer (ICP-OES) following USEPA Method 6010D (Element Symbol CAS Number, 2007).

Total phosphorus in the Hedley method extracts and USEPA method 1313 and 1314 samples was measured using ICP-OES to avoid interferences that affect colorimetric analysis (Ivanov et al., 2012). Inorganic phosphorus was measured as dissolved orthophosphate (PO_4^{3-}) by High-Performance Liquid Chromatography (HPLC) using direct injection by a Water® 515 pump following USEPA Method 300 (John D Pfaff, 1993).

All extracts were run at dilution factors of 1:1 – 1:100 (1:10 – 1:100 for digested samples) on both ICP-OES and HPLC to ensure all elements were within detection ranges for every sample. Triplicates, method blanks, and spiked extracts were also run on both ICP-OES and HPLC to ensure quality assurance and quality control.

Due to differences in the sludge versus post-treatment incinerated ash, all results were normalized in terms of the starting material: mass of element per mass of initial dry sludge (mg/kg–DS). Results in terms of dry matter (i.e., mg/kg–dm) can be found in Appendix A.3.

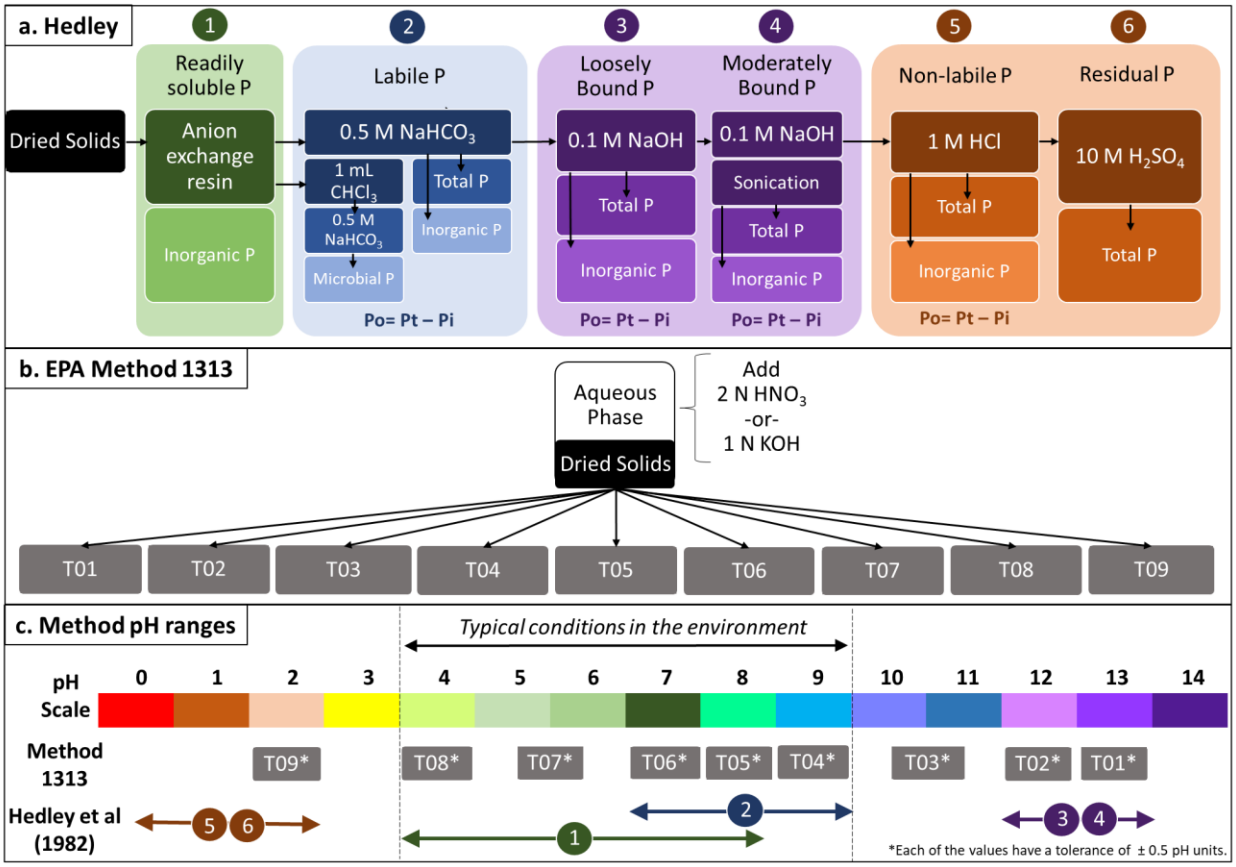

Figure 3.1: procedural schematics for a. the Hedley et al. (1982) fractionation procedure and b. USEPA Method 1313 parallel batch extraction. The 6 steps of the Hedley procedure (H1-H6) are outlined in a., including the chemical extractant and molarity used for to quantify each phosphorus pool. The phosphorus pools are assumed to decrease in plant availability from step (H1) being immediately available to step (H6) being unavailable. H1 is associated with readily soluble inorganic phosphorus (Zhang and Kovar, 2009). H2 is correlated to labile inorganic phosphorus from P-esters bound to surfaces of aluminum and iron (Cross and Schlesinger, 1995). H3 and H4 are moderately-labile phosphorus pools assumed to contain phosphorus chemisorbed to amorphous and some crystalline aluminum and iron oxides/hydroxides (Tiessen and Moir, 1993). H5 is assumed to be non-labile phosphorus bound to calcium-species (Cross and Schlesinger, 1995). The pH ranges corresponding to Hedley method pools and USEPA Method 1313 samples are provided in c. and compared to typical environmental pH conditions.

3.3 Results and Discussion

3.3.1 Phosphorus Analysis

3.3.1.1 Hedley Method

Figure 3.2 presents Hedley method results for sludge and incinerated ash. In the immediately soluble phosphorus pool (H1), 1100 mg/kg – dry sludge (i.e., mg/kg–DS) was extracted from both sludge and incinerated ash, comprising 2 and 5% of total phosphorus, respectively. Majority was from unavailable pools (H3 – H6): 57% and 79% for sludge and incinerated ash, respectively. The fraction of total phosphorus released from non-labile (H5) and residual (H6) pools increases from 32% in sludge to 62% in incinerated ash. Thermal treatment seems to have transformed a fraction of phosphorus to less available forms.

Hedley assumes organic phosphorus is the difference between total and inorganic phosphorus. The sludge seems to have larger proportions of organic phosphorus compared to the incinerated ash. Phosphorus in the sludge extracted by Hedley consists of 32% organic phosphorus distributed as 54% labile (H2), 16% loosely bound (H3), 10% moderately bound (H4), and 85% non-labile (H5). In contrast, only 10% of phosphorus in the incinerated ash is present as organic, distributed as 14% labile (H2), <1% loosely bound (H3), 10% moderately bound (H4), and <1% non-labile (H5). This reduction in organic phosphorus during thermal treatment is also evident when comparing microbial phosphorus: ~310 mg/kg–DS of microbial phosphorus for sludge versus negligible for incinerated ash. This is due to the destruction of any microbial biomass present in the sludge which would cause subsequent release of any microbially-bound phosphorus.

Phosphorus recovered from all steps of Hedley accounted for only 60% of total phosphorus extracted by microwave digestion from sludge and 80% from incinerated ash (Figure 3.2). This is consistent with unextracted phosphorus of 20-70% in other studies (Lehmann and Kleber, 2015; Tiessen and Moir, 1993). Hedley was developed for use in soils that have significantly less organic matter than sludges. In sludges, the optimal application of Hedley may be to compare the relative changes to functional phosphorus pools between samples.

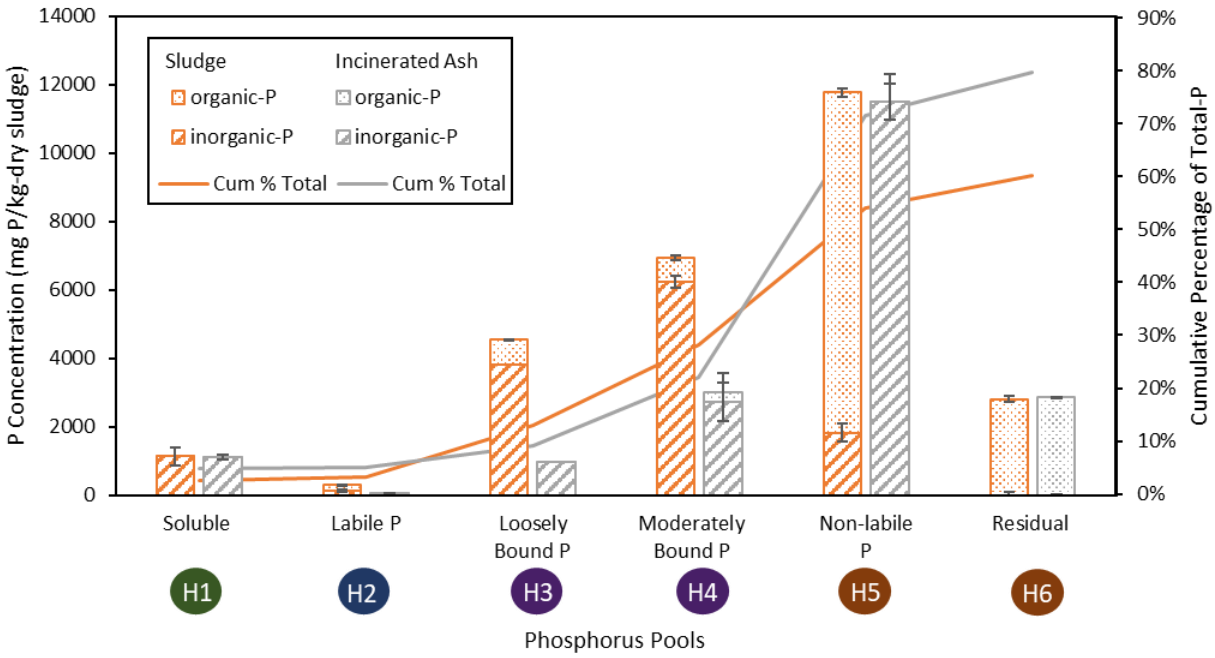

Figure 3.2: Results from the Hedley method on sludge and incinerated ash presented in orange and gray, respectively. The different P-pools are shown on the x-axis and labelled with numbers corresponding to the respective extraction steps shown in the Hedley procedural schematic (Figure 3.1a.). The full bar represents the total-P in that fraction. The bars are subdivided into inorganic- and organic-P which are shown with diagonal stripes and dots, respectively. The P concentration is given in mg of P per kg of dry sludge. The cumulative percentage of P extracted by the Hedley method compared to the total-P for the sludge and incinerated ash are plotted as lines on the secondary axis.

3.3.1.2 USEPA Method 1313

USEPA Method 1313 was used to quantify pH-dependent phosphorus availability (Figure 3.3). Sludge is slightly acidic while incinerated ash is slightly alkaline with native pH of 5.8 and 8.0, respectively. At native pHs, phosphorus availabilities were at a minimum from both sludge and incinerated ash; increasing significantly under strongly acidic and alkaline conditions.

At pH < 7, phosphorus availability was greater in incinerated ash than sludge, whereas at pH > 7, the opposite was true. Under acidic conditions (pH < 6), the concentration of total available phosphorus in incinerated ash increased from 370 to 3800 mg/kg–DS and from 150 to 1300 mg/kg–DS in sludge under the same conditions. Organic phosphorus accounts for an important fraction of available phosphorus in both materials in these conditions: 15 – 80% in sludge and 17 – 83% in incinerated ash. Most of the available organic phosphorus in incinerated ash becomes available at pH = 4, whereas, in sludge, available organic phosphorus varies more with pH. This difference likely reflects the absence of organic matter in incinerated ash.

Above pH 7, the concentration of available phosphorus in sludge increases almost linearly with increasing pH. In slightly alkaline conditions ($7.5 \leq pH \leq 9.5$), available phosphorus from incinerated ash was 0.4% of available phosphorus from sludge. As alkalinity increased (pH > 9.5), available phosphorus increased linearly in both sludge and incinerated ash. Available phosphorus in incinerated ash remained 20 – 40% of that available in sludge (3100 – 17,000 mg/kg–DS and 650 – 6400 mg/kg–DS in sludge and incinerated ash, respectively). Organic phosphorus accounts for a significantly larger

fraction of available phosphorus in sludge than incinerated ash in alkaline conditions: 29 – 68% versus 0 – 61%.

In summary, sludge shows generally higher concentrations of immediately available phosphorus across environmentally relevant pH conditions ($3.5 < pH < 8.5$) while incinerated ash contains higher available phosphorus under increasingly acidic conditions ($pH \leq 4$). Thermal treatment of sludge is likely transforming a portion of immediately available phosphorus at native pH into more recalcitrant forms (Qian and Jiang, 2014). This transformation may have important benefits since, after land application, immediately available phosphorus may be flushed rapidly from the system causing eutrophication of nearby surface waters. Conducting dynamic leaching tests (Method 1314) allows this potential impact to be directly studied.

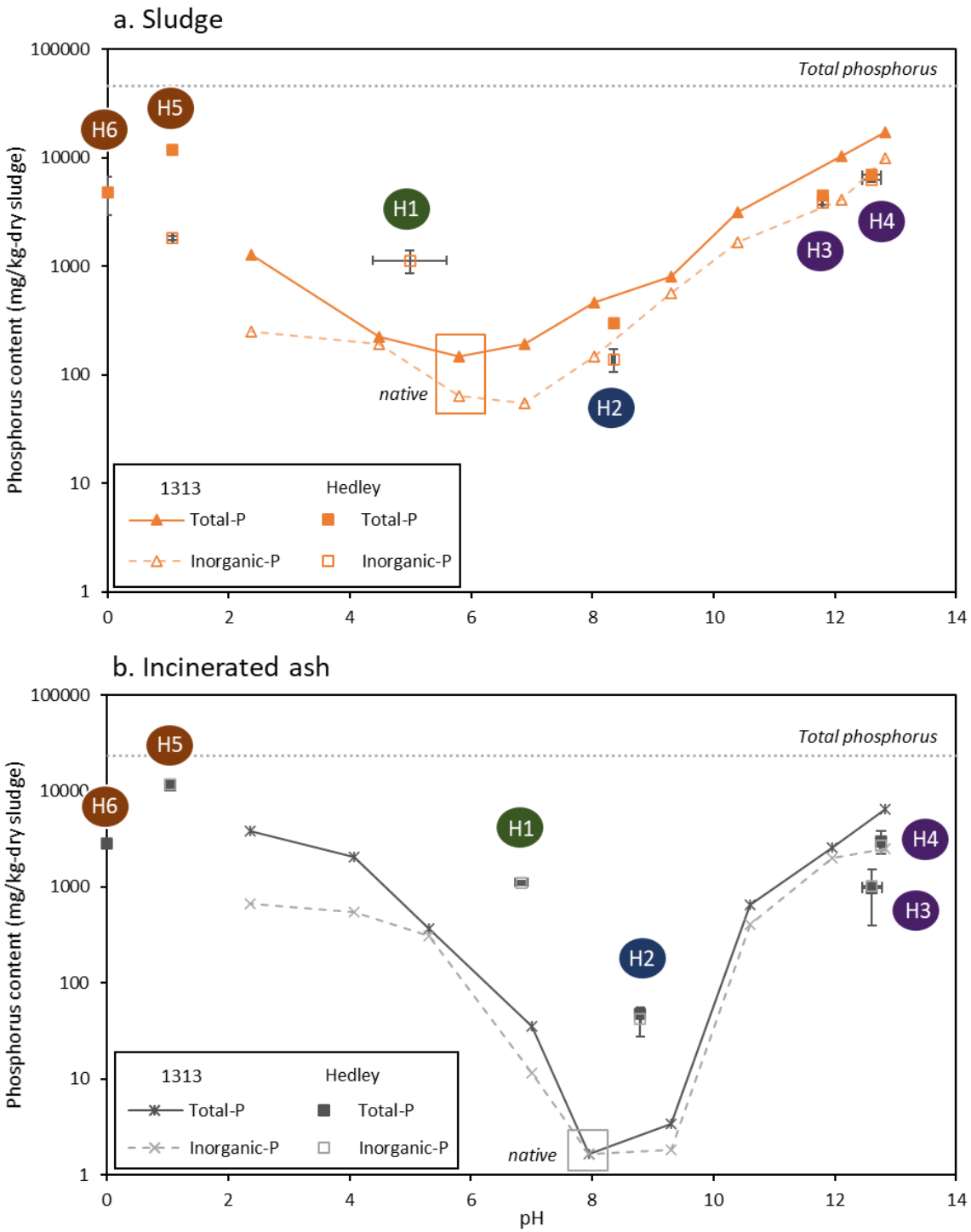

Figure 3.3: Comparison of the available-P as a function of pH for a. sludge and b. incinerated ash using the results of the EPA leaching method 1313 and the Hedley fractionation procedure. Method 1313 results are plotted along the curves while the Hedley results are plotted as discrete points using square markers. The extraction steps corresponding to each of the points are labelled as 1-6 (see Figure 3.1 for the full procedure). Total phosphorus is presented as the dotted line. The native pH of each material is outlined in a box.

3.3.1.3 USEPA Method 1314

USEPA Method 1314 dynamic leaching tests evaluate constituent release from materials as a function of increasing L/S ratio. The highest concentration of phosphorus is released immediately from both sludge and incinerated ash (Figure 3.4); however, important differences were observed between their release profiles.

In sludge, an initial slug of 9.5 mg/kg–DS of phosphorus was released (L/S = 0.2) followed by diminishing rates. Phosphorus rapidly becomes availability – limited as minimal release occurs with additional percolation ($0.5 \leq L/S \leq 10$), leading to a cumulative release of 19.7 mg/kg–DS. Of the total eluted phosphorus, 48% is released immediately. This behaviour is consistent with applications of sludge to soil where a rapid initial release of phosphorus, which can be linked to eutrophication (Johnston and Steen, 2002).

In incinerated ash, the initial slug of phosphorus leached was smaller - 92% less than in sludge - and released more slowly (0.8 mg/kg–DS over $0.2 \leq L/S \leq 2.0$). Organic phosphorus accounted for 37% of this initial slug as compared to 95% of the initial slug in sludge. Total and inorganic phosphorus then exhibited a continued slow release for the remainder of the incinerated ash experiment ($2.0 \leq L/S \leq 10$), exhibiting solubility-limited behaviour. Importantly, approximately 81% of total eluted phosphorus from incinerated ash was in the inorganic form, compared to 52% from sludge.

Early washout of soluble ions did not have a substantial impact on eluate pH in either material, although thermal treatment affected the initial pH (Figure 3.4). The elevated temperatures of incineration are associated with processes such as denaturation of organic acids and combustion of organic materials that have been observed to cause similar

increases in soil pH (Ulery and Graham, 1993). Combustion of organic matter within sludge resulted in about 50% of phosphorus being released through volatilization (see Appendix A.1), illustrating an important mechanism for recovery during thermal treatment. Most of what remained within the incinerated ash was likely transformed into more crystalline forms (Thygesen et al., 2011). The net result was a decrease in immediate phosphorus leaching, agreeing with the Method 1313 results at native pH.

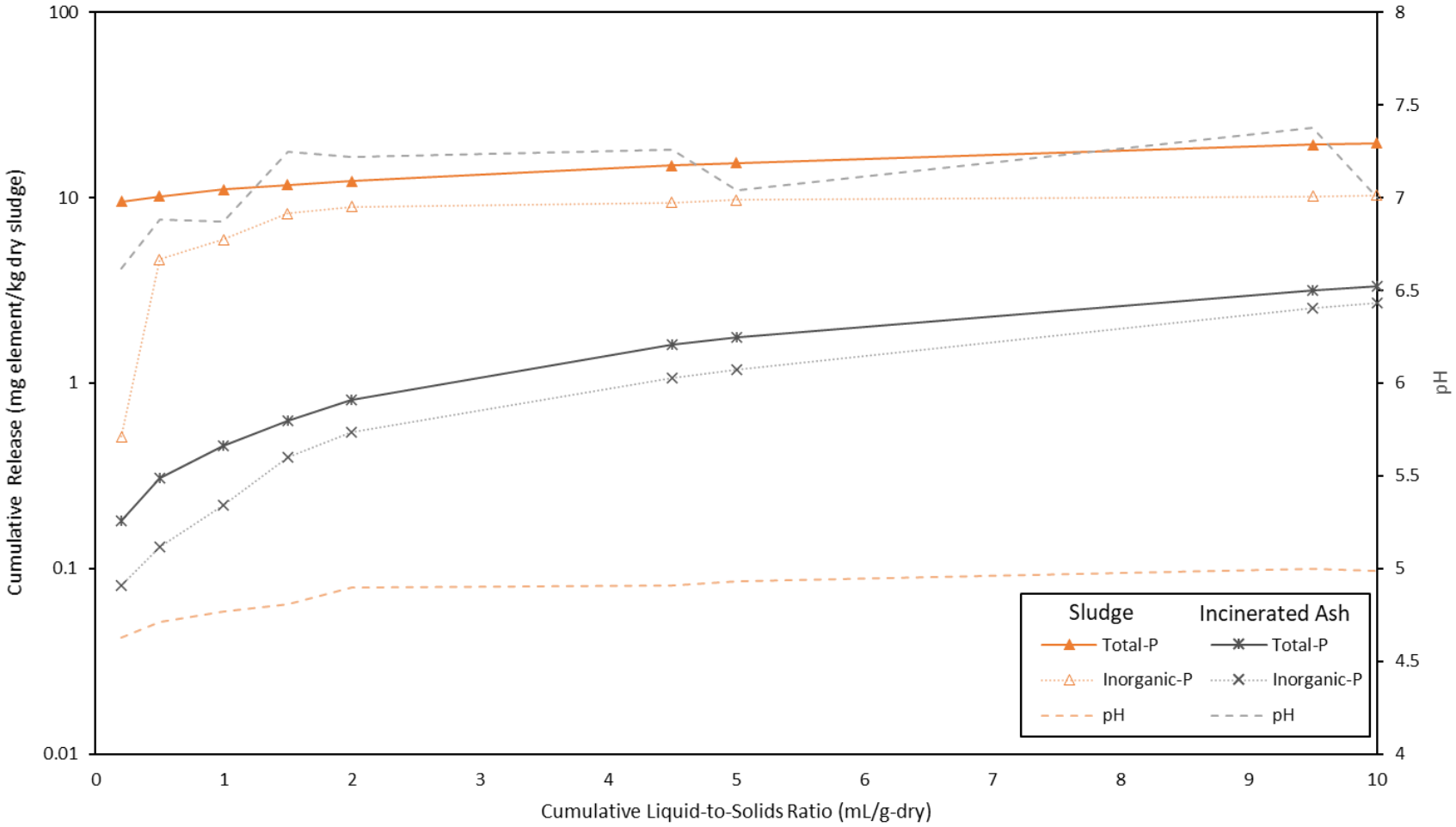

Figure 3.4: The USEPA method 1314 column percolation experiments for sludge (orange) and incinerated ash (grey). The concentrations of released phosphorus are shown in mg of phosphorus per kg dry sludge. The darker solid lines and lighter broken lines show total- and inorganic-P release, respectively. The pH changes over the column leaching experiment are plotted as dotted lines on the secondary y-axis.

3.3.2 Potentially Toxic Element Availability and Leaching

One of the barriers to land application of sludge, with or without further treatment, is potential release of PTEs. LEAF Methods 1313 and 1314 provide additional data to evaluate their potential release. Figure 3.5 shows Method 1313 plots of 8 elements of concern identified in Ontario Regulation 338/09 (O. Reg. 338 CM1 NASM) from the Nutrient Management Act (2002) (see Appendix A for PTE results from Method 1314).

All elements generally had higher availabilities from sludge compared to incinerated ash. The exceptions typically occurred in limited circumstances not relevant to conditions for land application (pH = 4). Cadmium, molybdenum, and lead all had similar availabilities from sludge and incinerated ash under neutral to acidic conditions and higher availabilities from sludge than incinerated ash under alkaline conditions. To understand how availability translates to potential release behaviour upon potential land application, results from Methods 1313 and 1314 must be viewed together.

Cumulative releases of all elements apart from molybdenum were higher from sludge than incinerated ash, often significantly higher (Figures A.2-2 and A.2-3, Appendix A.2). The lower release from the incinerated ash may partially be due to losses to emissions during thermal treatment. Importantly, although lead had higher available concentration at neutral pH (Figure 3.5), lead release from incinerated ash was small and 5% of lead released from sludge (Figure A.2-2, Appendix A.2). Among the other 6 PTEs, similar release trends were observed; cumulative releases from incinerated ash were <1-10% of the cumulative releases from sludge, usually because of a relatively large initial slug

released from the sludge. The thermal treatment process appears to affect the availability and leaching of PTEs in the resulting material, similar to phosphorus.

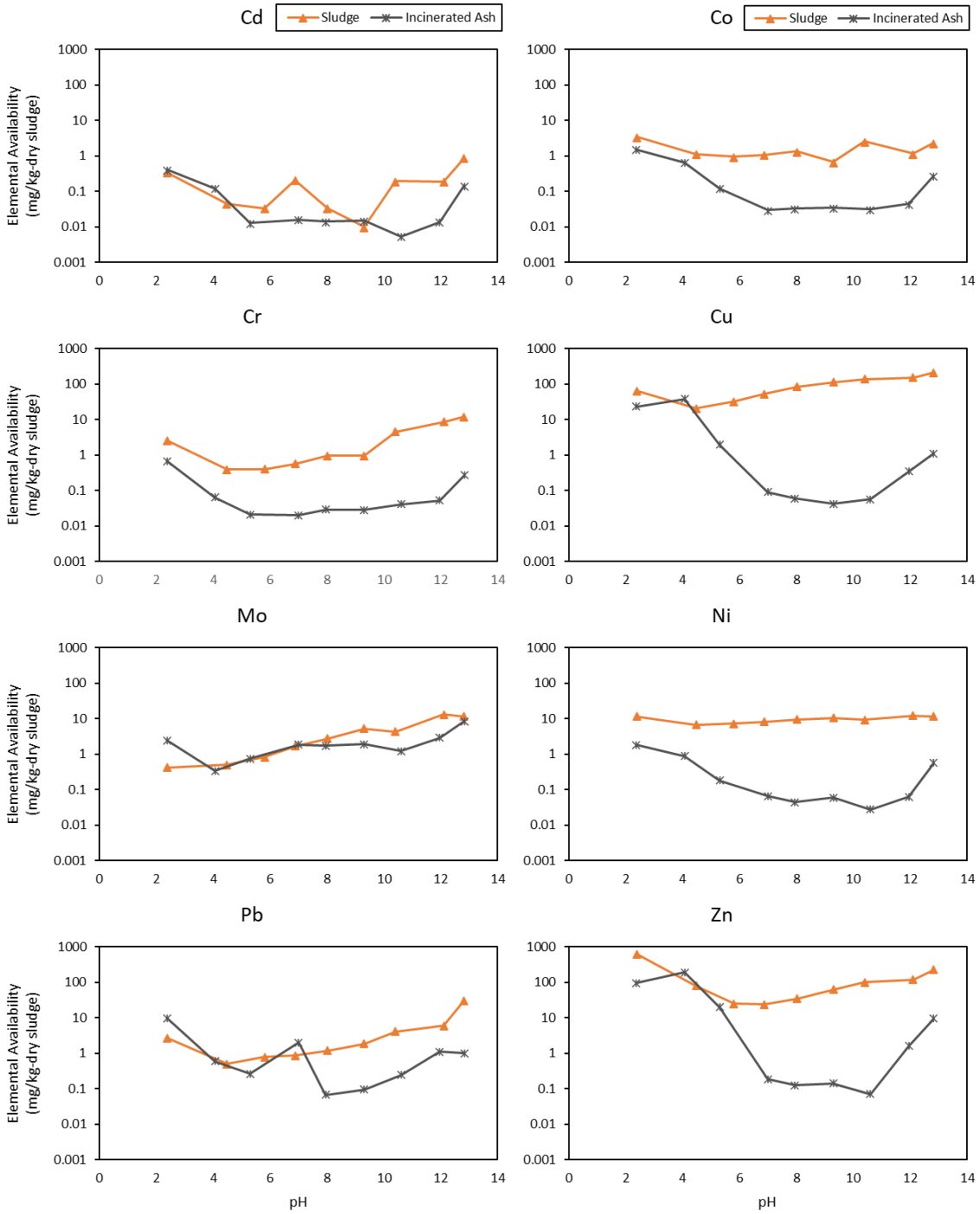

Figure 3.5: pH-dependent leaching curves for 8 PTEs of concern from O. Reg. 338 CM1 NASM for both sludge and incinerated ash, following USEPA Method 1313. Values have been normalized per kg dry sludge.

3.3.3 Discussion: Comparing Hedley and LEAF Methods

LEAF methods are easier to execute than sequential fractionation procedures. Hedley uses 6 different chemical extractants of varying molarities while Method 1313 requires only 2 and Method 1314 only 1 (deionized water). Method 1313 consists of 9 parallel batch extractions that are performed simultaneously, yielding independent results. Although Method 1314 is technically also a series extraction from the percolation column, compared to sequential fractionation the sample collection is simplistic. Sample quantity may also influence results. Hedley indicates 1 g dried sample which may not fully represent material characteristics. Method 1313 utilizes 10 g (or more) dried sample for each extraction and Method 1314 uses at least 300 g dried sample in the column. Although likely more characteristic, the larger sample sizes used in LEAF may also be a drawback compared to Hedley if sample amount is limited.

Quantifying release of phosphorus from each material is important to evaluate what plants may receive. Inconsistencies between Hedley and LEAF methods have important implications. Hedley soluble (H1) and labile (H2) pools typically correspond to points between T04 and T08 in Method 1313 (Figure 3.1c). In this work, soluble (H1) and labile (H2) pools correspond to T07 (pH = 5.5) and T05 (pH = 8), respectively, in the sludge and to T06 (pH = 7) and T04 (pH = 9), respectively, in the incinerated ash (Figure 3.1c). Phosphorus released at native pH in Method 1313 is inconsistent with soluble (H1) pool from Hedley, releasing ~6% and <1% from the sludge and incinerated ash, respectively (Figure 3.3). Furthermore, in sludge, soluble (H1) pool exceeds available phosphorus determined by Method 1313 at $3.5 < pH < 9.5$ (i.e., samples T04 – T08) making it only comparable at pH extremes, which is not relevant to land application. Similarly, in

incinerated ash, soluble (H1) pool only matches the magnitude of available phosphorus from Method 1313 determined in more extreme conditions (pH <5 or pH >11). Additional discrepancies arise considering Method 1314 results. Cumulative inorganic phosphorus released from Method 1314 was <1% of the quantity released in soluble (H1) pool for both sludge and incinerated ash, even when differences in L/S ratios between methods were considered. This lack of alignment is problematic. Readily soluble phosphorus is the primary concern for receiving waters (Johnston and Steen, 2002). Overestimation of this pool could result in insufficient phosphorus being applied to crops whereas underestimation risks contributing to eutrophication. The discrepancy between the LEAF and Hedley results for readily soluble phosphorus is probably caused by the Hedley's use of anion exchange resin, which likely extracts low-leachability phosphorus bound to solids (Koopmans et al., 2007; Schoumans and Groenendijk, 2000).

Hedley is also inconsistent with Method 1313 for the labile (H2), loosely bound (H3), and moderately bound (H4) phosphorus pools (Figure 3.3), whereas non-labile (H5) and residual (H6) pools were in line with Method 1313 results; however, pH values in Hedley are outside the range of Method 1313 (Figure 3.1c). For sludge, the quantities of labile (H2) and loosely bound (H3) phosphorus are consistently lower than available phosphorus from corresponding Method 1313 points, opposite to the case for readily soluble (H1) phosphorus (Figure 3.3). The resin used in soluble (H1) pool may have extracted some phosphorus that would otherwise appear in these subsequent pools, as was observed by (Soinne, 2009). For incinerated ash, an order of magnitude more phosphorus is released in Hedley labile (H2) fraction than by Method 1313 at the same pH. The phosphorus concentrated in incinerated ash following thermal treatment of sludge may

have exceeded the capacity of the resin used in soluble (H1), enabling release into subsequent pools. Consistent with sludge, phosphorus concentrations in Hedley loosely bound (H3) and moderately bound (H4) pools in incinerated ash are lower than corresponding points in Method 1313. The large portion of sorbed phosphorus removed within labile (H2) pool may have caused only more strongly bound phosphorus to remain, reducing the proportion of phosphorus extracted within the loosely bound (H3) pool. These discrepancies demonstrate an important drawback to Hedley and other sequential fractionation procedures: pools quantified in each extraction step influence pools quantified in subsequent steps (Soinne, 2009; Turner et al., 2005). Incorporating mineralogy into phosphorus analyses has the potential to improve our interpretation and understanding of these results (Han et al., 2019; Qian and Jiang, 2014). Phosphorus mineralogy of virgin sewage sludge is challenging (Smith et al., 2002) and research in this area is limited. Minerals such as hydroxyapatite, brushite, monetite, and others have been identified in sludges (Frossard et al., 1994; Smith et al., 2002). Mineral phases seem to depend on source materials; wastewater treatment processes and operating conditions; and subsequent sludge handling processes. For example, phosphorus mineral transformations have been observed after low temperature drying processes (Smith et al., 2002). High temperature treatment likely causes further transformations (Han et al., 2019; Qian and Jiang, 2014). This work provides important groundwork for future research exploring phosphorus mineralogy of sewage sludge and transformations brought about by thermal treatment.

3.4 Conclusions

Hedley and LEAF methods provide trends in available phosphorus that are qualitatively consistent. In this study, both suggest that thermal treatment of the sludge changes phosphorus minerals into forms that are more strongly bound to the solid surfaces. Therefore, phosphorus is less likely to leach from the incinerated ash in the short term, providing a more regulated source of gradual inorganic phosphorus with less potential harm to downstream water bodies.

However, Hedley and LEAF methods provide quantitative differences and LEAF is concluded to be superior for the following reasons. First, more incomplete phosphorus extraction from sludge than incinerated ash using Hedley suggests that it may be less appropriate for organic materials; this is consistent with previous studies and limits its applicability. Second, Hedley phosphorus pools were mostly at extreme pH conditions while LEAF (Method 1313) provided results across a range of controlled pH conditions relevant to land application. Third, Hedley overpredicted readily available phosphorus and underpredicted less soluble forms. Moreover, Hedley overpredicted the amount that would rapidly leach as inferred by LEAF (Method 1313) and directly quantified in LEAF (Method 1314). LEAF avoids the problem of sequential fractionation procedures where pools quantified in each extraction step influence pools quantified in subsequent steps. Fourth, LEAF was found to be practically simpler to execute and, while requiring more sample, the results may be more representative. Fifth, LEAF additionally provides analysis of PTEs, which are valuable for decision-making. In this study, smaller initial releases, lower availability in environmentally relevant conditions, and lower total contents in incinerated ash are promising indicators that land application of incinerated ash would likely result in

less PTE release to soil compared to land application of sludge. Although these elements could be analyzed in the Hedley extracts, that method was not designed for such purposes.

This analysis shows the value of the USEPA LEAF Methods in understanding phosphorus availability from materials such as sewage sludge before and after treatment. Land application of a material will change soil pH, which influences phosphorus availability and leaching of PTEs. LEAF was shown to provide valuable and superior insights into the effects of fluctuations in pH, dynamic leaching, and availability of PTEs. This information is essential for assessing material reuse and land application options. It is expected that LEAF will be similarly beneficial, relative to sequential fractionation methods (e.g., Hedley), when applied to soils and other relevant matrices.

3.5 References

Abdala, D.B., da Silva, I.R., Vergütz, L., Sparks, D.L., 2015. Long-term manure application effects on phosphorus speciation, kinetics and distribution in highly weathered agricultural soils. Chemosphere 119, 504–514. https://doi.org/10.1016/j.chemosphere.2014.07.029

Bolan, N.S., Hedley, M.J., 1990. Dissolution of phosphate rocks in soils. 2. Effect of pH on the dissolution and plant availability of phosphate rock in soil with pH dependent charge. Fertil. Res. 24, 125–134. https://doi.org/10.1007/BF01073580

Cade-Menun, B.J., Preston, C.M., 1996. A comparison of soil extraction procedures for 31P NMR spectroscopy. Soil Sci. 161, 770–785. https://doi.org/10.1097/00010694-199611000-00006

Chen, M., Ma, L.Q., 2001. Taxonomic and Geographic Distribution of Total Phosphorus in Florida Surface Soils. Soil Sci. Soc. Am. J. 65, 1539–1547. https://doi.org/10.2136/sssaj2001.6551539x

Condron, L.M., Frossard, E., Tiessen, H., Newmans, R.H., Stewart, J.W.B., 1990. Chemical nature of organic phosphorus in cultivated and uncultivated soils under different environmental conditions. J. Soil Sci. 41, 41–50. https://doi.org/10.1111/j.1365-2389.1990.tb00043.x

Cross, A.F., Schlesinger, W.H., 1995. A literature review and evaluation of the. Hedley

fractionation: Applications to the biogeochemical cycle of soil phosphorus in natural ecosystems. Geoderma 64, 197–214. https://doi.org/10.1016/0016-7061(94)00023-4

Element, C., 2007. SW-846 Method 3051A: Microwave Assisted Acid Digestion of Sediments, Sludges, Soils, and Oils.

Element Symbol CAS Number, 2007. Method 6010C Inductively Coupled Plasma-Atomic Emission Spectrometry. Cincinnati, Ohio.

Fang, W., Wei, Y., Liu, J., 2016. Comparative characterization of sewage sludge compost and soil: Heavy metal leaching characteristics. J. Hazard. Mater. 310, 1–10. https://doi.org/10.1016/j.jhazmat.2016.02.025

Frossard, E., Tekely, P., Grimal, J.Y., 1994. Characterization of phosphate species in urban sewage sludges by high-resolution solid-state 31P NMR. Eur. J. Soil Sci. 45, 403–408. https://doi.org/10.1111/j.1365-2389.1994.tb00525.x

Gerdes, P., Kunst, S., 1998. Bioavailability of phosphorus as a tool for efficient P reduction schemes, in: Water Science and Technology. Elsevier Sci Ltd, pp. 241–247. https://doi.org/10.1016/S0273-1223(98)00076-6

Gikonyo, E.W., Zaharah, A.R., Hanafi, M.M., Anuar, A.R., 2011. Degree of phosphorus saturation and soil phosphorus thresholds in an ultisol amended with triple superphosphate and phosphate rocks. ScientificWorldJournal. 11, 1421–1441. https://doi.org/10.1100/tsw.2011.131

González Medeiros, J.J., Pérez Cid, B., Fernández Gómez, E., 2005. Analytical phosphorus fractionation in sewage sludge and sediment samples. Anal. Bioanal. Chem. 381, 873–878. https://doi.org/10.1007/s00216-004-2989-z

Guggenberger, G., Christensen, B.T., Rubaek, G., Zech, W., 1996. Land-use and fertilization effects on P forms in two European soils: resin extraction and 31P-NMR analysis. Eur. J. Soil Sci. 47, 605–614. https://doi.org/10.1111/j.1365-2389.1996.tb01859.x

Han, X., Wang, F., Zhou, B., Chen, H., Yuan, R., Liu, S., Zhou, X., Gao, L., Lu, Y., Zhang, R., 2019. Phosphorus complexation of sewage sludge during thermal hydrolysis with different reaction temperature and reaction time by P K-edge XANES and 31P NMR. Sci. Total Environ. 688, 1–9. https://doi.org/10.1016/j.scitotenv.2019.06.017

Hartikainen, H., Yli-Halla, M., 1996. Solubility of soil phosphorus as influenced by urea. Zeitschrift für Pflanzenernährung und Bodenkd. 159, 327–332. https://doi.org/10.1002/jpln.1996.3581590403

Hartmann, T., Wollmann, I., You, Y., Müller, T., 2019. Sensitivity of Three Phosphate Extraction Methods to the Application of Phosphate Species Differing in Immediate Plant Availability. Agronomy 9, 29. https://doi.org/10.3390/agronomy9010029

Hedley, M.J., Stewart, J.W.B., 1982. Method to measure microbial phosphate in soils. Soil Biol. Biochem. 14, 377–385. https://doi.org/10.1016/0038-0717(82)90009-8

Hedley, M.J., Stewart, J.W.B., Chauhan, B.S., 1982. Changes in Inorganic and Organic Soil Phosphorus Fractions Induced by Cultivation Practices and by Laboratory Incubations. Soil Sci. Soc. Am. J. 46, 970–976. https://doi.org/10.2136/sssaj1982.03615995004600050017x

Huang, X.-L., Chen, Y., Shenker, M., 2008. Chemical Fractionation of Phosphorus in Stabilized Biosolids. J. Environ. Qual. 37, 1949–1958. https://doi.org/10.2134/jeq2007.0220

Ivanov, K., Zaprjanova, P., Petkova, M., Stefanova, V., Kmetov, V., Georgieva, D., Angelova, V., 2012. Comparison of inductively coupled plasma mass spectrometry and colorimetric determination of total and extractable phosphorus in soils, in: Spectrochimica Acta - Part B Atomic Spectroscopy. Elsevier, pp. 117–122. https://doi.org/10.1016/j.sab.2012.05.013

Iyamuremye, F., Dick, R.P., Baham, J., 1996. Organic amendments and phosphorus dynamics: II. distribution of soil phosphorus fractions. Soil Sci. 161, 436–443. https://doi.org/10.1097/00010694-199607000-00003

Jalali, M., Ostovarzadeh, H., 2009. Evaluation of phosphorus leaching from contaminated calcareous soils due to the application of sheep manure and ethylenediamine tetraacetic acid. Environ. Earth Sci. 59, 441–448. https://doi.org/10.1007/s12665-009-0042-4

Jiang, L., Yin, C., Liang, B., 2016. Effects of environmental pH on phosphorus leaching characteristics of phosphate waste rock deposited within Xiangxi River watershed. Chinese J. Environ. Eng. 10, 2674–2680. https://doi.org/10.12030/j.cjee.201511004

Jiang, L.G., Liang, B., Xue, Q., Yin, C.W., 2016. Characterization of phosphorus leaching from phosphate waste rock in the Xiangxi River watershed, Three Gorges Reservoir, China. Chemosphere 150, 130–138. https://doi.org/10.1016/j.chemosphere.2016.02.008

Johnson, A.H., Frizano, J., Vann, D.R., 2003. Review: Biogeochemical implications of labile phosphorus in forest soils determined by the Hedley fractionation procedure. Oecologia 135, 487–499. https://doi.org/10.1007/s00442-002-1164-5

Johnston, A., Steen, I., 2002. Understanding phosphorus and its use in agriculture. European Fertilizer Manufacturers Association, Brussels.

Koopmans, G.F., Chardon, W.J., McDowell, R.W., 2007. Phosphorus Movement and Speciation in a Sandy Soil Profile after Long-Term Animal Manure Applications. J. Environ. Qual. 36, 305–315. https://doi.org/10.2134/jeq2006.0131

Kosson, D.S., Garrabrants, A., Thorneloe, S., Fagnant, D., Helms, G., Connolly, K.,

Rodgers, M., 2017. Leaching Environmental Assessment Framework (LEAF) How-To Guide: Understanding the LEAF Approach and How and When to Use It. Nashville, TN.

Kosson, D.S., Garrabrants, A.C., DeLapp, R., van der Sloot, H.A., 2014. PH-dependent leaching of constituents of potential concern from concrete materials containing coal combustion fly ash. Chemosphere 103, 140–147. https://doi.org/10.1016/j.chemosphere.2013.11.049

Lehmann, J., Kleber, M., 2015. The contentious nature of soil organic matter. Nature. https://doi.org/10.1038/nature16069

Linquist, B.A., Singleton, P.W., Cassman, K.G., 1997. Inorganic and organic phosphorus dynamics during a build-up and decline of available phosphorus in an ultisol. Soil Sci. 162, 254–264. https://doi.org/10.1097/00010694-199704000-00003

Maguire, R.O., Sims, J.T., 2002. Soil Testing to Predict Phosphorus Leaching. J. Environ. Qual. 31, 1601–1609. https://doi.org/10.2134/jeq2002.1601

Neyroud, J.-A., Lischer, P., 2003. Do different methods used to estimate soil phosphorus availability across Europe give comparable results? J. Plant Nutr. Soil Sci. 166, 422–431. https://doi.org/10.1002/jpln.200321152

Pansu, M., Gautheyrou, J., 2007. Handbook of soil analysis: mineralogical, organic and inorganic methods. Springer Science & Business Media.

Pfaff, J.D., 1993. Method 300.0 Determination of Inorganic Anions by Ion Chromatography. Cincinnati, Ohio.

Qian, T.T., Jiang, H., 2014. Migration of phosphorus in sewage sludge during different thermal treatment processes. ACS Sustain. Chem. Eng. 2, 1411–1419. https://doi.org/10.1021/sc400476j

Schoumans, O.F., Groenendijk, P., 2000. Modeling Soil Phosphorus Levels and Phosphorus Leaching from Agricultural Land in the Netherlands. J. Environ. Qual. 29, 111–116. https://doi.org/10.2134/jeq2000.00472425002900010014x

Self-Davis, M., Moore Jr, P., 2000. Determining water-soluble phosphorus in animal manure, in: Soil Sampling and Methods of Analysis. Raleigh, NC, pp. 74–76.

Smith, S.R., Triner, N.G., Knight, J.J., 2002. Phosphorus Release and Fertiliser Value of Enhanced-Treated and Nutrient-Removal Biosolids. Water Environ. J. 16, 127–134. https://doi.org/10.1111/j.1747-6593.2002.tb00383.x

Soinne, H., 2009. Extraction methods in soil phophorus characterisation- Limitations and applications. University of Helsinki, Helsinki, Finland.

Telliard, W., 2001. Method 1684: Total, fixed, and volatile solids in water, solids, and

biosolids. Washington.

Thygesen, A.M., Wernberg, O., Skou, E., Sommer, S.G., 2011. Effect of incineration temperature on phosphorus availability in bio-ash from manure. Environ. Technol. 32, 633–638. https://doi.org/10.1080/09593330.2010.509355

Tiessen, H., Moir, J., 1993. Characterization of available P by sequential extraction, in: Soil Sampling and Methods of Analysis. pp. 5–229.

Tiwari, M.K., Bajpai, S., Dewangan, U.K., Tamrakar, R.K., 2015. Suitability of leaching test methods for fly ash and slag: A review. J. Radiat. Res. Appl. Sci. 8, 523–537. https://doi.org/10.1016/j.jrras.2015.06.003

Turner, B.L., Cade-Menun, B.J., Condron, L.M., Newman, S., 2005. Extraction of soil organic phosphorus. Talanta 66, 294–306. https://doi.org/10.1016/j.talanta.2004.11.012

Turner, B.L., Haygarth, P.M., 2000. Phosphorus Forms and Concentrations in Leachate under Four Grassland Soil Types. Soil Sci. Soc. Am. J. 64, 1090–1099. https://doi.org/10.2136/sssaj2000.6431090x

Ulery, A.L., Graham, R.C., 1993. Forest Fire Effects on Soil Color and Texture. Soil Sci. Soc. Am. J. 57, 135–140. https://doi.org/10.2136/sssaj1993.03615995005700010026x

USEPA, 2012a. Method 1313: Liquid-Solid Partitioning as a Function of pH for Constituents in Solid Materials Using a Parallel Batch Extraction Procedure. Nashville, TN.

USEPA, 2012b. Method 1314: Liquid-Solid Partitioning as a Function of Liquid-to-Solid Ratio for Constituents in Solid Materials Using a Percolation Column Procedure. Nashville, TN.

Xu, H., He, P., Gu, W., Wang, G., Shao, L., 2012a. Recovery of phosphorus as struvite from sewage sludge ash. J. Environ. Sci. (China) 24, 1533–1538. https://doi.org/10.1016/S1001-0742(11)60969-8

Xu, H., Zhang, H., Shao, L., He, P., 2012b. Fraction distributions of phosphorus in sewage sludge and sludge ash. Waste and Biomass Valorization 3, 355–361. https://doi.org/10.1007/s12649-011-9103-5

Zhang, H., Kovar, J., 2009. Fractionation of soil phosphorus, in: Methods of Phosphorus Analysis for Soils, Sediments, Residuals, and Waters. pp. 50–60.

Zhang, Y., Chen, J., Likos, W.J., Edil, T.B., 2016. Leaching Characteristics of Trace Elements from Municipal Solid Waste Incineration Fly Ash, in: Geo-Chicago 2016. American Society of Civil Engineers, Reston, VA, pp. 168–178. https://doi.org/10.1061/9780784480168.018

Chapter 4

4 Phosphorus Recovery and Reuse Potential from Smouldered Sewage Sludge Ash

4.1 Introduction

Increases in the proportion of waste components being recycled and reused compared to landfilled are evidence of societal shifts towards more sustainable practices. Recent research and regulations have demonstrated growing interest in circular economies, with significant focus on making waste disposal processes more cyclic (Canadian Municipal Water Consortium, 2015; Donatello and Cheeseman, 2013b; Fang et al., 2020; Gorazda et al., 2017; Mayer et al., 2016; Mulchandani and Westerhoff, 2016). Resource recovery, in particular, for nutrients and metals, not only relieves the depletion of essential elements but can also have environmental and economic benefits for wastewater treatment plants (WWTPs) (Neczaj and Grosser, 2018). Phosphorus is a key opportunity. Required in large quantities to produce agricultural fertilizers (Mayer et al., 2016), global phosphate reserves are expected to be depleted in the upcoming decades (Fang et al., 2020; Li et al., 2016). Therefore, there is significant interest in exploring recovery methods to extract phosphorus and other limited resources from human waste streams. Currently at WWTPs, >90% of all phosphorus ends up concentrated in sewage sludge (Fang et al., 2020). For an average Canadian WWTP servicing 200,000 people, approximately 1300 tonnes of phosphorus is present in the sewage sludge annually (London, 2019a), making it an important reservoir and promising source of phosphorus recovery.

However, recovery and reuse of phosphorus from sludge remains a challenge for numerous reasons. For example, several concerns arise when considering the direct

application of sewage sludge as a fertilizer. High water and organic matter content, pathogens, and numerous compounds of concern in the sludge can require sludge processing prior to such use (Donatello & Cheeseman, 2013; Hossain et al., 2011). Thermal processes for managing sewage sludge are now common in the industry. For example, incinerating allows for volume reduction and contaminant destruction (Adam et al., 2009). However, the pre-drying required to facilitate sludge incineration makes the treatment process energy intensive and expensive (Khiari et al., 2004; Werther and Ogada, 1999).

Another emerging thermal option is 'STAR' (Self-Sustaining Treatment for Active Remediation). First shown to treat sewage sludge in 2016 (Rashwan et al., 2016), STAR is now a fully commercial technology applied regularly to remediate soil contaminated with hydrocarbons, tars, and emerging contaminants such as PFAS (Duchesne et al., 2020; Scholes et al., 2015; Switzer et al., 2009). STAR utilizes smouldering combustion, a flameless form of burning that occurs on the surface of a fuel within a porous media, for example, glowing red charcoal in a barbecue (Rein, 2016). The smouldering process burns the sludge, like an incinerator, but operates at lower temperatures, is more resistant to quenching, and is more energy efficient (Rashwan et al., 2016; Torero et al., 2020). To initiate smouldering, a heater provides short term, localized energy input to the system (Yermán, 2016). Then the injection of air (oxygen) creates a 'smouldering front' that propagates forward (in the direction of air flow) through the waste bed. This front involves numerous zones (drying, pyrolysis, oxidation, and cooling) (Torero et al., 2020). A positive local energy balance around the front, occurring when energy generation by fuel oxidation exceeds energy lost to endothermic process and lateral heat losses (Zanoni et al., 2019), allows the smouldering front to propagate with a steady velocity and in a 'self-sustaining'

manner (i.e., without additional, external energy input) (Switzer et al., 2009). This feature means that smouldering treatment ranks highly for energy efficiency metrics and sustainability rankings (Gerhard et al., 2020).

Smouldering can only occur within a porous fuel or fuels embedded in a porous medium. The porous matrix (1) increases the surface area for reaction, (2) creates pathways for oxygen to flow to the reaction, and (3) insulates the reaction thereby reducing heat losses (Ohlemiller, 1985; Torero et al., 2020). Smouldering has been shown to effectively treat high moisture content and low permeability fuels, including faeces (up to 75% moisture content by mass) (Yermán et al., 2015) and biosolids (up to 80% moisture content by mass) (Rashwan et al., 2016). For such fuels/wastes, silica sand is usually added to create the porous medium (Rashwan et al., 2016; Yermán et al., 2015). This works well but has the associated post-treatment challenges of (i) separating the sand from post-treatment ash (if elemental recovery is the goal), and (ii) potential large volumes of typically clean and dry sand requiring management. A second option involves adding granular biomass (e.g., woodchips, waste crushed carbon, nut shells) to sewage sludge prior to thermal treatment to supplement low calorific values and improve treatment (Feng et al., 2021; Gorazda et al., 2017; Kijo-Kleczkowska et al., 2016). The use of biomass for smouldering treatment of sewage sludge is not well studied (Torero et al., 2020; Wyn et al., 2020).

A recent study identified that smouldered sewage sludge ash is likely safe for landfilling (Feng et al., 2020). However, landfilling ignores the recovery potential of limited resources such as phosphorus (Donatello and Cheeseman, 2013a; Fang et al., 2020). Moreover, recovering potential toxic elements (PTEs) – such as chromium and zinc – from

sewage sludge ash has a twofold benefit of removing these PTEs from a pathway into the environment and providing value-added recovery (Westerhoff et al., 2015), especially from compounds present in high concentrations (Bosshard et al., 1996).

Leaching methods are often applied to extract metals from post-treatment waste ashes, including bioleaching (Bosshard et al., 1996; Wu and Ting, 2006; Xu et al., 2014; Yang et al., 2009), chemical leaching (Gorazda et al., 2017; Petzet et al., 2012; Stark et al., 2006; Wu and Ting, 2006), and water-washing (Wang et al., 2001). Element extraction from ashes is a crucial first step towards recovery since it dictates the quantity available (Fang et al., 2020). Although several studies have assessed the recovery potential from incinerated sewage sludge ash (Krüger and Adam, 2014; Petzet et al., 2012; Schaum et al., 2007), it is novel to evaluate the recovery opportunities from smouldered sewage sludge ash.

This paper examines opportunities for recovering phosphorus from smouldered sewage sludge ash for potential reuse. This research seeks to explore the effects of bulking with (1) sand and with (2) particulate organic wastes (such as woodchips, herein referred to as 'co-smouldering'). Total elemental contents of ashes from both systems were determined and compared to Canadian land application guidelines to explore the suitability of each for direct land application. A combination of pH-dependent leaching tests and column percolation experiments, following USEPA Leaching Environmental Assessment Framework (LEAF) Methods 1313 (USEPA, 2012a) and 1314 (USEPA, 2012b), were used to explore the land application potential and extraction potential of the post-treatment ashes. This work progresses smouldering towards a more sustainable and cyclic process that produces beneficial by-products and helps preserve the environment. In addition, the

practical considerations for reuse and recovery from the post-treatment materials support further scaling the smouldering treatment to commercial applications.

4.2 Materials and Methods

4.2.1 Smouldering Experiments

4.2.1.1 Treatment System

The STAR reactor set-up and instrumentation followed established smouldering research methods fully described elsewhere (Rashwan, 2020; Rashwan et al., 2021b). Briefly, smouldering tests were performed in a cylindrical, stainless-steel reactor, with outer dimensions of 1.0 m height and 0.6 m diameter (see Figure B.1-1, Appendix B.1 for the full reactor set-up). The reactor was wrapped in 5.10 cm thick insulation (ASTM C518 R-Value = 9.6 at 24°C, FyreWrap® Elite® Blanket, Unifrax) to best represent field (low heat loss) conditions. The reactor was on a load cell (KD1500, Mettler Toledo) to measure moisture loss and the sludge destruction rate in real time. Thermocouples (Type K, 0.0064 m diameter Kelvin Technologies) installed along the full height of the reactor recorded process temperatures. A continuous emissions monitoring system (CEMS, ABB Ltd.) measured CH_4, CO_2, CO, and unburned hydrocarbons. The CEMS and mass balance data were recorded every 5 and 2 seconds, respectively. All other instruments were connected to a data logger (Multifunction Switch/Measure Unit 34980A, Agilent Technologies) and personal computer that logged every 3 seconds.

4.2.1.2 Sludge Mixed with Sand (“Sludge/Sand”)

Sludge was collected from Greenway Wastewater Treatment Plant (Greenway), London, Canada. The sludge had a volatile matter content of 61.0% (ASTM-D5832-98),

ash content of 27.5% (ASTM-D2866-11), and fixed carbon content of 11.4% (calculated as the difference), all on a dry-mass basis. An established method of sludge processing for laboratory experiments was employed (Fournie et al., 2021; Rashwan et al., 2016) and is briefly summarized below. Two experimental preparation methods have been used prior to smouldering treatment, (1) batch drying the sewage sludge (Rashwan et al., 2016) and (2) immediate use of unprocessed sewage sludge (Rashwan, 2020). The first was used for the sludge/sand test and the second for the sludge/woodchips test. Both methods result in statistically similar smouldering behaviour and performance (Rashwan, 2020) and is therefore not expected to influence any results or conclusions.

For the sludge/sand test, the sludge was batch dried in an oven at 105°C, achieving a moisture content of 3.81% (ASTM-D267-17). Coarse silica sand (1.180 ≤ mean grain diameter ≤ 2.000 mm, porosity = 0.37, bulk density = 1670 kg/m^3, Number 12, Bell & Mackenzie) was mixed with processed sludge as is typical for industrial smouldering treatments. For this experiment, 8.53 kg of sludge was mechanically mixed with 218 kg of coarse silica sand to achieve a sand-to-sludge ratio of 25.5:1 on a dry-mass basis. If the sludge had not been dried, the sand-to-sludge ratio would have been 6.5:1 on a wet-mass basis which has been shown to result in self-sustaining smouldering (Rashwan et al., 2021a) The mixture was prepared in small batches of ~22 kgs in a mechanical mixer before being transferred to sealed 19 L buckets for storage prior to loading. This methodology provided a homogeneous sludge sample that was stable over time.

On the experiment day, the sludge mixture was carefully added into the reactor in a way that ensure homogeneity and limited material compaction (Appendix B.1). The emptied buckets were reweighed to account for any material retained during packing. A

clean sand cap (3 – 6 cm thick) was added on top of the sludge pack as done in commercial applications. Air was injected into the reactor base at a Darcy flux of 5.0 cm/s throughout the test via a mass flux controller (8290B045PDB67 ASCO Numatics). An inline air heater (F074736 36 kW SureHeat® MAX, Osram Sylvania), operated at 300 – 400°C from the beginning of the test, provided convective ignition of smouldering as is done in the field (Solinger et al., 2020). The experiment required ~61 min for ignition (~34 min to increase the heater temperature and an additional ~27 min preheat). Smouldering of the sludge was confirmed when the first thermocouple within the contaminant pack peaked at 480°C (Figure B.1-2, Appendix B.1). Following ignition, the heater was turned off and ambient air was injected into the reactor, supporting a self-sustaining smouldering reaction propagating up the reactor. The reaction velocity was 0.38 cm/s ± 10% and the average centreline peak temperature was 525°C ± 4%, which are representative of laboratory and field applications (Torero et al., 2020; Wyn et al., 2020). The experiment was complete and self-terminated once the smouldering front reached the end of the contaminant pack (after 180 minutes). The emissions data aligned with what is typically observed during smouldering (Wyn et al., 2020) and showed that smouldering was robust, and the fuel was fully oxidized. These results were confirmed upon excavation.

The post-treatment bed consisted of coarse silica sand (conserved during treatment) and sewage sludge ash. Dry sieving separated them, with sand grains quantified as >0.250 mm (#60 ASTM sieve) and ash quantified as the finer inert mass. The sand summed to 26.5 kg while ash comprised 0.56 kg (97.9% and 2.1% of post-treatment materials, respectively).

4.2.1.3 Sludge Mixed with Woodchips ("Co-Smouldering")

The woodchips utilized in the co-smouldering tests were obtained from construction waste material (BRQ Fibre et Broyure Inc., Trois Rivieres, QC) (Cuthbertson, 2018; Rashwan et al., 2021b). Proximate analysis determined that woodchips had a moisture content of 10.9% (ASTM-D267-17), volatile matter content of 77.6% (ASTM-D5832-98), ash content of 10.7% (ASTM-D2866-11), and fixed carbon content of 11.8% (calculated as the difference), all on a dry-mass basis.

The moisture content of the virgin sewage sludge was 74.8%. For the smouldering test, 40.8 kg of sewage sludge was mechanically mixed with 16.0 kg of woodchips and 12.1 kg of water to achieve a ratio of woodchips: extra water: sludge of 0.4: 0.3: 1. The addition of water partially reconstituted the sludge to better understand the limits of the fuel moisture content that would still promote self-sustaining smouldering. The ability to smoulder higher moisture content fuels is important since it reduces the energy cost associated with dewatering. Mixing procedures were performed in batches of 6 kg. Loading the reactor followed the same process as other tests (Appendix B.1).

Ignition by convection was completed in 58 min (~39 min to increase the heater temperature and an additional ~19 min preheat). The heating period caused moisture loss via evaporation and boiling, only in the bottom ~2 cm of the 45 cm tall bed. As expected, – and in contrast to the sludge/sand test – the front did not migrate up the column. Instead, the self-sustained reaction slowly consumed the base of the pack – since it was nearly entirely smoulderable – and the pack steadily shrunk downwards. The experiment was complete after 280 minutes, when the fuels were completely consumed (Figure B.1-3, Appendix B.1). The average centreline temperature was 812°C ± 4%. The post-treatment

ash was 20% of the initial mass of the mixture (i.e., 13.5 kg), and was estimated to comprise 87% sludge ash and 13% woodchip ash. Since a single post-treatment ash was produced, no sieving was required prior to analysis. The top sand cap was not used in this experiment.

4.2.2 Analytical Materials and Methods

The chemical composition of the solids and elemental concentrations in all extracts were determined using an Agilent 720 Inductive Coupled Plasma Optical Emission Spectrometer (ICP-OES) (Agilent Technologies). Analyses were conducted in accordance with standard procedures, including quality control/quality assurance, outlined by USEPA Method 6010D (Element Symbol CAS Number, 2007). Solids were analyzed after acid extraction with a 3:1 ratio of concentrated nitric acid (HNO_3) and hydrochloric acid (HCl), assisted by microwave digestion (170 °C for 10 min in a CEM MARS 6® Microwave Accelerated Reactor System, MFR) according to USEPA Method 3051A (Element, 2007).

Inorganic phosphorus was measured as dissolved orthophosphate (PO_4^{3-}), the most reactive form of inorganic phosphorus, which is readily soluble and therefore easily utilized by plants (Johnston et al., 2014). High-Performance Liquid Chromatography (HPLC) was used to quantify PO_4^{3-} via direct injection using a Water® 515 pump following the standard procedure outlined by USEPA Method 300 (J. D. Pfaff, 1993).

Elements analyzed by ICP-OES included phosphorus, aluminum, cadmium, cobalt, chromium, copper, iron, magnesium, manganese, molybdenum, nickel, lead, and zinc, all of which are regulated at WWTPs in Ontario, Canada. For reuse applications, cadmium, cobalt, chromium, copper, molybdenum, nickel, lead, and zinc are also regulated under Ontario Regulation 338/09 (O. Reg. 338) from the Nutrient Management Act (2002). O.

Reg. 338 classifies sewage sludge as a category 3 non-agricultural source material (NASM) and sets guideline values for reuse applications. CM1 is the most stringent set of NASM guideline values in the O. Reg. 338 guideline.

4.2.3 pH-Dependent Leaching Tests (USEPA Method 1313)

This study conducted a series of batch extractions on 5 pre- and post-treatment materials following USEPA Method 1313, measuring phosphorus and 12 other PTEs in the extracts. USEPA Method 1313 consists of 9 parallel batch extractions to produce a liquid-solid partitioning curve of the material of interest over eluate pH range $2 \leq pH \leq 13 \pm 0.5$ (USEPA, 2012a). Briefly, for each extraction, 10 g of material was combined with 100 mL of extraction solution that consisted of deionized water with varied amounts of either 2 N nitric acid (HNO_3) or 1 N potassium hydroxide (KOH) to achieve the 9 specified target pH values. All extractions took place over 24 hours to achieve equilibrium between the solid and liquid phases. The pH and electrical conductivity of the supernatants were measured, and eluate samples were filtered and preserved for further analysis.

4.2.4 Column Percolation Tests (USEPA Method 1314)

Percolation tests were also conducted on 3 materials to measure phosphorus and 12 other PTEs using the USEPA Method 1314. This method uses a percolation column experiment to evaluate constituent release from the material of interest as a function of the liquid-to-solid ratio (L/S) (USEPA, 2012b). A full description of the process has been described elsewhere (Fournie et al., 2021). Briefly, 300 g of pulverized, air-dried sample is packed into a 30 cm tall glass column. Deionized water was injected using a Masterflex® L/S® digital peristaltic pump with flow moving upwards through the column. Prior to continuous percolation, the column was rested for 24 hours in a fully saturated state. After

the rest period, the flow rate of the water through the column was maintained at 0.75 ± 0.5 L/S per day to collect the nine eluate samples (T01-T09) at liquid-to-solid ratios of 0.2, 0.5, 1.0 ± 0.1, and 1.5, 2.0, 4.5, 5.0, 9.5, 10.0 ± 0.2 mL/g-dry matter. Each eluate sample was analyzed for pH and conductivity using a Fisher Scientific Accumet® AB200 pH/mV/Conductivity meter within one hour of sample collection. Subsamples were filtered and preserved with 1 N nitric acid for further analysis.

4.2.5 Extraction Potential

For this study, extraction potential was defined as the elemental concentration in the extracted supernatant divided by the total elemental concentration within the solids. Extractions were performed following the procedures outlined in section 2.3, under three pH conditions: native, acidic (pH 2 ± 0.5), and alkaline (pH 13 ± 0.5). Water washing was used for the extraction under native pH conditions, 2 N HNO_3 for acid extraction, and 1 N KOH for alkaline extraction. The total elemental contents for each material were determined according to section 2.2. Extraction potentials, initially determined as percentages, were converted to a mass of potentially extractable element per mass of material (results presented in Table B.2-1, Appendix B.2). This was done using a mass balance of the pre- and post-treatment materials. All extraction potential results were normalized in terms of kg of virgin sludge to allow comparison between samples. Subsequently, each element was identified as either solubility- or availability-limited by plotting cumulative element release as a function of the liquid-to-solid ratio measured in Method 1314 on a log-log scale (Kosson et al., 2017).

Table 4.1: Material composition and experimental data

Experiment		Units	Sludge & Sand		Sludge & Woodchips		
Proximate Analysis							
			Sludge	Mixture	Sludge	Woodchips	Mixture
Moisture Content [a]		%	3.81	3.22	74.8	10.9	65.4
Volatile Matter [b]		% (dry basis)	61.0	-	62.7	77.6	-
Ash Content [c]		% (dry basis)	27.5	26.6	28.8	10.7	20.0
Fixed Carbon [d]		% (dry basis)	11.4	-	8.53	11.8	-
Experimental Data							
			Sand: Sludge		Woodchips: Extra Water [e]: Sludge		
Mixture Ratio	Wet Basis	(g/g)	6.5: 1		0.4: 0.3: 1		
	Dry Basis	(g/g)	25.5: 1		-		
Mass of Materials Added	Sludge	kg	8.5		39.4		
	Sand	kg	217.7		-		
	Woodchips	kg	-		16.0		
	Water	kg	-		12.1		
Air Flux		cm/s	5.5		2.5 – 5.0		
Average Centreline Temperature		°C	525 [f]		812 [f]		

[a] Determined according to ASTM-D267-17
[b] Determined according to ASTM-D5832-98
[c] Determined according to ASTM-D2866-11
[d] Calculated as the difference
[e] Water was added to the fuel mixture to reduce treatment temperatures
[f] The thermocouple temperature results have an associated error of ± 4%

4.3 Results and Discussion

4.3.1 Material Characterization

Smouldering resulted in the 75 ± 3% mass reduction of sludge (i.e., 25 ± 3% ash content and the rest organic material that was oxidized). For the sludge/sand test, sand comprised 85% of the pre-treatment mixture by mass (sludge was 15%) and the sand mass was conserved during smouldering. The average temperature during 180 minutes of smouldering was 525°C ± 4% (Figure B.1-2, Appendix B.1). The post-treatment mixture comprised 98% sand and 2% ash. The phosphorus content initially present in the sludge was 26,000 mg/kg-dry sludge, split 57/43 (± 5%) as organic/inorganic. Following smouldering of the sludge/sand, 78% of phosphorus was retained by solids and the other 22% was potentially recoverable from process emissions. In the solids, 39% of phosphorus was retained in ash, split 7/93 (± 11%) organic/inorganic, and 30% retained in sand, split 49/51 (± 6%) organic/inorganic. When smouldering sludge with sand, total phosphorus was not conserved. Inorganic phosphorus seems to be conserved and potentially increased by transformation of organic phosphorus.

For the co-smouldering test, the woodchips comprised 23% of the pre-treatment mixture, sludge was 59%, and water was 18%. This test experienced higher energy smouldering (due to increased fuel loading), with average peak temperatures of 812°C ± 4% (Figure B.1-3, Appendix B.1). The temperatures were more similar to temperatures observed during sludge incineration. The post-treatment mixture (herein referred to as ‘mixed ash’) was 20% of the initial mass (i.e., 20% ash content). Initial phosphorus was 19,000 mg/kg-dry starting material in the co-smouldering test, diluted in comparison to the test with sand because of much higher water content and addition of woodchips. After the

higher energy combustion, 22% of phosphorus (split 32/68 ± 13% organic/inorganic) was retained in mixed ash and 78% was recoverable from process emissions.

Concentrations of the 12 quantified PTEs are presented in Table 2. The PTE concentrations are presented on a dry-mass basis for direct comparison to the O. Reg. 338 NASM CM1. All 12 PTEs were detected in all materials. However, PTE concentrations within sand were very low, 1 – 4% of the concentration originally present in the sludge. Concentrations in ash were often higher than those in virgin sludge (aluminum, cobalt, chromium, copper, magnesium, manganese, molybdenum, nickel, lead, and zinc) on this basis because smouldering reduced total mass by nearly 80%, which had a concentrating effect on elements not released to emissions or retained by sand. With negligible PTE content in the sand prior to smouldering, the observed PTE concentrations were likely contributed by ash retention within the sand fraction during dry sieve separation and/or condensation onto sand surfaces. However, because of its large mass in the system, sand provided an important sink for some elements such as lead, nickel, and chromium (Table B.2-2, Appendix B.2), reducing their total content in ash. The PTE concentrations in the mixed ash were lower than the virgin sludge for 10 of the 12 elements (aluminum, cadmium, cobalt, chromium, copper, iron, molybdenum, nickel, lead, and zinc) by 30 – 70%. The reduced PTE concentrations in the mixed ash were likely due to dilution by the woodchips and release to emissions via the higher energy smouldering.

When considered on a dry-sludge basis, total elemental contents between the materials are similar (Figure B.2-1, Appendix B.2). Essentially complete retention of aluminum, cobalt, chromium, manganese, nickel, and lead by bottom ash (i.e., material retained in the reactor) was observed with 100% retained in ash and sand (Table B.2-2,

Appendix B.2). Less than complete retention was observed for cadmium (87%), copper (67%), iron (60%), magnesium (74%), molybdenum (56%), phosphorus (69%), and zinc (93%), suggesting availability for recovery via emissions. For the mixed ash, low retention in the bottom ash is observed for all elements; aluminum (15%), cadmium (15%), cobalt (28%), chromium (14%), copper (25%), iron (14%), magnesium (29%), manganese (27%), molybdenum (11%), nickel (17%), phosphorus (22%), lead (6%), and zinc (22%) (Table B.2-3, Appendix B.2). These elements are available for recovery via emissions capture, which is commonly employed for incinerators (Cieślik and Konieczka, 2017). Lower retention in mixed ash was likely the result of (1) increased volatilization due to the higher energy smouldering (see Table 4.1), and (2) physical mobilization of elements in the exhaust gas.

The O. Reg. 338 NASM CM1 (Government of Ontario, 2009) PTE thresholds for land application are given in Table 4.2. Based on the guidelines, copper, molybdenum, nickel, and zinc were exceeded in the sludge, ash, or both. Conversely, cadmium, cobalt, chromium, and lead were not exceeded in any material. Only copper and molybdenum were exceeded in the mixed ash. Sludge and ash exceeded the guideline values for copper, molybdenum, zinc, and ash additionally exceeded for nickel. The current land application guidelines under O. Reg. 338 specify the maximum quantity of total regulated PTEs that can be added to a specific area of soil in a 5-year period (Government of Ontario, 2009). If the amount of ash required for land application is lowered because of well-regulated phosphorus, these exceedances may be avoidable. The following sections discuss reuse options for the smouldered ash via land application and alternatively, extraction of elements from the ash to subsequently recycle.

Table 4.2: Total elemental concentrations

Element	Concentration (mg/kg-dry matter) ± SE[a]						Regulatory standard O. Reg. 338: NASM CM1 (mg/kg-dry mass)
	Sludge	Woodchips	Ash [b]	Mixed Ash [c]	Woodchip Ash [d]	Sand [e]	
Target							
P	26000 ± 3000	480 ± 90	43000 ± 6000	13000 ± 20	970 ± 20	290 ± 50	
PTEs							
Al	5400 ± 300	1100 ± 400	13000 ± 1000	2400 ± 90	3200 ± 600	300 ± 100	
Cd	2.6 ± 0.2	0.3 ± 0.4	2.0 ± 0.8	1.0 ± 0.1	1.2 ± 0.05	0.06 ± 0.01	3
Co	3.8 ± 0.3	0.4 ± 0.4	5.7 ± 1	2.8 ± 0.3	2.8 ± 0.3	0.15 ± 0.01	34
Cr	120 ± 10	34 ± 2	160 ± 40	53 ± 2	13 ± 10	4.2 ± 0.7	210
Cu	480 ± 40	16 ± 4	1500 ± 400	290 ± 7	23 ± 8	3.5 ± 2	100
Fe	53000 ± 5000	2100 ± 600	56000 ± 20000	18000 ± 1000	4200 ± 800	620 ± 200	
Mg	4200 ± 400	1600 ± 300	9000 ± 1000	4200 ± 90	2900 ± 500	37 ± 13	
Mn	260 ± 30	200 ± 40	690 ± 50	330 ± 9	540 ± 30	4.1 ± 1	
Mo	22 ± 2	1.4 ± 0.6	26 ± 2	6.2 ± 0.3	3.7 ± 1	1.9 ± 0.3	5
Ni	47 ± 6	13 ± 2	87 ± 10	25 ± 1	25 ± 4	1.7 ± 0.2	62
Pb	110 ± 10	70 ± 10	110 ± 60	31 ± 4	29 ± 4	8.4 ± 0.2	150
Zn	630 ± 90	64 ± 30	1400 ± 500	350 ± 10	77 ± 7	7.8 ± 3	500

[a] Standard error calculated as $\frac{\sigma}{\sqrt{n}}$

[b] Ash is considered all materials from smouldering experiments of sand mixed with sludge finer than 0.250 mm (< #60 sieve)

[c] Post-treatment ash from co-smouldering experiments consisted of sludge mixed with woodchips

[d] Woodchip ash generated in the lab according to ASTM-D2866-11

[e] The sand is considered all materials from smouldering experiments of sand mixed with sludge coarser than 0.250 mm (> #60 sieve)

4.3.2 Suitability for Land Application

4.3.2.1 Phosphorus Availability and Release

Phosphorus release during column percolation, and pH-dependent availability from sludge, ash, and sand are shown in Figure 4.1. The values have been normalized in terms of mg of elemental release per kg of dry sludge (mg/kg – DS) so that all materials are weighted consistently based on starting material.

A large slug of phosphorus (60% of total release, 98% organic, <0.1% of total content) was immediately released from the sludge (Figure 4.1a). This initial release was followed by a significant decline, reaching a steady release after an L/S of 2 mL/g-dry. Most of the available phosphorus in the sludge was released early in the experiment, at low L/S. Of the cumulative phosphorus released from the sludge, 0.08% of total phosphorus, 74% was organic phosphorus and 26% was inorganic. Released phosphorus appears to be availability-limited as it reached an equilibrium within the duration of the experiment, which means that more phosphorus will not become available with additional water percolation alone (Figure B.3-1, Appendix B.3).

In contrast, a smaller initial slug, 81% organic, was released from the ash representing <0.001% of total phosphorus content in ash and <1% of total release (Figure 4.1a). The release profile transitioned to 36-59% inorganic phosphorus later in the test. Release never reached an equilibrium and seemed likely to continue releasing primarily inorganic phosphorus beyond the cumulative L/S of 10 mL/g-dry. Therefore, smouldering transformed phosphorus species into more solubility-limited forms (Figure B.3-1, Appendix B.3). Of the cumulative phosphorus released from the ash, 0.09% of total

phosphorus, 41% was organic phosphorus and 59% was inorganic. Over time, ash became a better source of inorganic phosphorus that is more valuable to plants. The available phosphorus from the ash was also primarily inorganic, composing 70-100% and varying with pH (Figure 4.1b). At native pH, ash had less available total and inorganic phosphorus compared to sludge at its native pH, i.e., pH 7.82 for the ash and 5.8 for the sludge. As pH changes, availability from ash increased by 4400 mg/kg – DS at pH 1.57 or 1800 mg/kg – DS at pH 13.

Release from the sand fraction showed similar patterns to both sludge and ash (Figure 4.1a). Initial phosphorus release from the sand, 88% organic, represents 0.2% of total phosphorus content in sand and 7% of total release. The normalized release from the sand was immediately higher than the ash and rapidly exceeded the release from the sludge between an L/S of 1 and 1.5 mL/g-dry. Of the cumulative phosphorus released from the sand (i.e., 2.4% of its total content), 90% was organic phosphorus and 10% was inorganic, suggesting a condensation effect on the sand. Some of the organic phosphorus that was volatilized during smouldering may condense within the cooler fixed sand bed ahead of the reactions, retaining a portion of it within the sand that would otherwise be released in the emissions. This was consistent throughout the experiment (88 – 90% organic and 10 – 12% inorganic) and further observed from the pH-dependent availability results (89 – 94% organic) (Figure 4.1b). Based on the release profile, sand seemed likely to continue to release phosphorus beyond the highest L/S in Figure 4.1a, thereby demonstrating a solubility-limited process similar to the ash. Furthermore, sand has minimal pH-dependence (Figure 4.1b), achieving a limited range of phosphorus availability, 440-770 mg/kg – DS, over environmental relevant pH conditions ($3.55<pH<10.98$).

Mixed ash was not evaluated for its applicability for land application because of its low retention of phosphorus (22%) (Table B.2-3, Appendix B.2), which translated to a low phosphorus availability (Figure B.3-5, Appendix B.3).

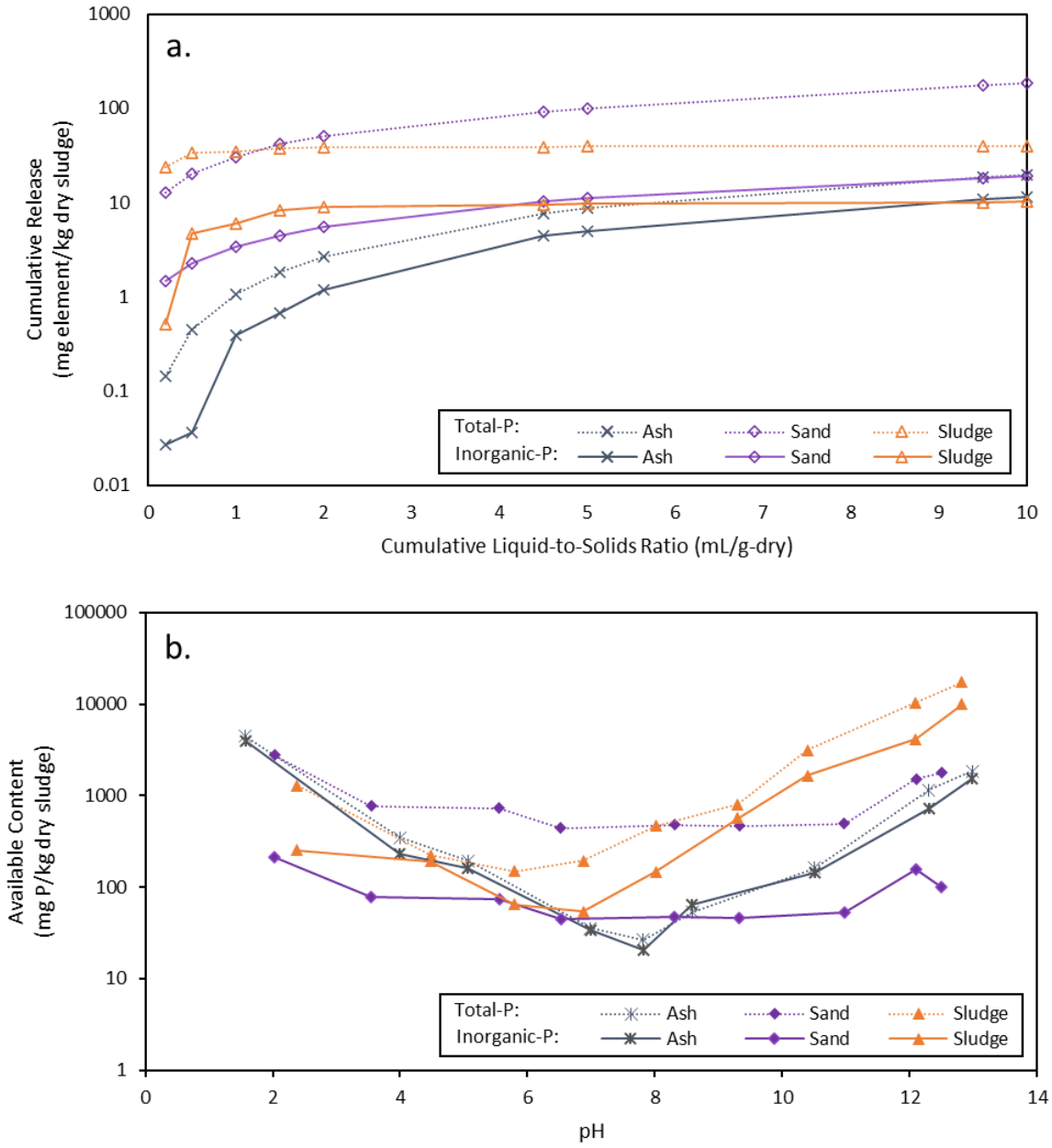

Figure 4.1: a. column percolation experimental results (following USEPA Method 1314), b. pH-dependent leaching (following USEPA Method 1313) of phosphorus from the virgin sludge and post-treatment ash and sand. The total phosphorus is shown with dotted lines and inorganic phosphorus with solid lines. All values have been normalized to mg of P per kg of dry sludge, and the release is presented as a function of the cumulative liquid-to-solids ratio.

4.3.2.2 Potentially Toxic Elements

Understanding the availability and leaching behaviour of PTEs is important for assessing the environmental impacts of disposal and/or reuse options for sludge and ash. Releases of 8 commonly regulated PTEs from the column percolation experiments are shown in Figure 4.2, and pH-dependent availabilities are shown in Figure 4.3.

Ash exhibited lower releases of 6 of 8 PTEs (Figure 4.2). Initial releases of cadmium, cobalt, copper, nickel, lead, and zinc from sludge exceeded those from ash by 93-99%, and cumulative releases from sludge exceeded ash by 50-96%. Of these, cobalt, copper, and nickel were availability-limited in the sludge (Figure 4.3). The lower relative pH of the sludge (pH 5.8) compared to the ash (pH 7.8), may explain the higher initial release of the availability-limited PTEs from the sludge since chemical changes would influence the release of these elements more than increased percolation (Figure B.3-2, Appendix B.3). While ash had higher total elemental concentrations compared to sludge (Table 4.2), higher total elemental concentrations did not translate to higher element releases. The relatively higher release of the other PTEs from the sludge than ash could be the result of mineralization during smouldering.

Releases of chromium and molybdenum, the two elements where release from ash exceeded that from sludge, were low from both materials. These two PTEs and lead were similar to or slightly more available from the ash than sludge under environmentally relevant conditions (i.e., pH 5.5 – 8.5; Figure 4.3). In contrast, availabilities of cobalt, copper, nickel, and zinc from sludge exceeded their availabilities from ash across the pH range most relevant to land application.

Although sand meets land application guidelines for PTEs (Table 4.2), a large mass of sand would be required to meet plant nutrient requirements, which would be labour intensive and costly. Moreover, operational challenges make direct land application of the sand infeasible. Wet sieving of sand to recover phosphorus is more practical and sequesters other PTEs, primarily lead, nickel, and chromium which are retained in the sand fraction. Therefore, the release and availability of other PTEs in the sand were not assessed here, but more information is available in the Appendix B.

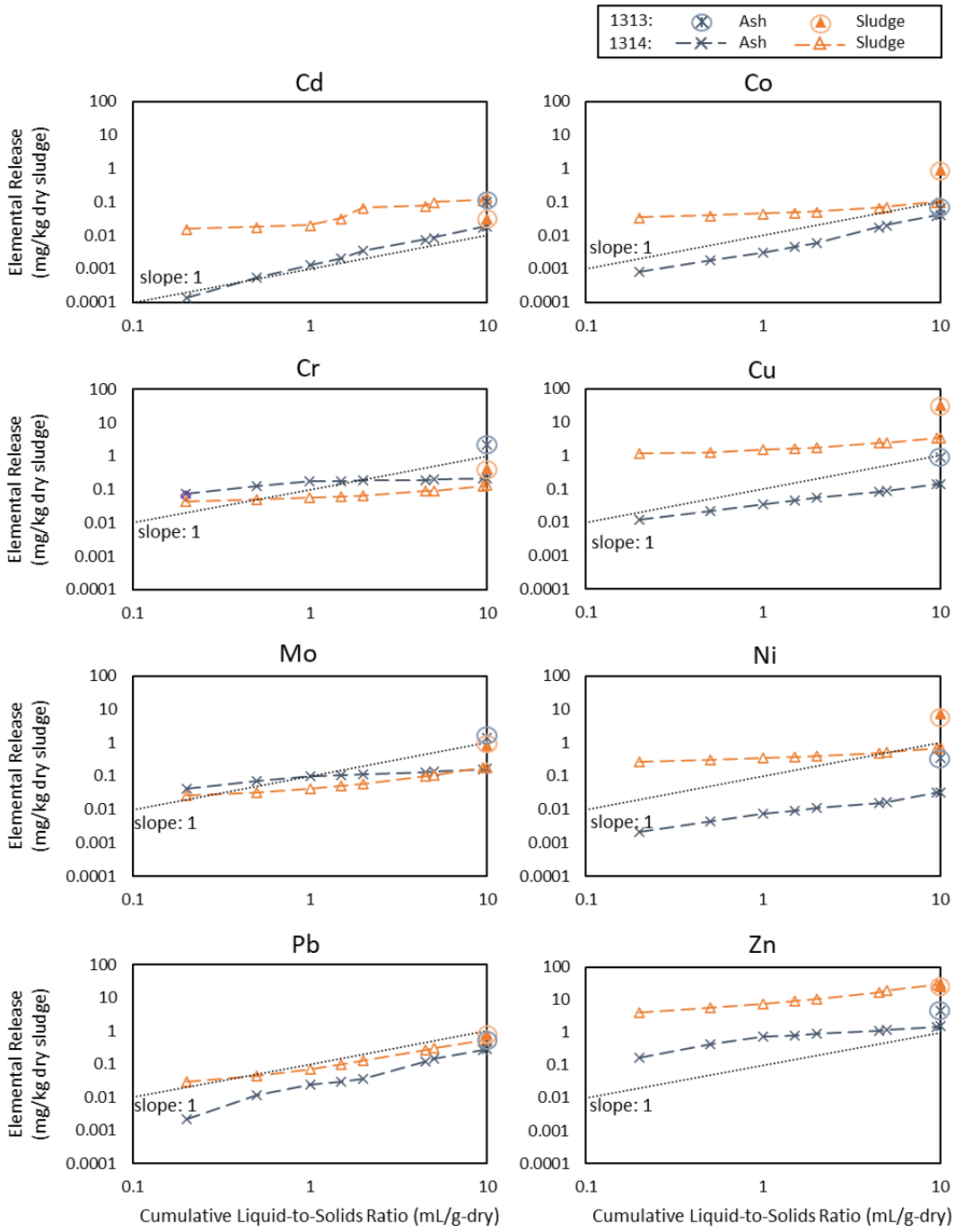

Figure 4.2: column percolation experimental results (following USEPA Method 1314) for 8 commonly regulated potentially toxic elements from the virgin sludge and post-treatment ash and sand. The elemental release is shown as cumulative release as a function of the liquid-to-solid ratio. The values have been normalized to mg of element per kg of dry sludge. The available content of the materials from USEPA Method 1313 at native pH has been plotted at an L/S of 10 mL/g-dry. A dotted line with a slope of 1 has been added to each plot. A slope of an element release curve near 1 demonstrates solubility-limited processes governing elemental release while a slope less than 1 demonstrates that availability-limited processes.

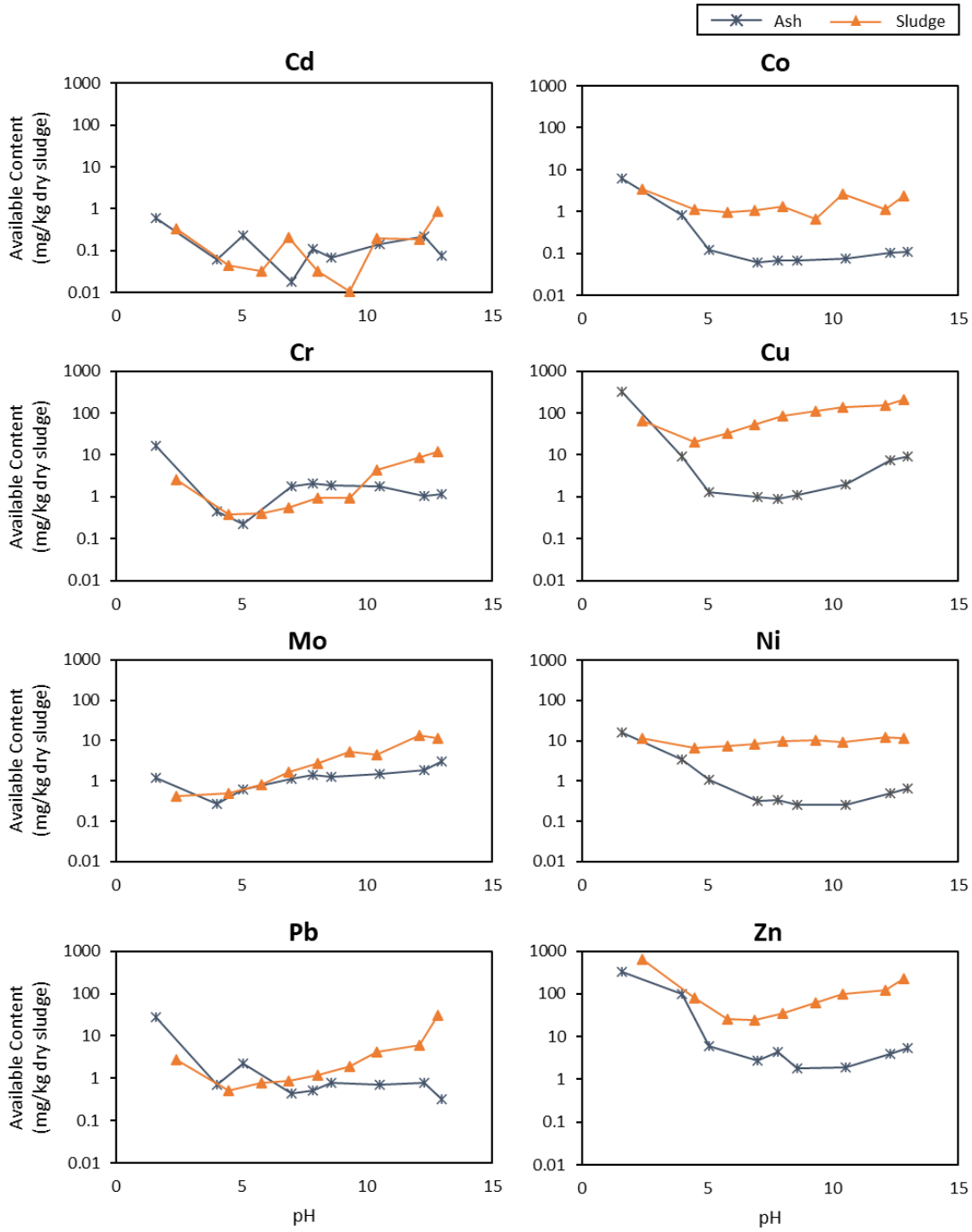

Figure 4.3: pH-dependent leaching (following USEPA Method 1313) of 8 potentially toxic elements from the virgin sludge compared to the post-treatment ash and sand. All values have been normalized to mg of phosphorus per kg of dry sludge.

4.3.3 Extraction Potential

The extraction potential of phosphorus from the sludge/sand test was determined for the post-treatment ash and sand using three different extractants and compared to virgin sludge (Table 4.3). A 10:1 L/S acidic extraction from ash and sand recovered 42% of initial phosphorus (10,900 mg/kg – initial sludge [IS]). The extractant solution was also enriched with iron (30%, 15,900 mg/kg – IS), magnesium (65%, 2730 mg/kg – IS), and aluminium (32%, 1730 mg/kg – IS) and contained measurable amounts of copper (60%, 290 mg/kg – IS), manganese (73%, 190 mg/kg – IS), zinc (22%, 140 mg/kg – IS), lead (32%, 35 mg/kg – IS), chromium (14%, 17 mg/kg – IS) and nickel (18%, 8.5 mg/kg – IS). The additional PTEs present in the extractant solution would likely require subsequent separation. All other measurable elements are below 15 mg/kg – IS. Phosphorus released from ash and sand were both solubility-limited (Figure 4.1); increasing the L/S above 10:1 could further increase the amount of phosphorus recovered from ash and sand. However, increasing the L/S would also increase PTE content in the solution, especially of cadmium, cobalt, lead, and zinc, which were all identified as solubility-limited (see Table 4.2).

Acidic extraction from sludge recovered only 5% of initial phosphorus (1300 mg/kg – IS) and is therefore not suitable on its own for phosphorus recovery. However, its high yields of PTEs from the initial sludge (magnesium (72%, 3020 mg/kg – IS), zinc (100%, 630 mg/kg – IS), and manganese (75%, 190 mg/kg – IS)) may make it attractive as a pre-treatment prior to smouldering or another recovery method. Phosphorus released from sludge is availability-limited (Figure 4.1), so increasing L/S would not provide much additional benefit.

Alkaline extraction from ash and sand recovered 19% of initial phosphorus (4940 mg/kg – IS) and was also enriched with aluminium (19%, 1030 mg/kg – IS). It also contained measurable amounts of iron (0.1%, 53 mg/kg – IS), copper (11%, 53 mg/kg – IS), and magnesium (0.4%, 17 mg/kg – IS). Although the phosphorus recovery was somewhat poor, the low abundance of other extractable elements may make it an attractive step in a more complex recovery effort.

Alkaline extraction from sludge recovered 68% of initial phosphorus (17,700 mg/kg – IS) and was also enriched with iron (11%, 5830 mg/kg – IS) and aluminium (60%, mg/kg – IS). The extractant solution also contained measurable amounts of magnesium (7%, mg/kg – IS), zinc (37%, 230 mg/kg – IS), copper (44%, 210 mg/kg – IS), manganese (16%, 42 mg/kg – IS), lead (27%, 30 mg/kg – IS), chromium (10%, 12 mg/kg – IS), nickel (26%, 12 mg/kg – IS), and molybdenum (55%, 12 mg/kg – IS). Subsequent separation of PTEs would likely be required, similar to acidic extraction from the ash. Water extraction was not a viable method for any material.

For the post-treatment materials (i.e., ash and sand): in addition to phosphorus recovery using either acidic or alkaline solutions, 30% of phosphorus could be recovered from the emissions stream. Emissions recovery could bring total phosphorus recovery from post-treatment materials to 70% with acidic extraction, and 50% with alkaline extraction.

For co-smouldering sludge and woodchips, the largest fraction of potentially recoverable phosphorus is from process emissions (78%). Both acidic and alkaline extractions from mixed ash provided some further recovery (Figure B.3-5, Appendix B.3). In particular, acidic extraction yielded a further 21% of initial phosphorus (2,500 mg/kg of

initial sludge/woodchip content [IS/WC]), bringing total phosphorus recovery to nearly 100%. Acidic extraction of mixed ash was also enriched in magnesium (32%; 850 mg/kg – IS/WC), iron (<1%; 190 mg/kg – IS/WC), zinc (24%; 72 mg/kg – IS/WC), aluminum (2.5%; 72 mg/kg – IS/WC), manganese (31%; 69 mg/kg – IS/WC), and copper (12%; 24 mg/kg – IS/WC). All other measurable elements were below 10 mg/kg – IS/WC. In contrast, alkaline extraction yielded only 2% additional phosphorus, making the total potentially recoverable phosphorus 80%. Alkaline extraction of mixed ash requires less additional separation of other elements. Only aluminum had significant presence in the extractant (3%; 96 mg/kg – IS/WC). All other PTEs were < 2 mg/kg – IS/WC. However, this benefit is small given its poor phosphorus yield at high pH. Therefore, the optimal method of phosphorus recovery from the mixed ash is via the process emissions combined with acidic extraction of the bottom ash.

Table 4.3: Extraction Potential from the Sludge and Sand with Ash

Element	Initial Content (mg/kg-dry matter) ± SE [a]	Percentage extracted from total content in sludge ± SE [a] (%)						
		Water [b]		pH 2 [c]		pH 13 [c]		
	Sludge	Sludge	Sand + Ash [d]	Sludge	Sand + Ash [d]	Sludge	Sand + Ash [d]	
Target								
P	26000 ± 3000	0.6 ± 0.06 [AL]	1.8 ± 0.4 [SL]	5 ± 0.5	42 ± 8	68 ± 7	19 ± 3	
High Recoverable Content (> 100 mg /kg-dry sludge)								
Fe	53000 ± 5000	0.1 ± 0.01 [SL]	0.3 ± 0.1 [SL]	5 ± 0.4	30 ± 9	11 ± 1	0.1 ± 0.1	
Al	5400 ± 300	0.04 ± 0.01 [AL]	0.2 ± 0.1 [SL]	4 ± 0.2	32 ± 11	60 ± 3	19 ± 7	
Mg	4200 ± 400	16 ± 2 [SL]	31 ± 15 [AL]	72 ± 7	65 ± 24	7 ± 1	0.4 ± 0.1	
Zn	630 ± 90	4 ± 1 [SL]	0.3 ± 0.1 [SL]	100 ± 14	22 ± 6	36 ± 5	0.7 ± 0.2	
Cu	480 ± 40	7 ± 1 [AL]	5 ± 4 [AL]	14 ± 1	61 ± 27	43 ± 3	11 ± 8	
Mn	260 ± 30	5 ± 1 [AL]	7 ± 3 [AL]	75 ± 7	74 ± 33	16 ± 2	0.4 ± 0.2	
Low Recoverable Content (< 40 mg /kg-dry sludge)								
Cr	120 ± 10	0.3 ± 0.02 [AL]	2 ± 1 [AL]	2 ± 0.2	14 ± 5	10 ± 1	3 ± 1	
Pb	110 ± 10	0.7 ± 0.1 [SL]	1.2 ± 0.6 [SL]	2 ± 0.3	32 ± 18	27 ± 3	0.9 ± 0.3	
Ni	47 ± 6	16 ± 2 [AL]	1.4 ± 0.8 [AL]	25 ± 3	18 ± 12	25 ± 3	4 ± 2	
Mo	22 ± 2	4 ± 0.4 [SL]	9 ± 6 [AL]	2 ± 0.2	7 ± 4	54 ± 6	30 ± 19	
Co	3.8 ± 0.3	25 ± 2 [AL]	1 ± 1 [SL]	90 ± 7	42 ± 10	62 ± 5	2 ± 2	
Cd	2.6 ± 0.2	1.3 ± 0.1 [SL]	1.2 ± 0.4 [SL]	13 ± 1	18 ± 5	34 ± 3	3 ± 1	

[a] Standard error calculated as $\frac{\sigma}{\sqrt{n}}$

[b] Extraction at native pH where samples were mixed with only deionized water (pH 6 for sludge, 7 for sand, and 8 for ash)

[c] The actual sample pH values are within ± 0.5 pH units of the specified value

[d] Combined post-treatment materials (i.e., coarse-grained quartz sand and smouldered ash)

[SL] Material identified as 'solubility-limited' based on the column percolation results following USEPA Method 1314

[AL] Material identified as 'availability-limited' based on the column percolation results following USEPA Method 1314

4.3.4 Discussion of Land Application and Recovery Opportunities

4.3.4.1 Sludge Smouldering in an Inert Porous Media

The best opportunity to create a valuable product for land application is smouldering sludge with sand which resulted in 78% phosphorus retention in the bottom ash. Furthermore, the ash contained more inorganic phosphorus than either the sludge or sand fraction which is more beneficial to plants. This inorganic phosphorus was released more slowly than the phosphorus from sludge, which experienced early washout, losing 60% of total released content almost immediately. Following the early release, remaining phosphorus species within the sludge were less available and therefore less useful to plants without additional weathering or solubilization by plants and microbes, which can be slow and often insufficient for plant needs (Arcand and Schneider, 2006). Interpreting column percolation (Figure 4.1a) and pH-dependent availability (Figure 4.1b) results together suggests that the sludge was already more acidic when applied and therefore its phosphorus was already more available in the immediate term. Early washout of available phosphorus from sludge can (1) contribute to eutrophication and (2) require sludge to be applied more frequently to meet plant nutrient needs. Comparatively, the phosphorus from the ash became more available with decreasing pH (relative to starting pH), which means a steadier supply of phosphorus to plants as pH becomes slightly more acidic with repeated plant growth cycles. With a high abundance of desirable, inorganic phosphorus in the ash, significantly less ash is likely to be needed for land application relative to sludge. Release of most retained PTEs was already lower from the ash and applying less ash would further reduce PTE release. The behaviour of phosphorus release and availability for the sand, supports the idea that a small amount of ash was retained in the sand fraction during dry

sieving. Since sand comprises 98% of the mass of post-treatment materials (2% ash), mechanical separation of the ash and sand would make land application of the ash more practical and economically feasible. Moreover, although sand meets land application guidelines for PTEs (Table 4.2), a large mass of sand would be required to meet plant nutrient requirements, which would be labour intensive and costly. Since the sand retained 30% of phosphorus (90% organic), wet sieving could be used to fully remove ash from the sand fraction and potentially recover some of the additional phosphorus retained on the sand while removing other PTEs (most notably lead, nickel, and chromium). Future work involving plant growth studies and multiple growth cycles may be beneficial to (1) optimize amounts of ash required to support plant growth and (2) determine the phosphorus flux from ash.

The maximum recoverable phosphorus from smouldering sludge mixed with sand was around 70% with approximately 30% from emissions and 40% from ash and sand with acidic extractant (pH 2). The lower observed phosphorus recovery using an alkaline extractant (19%) is unsurprising, as it has been observed consistently among other studies (Biswas et al., 2009; Petzet et al., 2012; Stark et al., 2006). The phosphorus yield using an acidic extractant may be improved further with more extractant volume. Furthermore, because the ash was the most concentrated source of retained phosphorus after treatment (50%) but only 2% of the post-treatment mass, extraction from the ash alone at low pH could minimize extractant volume requirements (0.69 m^3/tonne virgin sludge) while only slightly reducing phosphorus recovery (32% from ash alone). Comparatively, a significantly larger extractant volume would be required for a 10:1 L/S extraction ratio from both the sand and ash (66 m^3/tonne virgin sludge), or from the sludge (10 m^3/tonne

virgin sludge). Reduced extractant requirements also results in less processing solution waste which can be expensive and challenging to dispose of (Donatello and Cheeseman, 2013a). Therefore, when considering phosphorus recovery, it would make more economical sense to physically separate the ash and sand and reuse the sand in future smouldering applications.

4.3.4.2 Co-Smouldering Sludge with Organic Waste

Of the alternatives assessed, the best opportunity for direct recovery of phosphorus is smouldering sludge with woodchips (or another low-impurity, high-energy fuel) and capturing the gases (Table B.3-3, Appendix B.3). While emissions recovery was not rigorously quantified in this research, it is an important source of recoverable phosphorus that will be explored in future work on smouldering systems. The remaining phosphorus in the resultant mixed ash can be recovered easily with an acidic extractant (pH 2). Between the emissions capture (78%) and extraction from ash (21% at pH 2), close to 100% of phosphorus could be recovered from sludge (and woodchips). The significant phosphorus volatilization observed during co-smouldering of sewage sludge is commonly observed during incineration (Cieślik and Konieczka, 2017). Similar to chemical extraction, recovering phosphorus from the emissions stream would require additional processing to separate out other PTEs. To minimize disposal requirements from processing, the extraction waste and emissions waste could be combined and recycled for other purposes such as an additive in construction materials (Cieślik and Konieczka, 2017). Co-smouldering presents both operational and procedural advantages. Since both the sludge and woodchips are combustible, only inert ash remains (20% initial mass) making phosphorus recovery simpler and more economical. Phosphorus extraction from the mixed

ash would require 1.3 m^3 extractant solution/tonne virgin sludge which is 88% less extractant volume than would be required for virgin sludge. Another advantage of treating fully organic waste beds is their capacity to be straightforwardly designed as continuous or semi-continuous smouldering systems, where fuel (e.g., sludge/woodchips) is continuously added to the reactor with potential to remove ash from the base. A system of this nature could eliminate time and costs of reignition. Furthermore, continuous smouldering would behave similarly to current incinerator configurations at WWTPs, making adaptation of the process highly feasible.

4.4 Conclusions

Smouldering enables phosphorus recovery from wastewater treatment sludge in several potentially beneficial forms. The best opportunity to create a valuable soil amendment with sufficient phosphorus available to plants in the longer term is smouldering with sand. The resulting ash retained 78% of the total phosphorus of the parent sludge and contained higher quantities of inorganic phosphorus in sorbed and mineral phases, providing beneficial slow phosphorus release and avoiding early washout. Furthermore, land application of ash is more favourable than sludge since it reduces co-dissolution of 6 of 8 commonly regulated PTEs. Although total elemental concentrations of sludge and ash exceeded O. Reg. 338 land application guidelines for some PTEs, release profiles suggest that smouldering treatment provides important benefits by creating a resource of high-quality phosphorus while sequestering other potentially more harmful elements. Since sand provided an important sink for phosphorus (30% of retained phosphorus, 90% organic), mechanical separation and washing at low L/S should be applied to recover this additional phosphorus from the large sand mass.

Considering extraction as an alternative to direct land application, no single extraction from any material is ideal for phosphorus recovery, before or after smouldering. However, co-smouldering sludge with woodchips could enable close to 100% phosphorus recovery when extraction from the post-treatment ash (21% phosphorus at pH 2) is combined with emissions capture (78% phosphorus). Further separation of phosphorus and PTEs would still be required from the emissions stream which contained >70% of PTEs originally present in the parent sludge. Overall, co-smouldering sewage sludge with woodchips (or another low-impurity, high-energy fuel) has numerous benefits, including (1) treating multiple waste streams, (2) producing a single post-treatment ash, (3) being apt for continuous operation, and (3) increasing treatment temperatures, which may provide further opportunities for treating additional persistent contaminants in the parent sewage sludge.

4.5 References

Adam, C., Peplinski, B., Michaelis, M., Kley, G., Simon, F.G., 2009. Thermochemical treatment of sewage sludge ashes for phosphorus recovery. Waste Manag. 29, 1122–1128. https://doi.org/10.1016/j.wasman.2008.09.011

Arcand, M.M., Schneider, K.D., 2006. Plant- And microbial-based mechanisms to improve the agronomic effectiveness of phosphate rock: A review. An. Acad. Bras. Cienc. https://doi.org/10.1590/S0001-37652006000400013

Biswas, B.K., Inoue, K., Harada, H., Ohto, K., Kawakita, H., 2009. Leaching of phosphorus from incinerated sewage sludge ash by means of acid extraction followed by adsorption on orange waste gel. J. Environ. Sci. 21, 1753–1760. https://doi.org/10.1016/S1001-0742(08)62484-5

Bosshard, P.P., Bachofen, R., Brandl, H., 1996. Metal leaching of fly ash from municipal waste incineration by Aspergillus niger. Environ. Sci. Technol. 30, 3066–3070. https://doi.org/10.1021/es960151v

Canadian Municipal Water Consortium, 2015. Canadian Municipal Water Priorities Report- Towards Sustainable and Resilient Water Management.

Cieślik, B., Konieczka, P., 2017. A review of phosphorus recovery methods at various steps of wastewater treatment and sewage sludge management. The concept of "no solid waste generation" and analytical methods. J. Clean. Prod. 142, 1728–1740. https://doi.org/10.1016/J.JCLEPRO.2016.11.116

Cuthbertson, D., 2018. The Production of Pyrolytic Biochar for Addition in Value-Added Composite Material. Electron. Thesis Diss. Repos. University of Western Ontario, London.

Donatello, S., Cheeseman, C.R., 2013a. Recycling and recovery routes for incinerated sewage sludge ash (ISSA): A review. Waste Manag. https://doi.org/10.1016/j.wasman.2013.05.024

Donatello, S., Cheeseman, C.R., 2013b. Recycling and recovery routes for incinerated sewage sludge ash (ISSA): A review. Waste Manag. 33, 2328–2340. https://doi.org/10.1016/j.wasman.2013.05.024

Duchesne, A.L., Brown, J.K., Patch, D.J., Major, D., Weber, K.P., Gerhard, J.I., 2020. Remediation of PFAS-Contaminated Soil and Granular Activated Carbon by Smoldering Combustion. Environ. Sci. Technol. 54, 12631–12640. https://doi.org/10.1021/acs.est.0c03058

Element, C., 2007. SW-846 Method 3051A: Microwave Assisted Acid Digestion of Sediments, Sludges, Soils, and Oils.

Element Symbol CAS Number, 2007. Method 6010C Inductively Coupled Plasma-Atomic Emission Spectrometry. Cincinnati, Ohio.

Fang, L., Wang, Q., Li, J.-S., Poon, C.S., Cheeseman, C.R., Donatello, S., Tsang, D.C.W., 2020. Feasibility of wet-extraction of phosphorus from incinerated sewage sludge ash (ISSA) for phosphate fertilizer production: A critical review. Crit. Rev. Environ. Sci. Technol. 1–33. https://doi.org/10.1080/10643389.2020.1740545

Feng, C., Cheng, M., Gao, X., Qiao, Y., Xu, M., 2020. Occurrence forms and leachability of inorganic species in ash residues from self-sustaining smouldering combustion of sewage sludge. Proc. Combust. Inst. 000, 1–8. https://doi.org/10.1016/j.proci.2020.06.008

Feng, C., Huang, J., Yang, C., Li, C., Luo, X., Gao, X., Qiao, Y., 2021. Smouldering combustion of sewage sludge: Volumetric scale-up, product characterization, and economic analysis. Fuel 305, 121485. https://doi.org/10.1016/J.FUEL.2021.121485

Fournie, T., Switzer, C., Gerhard, J.I., 2021. USEPA LEAF methods for characterizing phosphorus and potentially toxic elements in raw and thermally treated sewage sludge. Chemosphere 275, 130081. https://doi.org/10.1016/j.chemosphere.2021.130081

Gerhard, J.., Grant, G.P., Torero, J.L., 2020. STAR: A Uniquely Sustainable In Situ and

Ex Situ Remediation Process, in: Sustainable Remediation of Contaminated Soil and Groundwater: Materials, Processes, and Assessment. Butterworth-Heinemann, pp. 221–245.

Gorazda, K., Tarko, B., Wzorek, Z., Kominko, H., Nowak, A.K., Kulczycka, J., Henclik, A., Smol, M., 2017. Fertilisers production from ashes after sewage sludge combustion – A strategy towards sustainable development. Environ. Res. 154, 171–180. https://doi.org/10.1016/j.envres.2017.01.002

Government of Ontario, 2009. O. Reg. 338/09: GENERAL. Government of Ontario, Ottawa.

Hossain, M.K., Strezov Vladimir, V., Chan, K.Y., Ziolkowski, A., Nelson, P.F., 2011. Influence of pyrolysis temperature on production and nutrient properties of wastewater sludge biochar. J. Environ. Manage. 92, 223–228. https://doi.org/10.1016/j.jenvman.2010.09.008

Johnston, A.E., Poulton, P.R., Fixen, P.E., Curtin, D., 2014. Phosphorus: Its Efficient Use in Agriculture. Adv. Agron. 123, 177–228. https://doi.org/10.1016/B978-0-12-420225-2.00005-4

Khiari, B., Marias, F., Zagrouba, F., Vaxelaire, J., 2004. Analytical study of the pyrolysis process in a wastewater treatment pilot station. Desalination 167, 39–47. https://doi.org/10.1016/j.desal.2004.06.111

Kijo-Kleczkowska, A., Środa, K., Kosowska-Golachowska, M., Musiał, T., Wolski, K., 2016. Experimental research of sewage sludge with coal and biomass co-combustion, in pellet form. Waste Manag. 53, 165–181. https://doi.org/10.1016/j.wasman.2016.04.021

Kosson, D.S., Garrabrants, A., Thorneloe, S., Fagnant, D., Helms, G., Connolly, K., Rodgers, M., 2017. Leaching Environmental Assessment Framework (LEAF) How-To Guide: Understanding the LEAF Approach and How and When to Use It. Nashville, TN.

Krüger, O., Adam, C., 2014. Recovery potential of German sewage sludge ash. Waste Manag. 45, 400–406. https://doi.org/10.1016/j.wasman.2015.01.025

Li, X., Zhang, D., Yang, T., Bryden, W., 2016. Phosphorus Bioavailability: A Key Aspect for Conserving this Critical Animal Feed Resource with Reference to Broiler Nutrition. Agriculture 6, 25. https://doi.org/10.3390/agriculture6020025

London, C. of, 2019. Greenway Wastewater Treatment Centre 2018 Annual Report.

Mayer, B.K., Baker, L.A., Boyer, T.H., Drechsel, P., Gifford, M., Hanjra, M.A., Parameswaran, P., Stoltzfus, J., Westerhoff, P., Rittmann, B.E., 2016. Total Value of Phosphorus Recovery. Environ. Sci. Technol. 50, 6606–6620. https://doi.org/10.1021/acs.est.6b01239

Mulchandani, A., Westerhoff, P., 2016. Recovery opportunities for metals and energy from sewage sludges. Bioresour. Technol. https://doi.org/10.1016/j.biortech.2016.03.075

Neczaj, E., Grosser, A., 2018. Circular Economy in Wastewater Treatment Plant–Challenges and Barriers. Proceedings 2, 614. https://doi.org/10.3390/proceedings2110614

Ohlemiller, T.J., 1985. Modeling of smoldering combustion propagation. Prog. Energy Combust. Sci. 11, 277–310. https://doi.org/10.1016/0360-1285(85)90004-8

Petzet, S., Peplinski, B., Cornel, P., 2012. On wet chemical phosphorus recovery from sewage sludge ash by acidic or alkaline leaching and an optimized combination of both. Water Res. 46, 3769–3780. https://doi.org/10.1016/j.watres.2012.03.068

Pfaff, J.D., 1993. Method 300.0 Determination of inorganic anions by ion chromatography.

Rashwan, T., 2020. Sustainable Smouldering for Waste-to-Energy: Scale, Heat Losses, and Energy Efficiency. Electron. Thesis Diss. Repos.

Rashwan, T.L., Fournie, T., Torero, J.L., Grant, G.P., Gerhard, J.I., 2021a. Scaling up self-sustained smouldering of sewage sludge for waste-to-energy. Waste Manag. 135, 298–308. https://doi.org/10.1016/J.WASMAN.2021.09.004

Rashwan, T.L., Gerhard, J.I., Grant, G.P., 2016. Application of self-sustaining smouldering combustion for the destruction of wastewater biosolids. Waste Manag. 50, 201–212. https://doi.org/10.1016/j.wasman.2016.01.037

Rashwan, T.L., Torero, J.L., Gerhard, J.I., 2021b. The improved energy efficiency of applied smouldering systems with increasing scale. Int. J. Heat Mass Transf. 177, 121548. https://doi.org/10.1016/J.IJHEATMASSTRANSFER.2021.121548

Rein, G., 2016. Smoldering Combustion, in: Hurley, M.J., Gottuk, D.T., Hall Jr., J.R., Harada, K., Kuligowski, E.D., Puchovsky, M., Torero, J.L., Watts Jr., J.M., Wieczorek, C.J. (Ed.), SFPE Handbook of Fire Protection Engineering. Springer New York, New York, pp. 581–603.

Schaum, C., Cornel, P., Jardin, N., 2007. Phosphorus recovery from sewage sludge ash–a wet chemical approach, in: Proceeding of the IWA Conference on Biosolids, Moving Forward Wastewater Biosolids Sustainability: Technical, Managerial, and Public Synergy.

Scholes, G.C., Gerhard, J.I., Grant, G.P., Major, D.W., Vidumsky, J.E., Switzer, C., Torero, J.L., 2015. Smoldering Remediation of Coal-Tar-Contaminated Soil: Pilot Field Tests of STAR. Environ. Sci. Technol. 49, 14334–14342. https://doi.org/10.1021/ACS.EST.5B03177

Solinger, R., Grant, G.P., Scholes, G.C., Murray, C., Gerhard, J.I., 2020. STARx Hottpad for smoldering treatment of waste oil sludge: Proof of concept and sensitivity to key design parameters: https://doi.org/10.1177/0734242X20904430 38, 554–566. https://doi.org/10.1177/0734242X20904430

Stark, K., Plaza, E., Hultman, B., 2006. Phosphorus release from ash, dried sludge and sludge residue from supercritical water oxidation by acid or base. Chemosphere 62, 827–832. https://doi.org/10.1016/j.chemosphere.2005.04.069

Switzer, C., Pironi, P., Gerhard, J.I., Rein, G., Torero, J.R., 2009. Self-sustaining smoldering combustion: A novel remediation process for non-aqueous-phase liquids in porous media. Environ. Sci. Technol. 43, 5871–5877. https://doi.org/10.1021/es803483s

Torero, J.L., Gerhard, J.I., Martins, M.F., Zanoni, M.A.B., Rashwan, T.L., Brown, J.K., 2020. Processes defining smouldering combustion: Integrated review and synthesis. Prog. Energy Combust. Sci. https://doi.org/10.1016/j.pecs.2020.100869

USEPA, 2012a. Method 1313: Liquid-Solid Partitioning as a Function of pH for Constituents in Solid Materials Using a Parallel Batch Extraction Procedure. Nashville, TN.

USEPA, 2012b. Method 1314: Liquid-Solid Partitioning as a Function of Liquid-to-Solid Ratio for Constituents in Solid Materials Using a Percolation Column Procedure. Nashville, TN.

Wang, K.S., Chiang, K.Y., Lin, K.L., Sun, C.J., 2001. Effects of a water-extraction process on heavy metal behavior in municipal solid waste incinerator fly ash. Hydrometallurgy 62, 73–81. https://doi.org/10.1016/S0304-386X(01)00186-4

Werther, J., Ogada, T., 1999. Sewage sludge combustion. Prog. Energy Combust. Sci. https://doi.org/10.1016/S0360-1285(98)00020-3

Westerhoff, P., Lee, S., Yang, Y., Gordon, G.W., Hristovski, K., Halden, R.U., Herckes, P., 2015. Characterization, Recovery Opportunities, and Valuation of Metals in Municipal Sludges from U.S. Wastewater Treatment Plants Nationwide. Environ. Sci. Technol. 49, 9479–9488. https://doi.org/10.1021/es505329q

Wu, H.Y., Ting, Y.P., 2006. Metal extraction from municipal solid waste (MSW) incinerator fly ash - Chemical leaching and fungal bioleaching. Enzyme Microb. Technol. 38, 839–847. https://doi.org/10.1016/j.enzmictec.2005.08.012

Wyn, H.K., Konarova, M., Beltramini, J., Perkins, G., Yermán, L., 2020. Self-sustaining smouldering combustion of waste: A review on applications, key parameters and potential resource recovery. Fuel Process. Technol. 205, 106425. https://doi.org/10.1016/J.FUPROC.2020.106425

Xu, T.J., Ramanathan, T., Ting, Y.P., 2014. Bioleaching of incineration fly ash by

Aspergillus niger - Precipitation of metallic salt crystals and morphological alteration of the fungus. Biotechnol. Reports 3, 8–14. https://doi.org/10.1016/j.btre.2014.05.009

Yang, J., Wang, Qunhui, Wang, Qi, Wu, T., 2009. Heavy metals extraction from municipal solid waste incineration fly ash using adapted metal tolerant Aspergillus niger. Bioresour. Technol. 100, 254–260. https://doi.org/10.1016/j.biortech.2008.05.026

Yermán, L., 2016. Self-sustaining Smouldering Combustion as a Waste Treatment Process, in: Developments in Combustion Technology. InTech. https://doi.org/10.5772/64451

Yermán, L., Hadden, R.M., Carrascal, J., Fabris, I., Cormier, D., Torero, J.L., Gerhard, J.I., Krajcovic, M., Pironi, P., Cheng, Y.L., 2015. Smouldering combustion as a treatment technology for faeces: Exploring the parameter space. Fuel 147, 108–116. https://doi.org/10.1016/j.fuel.2015.01.055

Zanoni, M.A.B., Torero, J.L., Gerhard, J.I., 2019. Determining the conditions that lead to self-sustained smouldering combustion by means of numerical modelling. Proc. Combust. Inst. 37, 4043–4051. https://doi.org/10.1016/J.PROCI.2018.07.108

Chapter 5

5 Behaviour of PCDD/Fs and PTEs during smouldering treatment of sewage sludge

5.1 Introduction

Sewage sludge contains high quantities of potentially toxic elements (PTEs) and emerging contaminants including antibiotic resistant bacteria and perfluorinated compounds (Jiwan and Ajah, 2011; Zhou et al., 2019), which have been shown to cause adverse health and environmental impacts (Zhang et al., 2017b). These hazards drive strong interest in thermal conversion techniques that limit their environmental release (Pudasainee et al., 2013; Werther and Ogada, 1999; Zabaniotou and Theofilou, 2008). Incineration is an attractive option for treating sewage sludge due to its ability to destroy organic contaminants (Werther and Ogada, 1999). However, the by-product emissions from sludge incineration often contain hazardous compounds that require additional treatment, particularly polychlorinated dibenzo-*p*-dioxins (PCDDs), polychlorinated dibenzofurans (PCDFs), and PTEs including heavy metals (Fullana et al., 2004; Pudasainee et al., 2013; Shao et al., 2008; Werther and Ogada, 1999).

Recently, smouldering combustion has been demonstrated as a novel sludge treatment technology to reduce energy and carbon demand in wastewater treatment plants (WWTPs) (Rashwan et al., 2016). Smouldering can manage high moisture content (MC) sludge (80-85% MC) with minimal pre-processing, an advantage that fundamentally draws on the slower smouldering combustion time scales compared to those in flaming combustion systems such as incinerators (Torero et al., 2020; Yermán et al., 2015). This key difference allows for more efficient energy transfer in the system. Smouldering-based

systems operate in a self-sustaining manner, without the need for supplemental energy after ignition, even in these very high moisture content conditions (Rashwan et al., 2016; Serrano et al., 2020). While smouldering has many advantages as a low-energy thermal treatment option, the lack of information regarding potential formation of by-products and treatments required to manage them is a barrier to widespread application.

Release of PCDD/Fs during sludge incineration is a major concern because these compounds are highly toxic and persistent (Fiedler, 2003; Reiner, 2016; Van den Berg et al., 2006). PCDD/F formation is possible from any thermal treatment process with sufficient quantities of carbon, chlorine, oxygen, and metal catalysts (Stanmore, 2004; Zhang et al., 2017a). Several studies have explored the mechanisms of PCDD/F formation during combustion processes (mostly incineration) and consensus is that major formation pathways are: (*i*) incomplete combustion of existing PCDD/Fs fed to the combustor; (*ii*) reactions from precursor compounds; and (*iii*) *de novo* synthesis from carbon and chlorine (Zhang, 2017; Hart, 2004; Stanmore, 2004; McKay, 2002). Heterogeneous reactions at the gas – solids interface are generally the dominant PCDD/F formation mechanisms in incinerators, although incomplete combustion of existing PCDD/Fs is also possible (Fullana et al., 2004; Stanmore, 2004; Zhang et al., 2017a). The extent of combustion completeness in incinerators has been shown to affect the release PCDD/Fs in incinerator emissions, where incomplete combustion favours higher amounts of PCDD/Fs released in the emissions and complete combustion favours lower release of PCDD/Fs (Fiedler, 2003; McKay, 2002). This is partially because products of incomplete combustion (e.g., volatile organic compounds (VOCs)) may promote PCDD/F formation via precursor pathways and, to a lesser extent, *de novo* synthesis (Tuppurainen et al., 1998). Fluidized bed incinerators

immediately subject sludge to high temperatures (750 – 925°C) at residence times of 2 – 5 seconds (USEPA, 1995) for complete destruction of PCDD/Fs originally present in the sludge (McKay, 2002). PCDD/Fs in incinerator emissions are typically produced through heterogeneous production pathways in the post-combustion chamber (Altwicker et al., 1992). Although the PCDD/Fs risks from sludge incineration are well-characterized (W. Deng et al., 2009; Fytili and Zabaniotou, 2008; Han et al., 2006), they are not well-understood for smouldering systems.

Smouldering systems for sludge often exhibit lower treatment temperatures (400-550 °C) and relatively high fractions of CO/CO_2 (0.05-0.4) (Torero et al., 2020). While these lower temperatures and high CO fractions indicate incomplete combustion, it is not necessarily clear if sludge smouldering systems foster the conditions needed for PCDD/F formation and/or release. Most applied smouldering systems exhibit efficient heat transfer ahead of smouldering as well as filtration, due to the use of inert porous media – typically coarse grained sand (Torero et al., 2020). As a result, the post-combustion chamber remains near ambient temperature throughout most of smouldering and contains less particulate matter than typical incinerators (Torero et al., 2020); these conditions are not expected to foster PCDD/F formation. These key differences between smouldering systems and incinerators are expected to govern the differences in mechanisms of PCDD/F formation and/or release in these two systems (Yerman, 2016). Therefore, it is not appropriate to extrapolate PCDD/F destruction findings from incinerators to smouldering systems. Instead, this work seeks to evaluate potential PCDD/Fs formation and/or release during smouldering with direct experiments.

Like PCDD/Fs, fate of PTEs during incineration of sewage sludge has been extensively studied (Han et al., 2006; Marani et al., 2003; Pudasainee et al., 2013); however, the fundamental differences between incineration and smouldering mean that analogies between these systems are not straightforward. Sewage sludge provides a natural accumulation point for PTEs and during incineration they can be retained in ash or mobilized in the process emissions. The distribution of PTEs during incineration is affected by type of waste and its characteristics; physicochemical properties of the PTEs; reactor type; residence time; and incineration operating conditions such as temperature and airflow rate (Nowak et al., 2013; Zhang et al., 2008). These factors likely affect the distribution of PTEs during smouldering treatment. Although smouldered sewage sludge ash is likely safe for landfilling (Feng et al., 2020), more work is still needed to understand compounds being formed and/or released from sewage sludge smouldering, especially within process emissions.

This work aims to improve the understanding of risks associated with smouldering treatment and is the first study to evaluate PCDD/F formation and release from smouldering sewage sludge. The objectives are to evaluate the mechanisms of potential formation and release of PCDD/Fs and VOCs and establish the fate of PTEs from treating sewage sludge with smouldering. To address these goals, smouldering tests were conducted in laboratory and oil-drum sized reactors varying moisture content and sand-to-sludge ratio widely to challenge the system. This approach was used to evaluate potential emissions hazards under a wide range of operating conditions.

5.2 Materials and Methods

5.2.1 Experimental Set-up and Procedure

Sewage sludge was obtained from Greenway Pollution Control Plant (Greenway) in London, Ontario, Canada. Complete details on wastewater processing and sludge generation at Greenway can be found elsewhere (Rashwan et al., 2016). In these tests, sewage sludge produced from a dewatered slurry of primary and secondary sludge was collected in batches of 40 – 55 kgs ahead of each smouldering test. Virgin sludge was typically collected one day prior to smouldering to allow for experiment set-up and preparation.

Cylindrical reactors fabricated from stainless steel were used for both laboratory experiments (with 0.16 m diameter, LAB) and larger scale tests in an oil-drum sized reactor (with 0.6 m diameter, DRUM). Well-established smouldering equipment and procedures were used for both the LAB (Rashwan et al., 2016), and DRUM (Fournie et al., 2022; Rashwan et al., 2021a) tests. A basic summary is provided here. Figure 5.1 illustrates the DRUM reactor set-up and sampling points. The LAB reactor set-up was similar, but it required a scaled-down and simplified sampling approach (Figure C.1-1, Appendix C). The reactors were wrapped in 0.051 m thick insulation (LAB: MinWool®, Johns Manville; DRUM: FyreWrap® Elite® Blanket, Unifrax).

The sewage sludge had an average moisture content of 74% and ash content of 1% (both wet mass-basis), determined using USEPA Method 1684 (Telliard, 2001). Eight DRUM and three LAB tests were conducted, summarized in Table 5.1. DRUM 1 and LAB 1a and 1b used dried sewage sludge (3% MC). DRUM 1 was the same sand and sludge

DRUM test used to evaluate phosphorus in Chapter 4. This sludge was batch dried in an oven at 105°C until there were no measurable changes in the sludge mass. DRUM 2 and LAB 2 involved sludge as-received (74% MC). DRUM 3 and 5 were similar but used lower sand concentrations. For DRUM 4, the sludge was tumbled in a large mechanical mixer until the moisture content was reduced by 45%. DRUM 6 and 7 were replicates of DRUM 2. DRUM 8 increased sludge content by 1.5x, but otherwise maintained the same conditions as DRUM 2, 6, and 7.

In each test, the specified mass of sludge was mixed with coarse silica sand (Bell & Mackenzie Number 12; 1.180 ≤ mean grain diameter ≤ 2.000 mm; porosity (ϕ) = 0.37; bulk density ($[1-\phi]\rho_s$) = 1670 kg m^{-3}; 0.04 – 0.4% MC) to achieve the specified sand-to-sludge ratio (Table 5.1) in a mechanical drum mixer (Rashwan et al., 2016). All experiments were packed carefully into the reactor to minimize packing heterogeneities; however, the mixtures in DRUM 3 and 5 were slightly more densely packed than the other high MC experiments, which contributed to poor smouldering performance. A clean sand cap (2.5-5 cm thick) was added on top of sand/sludge mixtures in all LAB and DRUM tests to lower the exiting emissions temperatures for safety purposes.

The reactors were placed on load cells (KCC150 (LAB) and KD1500 (DRUM), Mettler Toledo) to measure mass loss during smouldering. Thermocouples (Type K 0.0032 m diameter Omega Ltd (LAB); 0.0064 m diameter Kelvin Technologies (DRUM)) were installed along the full height of the reactors to record process temperatures throughout each test. Air was injected into the base of the reactors and was operated using a mass flux controller (FMA5400/5500 Series, Omega Ltd. (LAB); 8290B045PDB67 ASCO Numatics (DRUM)). The base of the reactor was then heated via a convective heater (F074719 2 kW

SureHeat® JET (LAB); F074736 36 kW SureHeat® MAX (DRUM), Osram Sylvania) until ignition, which was identified when the first thermocouple in the sand/sludge mixture peaked (i.e., 0.02 and 0.06 m up the column in the LAB and DRUM experiments, respectively). Following ignition, the heater was turned off and air flow was maintained to support self-sustaining smouldering. The end of each experiment was identified when the smouldering front reached the end of the sand/sludge mixture in the reactor.

Representative samples, 19 – 100L per DRUM test, of the post-treatment material (i.e., ash mixed with silica sand) were collected in 19 L buckets that aimed to capture heterogeneities throughout the reactor. Post-treatment materials were then separated into sand and ash fractions as defined by grain sizes greater than and less than 0.25 mm, respectively.

PCDD/Fs were measured in emissions LAB 1a, 1b, and 2 and DRUM 1, 2, 3, and 4. VOCs were measured in the emissions from DRUM 3 and 5. Elemental analyses were performed on the virgin sludge and remaining ash from DRUM 1, 2, 6, 7, and 8.

5.2.2 Emissions Monitoring

Continuous emissions monitoring systems (CEMS) measured oxygen, carbon dioxide, and carbon monoxide data from the LAB tests every two seconds (MGA3000C, ADC), and methane, carbon dioxide, carbon monoxide, and total hydrocarbons from the DRUM tests every five seconds (ABB Ltd.). The locations of all emissions sampling points for DRUM tests are shown in Figure 5.1, and LAB tests in Figure C.1-1 (Appendix C).

The PCDD/F emissions sampling train was constructed based on USEPA Method 23, modified following Wallbaum et al. (1995). An XAD tube containing XAD-2 resin

(Sigma-Alderich, USA) was used to capture PCDD/Fs within the emissions. A cold-water condenser ahead of the XAD tube was used to rapidly cool the emissions. In the LAB tests, a single emissions sample was collected from the reactor (Section C.1, Appendix C). In the DRUM tests, emission samples were collected at two locations along the experimental system: (*i*) just above the fixed bed, and (*ii*) at the exhaust of the onsite emissions treatment system (Figure 5.1). The two emissions sampling locations were used to analyze PCDD/Fs that may have been produced/released during smouldering and verify the effectiveness of the emissions treatment system. A flow meter ahead of the LAB and DRUM reactor sampling train was used to measure air flow through the sampling system and adjust valves to maintain constant flow throughout the sampling period. Oxygen content was measured immediately after the reactor sampling trains (LAB: MGA3000C, ADC; DRUM: Landtec GEM2000 portable gas analyzer). The duration of the PCDD/F emissions sampling was recorded from when the pump was turned on, thereby diverting a fraction of the emissions from the reactor outlet through the PCDD/F sampling train, until the pump was turned off. The timing and duration of PCDD/F sampling varied between tests to predominantly capture PCDD/F emissions away from initial- and end-effects (Table 5.1). The condensate that accumulated during emissions sampling was collected from the condenser and analyzed with the XAD-2 resin.

An evacuated Summa® canister (ALS Canada Ltd.) was used to collect emissions samples from DRUM 3 and 5. The canister was connected to the reactor hood directly above the PCDD/F sampling train (Figure 5.1). A flow controller was used to collect the emissions samples at a constant rate throughout each test. Sampling occurred for 270 min for DRUM 3, and 200 min for DRUM 5 (due to less smoulderable material in this test), as

the smouldering front progressed up the reactor. The emissions samples were analyzed benzene, benzyl chloride, chlorobenzene, 1,2-dichlorobenzene, 1,3- dichlorobenzene, 1,4-dichlorobenzene, ethylbenzene, 4-ethyltoluene, styrene, toluene, 1,2,4-trichlorobenzene, 1,2,4- trichlorobenzene, 1,3,5- trichlorobenzene, o-xylene, m&p-xylene by ALS using Gas Chromatography/Mass Spectrometry (GC/MS) complying with USEPA Method T0-15, i.e., as recommended by the National Environmental Protection (Air Toxics) Measure (USEPA, 1999).

To ensure that all measurements were independent of previous experiments, background samples were taken while injecting hot air (50 – 60°C) through the empty DRUM and LAB setups to quantify the background concentration of PCDD/Fs. Background concentrations were all below detection limits.

All LAB tests were performed in fume hoods that collected the emissions exiting the reactor into a centralized collection system. Emissions exiting the DRUM reactors were passed through an onsite treatment system prior to release from a stack. The custom treatment system (Newterra Ltd.) consisted of two granular activated carbon vessels (820 and 75 kg, respectively), followed by a vessel with impregnated potassium permanganate media (with 150 kg of material).

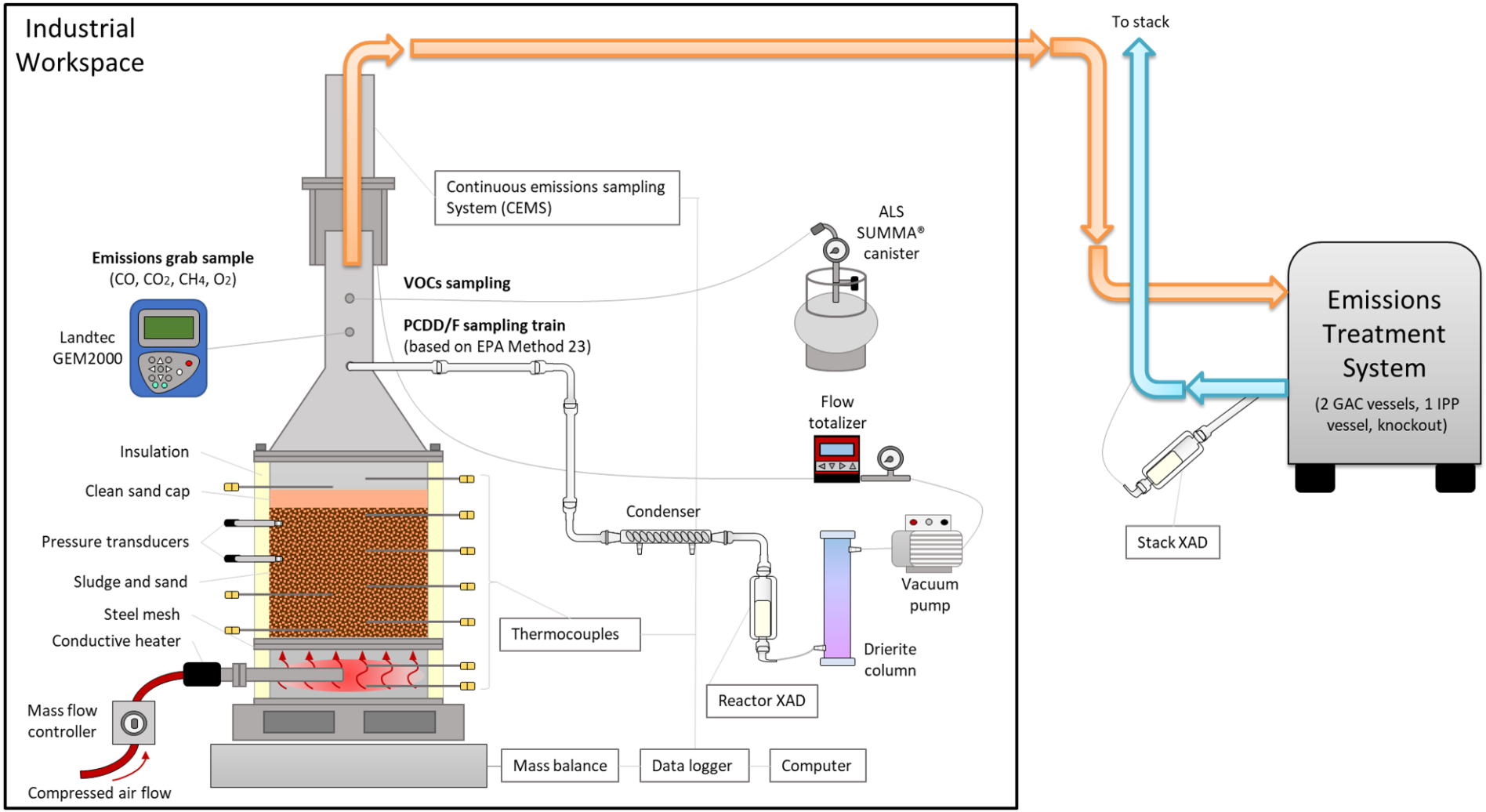

Figure 5.1: Experimental set-up and sampling for DRUM tests.

Table 5.1: Summary of smouldering experiments

Test	Sludge Properties		Sand: Sludge [1]	Sludge Added	Sand Added	Bulk Density	Air Flux	Peak Temp	Propagation Velocity	Other Analyses Performed	Comments
	MC (wet mass %)	Ash (dry mass %)	(g/g)	(kg)	(kg)	(kg/m^3)	(cm/s)	(°C)	(cm/min)		
LAB											
1a	3.2	29	24:1	0.52	12	1626	5.0	516	0.53	PCDD/F	Robust, some edge effects
1b	3.2	29	24:1	0.27	6.27	1490	4.6	569	0.46	PCDD/F	Robust, some edge effects
2	74	29	6.5:1	1.84	12	1148	5.0	458	0.29	PCDD/F	Extinction part way up the column, edge effects similar to DRUM 2
DRUM											
1	3.2	28	24:1	8.5	218	1472	5.0	533	0.38	PCDD/F, PTEs	Robust, minimal pyrolyzed crust similar to DRUM 4
2	72	23	6.5:1	29.2	191	1191	5.0	500	0.27	PCDD/F, PTEs	Robust, some edge effects
3	75	27	4.5:1	33.5	151	1355	1.0 [2]	427	0.09	VOCs, PCDD/F	Weak, significant unburned/crust regions
4	40	24	12:1	28.5	186	1435	5.0	512	0.40	PCDD/F	Robust, minimal edge effects
5	75	28	4.5:1	26.5	119	1378	5.0	324	0.23	VOCs	Weak, significant unburned/crust regions
6	72	27	6.5:1	29.2	191	1265	5.0	475	0.23	PTEs	Robust, some edge effects similar to DRUM 2
7	74	22	6.5:1	29.2	191	1296	5.0	481	0.24	PTEs	Robust, minimized edge effects compared to DRUM 2 & 6
8	73	24	4.5:1	42.5	191	1267	5.0	528	0.20	PTEs	Robust, some edge effects

[1] The total sand to fuel mass ratio is presented, although the MC (%) and Ash (%) varied between tests
[2] Ignited at a higher air flux

5.2.3 Elemental Analysis and Mass Balance Calculations

Total contents of aluminum, cadmium, cobalt, chromium, copper, iron, manganese, molybdenum, nickel, lead, and zinc in the virgin sewage sludge, virgin sand, and post-treatment ash and sand were determined with inductively coupled plasma, optical emission spectroscopy, and mass spectrometry (ICP-OES). These elements were selected because they are currently monitored at WWTPs. Triplicate samples of solids were extracted by microwave assisted acid digestion following USEPA Method 3051A (Element, 2007).

Experimental data was used to determine the distribution of mass of each element within the reactor pre- and post-smouldering. Masses of sand and sewage sludge added into the systems was carefully tracked during mixing, packing, and unpacking. The mass of post-treatment ash generated was determined based on the quantity of sewage sludge added to the system and the mass removed during smouldering as measured by the load cell. Due to the nature of a fixed bed reactor, the sand matrix is conserved with no losses during treatment (Yermán et al., 2015).

The total masses of sand and ash size fractions were extrapolated based on sieve analysis from 6 subsamples taken from each test (Section C.2, Appendix C). The total quantity of each element was similarly extrapolated for each size fraction and compared to the total quantities originally in virgin sewage sludge and sand. Differences were assumed as losses via volatilization.

5.2.4 Dioxin and Furan Analysis

A modified QuEChERS method (Haimovici et al., 2016) was used to extract the aliquot from the XAD-2 and condensate samples for PCDD/Fs analysis by Gas Chromatography/High-Resolution Mass Spectrometry (GC/HRMS). All analyses were performed at the mass spectrometry laboratory, Ministry of Environment, Conservation, and Parks, Toronto, ON. The measured masses of the 17 most toxic PCDD/F congeners (i.e., the PCDD/Fs containing chlorine atoms in the 2,3,7,8 positions on the benzene rings) (Reiner, 2016) were converted into concentrations in the emissions based on measurements from a downstream flow totalizer (see Section C.3, Appendix C for full method and calculations).

PCDD/F emissions concentrations were normalized to account for sampling volume, reactor scale, air flux into the reactor, bulk density of the sludge and sand mixture, MC of the fuel, ash content, sand-to-sludge mass ratio, smouldering propagation velocity, and the temperatures and pressures of the air entering and leaving the reactor (Section C.4, Appendix C).

According to the Canadian Council of Ministers of the Environment Environmental Compliance Approval (ECA), the allowable maximum concentration of PCDD/Fs in the undiluted flue gas, emitted from sewage sludge incinerator stacks is 80 pg/m^3 toxic equivalent quantity (TEQ) corrected to 11% O_2 at a reference temperature and pressure of 25°C and 101.3 kPa, respectively. To compare the PCDD/F concentrations to regulatory standards, experimental values were corrected to these reference conditions (see Section C.3, Appendix C for full calculations).

5.3 Results and Discussion

5.3.1 Smouldering Behaviour

Smouldering destroyed more than 90% of the initial sludge biomass, leaving 1-10% as residual inorganic ash in the reactor. Peak temperatures ranged between 450 – 600°C in LAB tests and 325 – 550°C in DRUM tests (Table 5.1).

The evolution of three dominant smouldering burn patterns observed in the experiments are shown in Figure 5.2 (adapted from Rashwan et al., 2021). In robust smouldering, the smouldering front is well distributed in the cross-sectional area of the reactor and remained that way as the front propagated through the material. Robust smouldering, with minimal crust/unburned sections, was observed in LAB 1a and 1b and DRUM 1 and 4 (Figure 5.2A). Internal and external factors can reduce smouldering robustness. Heat losses at reactor walls (i.e., edge effects) inhibit smouldering at the walls while smouldering remains robust at the center of the reactor. These edge effects were observed as pyrolyzed crusts near the reactor walls after treatment in DRUM 2, and 6 – 8 (Figure 5.2B). In these tests, wall temperatures were less than 200 °C, thereby indicating that the material did not completely smoulder near the wall (Section C.2, Appendix C). Heterogeneities can further inhibit smouldering by inducing channeling and other irregularities in the porous media. Weak smouldering was observed in LAB 2, and DRUM 3 and 5. With extinction conditions near the reactor wall and non-uniform flow field, both driven by heat losses, large fractions in these experiments remained unburned (Rashwan, 2020; Rashwan et al., 2021c). These weak smouldering conditions led to non-self-sustaining conditions in LAB 2, evident with declining temperatures along the centreline until extinction halfway up the fuel pack (Section C.2, Appendix C), and borderline-self-

sustaining conditions in DRUM 3 and 5 (Figure 5.2C), with declining peak temperatures but no quenching (Section C.3, Appendix C). Therefore, these experiments as a whole represent a broad spectrum of conditions to evaluate process emissions, from robust self-sustaining to extinction of smouldering.

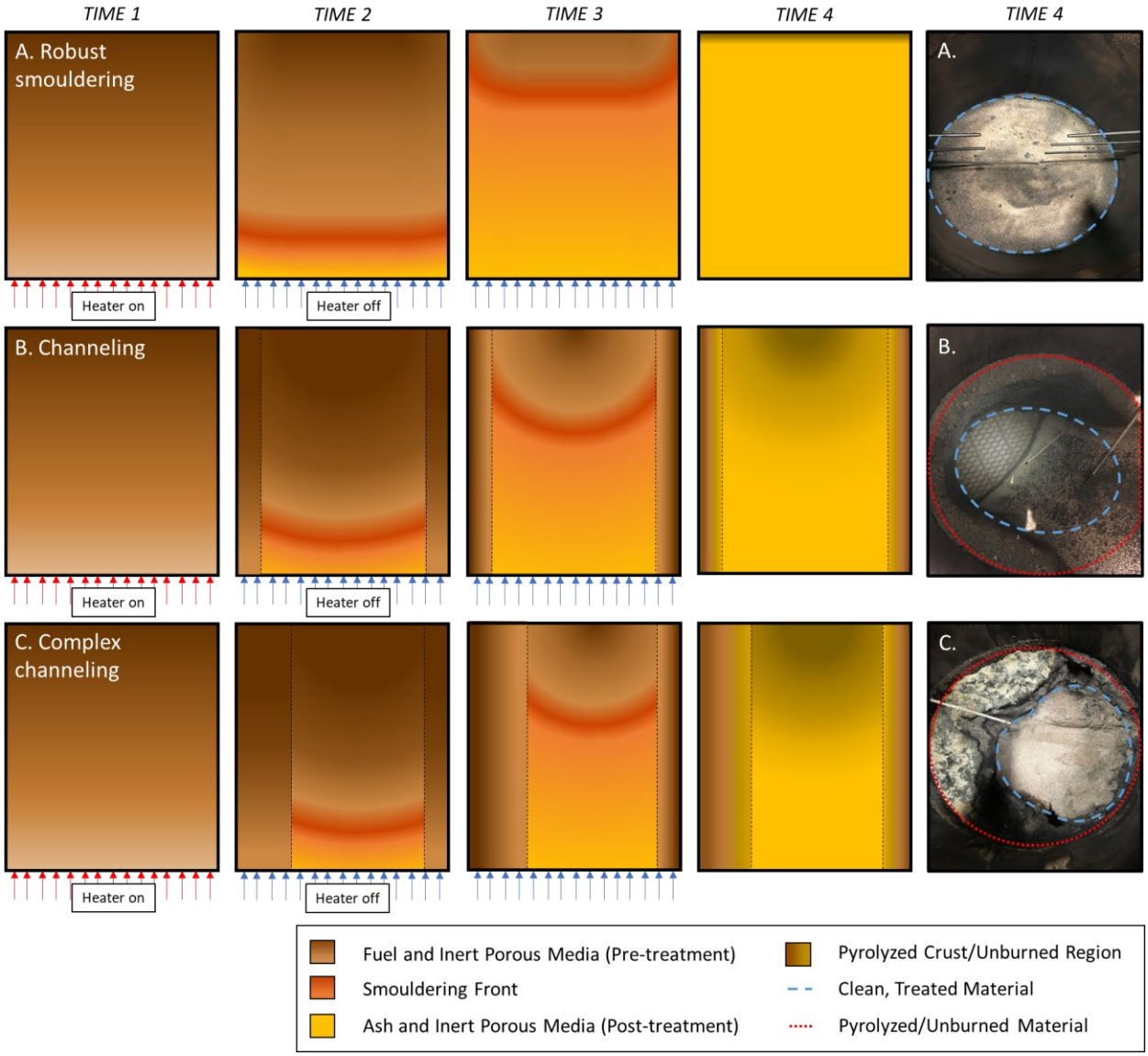

Figure 5.2: Summary of the different burn patterns observed in the experiments. Times 1 to 4 show smouldering front propagation, where Time 1 shows ignition at the reactor base, Time 2 shows when the front propagated part-way up the column, Time 3 shows when the smouldering front is approaching the top of the contaminant pack, and Time 4 shows the approximate post-treatment burn patterns. A. represents tests with no/minimal crust, B. shows pyrolyzed/unburned crust due to edge effects, and C. shows significant crust formation and large, unburned regions.

5.3.2 Fate of Potentially Toxic Elements (PTEs)

Table 5.2 presents a mass balance of elemental retention and volatilization during smouldering. The ash and sand fractions comprised ~2% and ~98% of the total post-treatment material mass, respectively. However, both fractions retained roughly equal amounts of PTEs, i.e., the ash retained 33 to 77 (± 15%) of PTEs, while the sand retained 28 to 78 (± 5%) of PTEs. Because dry sieving did not completely separate ash and sand, some ash was likely retained in the sand fraction (i.e., due to physical attachment). The high retention of some elements in the sand may be due to this retained ash, compounded because of the large relative mass of sand. In addition, some PTEs may have condensed on the sand during smouldering treatment.

Table 5.2 shows that, following smouldering treatment, most PTEs were retained within the reactor. Retentions of cadmium, chromium, copper, lead, nickel, and zinc were all ~100% (Table 5.2). In comparison, losses of 60-100% of cadmium, 30-50% of lead, and 20% of chromium, copper, nickel, and zinc are commonly observed during sewage sludge incineration (Zhang et al., 2008). Compared to incineration, the lower treatment temperatures during smouldering likely limited volatilization of these PTEs so they remained in the ash and were not released in the emissions. For example, from the 2018 National Pollutant Release Inventory Report (which summarizes elemental release from WWTPs through sludge incineration in London, Canada), one large WWTP reported losses of: 9 kg of cadmium, 76 kg of lead, 2.7 tonnes of zinc, and 4.1 tonnes of total particulate matter (City of London, 2019). Considering the initial elemental concentrations in the sludge and the annual quantity processed by this WWTP, elemental losses in incinerator emissions equate to ~38% of cadmium, ~6% of lead, and ~22% of zinc originally in the

sludge (Section C.5, Appendix C). In comparison, smouldering treatment retained 85 to 111 (± 16%) of all PTEs within post-treatment ash and sand (Table 5.2).

Low release of PTEs during smouldering relative to incineration is likely due to: (*i*) lower air flow rates; (*ii*) use of fixed beds instead of fluidized beds; (*iii*) lower smouldering temperatures; and (*iv*) less particulate release. These process differences likely reduce the potential for volatilized PTEs in the emissions.

Table 5.2: Average elemental content and mass balances of 12 commonly monitored PTEs at WWTPs

Element	Average Elemental Concentration (mg/kg-dry matter) ± SE [a]			Mass Balance (% total content) ± SE [a]		
	Sludge	Post-Treatment		Post-Treatment		
		Sand [b]	Ash [c]	Sand [b]	Ash [c]	Total [d]
Al	8100 ± 300	260 ± 90	17000 ± 2000	69 ± 24%	40 ± 14%	109 ± 28%
Cd	2 ± 0.2	0.05 ± 0.01	2.8 ± 0.9	61 ± 13%	42 ± 9%	103 ± 16%
Co	2.9 ± 0.4	0.11 ± 0.01	7.8 ± 1	80 ± 4%	42 ± 14%	122 ± 14%
Cr	100 ± 8	3.7 ± 1	130 ± 30	78 ± 30%	33 ± 16%	111 ± 34%
Cu	500 ± 30	7 ± 2	2700 ± 700	34 ± 11%	77 ± 14%	110 ± 18%
Fe	40000 ± 4000	830 ± 200	54000 ± 20000	45 ± 14%	39 ± 5%	85 ± 15%
Mg	4400 ± 400	58 ± 14	13000 ± 2000	29 ± 6%	62 ± 11%	91 ± 15%
Mn	240 ± 20	4.3 ± 4	800 ± 100	40 ± 14%	63 ± 11%	103 ± 18%
Mo	13 ± 2	0.21 ± 0.03	30 ± 2	36 ± 7%	53 ± 12%	89 ± 14%
Ni	41 ± 5	1.1 ± 0.1	100 ± 15	57 ± 25%	42 ± 19%	99 ± 31%
Pb	60 ± 14	1.6 ± 0.2	85 ± 60	57 ± 10%	43 ± 13%	101 ± 17%
Zn	680 ± 70	15 ± 40	2200 ± 500	48 ± 9%	62 ± 12%	110 ± 15%

[a] Standard error calculated as $\frac{\sigma}{\sqrt{n}}$

[b] Post-treatment sand (> #60 sieve size)

[c] Mostly post-treatment ash (< #200 sieve size)

[d] Content in post-treatment ash was determined from ash (< #200 sieve) and mixed sand fines and ash (i.e., between the #200 and #60 sieve sizes)

[e] The standard error was calculated from the uncertainties from each calculation added in quadrature

5.3.3 PCDD/F Formation and Release

5.3.3.1 PCDD/F Results from LAB and DRUM Tests

Smouldering removed >99% of 1234678-HpCDD, >99.9% of OCDF and OCDD, and ~100% of all other PCDD/F compounds initially present in the sewage sludge. Table 5.3 summarizes the quantities of PCDD/Fs released in the combustion gases from the LAB and DRUM tests, and Figure 5.3 presents the quantities normalized per mass of sludge destroyed.

Of the four DRUM tests that were monitored for PCDD/Fs, PCDD/Fs were not detected in the emissions from either DRUM 2 or DRUM 4, both of which were sampled during robust smouldering conditions. DRUM 1, which was sampled near the end of smouldering and captured end-effects, and DRUM 3, which exhibited less robust smouldering, released small concentrations: 45 and 48 pg TEQ /m^3 PCDD/Fs, respectively. These small PCDD/F concentrations in DRUM 1 and 3 were comparable to the LAB experiments, where LAB 1a and 1b released 26 - 35 pg TEQ /m^3 PCDD/Fs, and LAB 2 released 3.9 pg TEQ /m^3 PCDD/Fs (Table 5.3). All LAB and DRUM tests that had measurable PCDD/Fs in the emissions released some 2,3,7,8-TCDF, 1,2,3,4,6,7,8-HpCDD, and OCDD (Table 5.3). LAB 1a also released 1,2,3,6,7,8-HxCDD, which was also measured in DRUM 3, along with 1,2,3,4,6,7,8-HpCDF, OCDF, 1,2,3,4,7,8-HxCDD, and 1,2,3,7,8,9-HxCDD, which were not detected in any other experiment.

All measured PCDD/F values were exceptionally low. After correcting the reactor emissions to 11% oxygen (Table 5.3), the concentrations from the DRUM tests were 105 pg TEQ /m^3 PCDD/Fs from DRUM 1, 145 pg TEQ /m^3 PCDD/Fs from DRUM 3. The corrected concentrations from the LAB tests were slightly lower, with 70 pg TEQ /m^3

PCDD/Fs from LAB 1a, 63 pg TEQ /m^3 PCDD/Fs from LAB 1b, and 18 pg TEQ /m^3 PCDD/Fs from LAB 2. Therefore, the PCDD/F release from all LAB tests were below the standard 80 pg TEQ /m^3 ECA requirement for exhaust stack release. While the PCDD/F release from the DRUM tests were slightly higher than the ECA requirement, after passing through the onsite emissions treatment system, all emissions from every experiment fully complied with the ECA and most tests had no detectable stack release (Section C.3, Appendix C).

After smouldering, only three PCDD/F compounds were detected in the post-treatment ash from DRUM 1: OCDF, OCDD, and 1234678-HpCDD (Section C.3, Appendix C). These measurements were all above the detection limit but below the calibrated range. The ash contained ~1.27 pg/g 1234678-HpCDD, ~0.24 pg/g OCDF, and ~5.09 pg/g OCDD.

The normalized PCDD/F release amounts in Figure 5.3 accounted for variable experimental conditions across the LAB and DRUM scale tests. These results show that most experiments released similar amounts of common PCDD/Fs. In addition, the LAB tests generally exhibited slightly lower PCDD/F release than the DRUM tests, except for OCDD released from LAB 2. Figure 5.3 also includes hypothetical release values if all PCDD/Fs initially present in the sludge were released.

5.3.3.2 Interpretation of Results

The PCDD/F quantities measured in this study are similar to laboratory scale incineration studies (W. Deng et al., 2009) and commercial sludge incinerators (e.g., Werther & Ogada, 1999). Therefore, smouldering sewage sludge releases similarly low PCDD/Fs as incineration; however, the mechanisms leading to PCDD/Fs in the emissions are hypothesized to be different than those in incinerators (see Section 5.3.2.3.). Of the dioxins measured, the two lowest toxicity congeners, OCDD and 1,2,3,4,6,7,8-HpCDD, comprised most of the released PCDD/F compounds from both LAB and DRUM tests. OCDD comprised 69 – 90% of LAB and 55 – 58% of DRUM PCDD/F emissions by mass; 1,2,3,4,6,7,8-HpCDD comprised 9 – 26% of LAB and 24 – 32% of DRUM PCDD/F emissions by mass. The most toxic congener released from any smouldering experiment was 2,3,7,8-TCDF (TEF of 0.1), which contributed < 5% of the PCDD/F mass in the LAB tests, and < 10% PCDD/F mass in DRUM tests.

The two laboratory repeats, LAB 1a and 1b, both of which were characterized as having robust smouldering throughout the test, had very similar PCDD/F results indicating good repeatability. Comparatively, LAB 2 was characterized as non-robust since it fostered non-self-sustaining smouldering, which was evident from the large crust formation and declining temperatures (Section C.1, Appendix C). This experiment released less PCDD/Fs than LAB 1a and 1b, even under weaker conditions, which could be due to less overall material smouldered during LAB 2. Overall, a very small quantity of PCDD/Fs (consistently below the ECA regulations) were released during each LAB test, irrespective of smouldering performance. The quantities were similar to the PCDD/Fs measured in the

emissions from DRUM tests during less robust smouldering conditions (i.e., DRUM 1 and 3).

For the larger scale repeat of LAB 1a and 1b, i.e., DRUM 1, the PCDD/F sample may have captured end-effects when the smouldering front reached the end of the fuel bed (Figure 5.2). Similar to the behaviour of other condensable compounds in applied smouldering systems, PCDD/Fs may be released ahead of the smouldering front and retained by the porous media (i.e., sand) through (*i*) recondensation onto the cooler sand grains and/or (*ii*) physical filtration (e.g., if the PCDD/Fs are sorbed on unburned particulate material). If recondensation occurs, then some accumulated PCDD/Fs could be released when the smouldering front reached the end of the fuel bed, which has been demonstrated for other condensable compounds in smouldering systems (Kinsman, 2015; Martins et al., 2010; Rashwan et al., 2021b; Yermán et al., 2015). The total unburned hydrocarbons measured in the emissions from DRUM 2, 3, and 4 supports this recondensation hypothesis, as the total hydrocarbons relative to the CO_2 fraction increased throughout smouldering propagation (Section C.2, Appendix C). Therefore, this data indicates that condensable hydrocarbons, sometimes including PCDD/Fs, likely accumulated in the cool region ahead of the smouldering front and were released from the system when the temperatures rose as the smouldering front approached the end of the system, i.e., similar to a common distillation column. All other tests were not timed to capture this end-effect (Sections C.1 and C.2, Appendix C).

Under weaker smouldering conditions, the PCDD/Fs measured from DRUM 3 were generally similar to those measured when the smouldering front exited the fuel pack in DRUM 1. However, the weaker smouldering in DRUM 3 released additional PCDD/Fs

that were not measured during stronger smouldering (i.e., DRUM 2 and 4) or when the front exited the column (DRUM 1). This may be because this experiment did not facilitate the high temperatures and residence times to destroy these PCDD/Fs, and instead released them in the emissions; Section 5.3.2.3. discusses this hypothesized pathway in more detail.

In DRUM 2 and 4, the PCDD/Fs were sampled soon after self-sustaining smouldering was achieved and during robust smouldering (sample timing and temperature histories are presented in Section C.2, Appendix C). Therefore, these PCDD/F measurements demonstrate that very small amounts of PCDD/Fs were likely released during robust smouldering and recondensed locally, and a small amount of recondensed PCDD/Fs were likely released as an end-effect, as hypothesized in DRUM 1.

The normalized PCDD/F results in Figure 5.3 provide further insight into the conditions that influence PCDD/F release during smouldering. Interestingly, after accounting for all experimental and operational differences between LAB and DRUM tests, the PCDD/F results align more closely than in Table 5.3. While smaller LAB scale experiments exhibited slightly higher smouldering propagation velocities (Table 5.1), heating rates (Sections C.1 and C.2, Appendix C), and peak temperatures (Table 5.1) than the larger DRUM scale experiments, the characteristic smouldering behaviour in these two systems was similar. This similar system behaviour corresponds to similar PCDD/Fs released per mass of sludge smouldered (Figure 5.3), which demonstrates that PCDD/F released during sewage sludge smouldering may not be sensitive to changes in operational conditions (e.g., reactor scale or air flux). This is an important finding, as it demonstrates that the risk from PCDD/Fs may be low in commercial scale smouldering reactors for sewage sludge treatment.

Table 5.3: Summary of PCDD/F release in combustion gases from DRUM and LAB tests

Congener	TEF[1]	Concentration of PCDD/F in combustion gases (pg/m^3)						
		LAB			DRUM			
		1a	1b	2	1	2	3	4
2378-TCDD	1	B.D.L. [2]	B.D.L.	B.D.L.	B.D.L.	B.D.L.	B.D.L.	B.D.L.
12378-PeCDD	1	B.D.L.	B.D.L.	B.D.L.	B.D.L.	B.D.L.	B.D.L.	B.D.L.
23478-PeCDF	0.3	B.D.L.	B.D.L.	B.D.L.	B.D.L.	B.D.L.	B.D.L.	B.D.L.
123478-HxCDF	0.1	91	172	20	340	B.D.L.	116	B.D.L.
123678-HxCDF	0.1	B.D.L.	B.D.L.	B.D.L.	B.D.L.	B.D.L.	B.D.L.	B.D.L.
234678-HxCDF	0.1	B.D.L.	B.D.L.	B.D.L.	B.D.L.	B.D.L.	B.D.L.	B.D.L.
123789-HxCDF	0.1	B.D.L.	B.D.L.	B.D.L.	B.D.L.	B.D.L.	B.D.L.	B.D.L.
2378-TCDF	0.1	B.D.L.	B.D.L.	B.D.L.	B.D.L.	B.D.L.	B.D.L.	B.D.L.
123478-HxCDD	0.1	B.D.L.	B.D.L.	B.D.L.	B.D.L.	B.D.L.	13	B.D.L.
123678-HxCDD	0.1	164	B.D.L.	B.D.L.	B.D.L.	B.D.L.	167	B.D.L.
123789-HxCDD	0.1	B.D.L.	B.D.L.	B.D.L.	B.D.L.	B.D.L.	88	B.D.L.
12378-PeCDF	0.03	B.D.L.	B.D.L.	B.D.L.	B.D.L.	B.D.L.	B.D.L.	B.D.L.
1234678-HpCDF	0.01	B.D.L.	B.D.L.	B.D.L.	B.D.L.	B.D.L.	74	B.D.L.
1234789-HpCDF	0.01	B.D.L.	B.D.L.	B.D.L.	B.D.L.	B.D.L.	B.D.L.	B.D.L.
1234678-HpCDD	0.01	705	899	146	1087	B.D.L.	794	B.D.L.
OCDF	0.0003	B.D.L.	B.D.L.	B.D.L.	B.D.L.	B.D.L.	271	B.D.L.
OCDD	0.0003	2141	2381	1440	1969	B.D.L.	1862	B.D.L.
Total Mass Concentration [3]	pg / m³	3101	3452	1605	3396	0	3384	0
Total TEQ Concentration [4]	pg TEQ / m³	35	26	3.9	45	0	48	0
Oxygen content [5]	%	16.0	16.8	18.8	17.8	15.8	16.4	17
Oxygen correction factor [6]	-	2.0	2.4	4.7	3.2	1.9	2.2	2.5
TEQ Concentration (corrected to O_2) [7]	pg TEQ / m³	70	62	18	145	0	105	0

[1] Toxic equivalency factors (USEPA, 2010)
[2] Below the detection limit (B.D.L.), where these limits are summarized in the Supplementary Materials
[3] Sum of the PCDD/F mass measured in the emissions normalized per unit volume of emissions analyzed
[4] Total mass concentration considering the TEQs of the PCDD/Fs measured
[5] Measured immediately after the sampling train
[6] Calculated according to the Canadian Council of Ministers of the Environment (1989) equation: {*Concentration (at 11% O_2) = {Concentration x [(20.9-11.0)/20.9]}*
[7] TEQ concentration of PCDD/Fs in emissions normalized to 11% oxygen content

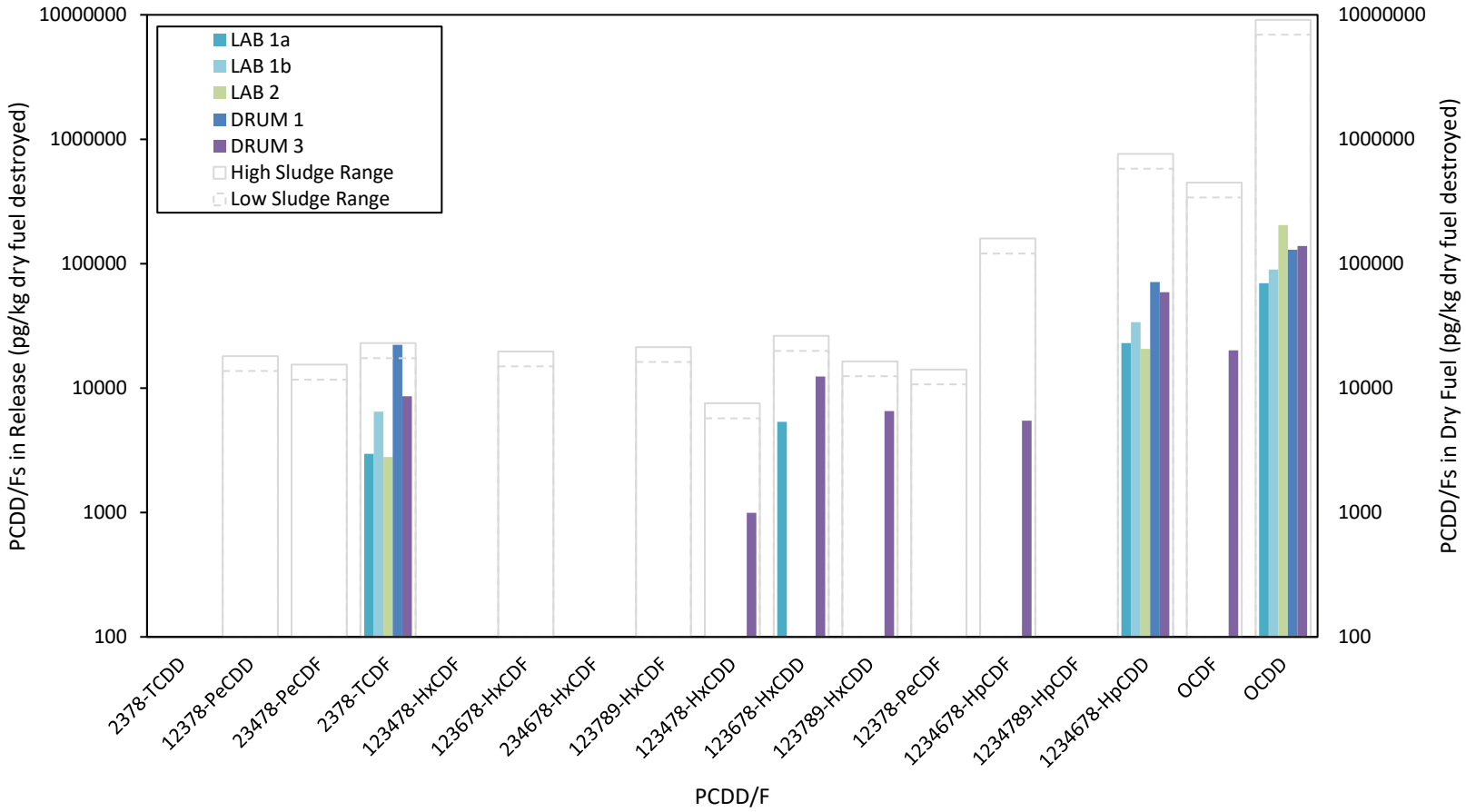

Figure 5.3: PCDD/F measured in the emissions from LAB and DRUM tests normalized per mass of dry fuel destroyed. The solid columns present the emissions results on the primary axis. DRUM tests 2 and 4 are not presented since both had no detection of any PCDD/F compound. The outlined columns show the upper and lower range of PCDD/F content in the virgin sewage sludge normalized per mass of dry fuel; thereby assuming the approximate maximum rates if all PCDD/Fs initially present in the sludge were released.

5.3.3.3 Pathways of PCDD/F Release

The sludge used in this study contained quantifiable amounts of 14 out of the 17 most toxic PCDD/F congeners. Figure 5.3 shows the PCDD/Fs originally present in the virgin sewage sludge normalized to the MC and range of ash contents typically observed in the sewage sludge (i.e., 22 – 29%). This illustrates a range of hypothetical maximum values if all PCDD/Fs initially present in the sludge were released. All the normalized PCDD/F releases from the DRUM and LAB experiments are lower than this hypothetical range. Moreover, all PCDD/F compounds released in the emissions were present in the virgin sludge, even the unique compounds released from DRUM 3 during weak smouldering. The mass fractions of PCDD/F congeners within the sludge are shown in Figure 5.4. The mass fractions also suggest that the measured compounds are being released rather than created, because they align with the distribution observed in the emissions, i.e., OCDD comprises the largest PCDD/F mass fraction at 86%, followed by 1,2,3,4,6,7,8-HpCDD at 7% (Section C.2, Appendix C).

Because the temperatures during smouldering treatment evolve in space in time, the sludge is heated from ambient temperature to peak smouldering temperatures at heating rates between 50-200 °C min^{-1}. Therefore, the PCDD/Fs originally present in the sludge may have transformed or changed phase due to the lower heating rates and transported out of the reactor instead of being completely destroyed. The drying, pre-heating, and pyrolysis zones (Figure 5.2) within a smouldering reactor provide the low-temperature conditions that may facilitate the release of PCDD/Fs originally present in the virgin sewage sludge. While most of these PCDD/Fs likely recondense within the sand-sludge matrix ahead of the smouldering front, some may be released with the emissions.

Non-uniform conditions (both in the flow field and reactions due to heat losses) within the fixed bed may produce localized zones of lower temperatures, typically at the reactor edges, that result in air channeling (Figure 5.2B/C). With the smouldering front moving unevenly through the waste pack, some regions will be subjected to extended low-temperature conditions and may be by-passed by the smouldering front (i.e., unburned areas). Therefore, non-uniform conditions during weak smouldering may result in higher quantities of PCDD/Fs released in emissions relative to stronger smouldering conditions. Furthermore, during weaker smouldering conditions (e.g., DRUM 3), the unburned sludge would likely still contain some amount of the original PCDD/Fs. Comparatively, during robust smouldering, the PCDD/Fs that are not released from the sludge are almost completely destroyed (>99% of all compounds; Section C.3, Appendix C).

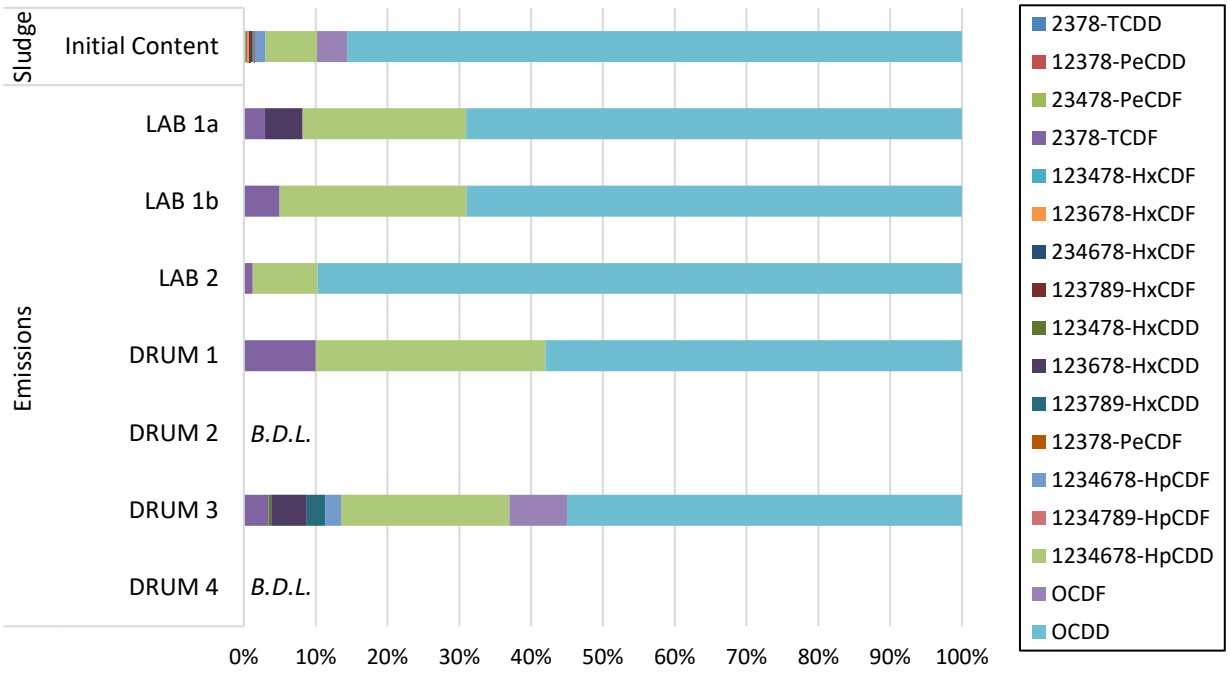

Figure 5.4: Mass fractions of the 17 PCDD/F congeners found in the emissions from DRUM and LAB tests compared to the virgin sewage sludge.

5.3.3.4 Pathways of Formation

During non-robust smouldering conditions, products of incomplete combustion (e.g., VOCs) are more likely to form. VOCs, particularly benzenes and chlorinated benzenes, were quantified to provide some insight into potential PCDD/F formation via precursor pathways. The concentrations of benzene-type aromatic VOCs within the combustion gases of DRUM 3 and 5 (the two experiments that monitored for VOCs) are shown in Figure 5.5. Since DRUM 5 and DRUM 3 supported weak smouldering that resulted in large quantities of unburned and pyrolyzed sludge, the VOCs produced during these tests provides a conservative estimate of precursors present in the emissions during non-robust conditions. Overall, few benzene-type aromatic VOCs were observed in the combustion gases, and the trends are relatively consistent between experiments. The highest concentration of aromatic VOCs was released from DRUM 3, 27,500 $\mu g/m^3$ of benzene, followed by 12,800 and 11,900 $\mu g/m^3$ of styrene and toluene, respectively. These compounds were also released from DRUM 5, but to lesser extents, i.e., 8,800 $\mu g/m^3$ of benzene, 5,600 $\mu g/m^3$ of styrene, and 10,100 $\mu g/m^3$ of toluene. Chlorobenzene, which is a known precursor of PCDD/Fs, was not present in detectable concentrations for DRUM 3 and relatively minor concentrations for DRUM 5 (254 $\mu g/m^3$). Additionally, all isomers of dichlorobenzene, and 1,2,4-trichlorobenzene were below detection limits for both tests. Therefore, even under weak combustion conditions, smouldering does not produce significant quantities of PCDD/F precursor compounds, making this an unlikely pathway of formation.

De novo synthesis accounts for significantly less PCDD/F formation in typical incinerators than precursor pathways (Tame et al., 2007), and the same is likely true for

smouldering. The chemistry, low process air fluxes, and filtration offered by the porous media minimize particulate matter and soot release in the emissions from smouldering systems (Torero et al., 2020). Therefore, *de novo* reactions, which occur on the surfaces of solid carbon in the combustion gases (e.g., soot; (Stanmore, 2004)), are probably negligible in sludge smouldering systems. However, more work is needed to better understand *de novo* reactions in smouldering systems.

Furthermore, the emissions temperatures directly above the fuel bed (between ~4 – 37 cm above pack for LAB tests and 40 – 60 cm DRUM tests) do not generally correspond to the range for optimal heterogeneous reactions (i.e., 200-400°C; Stanmore, 2004) until after the smouldering front reaches the end of the fuel pack (see Sections C.2 and C.3, Appendix C). These optimal temperatures are only achieved in the emissions following robust smouldering (e.g., LAB 1a and 1b, and DRUM 1 and 4) where robust smouldering would destroy any precursor compounds that could potentially form PCDD/Fs in the post-combustion region. During weaker smouldering (e.g., LAB 2, and DRUM 3), the emissions temperatures did not achieve this optimal range, even though PCDD/Fs were detected. This result further suggests that PCDD/Fs measured were released, not formed.

PCDD/F formation may be possible from heterogeneous pathways in smouldering, much like incineration; however, more work needs to be done to fully understand the mechanisms governing the risks of PCDD/F formation in smouldering systems. From these experiments, it is much more likely that PCDD/Fs originally present in the sludge were released from the sludge rather than formed.

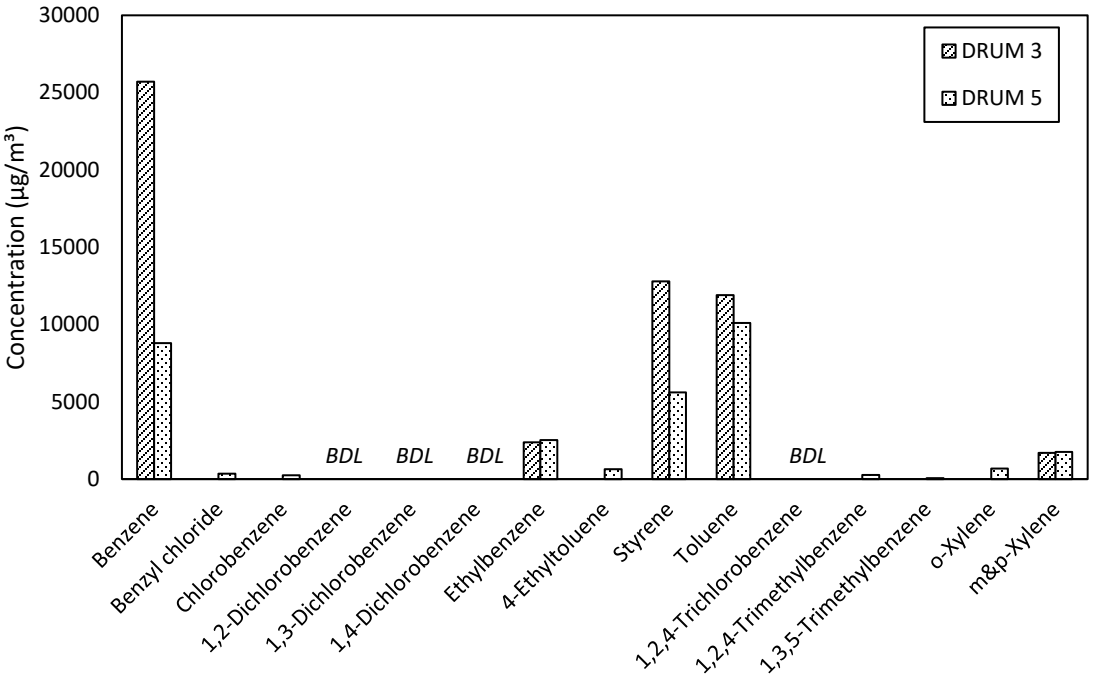

Figure 5.5: Concentrations of aromatic VOCs in the combustion gases from DRUM 3 and 5 during sewage sludge smouldering. Compounds below the detection limits have been labeled as 'BDL'.

5.4 Conclusions

Smouldering provides an economic and energy efficient alternative to incineration of sewage sludge and presents additional advantages by reducing hazardous by-product formation. Similar to incineration, smouldering combustion destroys sludge and concentrates potentially toxic elements (PTEs) within post-treatment ash. However, lower relative operational temperatures and filtration by the porous bed result in minimal PTE release in exhaust gases compared to traditional incineration. With relatively lower quantities of PTEs being released in the emissions, bulk removal and disposal of these compounds from the reactor sand and ash would be environmentally advantageous and operationally simpler. In terms of emissions by-products, there is strong evidence to suggest that PCDD/Fs were not formed in measurable amounts during smouldering treatment; instead, a fraction of the PCDD/Fs originally present in the virgin sludge were

released via volatilization – predominantly in less robust conditions. Altogether, smouldering acted as a sink for PCDD/Fs, releasing 0 – 3% of the originally present compounds into the emissions and destroying >99% of the remainder with <1% of originally present PCDD/Fs remaining in the post-treatment ash. This PCDD/Fs release was not highly sensitive to operational conditions, including reactor scale and applied air flux. This result highlights a strong benefit of smouldering combustion: the release of condensable compounds does not seem significantly influenced by system scale changes; this is important for emerging industrial smouldering applications. Moreover, due to recondensation ahead of smouldering, some PCDD/Fs may release at higher concentrations when the smouldering front reaches the end of the fuel bed. Since the quantity of PCDD/Fs released is near the allowable limit for stack emissions, minimal emissions treatment is necessary, thereby simplifying industrial application of smouldering treatment for sewage sludge. Further research linking PCDD/F release to operating conditions may facilitate selective application of emissions management measures when needed, instead of continuously as conducted during smouldering operation.

5.5 References

Altwicker, E.R., Konduri, R.K.N.V., Lin, C., Milligan, M.S., 1992. Rapid formation of polychlorinated dioxins/furans in the post combustion region during heterogeneous combustion. Chemosphere 25, 1935–1944. https://doi.org/10.1016/0045-6535(92)90032-M

Deng, W., Jianhua, Y., Xiaodong, L.I., Fei, W., Yong, C., Shengyong, L.U., 2009. Emission characteristics of dioxins, furans and polycyclic aromatic hydrocarbons during fluidized-bed combustion of sewage sludge. J. Environ. Sci. 21, 1747–1752. https://doi.org/10.1016/S1001-0742(08)62483-3

Element, C., 2007. SW-846 Method 3051A: Microwave Assisted Acid Digestion of Sediments, Sludges, Soils, and Oils.

Feng, C., Cheng, M., Gao, X., Qiao, Y., Xu, M., 2020. Occurrence forms and leachability

of inorganic species in ash residues from self-sustaining smouldering combustion of sewage sludge. Proc. Combust. Inst. 000, 1–8. https://doi.org/10.1016/j.proci.2020.06.008

Fiedler, H., 2003. Dioxins and Furans (PCDD/PCDF), in: Persistent Organic Pollutants. Springer-Verlag, pp. 123–201. https://doi.org/10.1007/10751132_6

Fournie, T., Rashwan, T.L., Switzer, C., Gerhard, J.I., 2022. Phosphorus recovery and reuse potential from smouldered sewage sludge ash. Waste Manag. 137, 241–252. https://doi.org/10.1016/J.WASMAN.2021.11.001

Fullana, A., Conesa, J.A., Font, R., Sidhu, S., 2004. Formation and destruction of chlorinated pollutants during sewage sludge incineration. Environ. Sci. Technol. 38, 2953–2958. https://doi.org/10.1021/es034896u

Fytili, D., Zabaniotou, A., 2008. Utilization of sewage sludge in EU application of old and new methods--A review. Renew. Sustain. Energy Rev. 12, 116–140.

Haimovici, L., Reiner, E.J., Besevic, S., Jobst, K.J., Robson, M., Kolic, T., MacPherson, K., 2016. A modified QuEChERS approach for the screening of dioxins and furans in sediments. Anal. Bioanal. Chem. 408, 4043–4054. https://doi.org/10.1007/s00216-016-9493-0

Han, J., Xu, M., Yao, H., Furuuchi, M., Sakano, T., Kanchanapiya, P., Kanaoka, C., 2006. Partition of heavy and alkali metals during sewage sludge incineration. Energy and Fuels 20, 583–590. https://doi.org/10.1021/ef0501602

Jiwan, S., Ajah, K.S., 2011. Effects of Heavy Metals on Soil, Plants, Human Health and Aquatic Life. Int. J. Res. Chem. Environ. 1, 15–21.

Kinsman, L.L., 2015. Smouldering Remediation: Transient Effects of Front Propogation. Western University.

London, C. of, 2019. 2018 National Pollutant Release Inventory (NPRI) Report. London, ON.

Marani, D., Braguglia, C.M., Mininni, G., Maccioni, F., 2003. Behaviour of Cd, Cr, Mn, Ni, Pb, and Zn in sewage sludge incineration by fluidised bed furnace. Waste Manag. 23, 117–124.

Martins, M.F., Salvador, S., Thovert, J.F., Debenest, G., 2010. Co-current combustion of oil shale - Part 2: Structure of the combustion front. Fuel 89, 133–143. https://doi.org/10.1016/j.fuel.2009.06.040

McKay, G., 2002. Dioxin characterisation, formation and minimisation during municipal solid waste (MSW) incineration: Review. Chem. Eng. J. 86, 343–368. https://doi.org/10.1016/S1385-8947(01)00228-5

Nowak, B., Aschenbrenner, P., Winter, F., 2013. Heavy metal removal from sewage sludge ash and municipal solid waste fly ash - A comparison. Fuel Process. Technol. 105, 195–201. https://doi.org/10.1016/j.fuproc.2011.06.027

Pudasainee, D., Seo, Y.C., Kim, J.H., Jang, H.N., 2013. Fate and behavior of selected heavy metals with mercury mass distribution in a fluidized bed sewage sludge incinerator. J. Mater. Cycles Waste Manag. 15, 202–209. https://doi.org/10.1007/s10163-013-0115-z

Rashwan, T., 2020. Sustainable Smouldering for Waste-to-Energy: Scale, Heat Losses, and Energy Efficiency. Electron. Thesis Diss. Repos.

Rashwan, T.L., Fournie, T., Torero, J.L., Grant, G.P., Gerhard, J.I., 2021a. Scaling up self-sustained smouldering of sewage sludge for waste-to-energy. Waste Manag. 135, 298–308. https://doi.org/10.1016/J.WASMAN.2021.09.004

Rashwan, T.L., Gerhard, J.I., Grant, G.P., 2016. Application of self-sustaining smouldering combustion for the destruction of wastewater biosolids. Waste Manag. 50, 201–212. https://doi.org/10.1016/j.wasman.2016.01.037

Rashwan, T.L., Torero, J.L., Gerhard, J.I., 2021b. Heat losses in a smouldering system: The key role of non-uniform air flux. Combust. Flame 227, 309–321. https://doi.org/10.1016/j.combustflame.2020.12.050

Rashwan, T.L., Torero, J.L., Gerhard, J.I., 2021c. The improved energy efficiency of applied smouldering systems with increasing scale. Int. J. Heat Mass Transf. 177, 121548. https://doi.org/10.1016/J.IJHEATMASSTRANSFER.2021.121548

Reiner, E.J., 2016. Analysis of Dioxin and Dioxin-Like Compounds, in: Dioxin and Related Compounds: Special Volume in Honor of Otto Hutzinger. Springer International Publishing, pp. 51–94.

Serrano, A., Wyn, H., Dupont, L., Villa-Gomez, D.K., Yermán, L., 2020. Self-sustaining treatment as a novel alternative for the stabilization of anaerobic digestate. J. Environ. Manage. 264, 110544. https://doi.org/10.1016/j.jenvman.2020.110544

Shao, J., Yan, R., Chen, H., Yang, H., Lee, D.H., Liang, D.T., 2008. Emission characteristics of heavy metals and organic pollutants from the combustion of sewage sludge in a fluidized bed combustor. Energy and Fuels 22, 2278–2283. https://doi.org/10.1021/ef800002y

Stanmore, B.R., 2004. The formation of dioxins in combustion systems. Combust. Flame 136, 398–427. https://doi.org/10.1016/j.combustflame.2003.11.004

Tame, N.W., Dlugogorski, B.Z., Kennedy, E.M., 2007. Formation of dioxins and furans during combustion of treated wood. Prog. Energy Combust. Sci. 33, 384–408. https://doi.org/10.1016/J.PECS.2007.01.001

Telliard, W., 2001. Method 1684: Total, fixed, and volatile solids in water, solids, and biosolids. Washington.

Torero, J.L., Gerhard, J.I., Martins, M.F., Zanoni, M.A.B., Rashwan, T.L., Brown, J.K., 2020. Processes defining smouldering combustion: Integrated review and synthesis. Prog. Energy Combust. Sci. https://doi.org/10.1016/j.pecs.2020.100869

Tuppurainen, K., Halonen, I., Ruokojärvi, P., Tarhanen, J., Ruuskanen, J., 1998. Formation of PCDDs and PCDFs in municipal waste incineration and its inhibition mechanisms: A review. Chemosphere. https://doi.org/10.1016/S0045-6535(97)10048-0

USEPA, 1999. Air Method, Toxic Organics-15 (TO-15): Compendium of Methods for the Determination of Toxic Organic Compounds in Ambient Air, Second Edition: Determination of Volatile Organic Compounds (VOCs) in Air Collected in Specially-Prepared Canisters and Analyzed . https://doi.org/EPA 625/R-96/010b

USEPA, 1995. Solid Waste Disposal 2.2-1 2.2: Sewage Sludge Incineration.

Van den Berg, M., Birnbaum, L.S., Denison, M., Vito, M. De, Farland, W., Feeley, M., Fiedler, H., Hakansson, H., Hanberg, A., Haws, L., Rose, M., Safe, S., Schrenk, D., Tohyama, C., Tritscher, A., Tuomisto, J., Tysklind, M., And, N.W., Peterson, R.E., 2006. The 2005 World Health Organization Reevaluation of Human and Mammalian Toxic Equivalency Factors for Dioxins and Dioxin-Like Compounds. Toxicol. Sci. 93, 223–241.

Wallbaum, U., Nestrick, T., Lamparski, L., Krueger, J., Wilken, M., 1995. Comparison of dioxin sampling methods; US EPA Method 23 versus two German VDI methods. Organohalogen Compd. 23, 53–57.

Werther, J., Ogada, T., 1999. Sewage sludge combustion. Prog. Energy Combust. Sci. https://doi.org/10.1016/S0360-1285(98)00020-3

Yermán, L., Hadden, R.M., Carrascal, J., Fabris, I., Cormier, D., Torero, J.L., Gerhard, J.I., Krajcovic, M., Pironi, P., Cheng, Y.L., 2015. Smouldering combustion as a treatment technology for faeces: Exploring the parameter space. Fuel 147, 108–116. https://doi.org/10.1016/j.fuel.2015.01.055

Zabaniotou, A., Theofilou, C., 2008. Green energy at cement kiln in Cyprus-Use of sewage sludge as a conventional fuel substitute. Renew. Sustain. Energy Rev. https://doi.org/10.1016/j.rser.2006.07.017

Zhang, H., He, P.-J., Shao, L.-M., 2008. Fate of heavy metals during municipal solid waste incineration in Shanghai. J. Hazard. Mater. 156, 365–373. https://doi.org/10.1016/j.jhazmat.2007.12.025

Zhang, Mengmei, Buekens, A., Li, • Xiaodong, 2017. Dioxins from Biomass Combustion: An Overview. Waste and Biomass Valorization.

https://doi.org/10.1007/s12649-016-9744-5

Zhang, Meng, Shi, Y., Lu, Y., Johnson, A.C., Sarvajayakesavalu, S., Liu, Z., Su, C., Zhang, Y., Juergens, M.D., Jin, X., 2017. The relative risk and its distribution of endocrine disrupting chemicals, pharmaceuticals and personal care products to freshwater organisms in the Bohai Rim, China. Sci. Total Environ. 590–591, 633–642. https://doi.org/10.1016/j.scitotenv.2017.03.011

Zhou, Y., Meng, J., Zhang, M., Chen, S., He, B., Zhao, H., Li, Q., Zhang, S., Wang, T., 2019. Which type of pollutants need to be controlled with priority in wastewater treatment plants: Traditional or emerging pollutants? Environ. Int. 131. https://doi.org/10.1016/j.envint.2019.104982

Chapter 6

6 Smouldering to treat PFAS contaminated sewage sludge

6.1 Introduction

Recently, compounds of concern in sewage sludge have expanded to include endocrine disrupting compounds, including, per- and polyfluorinated compounds (PFAS) (Clarke and Smith, 2011). PFAS are a group of thousands of chemicals, with the most common being perfluorooctane sulfonate (PFOS) and perfluorooctanoic acid (PFOA)(Buck et al., 2011). Due to their toxicity and persistence in the environment, both PFOS and PFOA production have been restricted around the world (UNEP, 2019; USEPA, 2020). The properties of PFAS, including chemical and thermal stability, have made them useful in many applications (Kissa, 2001). However, it is these same properties that make PFAS challenging to remediate.

PFAS are becoming ubiquitous in the environment, including at wastewater treatment plants (WWTPs) (Arvaniti et al., 2014, 2012; Gómez-Canela et al., 2012; Moodie et al., 2021; Sindiku et al., 2013; Sun et al., 2011; Venkatesan and Halden, 2013; Yan et al., 2012). Sources of PFAS to WWTPs include industrial discharge (Kunacheva et al., 2011; Washington et al., 2010), landfill leachate (Gallen et al., 2016), and domestic sources (Pan et al., 2010). Since conventional wastewater treatment methods are ineffective at treating PFAS, WWTPs tend to be a sink for these compounds (Ahrens et al., 2009). Additionally, WWTPs are potential sources of PFAS since they can be formed via precursor degradation (Houtz et al., 2018; Lakshminarasimman et al., 2021; Pan et al., 2010; Sepulvado et al., 2011). Within WWTPs, most PFAS tends to be concentrated in

sewage sludge (Clarke and Smith, 2011; Milinovic et al., 2016; Zhang et al., 2013). Therefore, sewage sludge management needs to consider the fate of these compounds. Landfilling sewage sludge can result in PFAS entering the environment via leachate (Ahrens et al., 2011; Gallen et al., 2016). A common alternative to landfilling sewage sludge is direct land application as a soil amendment. Land applied sludges can be a significant source of PFAS contamination to the environment through surface runoff or infiltration (Sepulvado et al., 2011), or circulate in the environment via plant uptake (Blaine et al., 2013).

With increasing regulations, especially for PFOS and PFOA (USEPA, 2021), there is significant interest in developing methods of removing and degrading PFAS from sewage sludge. While incineration may be an effective method of destroying contaminants present in sewage sludge (Ross et al., 2018), it is also an energy intensive and expensive process (Werther and Ogada, 1999). The use of thermal treatment methods to remove PFAS from sewage sludge is relatively limited. Current thermal methods being explored include incineration (Wang et al., 2013), pyrolysis (Kim et al., 2015; Kundu et al., 2021), and hydrothermal treatments (Yu et al., 2020a; Zhang and Liang, 2021). While these studies demonstrate the limited understanding and complexities of treating PFAS in sewage sludge, they also provide valuable information that can help advance treatment technologies. Overall, more work is needed in this area.

In 2020, smouldering combustion was shown to be an effective method of treating PFAS contaminated soils (Duchesne et al., 2020). Smouldering is a flameless form of burning that occurs on the surface of a fuel within a porous medium (Rein, 2016). This exothermic reaction produces heat from the heterogenous oxidation of the fuel (i.e., oxygen

directly attacks the fuel surface) (Ohlemiller, 1985). Smouldering has the potential to be self-sustaining (i.e., no additional energy input is required after ignition) if the oxidation reaction releases sufficient energy to overcome heat loses (Ohlemiller, 1985) and the system has a positive global energy balance (Zanoni et al., 2019). Smouldering combustion has been demonstrated to be an effective, energy efficient remediation strategy for both soil treatment (Grant et al., 2016; Pironi et al., 2009; Scholes et al., 2015; Switzer et al., 2009) and management of wastewater sludges (Rashwan et al., 2016) and faeces (Yermán et al., 2015). In this context, the organic contaminants and/or wastes are the fuel, and self-sustained smouldering destroys virtually all of it by oxidation; typically, only inert soil grains (e.g., quartz sand) and ash composed of inorganic compounds remains. To treat PFAS contaminated soil, a supplemental fuel was added (granular activated carbon (GAC)) to achieve sufficient temperature for PFAS degradation (~900°C) (Duchesne et al., 2020). While smouldering sewage sludge has been explored in the context of process optimization (Rashwan et al., 2016), scaling (Rashwan et al., 2021a), landfilling potential (Feng et al., 2020), and resource recovery potential (Fournie et al., 2022), it is not known how PFAS originally present in sewage sludge behaves during smouldering.

The aim of this study is to evaluate the use of smouldering to treat PFAS in sewage sludge. This was done in three phases: (I) evaluating PFAS removal, (II) assessing methods of improving degradation of PFAS, and (III) exploring the impact of scaling on PFAS removal. Phases I and II consisted of a series of laboratory smouldering experiments that evaluated PFAS fate in varied input and operating conditions, including treating high moisture content sludge, and CaO addition, which has been shown previously to improve PFAS mineralization in sewage sludge during thermal treatment (Wang et al., 2013).

Finally, Phase III explored how scale impacts PFAS removal. This work presents the first comprehensive evaluation of PFAS fate during smouldering treatment of sewage sludge.

6.2 Materials and Methods

6.2.1 Waste Collection and Preparation

Sewage sludge was obtained from a wastewater treatment plant in Ontario, Canada. Complete details on wastewater processing and sludge generation at Greenway can be found elsewhere (Fournie et al., 2021; Rashwan et al., 2016). The sewage sludge produced from a dewatered slurry of primary and secondary sludge had an average moisture content (MC) of 74.3%, determined using USEPA Method 1684 (Telliard, 2001). All sewage sludge utilized for the lab tests was collected in a single batch (~40 kgs) to minimize variability between tests. Sewage sludge utilized for the DRUM tests was collected in individual batches (~30 kg) immediately ahead of each test. DRUM tests were performed between January 2018 – August 2019.

Sewage sludge storage and preparation followed a modified procedure developed by Rashwan et al. (2016). Virgin sewage sludge was batch dried in an oven at 105°C to achieve a MC of <1%. The samples were dried until there were no measurable changes in the sludge mass. To homogenize the material, the dried sludge was pulverized using an immersion blender and sieved to ensure all material was <1 cm. The homogenized, dried sludge was then stored in 19 L sealed containers at 5°C until use.

Preliminary analysis of sewage sludge samples collected between January 2018 – August 2019 showed that concentrations of PFOS ranged from 224 – 2230 ng/g and PFOA was below the detection limit for all samples (Table D.1-1, Appendix D, Section D.1). The

sewage sludge contained similarly high PFOS compared to treatment studies that have spiked their sewage sludge (Hamid and Li, 2018; Yu et al., 2020a). Therefore, it was decided that the virgin sewage sludge would be utilized without additional PFAS spiking.

6.2.2 Smouldering Column Set-up and Procedure

Cylindrical reactors fabricated from stainless steel were used for all laboratory experiments (LAB: 0.08 m radius) and larger scale tests in oil-drum sized reactors (DRUM: 0.3 m radius). The reactors were wrapped in 0.051 m thick insulation (LAB: MinWool®, Johns Manville; DRUM: FyreWrap® Elite® Blanket, Unifrax). The reactor set-up and instrumentation for LAB tests is shown in Figure 6.1, and DRUM tests is summarized in Section D.3, Appendix D.

Seven new LAB and three DRUM tests were conducted; summarized in Table 6.1. The LAB tests were separated into two phases. Phase I consisted of three repeat LAB base case tests (I-1, I-2, and I-3) using dried sewage sludge (MC <1%) mixed with silica sand in a ratio of 6.5:1 sand-to-dried sludge (g/g). This ratio is higher than what has been used in previous studies smouldering dried sludge (Fournie et al., 2022; Rashwan et al., 2021a) to increase the fuel loading and therefore the ability to quantify PFAS products in the post-treatment materials and emissions. Phase II consisted of four LAB tests, two with higher MC sludge (75% by mass) combined with GAC (CAS: 7440-44-0, PTI Process Chemicals) in varying concentrations (II-1-1: 20 g GAC/kg sand; II-1-2: 30 g GAC/kg sand). The sludge was combined with sand in a ratio of 4.5:1 sand-to-sludge (g/g) on a wet-mass basis. The GAC was added to these higher MC tests to achieve temperatures >900°C by supplementing the low calorific value sludge. The concentrations were chosen based on previous research (Duchesne et al., 2020). The other two tests were similar to the base case,

6.5:1 sand-to-dried sludge, with the addition of CaO (CAS: 1305-788, Carmeuse Lime & Stone) in varying concentrations (II-2-1: 5 g CaO/kg sand; II-2-2: 10 g CaO/kg sand). The CaO was added to react with the PFAS in the sludge, mineralizing the fluorine at treatment temperatures <900°C (F. Wang et al., 2015; Wang et al., 2013). CaO concentrations were selected to explore how the content impacted the mineralization without significantly reducing the fuel permeability which could have resulted in extinction. Phase III consisted of three DRUM tests, the first with dried sludge (III-1 [same as the sand and sludge DRUM test in Chapter 4 and DRUM 1 in Chapter 5]), and the other two with high MC sludge (III-2: 72.3% by mass [same as DRUM 6 in Chapter 5]; III-3: 74.4% by mass). The sand-to-sludge ratio for III-1 and III-2 were 6.5:1, and III-3 was 4.5:1, all on a wet-mass basis. No CaO or GAC was added for these tests.

A specific mass of sludge was mixed with coarse silica sand (CAS: 14808-60-7, $1.18 \leq$ mean grain diameter ≤ 2.36 mm, WP #2, K & E) to achieve a specific sand-to-sludge ratio (see Table 6.1), and create a smoulderable mixture (Rashwan et al., 2016). For the higher MC LAB tests (II-1-1 and II-1-2), water was added in addition to the dried sludge and sand to reconstitute the sludge back to 75% MC following a method developed by (Rashwan et al., 2016). For the higher MC DRUM tests (III-2 and III-3), the sludge was collected the same day the reactor was set-up and therefore did not require any drying or rewetting prior to treatment. A clean sand cap (~5-10 cm thick) was added on top of the contaminant pack to lower the exiting temperatures when the smouldering front approached the top of the reactor.

Reactors were placed on load cells (LAB: KCC150, Metler Toledo; DRUM: KD1500, Mettler Toledo) to measure each experiment's fuel destruction rate.

Thermocouples (LAB: Type K, 0.0032 m diameter Omega Ltd; DRUM: 0.0064 m diameter Kelvin Technologies) were installed along the full height of the reactors to record process temperatures throughout each test. For the LAB tests, centreline (8 cm) and half-radius (5 cm) thermocouples were installed to better understand the temperature distribution across the reactor which has shown to vary more significantly at smaller scales (Rashwan et al., 2021b).

The DRUM test set-up and procedure using convective ignition is described in detail elsewhere (Fournie et al., 2022; Rashwan, 2020; Rashwan et al., 2021c) and can be found in Section D.3, Appendix D. The LAB test set-up and procedure using conductive ignition follows established methods (Duchesne et al., 2020; Rashwan et al., 2016), and is described briefly below (Figure 6.1).

The LAB reactor was ignited using a coiled resistive heater (450 W, 120 V, Watlow Ltd.), with no air flow. When the first thermocouple reached 200°C, air was injected into the reactor base at a Darcy flux of 5.0 cm/s – operated with a mass flux controller (FMA5400/5500 Series, Omega Ltd.) – for the remainder of the test, until temperatures reached ambient. Smouldering was confirmed when the first thermocouple within the fuel pack peaked (3.5 cm from the base). The heater was then turned off and the airflow supported the self-sustaining smouldering propagation. The end of each experiment was identified when the smouldering front reached the end of the contaminant pack in the reactor.

6.2.3 Emissions and Sample Collection

For every experiment, rigorous cleaning procedures were conducted based on (Duchesne et al., 2020). Ahead of each experiment, all glassware and tubing used for the emissions sampling train and sample bottles were rinsed three times with deionized (DI) water, isopropanol (CAS 67-63-0, Fisher Chemical), and methanol (CAS 67-56-1, Fisher Chemical).

During experiments, an NDIR infrared gas analyzer measured oxygen, carbon dioxide, and carbon monoxide data from the LAB tests every two seconds (Model: 7500ZA, Teledyne Analytical Instruments). Furthermore, two emissions sampling trains (Figure 6.1) were utilized for the LAB tests to subsample the emissions exiting the reactor for (1) PFAS, and (2) HF. The PFAS sampling train was adapted from (Duchesne et al., 2020), and the HF sampling train from EPA Method 26 (2019). These methods have been shown to effectively collect PFAS and HF in the emissions from LAB smouldering tests (Duchesne et al., 2020). Briefly, the PFAS emissions sample was collected using a vacuum pump (DOA-P704-AA, Gast) pulling sample at ~3 L/min. The emissions passed through two sorption tubes containing 50 g GAC and topped with 1 – 3 g glass wool (to secure the GAC). The sorption tubes were aligned in series to prevent breakthrough of PFAS. The HF emissions sample was similarly collected using a vacuum pump pulling sample at ~3 L/min. The emissions from the HF train passed through 4 glass impingers (impingers 1 and 4 were empty, impingers 2 and 3 contained 15 mL of 1% H_2SO_4) within an ice bath (4.0 °C). The total volume of emissions sample collected from each sampling train were quantified using flow totalizers (PFAS train: FMA6616 Series, Omega Ltd.; HF train:

FMA4316 Series, Omega Ltd.). Leakage of ambient air into each sampling train was quantified and minimized to <5% (see Section D.2, Appendix D for procedure).

Following emissions capture, the GAC from each sorption tube were collected in full and stored in PFAS free polypropylene bottles (VWR®). Additional PFAS samples included the glasswool, tubing rinse, and sorption tube rinses. The liquid from (1) the first and second impingers, and (2) the third and fourth impingers were combined into two HF samples. The tubing ahead of the HF emissions sampling train was rinsed using DI water and the rinse was also collected for analysis.

Representative samples of the post-treatment material (i.e., ash mixed with sand) were collected from three locations within the reactor, the sand cap (~38 – 48 cm from reactor base), the top of the fuel bed (~27 – 31 cm from reactor base), and the bottom of the fuel bed (~13 – 20 cm from reactor base) (see Section D.2, Appendix D for sample photos). Samples were 100 – 200 g and were stored in 250 mL jars at 5°C. Since samples collected at the top and bottom of the fuel bed had similar concentrations, these values were averaged to approximate the concentration in the fuel bed following smouldering treatment (herein referred to as 'ash'). The concentrations in the sand cap were presented separately (Section D.4, Appendix D).

6.2.4 Emissions and Solids Analyses

Solid samples were extracted with basic methanol (0.1% ammonium hydroxide (CAS: 1336-21-6, Fisher Scientific) v/v) using 5:1 extractant-to-sample (g/g). Samples were vortexed for 30 seconds, then placed on a shaker table at 30 RPM for 48 hours.

Samples were then centrifuged at 4000 RPM for 10 minutes, and a sub-sample transferred to a PFAS free HPLC vial for analysis.

All PFAS analyses were conducted by the Environmental Sciences Group at the Royal Military College of Canada. Analysis of samples was completed following a modified EPA 8327 method using liquid chromatography with tandem mass spectrometry (LC-MS/MS).

Mass-labelled internal standards of PFOA, PFOS, PFHxS were added to solid samples before extraction to examine matrix effects. Blank samples of (1) methanol, (2) DI water, (3) sand, (4) GAC, and (5) glasswool collected during each test were analyzed to ensure no cross-contamination during experimental procedures. Blanks included every 20 samples were analyzed and monitored to ensure no cross-contamination of samples occurred during analysis. Duplicate samples were included to ensure reproducibility of results.

Concentrations of 12 PFAS (TFA, PFPA, PFBA, PFBS, PFPeA, PFPeS, PFHxA, PFHxS, PFHpA, PFHpS, PFOA, PFOS) were calculated using a seven-point calibration curve across 0.4 ppb to 100 ppb. Internal standard recoveries were found to be between 70-120% and no correction was applied for internal standard. Two double injection blanks (basic methanol) were run before each method blank, reagent blank, calibration curve, post-treatment sample, and experimental blanks to eliminate contamination and carry-over from other samples. Sample duplicates within 30% relative percent difference (RPD) was considered acceptable according to EPA Method 531.1. The instrumental detection limit was 0.0004 ppm PFAS and the quantitation limit was 0.001 ppm PFAS.

The HF collected in the impinger liquids were analyzed using an ion probe (HQ30d-flexi, Hach). The analysis followed EPA Method 9214 (1996) and is outlined briefly here. The probe was calibrated using standards between 0.5 – 2 mg/L (BDH Chemicals, VWR®). Samples were prepared with 1:1 (v/v) sample-to-TISAB solution (Supelco, Sigma Aldrich) to neutralize the sample. Samples were analyzed in triplicates and an internal standard was run between each sample.

A combination of X-ray diffractometer (XRD) analysis and Scanning electron microscopy with energy dispersive X-ray spectroscopy (SEM/EDX) analysis were performed on the post-treatment ash from I-1, II-2-1, II-2-2, and III-1 tests to evaluate the use of calcium to mineralize fluorine from the sludge. These analyses were performed by Surface Science Western using a Rigaku SmartLab XRD, and a Hitachi SU8230 Regulus Ultra High-Resolution Field Emission SEM. Full specifications of the instrumentation, operating conditions, and QA/QC specifications can be found in the Section D.5, Appendix D.

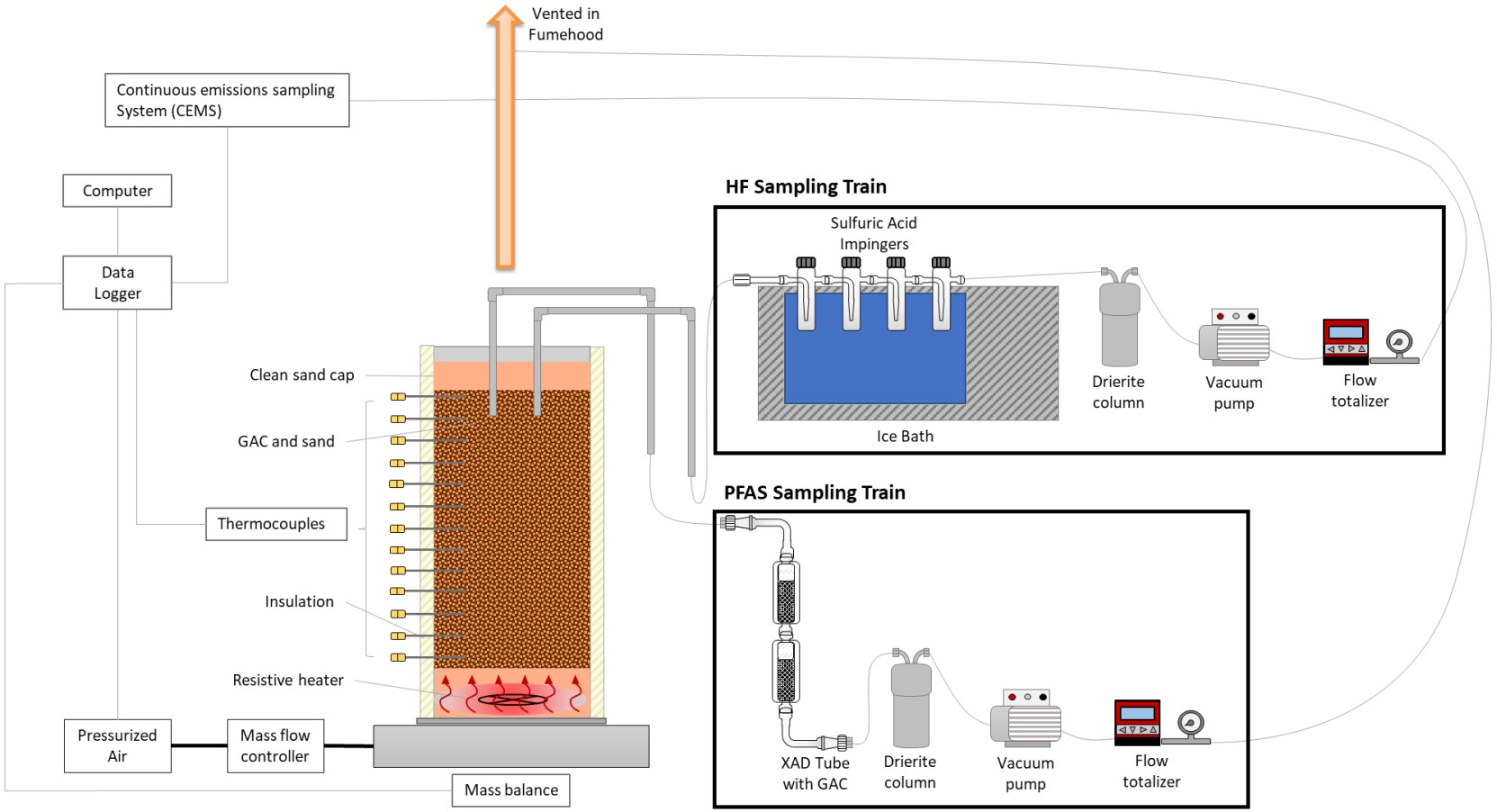

Figure 6.1: Experimental set-up and sampling for LAB tests.

Table 6.1: Summary of smouldering experiments

Experiment	Experimental Conditions						Results	
	Moisture Content	Sand/Sludge	GAC Concentration	CaO Added	Pack Height	Air Flux	Average Centreline Peak Temperature ± S.E. [a]	Smouldering Velocity ± S.E. [a]
	(%)	(g/g)	(g GAC/kg sand)	(g CaO/kg sand)	(cm)	(cm/s)	(°C)	(cm/min)
PHASE I: LAB Base case								
I-1	0	6.5 [b]	-	-	31.1	5.0	856 ± 34	0.44 ± 0.07
I-2	0	6.5 [b]	-	-	34.3	5.0	737 ± 37	0.42 ± 0.08
I-3	0	6.5 [b]	-	-	34.9	5.0	831 ± 41	0.46 ± 0.08
PHASE II: LAB High MC and Amendments								
II-1-1	75 [c]	4.5 [d]	20	-	29.2	5.0	746 ± 21	0.52 ± 0.13
II-1-2	75 [c]	4.5 [d]	30	-	29.2	5.0	905 ± 21	0.50 ± 0.09
II-2-2	0	6.5 [b]	-	5	28.6	5.0	818 ± 57	0.53 ± 0.11
II-2-1	0	6.5 [b]	-	10	29.2	5.0	824 ± 54	0.30 ± 0.14
PHASE III: DRUM								
III-1	3.2	25.5 [b]	-	-	53.5	5.0	542 ± 7.7	0.34 ± 0.04
III-2	72.3 [e]	6.5 [c]	-	-	61.6	5.0	473 ± 1.7	0.23 ± 0.01
III-3	74.4 [e]	4.5 [c]	-	-	61.9	5.0	469 ± 7.8	0.23 ± 0.03

[a] Standard error calculated as $\sigma\sqrt{n}$

[b] Measured on a dry-mass basis

[c] Moisture content of virgin sludge after drying and rehydrating

[d] Measured on a wet-mass basis

[e] Moisture content of virgin sludge, no drying occurred for these tests

6.3 Results and Discussion

6.3.1 Overview of Smouldering Experiments

Smouldering destroyed more than 90% of the initial sludge biomass under all experimental conditions, leaving <10% as residual inorganic ash in the reactor. Peak temperatures ranged between 700 – 926 °C in LAB tests and 461 – 550 °C in DRUM tests (Table 6.1).

Smouldering of dry sewage sludge in base case tests had an average peak centreline temperature of 808 °C ± 65 °C and average propagation velocity of 0.44 ± 0.13 cm/min (Table 6.1). The base case tests had the most consistent temperature distributions across the radius of the reactor (Section D.2, Appendix D). Higher MC is a source of heat losses that typically reduces peak temperatures in the reactor (Fournie et al., 2022; Rashwan et al., 2021a). These heat losses were offset by the addition of 20 g/kg GAC (centreline: 746 °C ± 21 °C) and exceeded by the addition of 30g/kg GAC (centreline: 905 °C ± 21 °C) (Phase II; Table 6.1). Both high MC/GAC tests had similar average propagation velocities (II-1-1: 0.52 ± 0.13; II-1-2: 0.50 ± 0.09). This aligns with previous research exploring the relationship between GAC content and smouldering temperature (Duchesne et al., 2020). The temperature profiles, sampling times, and heating rates can be found in the Section D.2, Appendix D for LAB tests, and Section D.3 for DRUM tests.

Addition of CaO at 5 and 10 g/kg did not alter the smouldering temperature, which remained consistent with base case tests, but it did impact the propagation velocities (Table 6.1) and heating rates of the tests (Section D.2, Appendix D). Increasing the CaO content in the fuel mixture reduced the propagation velocity from 0.53 ± 0.11 with 5 g CaO/kg

sand to 0.30 ± 0.14 with 10 g CaO/kg sand. Additionally, both CaO tests had slower heating rates than all other tests, consistently lower than 125°C/min (Section D.2, Appendix D). In comparison, the base case and high MC/GAC tests had heating rates between 125 – 300°C/min. The lower heating rates were likely driven by physical and chemical processes. The addition of CaO may have reduced the permeability of the fuel mixture. Reductions in permeability have been shown to slow the propagation velocity of smouldering; however, they should not impact the robustness of the reaction (Wang et al., 2021). Furthermore, reactions occurring due to the addition of CaO to the system may have consumed energy during heating and, later, fuel oxidation, and then released some energy during fluorine mineralization. The presence of these additional processes may have slowed energy transfer to adjacent fuel in the system resulting in decreased heating rates during these tests.

The DRUM scale tests (Phase III) had lower treatment temperatures and slower propagation velocities than were observed in any of the LAB tests. The dry sludge DRUM test, III-1, had average peak centreline temperatures between 534 – 550 °C (Table 6.1). The two higher MC DRUM tests (i.e., III-2 and III-3) had average peak centreline temperatures between 461 – 477 °C reflecting the additional energy to vaporize water ahead of smouldering.

For the LAB tests, the average peak half-radius temperatures varied, sometimes significantly, from the average peak centreline temperatures. These differences in temperatures across the radius of the reactor have important implications for treating PFAS since high temperatures (>900 °C) are required for effective degradation of these compounds (Duchesne et al., 2020; Mahinroosta and Senevirathna, 2020). Temperature gradients will likely not influence the removal of PFAS from the ash since it has been

shown previously that PFAS volatilize at low temperatures, <400 °C (Crownover et al., 2019; Winchell et al., 2021). However, temperature gradients will impact the degradation resulting in longer chain compounds in the emissions that would still need to be treated. The temperature differences across the reactor are likely due to a combination of heterogeneities in the fuel mixtures and heat losses (Rashwan et al., 2021b). Smouldering sludge at a larger scale – closer to what could be implemented at a WWTP – could minimize these heat losses and foster more uniform temperature gradients (Rashwan et al., 2021b), and thereby improve treatment.

Peak temperatures in the clean sand cap ranged from 434 – 661°C (Section D.2, Appendix D). The longer smouldering tests (i.e., CaO and DRUM tests) tended to have higher temperatures in the sand cap than the faster tests. This is likely because the sand had a longer period of the higher temperatures and was therefore able to retain more of the heat energy from smouldering.

6.3.2 PFAS in Virgin Sludge and Post-Treatment Ash

Figure 6.2 outlines the initial concentrations of 12 PFAS in the sewage sludge prior to smouldering compared to the post-treatment ashes from both LAB and DRUM tests. For all tests, there was complete removal of 3C – 8C PFAS from the ash.

6.3.2.1 LAB (Phase I and Phase II)

For all the base case and high MC/GAC tests, TFA (2C) was the primary compound measured in the ash. Traces of PFPA (3C) were also measured in the ash from one of the base case tests, I-2 (Section D.4, Appendix D). Increases of 120-590% TFA were measured in the ash during the base case tests compared to what was originally present in the dried

sludge. This increase in shorter chain compounds suggests some degradation of larger PFAS during smouldering. There was also some retention of PFAS, primarily TFA, PFPA, and/or PFHpS, in the sand cap during these tests due to re-condensation (Section D.4, Appendix D). The high MC tests had the lowest relative temperatures (Section D.2, Appendix D) and highest PFAS retentions in the sand cap. The presence of only TFA in the sand cap of higher GAC test compared to a distribution of TFA (2C), PFPA (3C), and PFHpS (7C) in the lower GAC test suggests that the higher temperature/energy smouldering improved degradation of PFAS, breaking down the larger chains into smaller compounds.

Similar to the high MC/GAC tests, both CaO tests (II-2-1 and II-2-2) only had retention of TFA in the ash. In addition to TFA, the top sand cap from both CaO tests contained PFCA (Section D.4, Appendix D). The top sand cap retained more PFAS than remained in the ash by 81% for the lower CaO test (II-2-1) and 34% for the higher CaO test (II-2-2). These results are further evidence of recondensation of PFAS in the top sand cap.

6.3.2.2 DRUM (Phase III)

While the LAB tests had some retention of short-chained PFAS in the ash (primarily TFA), the DRUM tests had complete removal of all PFAS from the ash (Figure 6.2). The removal was irrespective of the initial PFAS content in the sludge, which varied between sludge batches collected for each DRUM test (Figure 6.2). The DRUM tests had lower smouldering front propagation velocities than the LAB tests (Table 6.1). The slower front movement means that every location was exposed to the elevated treatment

temperatures for longer times, which likely facilitated complete removal of all PFAS from the ash.

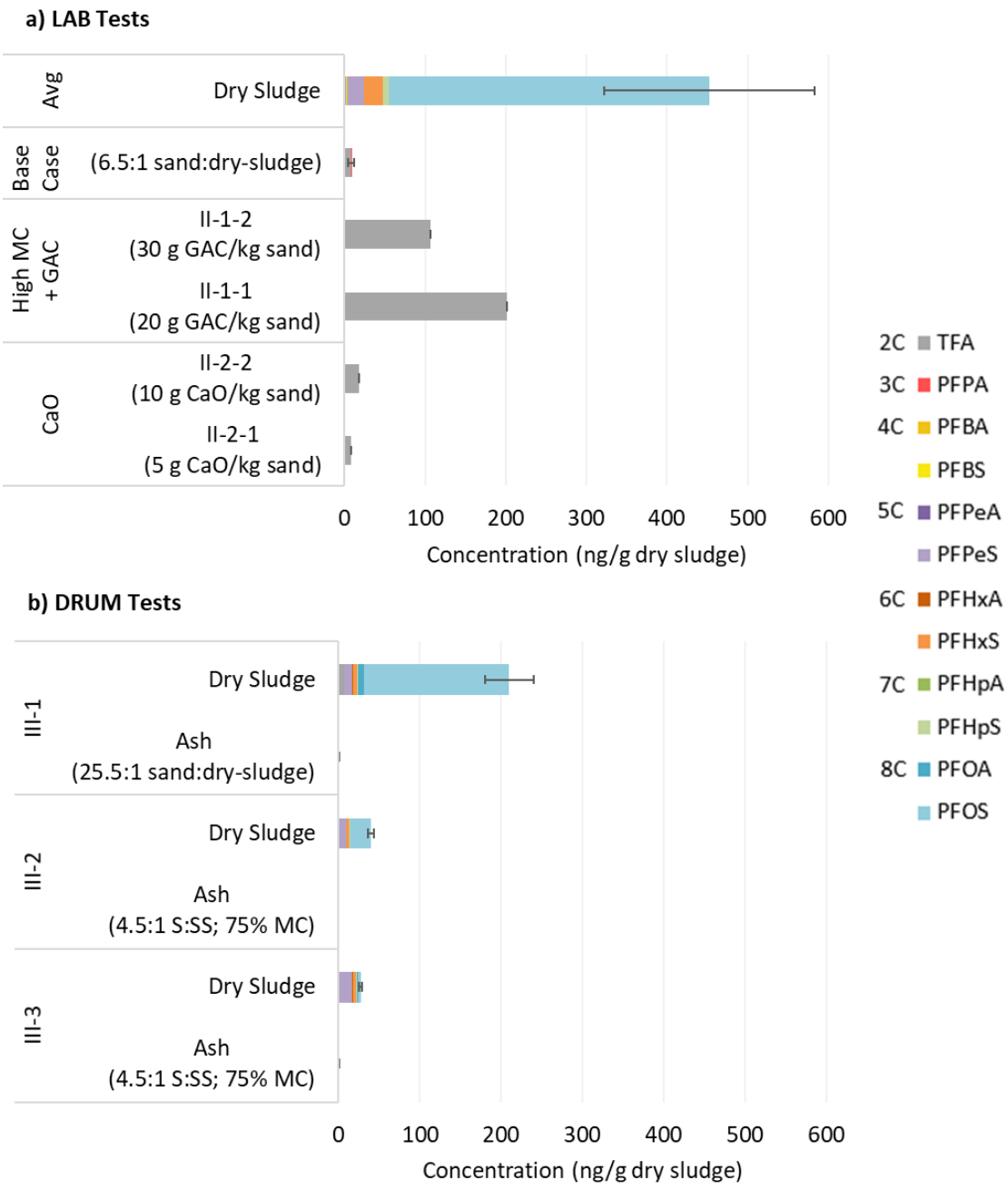

Figure 6.2: Content of 12 PFAS originally present in sludges and post-treatment ashes following smouldering treatment from a) LAB Phase I: base cases and Phase II: high MC (75%) and GAC, and CaO tests, and b) DRUM Phase III. Error bars represent standard error of the cumulative PFAS concentration determined from replicate samples, and base case tests from triplicate smouldering tests.

6.3.3 PFAS in Emissions

Figure 6.3 outlines the initial contents of 12 PFAS in the sewage sludge prior to smouldering compared to the content measured in the emissions from the LAB tests.

The emissions from the base case tests had the largest mass fractions of PFOS and PFOA (both 8C), comprising 79 – 97% by mass. With complete removal of PFOS from the ash, the higher content in the emissions suggests release into the emissions without degrading. Therefore, the emissions under base case smouldering conditions would require further treatment to collect and/or degrade the PFAS. Furthermore, since PFOA was not originally present in the sewage sludge, its presence in the emissions is evidence of formation during smouldering, possibly through precursors or breakdown of other compounds not analyzed in the sludge (Zhang and Liang, 2021). Future work could explore PFAS formation during smouldering.

Both higher MC/GAC tests had similar total PFAS in the emissions, 490 and 470 ng/g-dry sludge from II-1-1 and II-1-2, respectively, but the compounds differed. PFOS comprised the largest mass fraction from II-1-1 at 93% while TFA comprised the largest fraction from II-1-2 at 67%, suggesting improved degradation with higher treatment temperatures. The lower GAC test (II-1-1) behaved similarly to the base case tests, likely due to the similarly low temperatures achieved.

The PFAS content in the emissions from the CaO tests was lower than all other tests by 97 – 99% by mass. The treatment temperatures observed during both CaO tests (760 – 880 °C centreline; 670 – 810 °C half-radius) were likely sufficient to support mineralization of fluorine from PFAS in the presence of sufficient calcium, which has

been previously demonstrated at these temperatures (Wang et al., 2013). The primary PFAS found in the emissions following the CaO tests was TFA. A higher mass fraction of TFA was measured during the higher CaO test (II-2-2: 77% TFA by mass) compared to the lower CaO test (II-2-2: 58% TFA by mass). Adding more CaO increased the fraction of TFA in the emissions. The presence of calcium to mineralize fluorine from PFAS has been shown to prevent the release of short and longer-chained PFAS (>3C) in emissions (Wang et al., 2013) and reduces the production of secondary fluorinated compounds (Riedel et al., 2021). A higher concentration of CaO (10 g CaO/kg sand) reduced the total PFAS content in the emissions by 38% (relative to 5 g CaO/kg sand). In particular, the PFOA formation was reduced by 24% and PFOS content by 100%.

With DRUM tests achieving treatment temperatures between 460 – 550°C (Table 6.1), we hypothesize that most of the PFAS originally present in the sludge was released in the emissions with minimal degradation, similar to the LAB base case tests (I-1, I-2, & I-3) and lower concentration GAC test (II-1-1). Future work could examine the PFAS emissions by-products from smouldering sludge at larger scales and work to optimize treatment via process changes (e.g., air flow) and amendments (e.g., GAC or CaO).

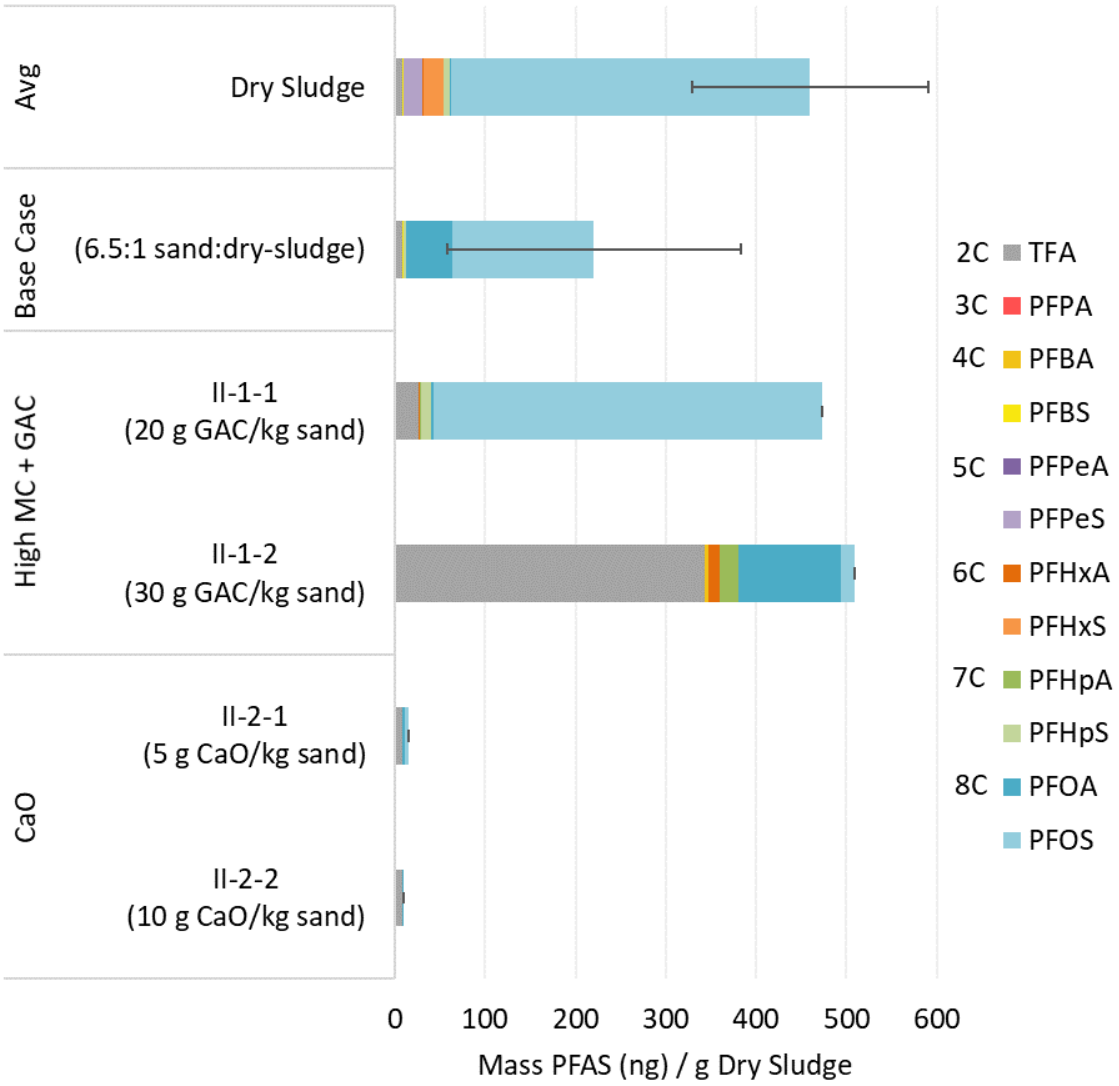

Figure 6.3: Content of 12 PFAS in the emissions during smouldering compared to the content originally present in the dried sludge. The content in the emissions has been normalized to account for differences between the experiments.

6.3.4 Defluorination

Minimal HF was measured in the emissions during the base case tests (I-1, I-2, and I-3) and the lower GAC test (II-2-1) (Figure 6.4). The lower relative temperatures (724 – 860 °C), slower heating rates, and lower propagation velocities likely supported release of longer chained PFAS in the emissions (Figure 6.3) rather than destroying these compounds.

The higher GAC test (II-1-2) had the highest production of HF. This is further evidence of improved degradation during the higher energy/temperature smouldering. Moreover, the faster heating rates (Section D.2, Appendix D) and smouldering propagation (Table 6.1) may reduce the time for the PFAS to volatilize ahead of being oxidized by the smouldering front. Therefore, a faster heating rate may be favourable to improve degradation when thermal destruction alone is used. Future work could explore the role of heating rates on PFAS destruction via smouldering.

The CaO tests had low HF emissions and low PFAS in emissions and ash. The most likely explanation is that some of the fluorine has mineralized with the calcium, forming new compounds that remained in the ash. Mineral analysis was conducted (Section D.7, Appendix D); however, the concentrations were below the instrument detection limits so more work is needed to understand the fate of fluorine during sewage sludge smouldering. Furthermore, future work could explore the use of a calcium amendment as an alternative to GAC supplementation to mineralize fluorine from high MC sludge at lower treatment temperatures (potentially as low as 400 °C (Wang et al., 2015, 2013)).

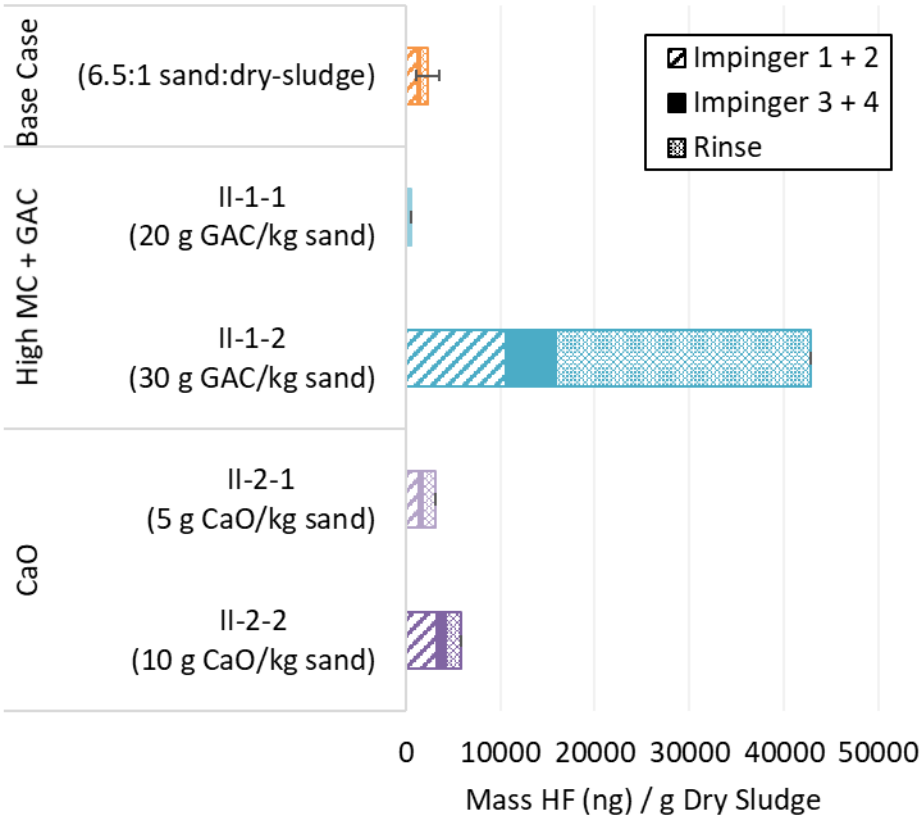

Figure 6.4: HF content measured in the emissions from each laboratory smouldering experiment. The content collected from two sections of the glassware sampling train and additionally the glassware rinse have been presented separately. The contents in the emissions have been normalized to account for differences between the experiments.

6.4 Conclusions

Smouldering combustion can be used to treat PFAS effectively in high moisture content (MC) sewage sludge with complete removal of PFAS compounds 4C – 8C. The most effective treatment of PFAS-laden sewage sludge involved the use of calcium oxide (CaO) to sequester fluorine in the resulting ash. An addition of 5 – 10 mg CaO per kg of dried sludge ahead of smouldering treatment achieved complete removal of PFAS 4C – 8C without significant PFAS or HF release in emissions. In contrast, smouldering of sludge bulked with only sand volatilized most of the PFAS, where some PFAS recondensed

downstream in cooler regions in the reactor and the rest released via emissions. Supplementing the sludge and sand mixture with higher calorific value fuel (i.e., 30 g GAC / kg sand) increased the energy content of the system, which fostered ~900 °C peak temperatures and improved PFAS degradation. Other high calorific value fuels such as wood chips could achieve these conditions. While higher energy smouldering supports thermal degradation of PFAS, it also generates HF emissions, which require further treatment. In contrast, CaO addition achieved similar PFAS 4C – 8C degradation at temperatures between 670 – 880 °C, which were lower than required to degrade PFAS by other thermal treatments and avoided HF production. Using a calcium amendment had the dual benefits of removing PFAS without producing other hazardous emission by-products. Future work should investigate the long-term stability of fluorine sequestered in ash produced by smouldering treatment of PFAS-laden sewage sludge with calcium amendments, and the use of calcium amendments to treat high MC sludges.

6.5 References

Ahrens, L., Felizeter, S., Sturm, R., Xie, Z., Ebinghaus, R., 2009. Polyfluorinated compounds in waste water treatment plant effluents and surface waters along the River Elbe, Germany. Mar. Pollut. Bull. 58, 1326–1333. https://doi.org/10.1016/j.marpolbul.2009.04.028

Ahrens, L., Shoeib, M., Harner, T., Lee, S.C., Guo, R., Reiner, E.J., 2011. Wastewater treatment plant and landfills as sources of polyfluoroalkyl compounds to the atmosphere. Environ. Sci. Technol. 45, 8098–8105. https://doi.org/10.1021/es1036173

Arvaniti, O.S., Andersen, H.R., Thomaidis, N.S., Stasinakis, A.S., 2014. Sorption of Perfluorinated Compounds onto different types of sewage sludge and assessment of its importance during wastewater treatment. Chemosphere 111, 405–411. https://doi.org/10.1016/j.chemosphere.2014.03.087

Arvaniti, O.S., Ventouri, E.I., Stasinakis, A.S., Thomaidis, N.S., 2012. Occurrence of different classes of perfluorinated compounds in Greek wastewater treatment plants and determination of their solid-water distribution coefficients. J. Hazard. Mater.

239–240, 24–31. https://doi.org/10.1016/j.jhazmat.2012.02.015

Blaine, A.C., Rich, C.D., Hundal, L.S., Lau, C., Mills, M.A., Harris, K.M., Higgins, C.P., 2013. Uptake of perfluoroalkyl acids into edible crops via land applied biosolids: Field and greenhouse studies. Environ. Sci. Technol. 47, 14062–14069. https://doi.org/10.1021/es403094q

Buck, R.C., Franklin, J., Berger, U., Conder, J.M., Cousins, I.T., Voogt, P. De, Jensen, A.A., Kannan, K., Mabury, S.A., van Leeuwen, S.P.J., 2011. Perfluoroalkyl and polyfluoroalkyl substances in the environment: Terminology, classification, and origins. Integr. Environ. Assess. Manag. 7, 513–541. https://doi.org/10.1002/IEAM.258

Clarke, B.O., Smith, S.R., 2011. Review of 'emerging' organic contaminants in biosolids and assessment of international research priorities for the agricultural use of biosolids. Environ. Int. 37, 226–247. https://doi.org/10.1016/J.ENVINT.2010.06.004

Crownover, E., Oberle, D., Kluger, M., Heron, G., 2019. Perfluoroalkyl and polyfluoroalkyl substances thermal desorption evaluation. Remediat. J. 29, 77–81. https://doi.org/10.1002/REM.21623

Duchesne, A.L., Brown, J.K., Patch, D.J., Major, D., Weber, K.P., Gerhard, J.I., 2020. Remediation of PFAS-Contaminated Soil and Granular Activated Carbon by Smoldering Combustion. Environ. Sci. Technol. 54, 12631–12640. https://doi.org/10.1021/acs.est.0c03058

Feng, C., Cheng, M., Gao, X., Qiao, Y., Xu, M., 2020. Occurrence forms and leachability of inorganic species in ash residues from self-sustaining smouldering combustion of sewage sludge. Proc. Combust. Inst. 000, 1–8. https://doi.org/10.1016/j.proci.2020.06.008

Fournie, T., Rashwan, T.L., Switzer, C., Gerhard, J.I., 2022. Phosphorus recovery and reuse potential from smouldered sewage sludge ash. Waste Manag. 137, 241–252. https://doi.org/10.1016/J.WASMAN.2021.11.001

Fournie, T., Switzer, C., Gerhard, J.I., 2021. USEPA LEAF methods for characterizing phosphorus and potentially toxic elements in raw and thermally treated sewage sludge. Chemosphere 275, 130081. https://doi.org/10.1016/j.chemosphere.2021.130081

Gallen, C., Drage, D., Kaserzon, S., Baduel, C., Gallen, M., Banks, A., Broomhall, S., Mueller, J.F., 2016. Occurrence and distribution of brominated flame retardants and perfluoroalkyl substances in Australian landfill leachate and biosolids. J. Hazard. Mater. 312, 55–64. https://doi.org/10.1016/J.JHAZMAT.2016.03.031

Gómez-Canela, C., Barth, J.A.C., Lacorte, S., 2012. Occurrence and fate of perfluorinated compounds in sewage sludge from Spain and Germany. Environ. Sci. Pollut. Res. 19, 4109–4119. https://doi.org/10.1007/s11356-012-1078-7

Grant, G.P., Major, D., Scholes, G.C., Horst, J., Hill, S., Klemmer, M.R., Couch, J.N., 2016. Smoldering Combustion (STAR) for the Treatment of Contaminated Soils: Examining Limitations and Defining Success. Remediat. J. 26, 27–51. https://doi.org/10.1002/rem.21468

Hamid, H., Li, L.Y., 2018. Fate of perfluorooctanoic acid (PFOA) in sewage sludge during microwave-assisted persulfate oxidation treatment. Environ. Sci. Pollut. Res. 25, 10126–10134. https://doi.org/10.1007/s11356-018-1576-3

Houtz, E., Wang, M., Park, J.S., 2018. Identification and Fate of Aqueous Film Forming Foam Derived Per- and Polyfluoroalkyl Substances in a Wastewater Treatment Plant. Environ. Sci. Technol. 52, 13212–13221. https://doi.org/10.1021/acs.est.8b04028

Kim, J.H., Ok, Y.S., Choi, G.H., Park, B.J., 2015. Residual perfluorochemicals in the biochar from sewage sludge. Chemosphere 134, 435–437. https://doi.org/10.1016/j.chemosphere.2015.05.012

Kissa, E., 2001. Fluorinated surfactants and repellents, Vol. 97. ed. CRC Press.

Kunacheva, C., Tanaka, S., Fujii, S., Boontanon, S.K., Musirat, C., Wongwattana, T., Shivakoti, B.R., 2011. Mass flows of perfluorinated compounds (PFCs) in central wastewater treatment plants of industrial zones in Thailand. Chemosphere 83, 737–744. https://doi.org/10.1016/J.CHEMOSPHERE.2011.02.059

Kundu, S., Patel, S., Halder, P., Patel, T., Hedayati Marzbali, M., Pramanik, B.K., Paz-Ferreiro, J., De Figueiredo, C.C., Bergmann, D., Surapaneni, A., Megharaj, M., Shah, K., 2021. Removal of PFASs from biosolids using a semi-pilot scale pyrolysis reactor and the application of biosolids derived biochar for the removal of PFASs from contaminated water. Environ. Sci. Water Res. Technol. 7, 638–649. https://doi.org/10.1039/d0ew00763c

Lakshminarasimman, N., Gewurtz, S.B., Parker, W.J., Smyth, S.A., 2021. Removal and formation of perfluoroalkyl substances in Canadian sludge treatment systems – A mass balance approach. Sci. Total Environ. 754. https://doi.org/10.1016/j.scitotenv.2020.142431

Mahinroosta, R., Senevirathna, L., 2020. A review of the emerging treatment technologies for PFAS contaminated soils. J. Environ. Manage. https://doi.org/10.1016/j.jenvman.2019.109896

Milinovic, J., Lacorte, S., Rigol, A., Vidal, M., 2016. Sorption of perfluoroalkyl substances in sewage sludge. Environ. Sci. Pollut. Res. 23, 8339–8348. https://doi.org/10.1007/s11356-015-6019-9

Moodie, D., Coggan, T., Berry, K., Kolobaric, A., Fernandes, M., Lee, E., Reichman, S., Nugegoda, D., Clarke, B.O., 2021. Legacy and emerging per- and polyfluoroalkyl substances (PFASs) in Australian biosolids. Chemosphere 270, 129143.

https://doi.org/10.1016/J.CHEMOSPHERE.2020.129143

Ohlemiller, T.J., 1985. Modeling of smoldering combustion propagation. Prog. Energy Combust. Sci. 11, 277–310. https://doi.org/10.1016/0360-1285(85)90004-8

Pan, Y., Shi, Y., Wang, J., Cai, Y., 2010. Evaluation of perfluorinated compounds in seven wastewater treatment plants in Beijing urban areas. Sci. China Chem. 2011 543 54, 552–558. https://doi.org/10.1007/S11426-010-4093-X

Pironi, P., Switzer, C., Rein, G., Fuentes, A., Gerhard, J.I., Torero, J.L., 2009. Small-scale forward smouldering experiments for remediation of coal tar in inert media. Proc. Combust. Inst. 32 II, 1957–1964. https://doi.org/10.1016/j.proci.2008.06.184

Rashwan, T., 2020. Sustainable Smouldering for Waste-to-Energy: Scale, Heat Losses, and Energy Efficiency. Electron. Thesis Diss. Repos.

Rashwan, T.L., Fournie, T., Torero, J.L., Grant, G.P., Gerhard, J.I., 2021a. Scaling up self-sustained smouldering of sewage sludge for waste-to-energy. Waste Manag. 135, 298–308. https://doi.org/10.1016/J.WASMAN.2021.09.004

Rashwan, T.L., Gerhard, J.I., Grant, G.P., 2016. Application of self-sustaining smouldering combustion for the destruction of wastewater biosolids. Waste Manag. 50, 201–212. https://doi.org/10.1016/j.wasman.2016.01.037

Rashwan, T.L., Torero, J.L., Gerhard, J.I., 2021b. The improved energy efficiency of applied smouldering systems with increasing scale. Int. J. Heat Mass Transf. 177, 121548. https://doi.org/10.1016/J.IJHEATMASSTRANSFER.2021.121548

Rashwan, T.L., Torero, J.L., Gerhard, J.I., 2021c. Heat losses in a smouldering system: The key role of non-uniform air flux. Combust. Flame 227, 309–321. https://doi.org/10.1016/j.combustflame.2020.12.050

Rein, G., 2016. Smoldering Combustion, in: Hurley, M.J., Gottuk, D.T., Hall Jr., J.R., Harada, K., Kuligowski, E.D., Puchovsky, M., Torero, J.L., Watts Jr., J.M., Wieczorek, C.J. (Ed.), SFPE Handbook of Fire Protection Engineering. Springer New York, New York, pp. 581–603.

Riedel, T.P., Wallace, M.A.G., Shields, E.P., Ryan, J. V., Lee, C.W., Linak, W.P., 2021. Low temperature thermal treatment of gas-phase fluorotelomer alcohols by calcium oxide. Chemosphere 272, 129859. https://doi.org/10.1016/J.CHEMOSPHERE.2021.129859

Ross, I., Mcdonough, J., Miles, J., Storch, P., Kochunarayanan, P.T., Kalve, E., Hurst, J., Dasgupta, S.S., Burdick, J., 2018. A review of emerging technologies for remediation of PFASs. Remediation 28, 101–126. https://doi.org/10.1002/rem.21553

Scholes, G.C., Gerhard, J.I., Grant, G.P., Major, D.W., Vidumsky, J.E., Switzer, C., Torero, J.L., 2015. Smoldering Remediation of Coal-Tar-Contaminated Soil: Pilot

Field Tests of STAR. Environ. Sci. Technol. 49, 14334–14342. https://doi.org/10.1021/ACS.EST.5B03177

Sepulvado, J.G., Blaine, A.C., Hundal, L.S., Higgins, C.P., 2011. Occurrence and fate of perfluorochemicals in soil following the land application of municipal biosolids. Environ. Sci. Technol. 45, 8106–8112. https://doi.org/10.1021/es103903d

Sindiku, O., Orata, F., Weber, R., Osibanjo, O., 2013. Per- and polyfluoroalkyl substances in selected sewage sludge in Nigeria. Chemosphere 92, 329–335. https://doi.org/10.1016/j.chemosphere.2013.04.010

Sun, H., Gerecke, A.C., Giger, W., Alder, A.C., 2011. Long-chain perfluorinated chemicals in digested sewage sludges in Switzerland. Environ. Pollut. 159, 654–662. https://doi.org/10.1016/j.envpol.2010.09.020

Switzer, C., Pironi, P., Gerhard, J.I., Rein, G., Torero, J.R., 2009. Self-sustaining smoldering combustion: A novel remediation process for non-aqueous-phase liquids in porous media. Environ. Sci. Technol. 43, 5871–5877. https://doi.org/10.1021/es803483s

Telliard, W., 2001. Method 1684: Total, fixed, and volatile solids in water, solids, and biosolids. Washington.

UNEP, 2019. SC-9/12: Listing of perfluorooctanoic acid (PFOA), its salts and PFOA-related compounds. Geneva.

USEPA, 2021. Contaminants on the Fourth Drinking Water Contaminant Candidate List. Environmental Protection Agency.

USEPA, 2020. Significant New Use Rule: Long-Chain Perfluoroalkyl Carboxylate and Perfluoroalkyl Sulfonate Chemical Substances. Environmental Protection Agency.

Venkatesan, A.K., Halden, R.U., 2013. National inventory of perfluoroalkyl substances in archived U.S. biosolids from the 2001 EPA National Sewage Sludge Survey. J. Hazard. Mater. 252–253, 413–418. https://doi.org/10.1016/j.jhazmat.2013.03.016

Wang, F., Lu, X., Li, X.Y., Shih, K., 2015. Effectiveness and mechanisms of defluorination of perfluorinated alkyl substances by calcium compounds during waste thermal treatment. Environ. Sci. Technol. 49, 5672–5680. https://doi.org/10.1021/es506234b

Wang, F., Shih, K., Lu, X., Liu, C., 2013. Mineralization Behavior of Fluorine in Perfluorooctanesulfonate (PFOS) during Thermal Treatment of Lime-Conditioned Sludge. Environ. Sci. Technol. 47, 2621–2627. https://doi.org/10.1021/es305352p

Wang, J., Grant, G.P., Gerhard, J.I., 2021. The influence of porous media heterogeneity on smouldering remediation. J. Contam. Hydrol. 237, 103756. https://doi.org/10.1016/J.JCONHYD.2020.103756

Washington, J.W., Yoo, H., Ellington, J.J., Jenkins, T.M., Libelo, E.L., 2010. Concentrations, distribution, and persistence of perfluoroalkylates in sludge-applied soils near Decatur, Alabama, USA. Environ. Sci. Technol. 44, 8390–8396. https://doi.org/10.1021/ES1003846/SUPPL_FILE/ES1003846_SI_001.PDF

Werther, J., Ogada, T., 1999. Sewage sludge combustion. Prog. Energy Combust. Sci. https://doi.org/10.1016/S0360-1285(98)00020-3

Winchell, L.J., Ross, J.J., Wells, M.J.M., Fonoll, X., Norton, J.W., Bell, K.Y., 2021. Per- and polyfluoroalkyl substances thermal destruction at water resource recovery facilities: A state of the science review. Water Environ. Res. 93, 826–843. https://doi.org/10.1002/WER.1483

Yan, H., Zhang, C.J., Zhou, Q., Chen, L., Meng, X.Z., 2012. Short- and long-chain perfluorinated acids in sewage sludge from Shanghai, China. Chemosphere 88, 1300–1305. https://doi.org/10.1016/j.chemosphere.2012.03.105

Yermán, L., Hadden, R.M., Carrascal, J., Fabris, I., Cormier, D., Torero, J.L., Gerhard, J.I., Krajcovic, M., Pironi, P., Cheng, Y.L., 2015. Smouldering combustion as a treatment technology for faeces: Exploring the parameter space. Fuel 147, 108–116. https://doi.org/10.1016/j.fuel.2015.01.055

Yu, J., Nickerson, A., Li, Y., Fang, Y., Strathmann, T.J., 2020. Fate of per- and polyfluoroalkyl substances (PFAS) during hydrothermal liquefaction of municipal wastewater treatment sludge. Environ. Sci. Water Res. Technol. 6, 1388–1399. https://doi.org/10.1039/c9ew01139k

Zanoni, M.A.B., Torero, J.L., Gerhard, J.I., 2019. Determining the conditions that lead to self-sustained smouldering combustion by means of numerical modelling. Proc. Combust. Inst. 37, 4043–4051. https://doi.org/10.1016/J.PROCI.2018.07.108

Zhang, C., Yan, H., Li, F., Hu, X., Zhou, Q., 2013. Sorption of short- and long-chain perfluoroalkyl surfactants on sewage sludges. J. Hazard. Mater. 260, 689–699. https://doi.org/10.1016/j.jhazmat.2013.06.022

Zhang, W., Liang, Y., 2021. Effects of hydrothermal treatments on destruction of per- and polyfluoroalkyl substances in sewage sludge. Environ. Pollut. 285, 117276. https://doi.org/10.1016/J.ENVPOL.2021.117276

Chapter 7

7 Conclusions

7.1 Summary

The goal of this research was to explore potential benefits from smouldering sewage sludge, while also understanding and minimizing any potential harmful by-products from the process. Smouldering experiments were performed under various test conditions at laboratory and oil-drum reactor scales. Emissions capture and analysis of the post-treatment ash was used to understand the behaviour of elements of value and potentially harmful by-products, and the conditions under which they are formed and/or released.

The first study compared the commonly used Hedley fractionation method to the USEPA LEAF pH-dependent, parallel batch tests (Method 1313) and dynamic leaching column test (Method 1314) to assess the bioavailability of phosphorus. The three methods were applied to wastewater treatment plant sludge before and after thermal treatment. Both methods revealed similar qualitative trends, namely that thermal treatment of the sludge changes phosphorus minerals into forms that are more strongly bound to the solid surfaces. Therefore, phosphorus is less likely to leach from the incinerated ash in the short term, providing a more regulated source of gradual inorganic phosphorus with less potential harm to downstream water bodies. However, the Hedley and LEAF methods were inconsistent in the forms and amounts of available phosphorus recovered from the solids. The Hedley method left 40% of phosphorus unextracted from sludge and 20% from incinerated ash, suggesting that it may be less appropriate for organic materials. Moreover, only 2 of the 6 Hedley phosphorus pools were within environmentally relevant pH

conditions (compared to 5 of 9 samples for LEAF Method 1313 and all samples for LEAF Method 1314). Furthermore, the Hedley method overpredicted the readily available phosphorus. In contrast, the LEAF methods allowed for a more detailed analysis of phosphorus availability - while simultaneously assessing PTEs - across a controlled pH range. Moreover, LEAF used simpler procedures and provided more easily interpreted results. Thus, LEAF facilitates more robust and valuable assessment of organic and inorganic solids being considered for land application.

After determining that USEPA LEAF methods were superior for analyzing phosphorus and PTEs in organic sludges and inorganic ashes, the next study applied these methods to understand the recovery and land application potential of smouldered sewage sludge ash. Compared to the parent sludge, post-treatment ash from smouldering sludge with sand contained higher quantities of inorganic phosphorus in sorbed and mineral phases, which can provide beneficial slow phosphorus release to plants and avoid early phosphorus washout during land application. Furthermore, land application of ash is more favourable than sludge since it reduces co-dissolution of 6 of 8 commonly regulated PTEs. As an alternative to land application, approximately 42% of retained phosphorus can be recovered directly using acidic extraction, and an additional 30% from emissions. Since sand provided an important sink for phosphorus, mechanical separation and washing at low L/S should be applied to recover this additional phosphorus from the large sand mass. In contrast, co-smouldering sludge with woodchips was more suited for direct recovery with 78% of phosphorus potentially recoverable via emissions capture and yield increasing to 99% with acidic extraction of resulting ash (21% phosphorus at pH 2). Further separation

of phosphorus and PTEs would still be required from the emissions stream which contained >70% of PTEs originally present in the parent sludge.

With all of the potential benefits from smouldering treatment of sewage sludge, there are also potential hazards that needed to be evaluated and addressed. This question was explored in two studies, the first assessing PCDD/Fs and PTEs, and the second analyzing PFAS. Both studies included smouldering tests at the LAB (0.08 m radius) and DRUM (0.3 m radius) reactor scales. These tests were evaluated for key compounds of interest – PCDD/Fs, PTEs, and PFAS – before and after treatment as well as in process emissions. VOCs were also measured. The first study found negligible PCDD/Fs in process emissions during robust smouldering and low levels of PCDD/Fs (45 – 48 pg TEQ /m^3) during weak smouldering, which were comparable to the PCDD/Fs typically released by incineration. Moreover, due to recondensation ahead of smouldering, PCDD/Fs may release at concentrations comparable to incineration systems when the smouldering front reaches the end of the fuel bed. Overall, smouldering acts as a sink for PCDD/Fs, releasing 0 – 3% of the originally present compounds and destroying >99% of the remainder. In addition, 94-100% of all the PTEs analyzed were retained in the post-treatment material following smouldering treatment, i.e., not released in the emissions, and minimal VOCs were measured in the emissions.

The final study explored the use of smouldering combustion to treat PFAS that accumulates in sewage sludge. Base case experiments were performed at the LAB scale. Iterations on these base case tests aimed at making the experimental conditions closer to requirements for industrial application (e.g., high MC sludge, larger reactor scale) and improve fluorine mineralization via a calcium amendment. Pre-treatment sludge and post-

treatment ash and sand samples from all tests were analyzed for 12 PFAS (2C-8C). Additional emissions samples were collected from all LAB tests and analyzed for 12 PFAS and additionally hydrogen fluoride. The results from this study demonstrated that smouldering completely removed all PFAS >3C from the post-treatment ash under all LAB conditions. While PFOS and PFOA were completely removed from the ash during the base case tests, 79-94% of the total PFAS that are measured in the emissions are PFOS and PFOA. This suggests that some of these compounds are being volatilized without degrading. Reaching temperatures of ~900°C while smouldering high MC sludge was demonstrated by supplementing with 30 g GAC/kg sand. These elevated temperatures improved PFAS degradation, releasing primarily shorter chain compounds in the emissions (67% TFA (2C) by mass) compared to primarily PFOS (93% by mass) when treatment temperatures were <800°C (i.e., 20 g GAC/kg sand was used). The PFAS content in the emissions from the CaO tests were lower than all other tests by 97 – 99% by mass. With minimal PFAS in the ash and also minimal HF production, it is likely that the fluorine from the PFAS reacted with CaO and mineralized in the ash. Compared to the LAB tests, smouldering at the DRUM scale effectively removed all PFAS from the ash.

7.2 Implications

In terms of emissions by-products, consistently low PCDD/F release highlights a strong benefit of smouldering combustion: the release of condensable compounds does not seem significantly influenced by system scale changes. This finding is important for emerging industrial smouldering applications. Furthermore, low PTE, VOC, and PCDD/F release (near the allowable limit for stack emissions) indicates that minimal emissions

treatment is necessary, thereby simplifying industrial application of smouldering treatment for sewage sludge.

The results from the PFAS study demonstrated that it is possible to smoulder 75% MC sewage sludge at sufficiently high temperatures (~900°C) to achieve the thermal destruction of PFAS. Since dewatering sludge is an energy intensive and expensive component of sludge management, reducing this requirement while still degrading contaminants in the sludge is essential.

Smouldering sewage sludge at the DRUM scale was shown to completely remove all PFAS from the ash. This is important when considering industrial application of smouldering for sewage sludge management. However, under the DRUM conditions assessed, the PFAS did not degrade significantly, but rather volatilized the compounds resulting in emissions that would need further treatment.

Smouldering enables phosphorus recovery from wastewater treatment sludge in several potentially beneficial forms. The best opportunity to create a valuable soil amendment with sufficient phosphorus available to plants in the longer term is smouldering with sand. Co-smouldering sewage sludge with another organic waste is an important alternative to the use of sand to create a porous matrix. Not only does co-smouldering treat multiple waste streams, but it also produces a single post-treatment ash and can be operated continuously, which aligns with current incinerator configurations at wastewater treatment plants and makes adaptation highly feasible. Furthermore, since co-smouldering can increase the treatment temperature, it could be a most cost-effective method of degrading contaminants in sewage sludge that require higher energy combustion, e.g., PFAS.

This research has demonstrated the value of the USEPA LEAF Methods in understanding phosphorus availability and leaching of PTEs from materials such as sewage sludge before and after thermal treatment. This information is essential for assessing material reuse and land application options. Moreover, relative to sequential fractionation methods (e.g., Hedley), LEAF facilitates more robust and valuable assessment of organic and inorganic solids and is a promising tool for evaluating land application potential.

Overall, industrial application of smouldering treatment for sewage sludge may be simpler than other thermal treatment methods due to reduced emissions treatment requirements, especially for PTEs, VOCs, and PCDD/Fs. Smouldering also presents unique opportunities for PFAS management, where larger scale reactors fully remove these compounds from the sewage sludge and amendments improve overall degradation. Finally, with phosphorus reuse potential for land application and direct recovery, smouldering sewage sludge creates an important opportunity for a phosphorus circular economy as part of wastewater treatment sludge management.

7.3 Recommendations for Future Work

Although this research advances the understanding of both the beneficial and potentially harmful by-products from smouldering sewage sludge, several recommendations have been presented for future work in these areas:

- This research attempted to understand the mineral phases formed with calcium and fluorine in the ash when a calcium amendment is added to sewage sludge. With concentrations of fluorine and fluorine containing compounds too low in the ash to be detected, the question of the fate of fluorine during sewage sludge smouldering is still largely unknown. Future work could seek to address this question.

- While this work demonstrated that significant PFAS degradation from high MC sludge is possible when supplemented with an additional fuel source (e.g., GAC), future work should investigate the use of a calcium amendments as an alternative to GAC supplementation for treating PFAS in high MC sludge.
- Future work could apply the LEAF methods to examine PFAS mobility from sludge and ash to better understand the risks associated with land application of these materials as soil amendments.
- Future work could examine the PFAS emissions by-products from smouldering sludge at larger scales and work to optimize treatment via amendments and process changes.
- Further research linking PCDD/F release to operating conditions may facilitate the ability to selectively apply emissions management measures as needed, instead of continuously during operation.
- PCDD/F formation may be possible from heterogeneous pathways in smouldering, much like incineration; however, more work needs to be done to fully understand the mechanisms governing the risks of PCDD/F formation in smouldering systems.
- While the extraction potential of phosphorus and other PTEs was explored in this research, this is only a first step towards recovery. Future work could explore methods of recovering the elements from the extractant solution into useful/useable forms.
- While emissions recovery was not rigorously quantified in this research, it is an important source of recoverable phosphorus that should be explored in future work on smouldering systems.

- Future work involving plant growth studies and multiple growth cycles may be beneficial to (1) optimize amounts of ash required to support plant growth and (2) determine the phosphorus flux from ash.
- Incorporating mineralogy into phosphorus analyses has the potential to improve our interpretation and understanding of these results. This work provides important groundwork for future research exploring phosphorus mineralogy of organic waste streams (including sewage sludge) and transformations brought about by thermal treatment.

Appendices

Appendix A: Supplementary Material for "USEPA LEAF methods for characterizing phosphorus and potentially toxic elements in raw and thermally treated sewage sludge"

A.1: Total Elemental Concentrations

Table A.1- 1: Total Amounts of 13 Potentially Toxic Elements

Element	Concentration ± SE [a]				Regulatory standard *O. Reg. 338:* NASM CM1
	Sludge	Incinerated Ash			
	(mg/kg-dry sludge)	(mg/kg-dry ash)	(mg/kg-dry sludge) [b]		(mg/kg-dry mass)
Al	11000 ± 320	28000 ± 280	7000 ± 70		
Cd	3 ± 0.1	3 ± 0.1	0.8 ± 0.02		3
Co	6 ± 0.6	17 ± 0.4	4 ± 0.1		34
Cr	120 ± 2	240 ± 4	60 ± 0.9		210
Cu	570 ± 14	1500 ± 20	370 ± 5		100
Fe	75000 ± 3100	73000 ± 3800	18000 ± 960		
Mg	6000 ± 180	18000 ± 420	4600 ± 100		
Mn	480 ± 17	1200 ± 6	290 ± 2		
Mo	22 ± 0.1	35 ± 0.3	9 ± 0.1		5
Ni	49 ± 3	120 ± 2	30 ± 0.4		62
P	46000 ± 1200	93000 ± 840	23000 ± 210		
Pb	90 ± 22	230 ± 52	57 ± 13		150
Zn	1100 ± 28	3000 ± 58	750 ± 15		500

[a] Standard error calculated as $\frac{\sigma}{\sqrt{n}}$

[b] A 25% ash content on a dry-mass basis of the sludge was used based on the results of the proximate analysis (see section 2.1)

A.2: Additional LEAF PTE results normalized per kg dry sludge

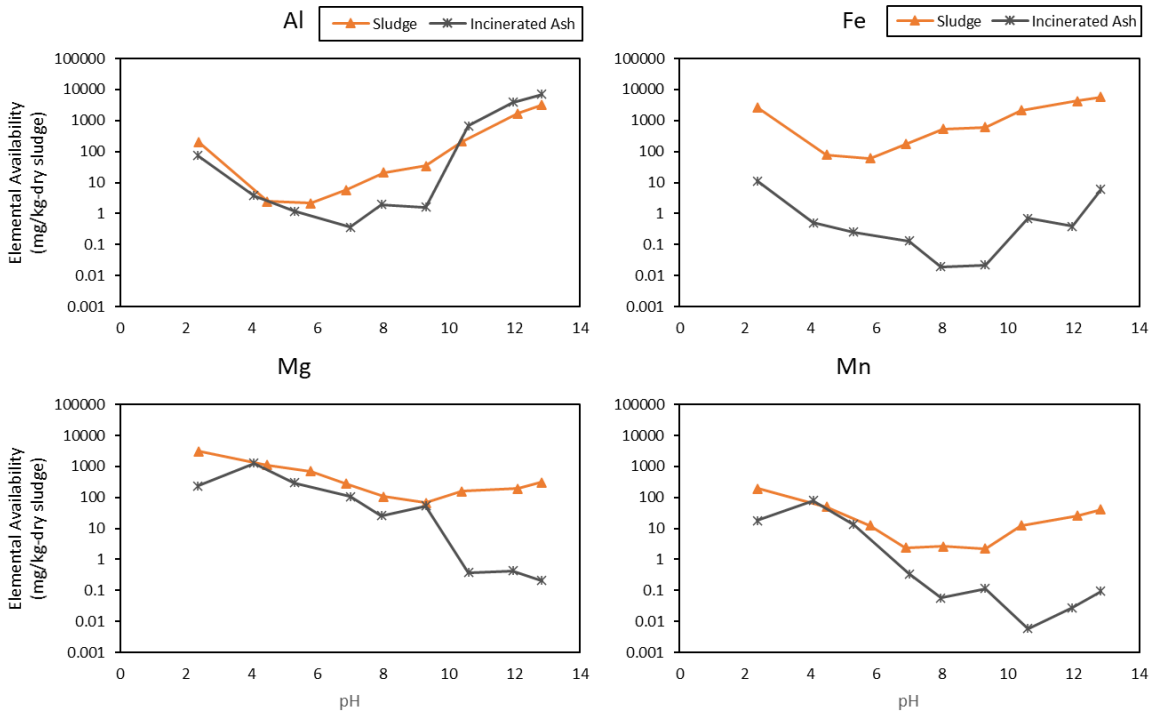

Figure A.2- 1: pH-dependent release of Al, Fe, Mg, and Mn following USEPA Method 1313 with values normalized per kg of dry sludge.

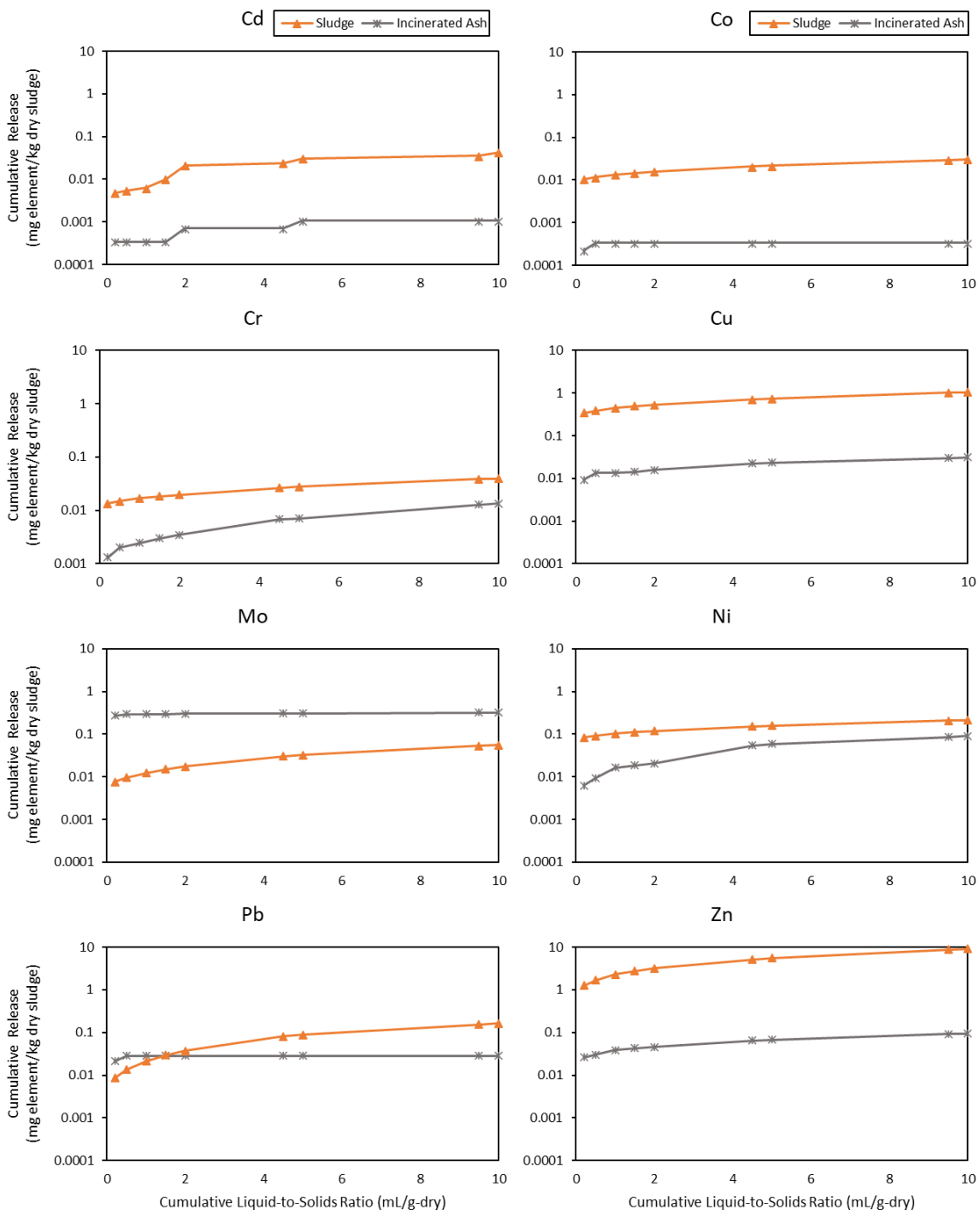

Figure A.2- 2: USEPA Method 1314 cumulative release of 8 PTEs of concern from O. Reg. 338 CM1 NASM for both sludge and incinerated ash. Values have been normalized per kg of dry sludge.

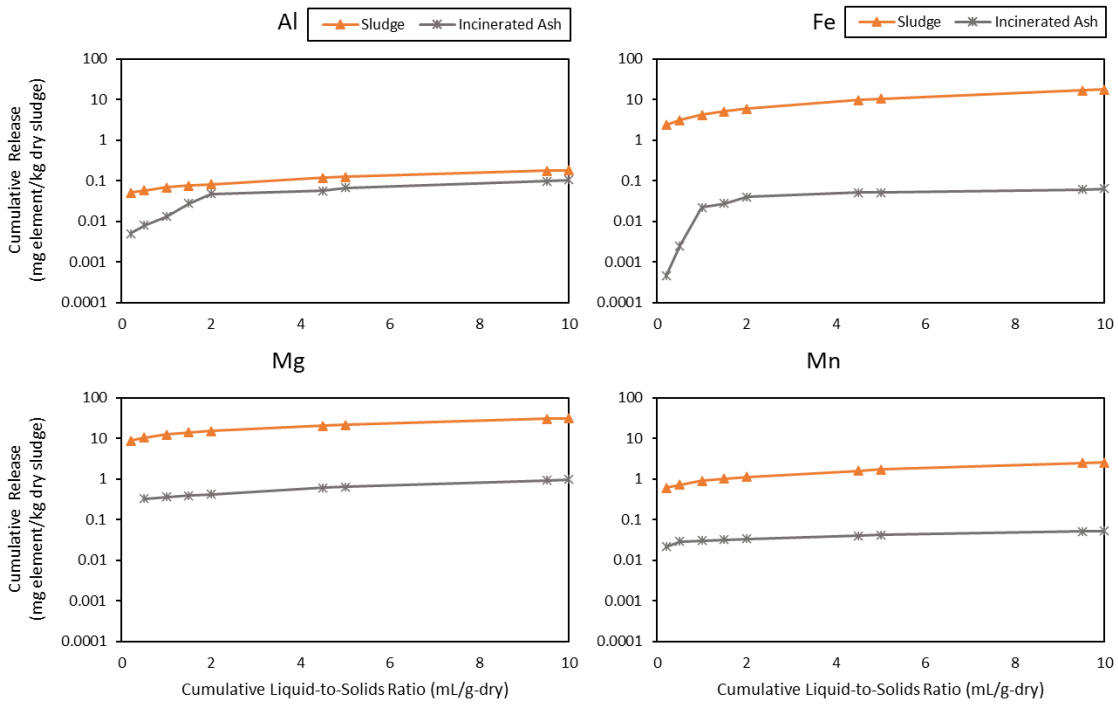

Figure A.2- 3: USEPA Method 1314 cumulative release of Al, Fe, Mg, and Mn normalized per kg of dry sludge.

A.3: All LEAF results per kg dry matter

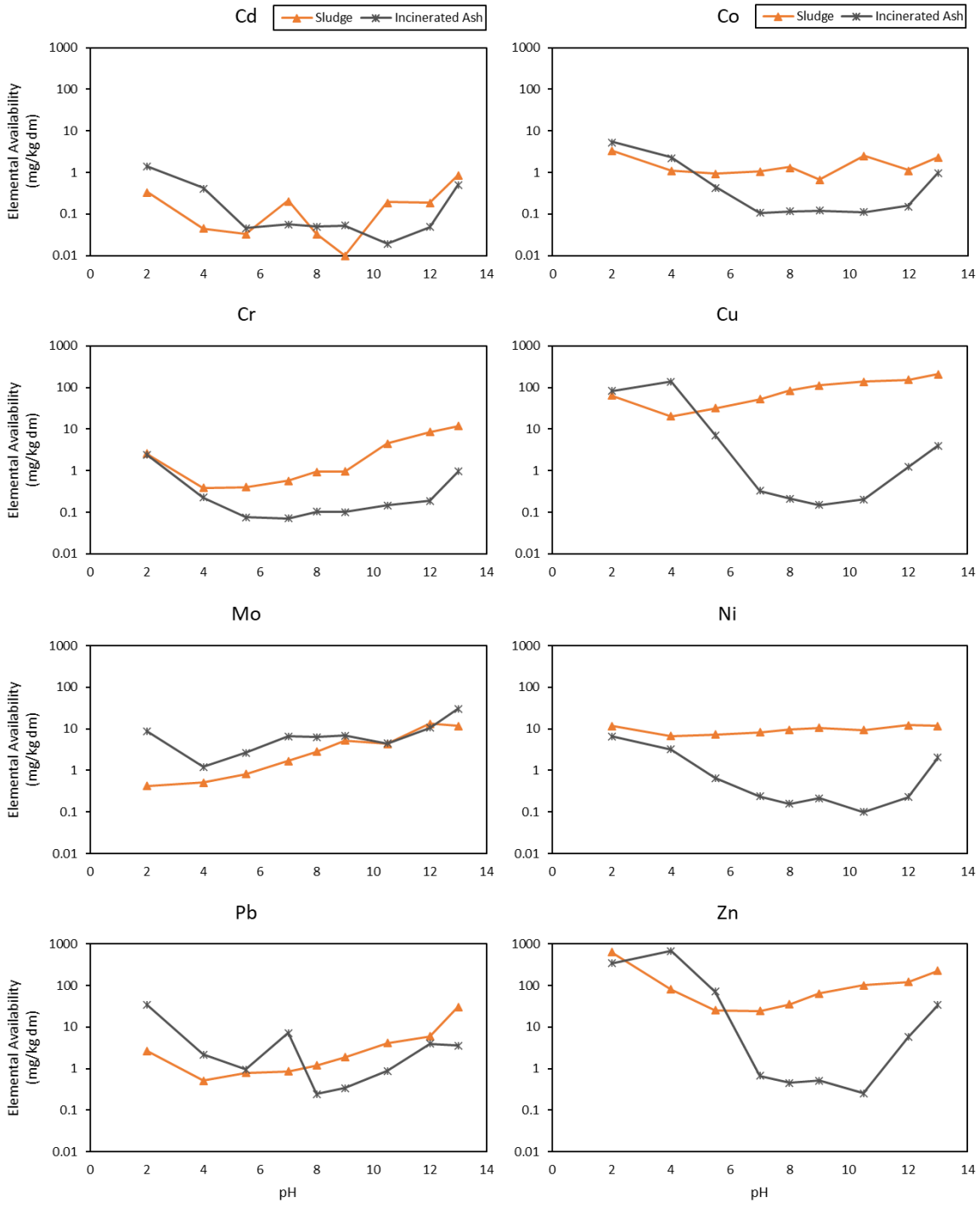

Figure A.3- 1: pH-dependent leaching curves for 8 PTEs of concern from O. Reg. 338 CM1 NASM for both sludge and incinerated ash, following USEPA Method 1313 per kg dry matter.

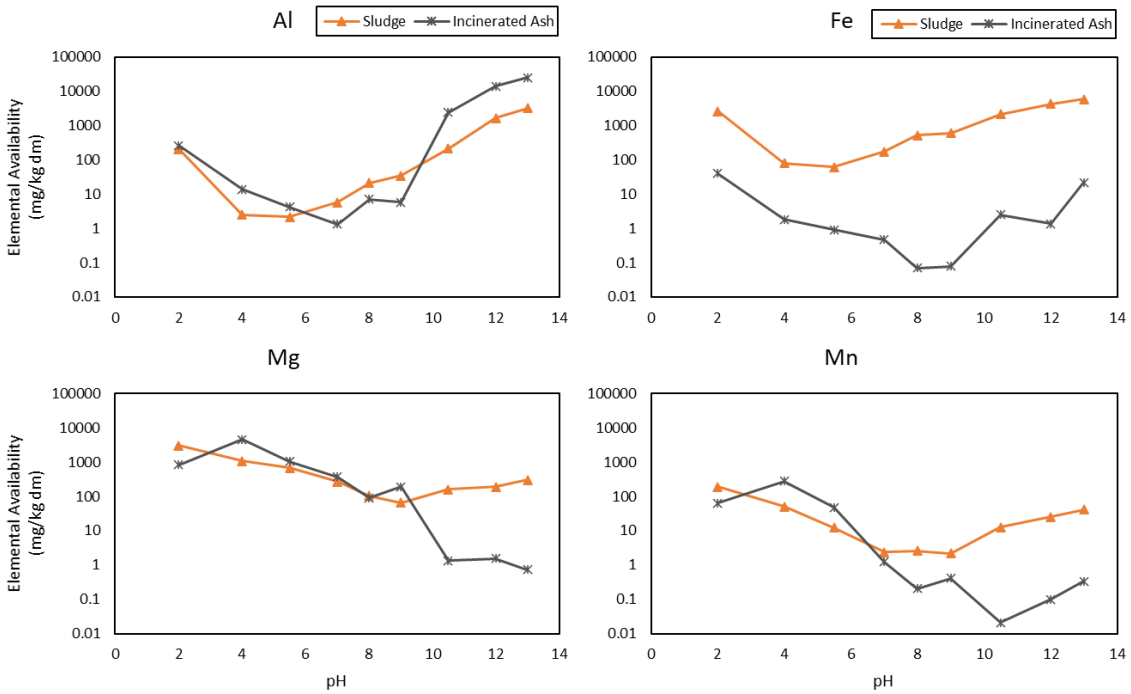

Figure A.3- 2: pH-dependent release of Al, Fe, Mg, and Mn following USEPA Method 1313 per kg dry matter.

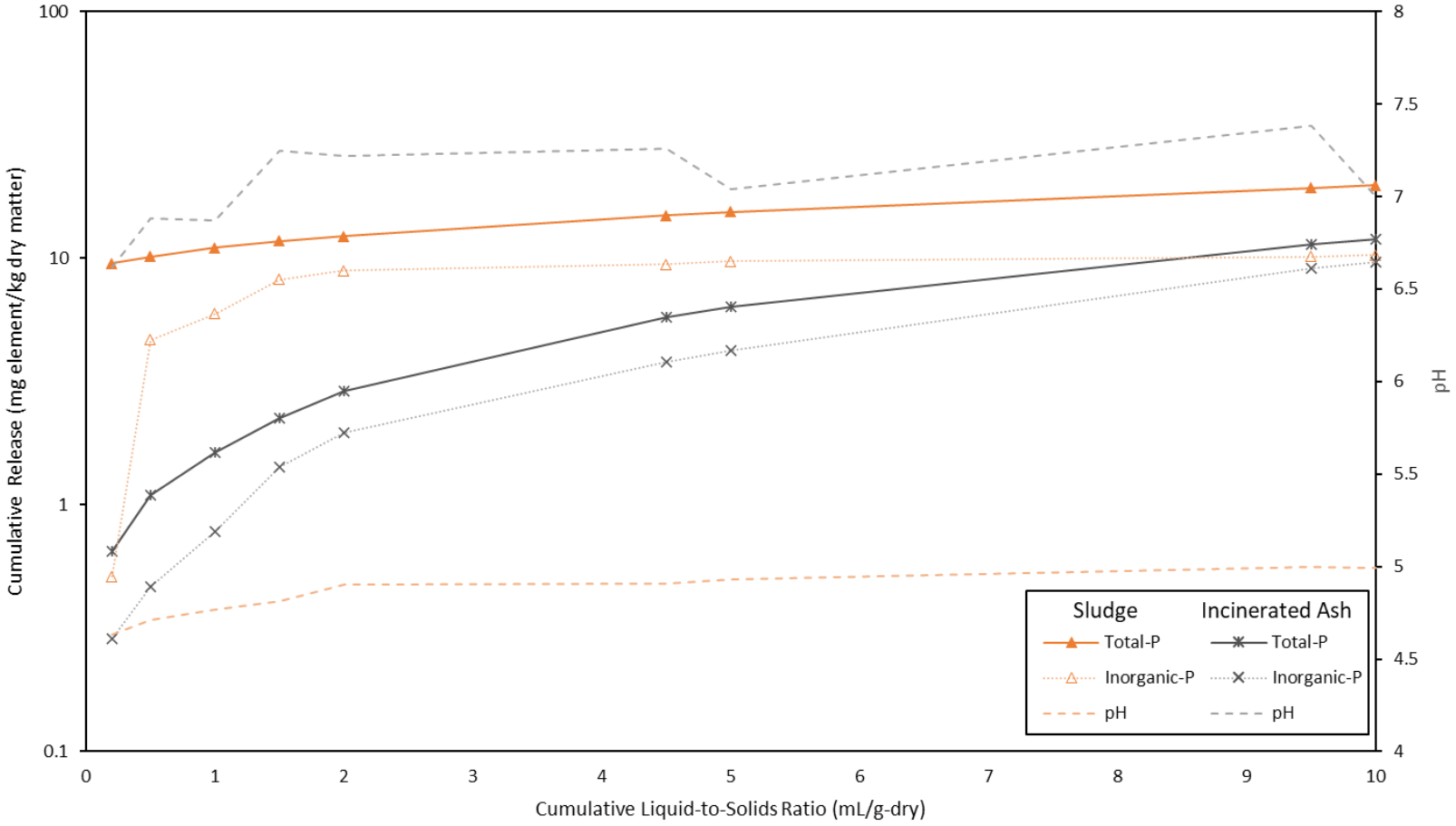

Figure A.3- 3: The USEPA method 1314 column percolation experiments for sludge (orange) and incinerated ash (grey). The concentrations of released phosphorus are shown in mg of phosphorus per kg dry matter. The darker solid lines and lighter broken lines show total- and inorganic-P release, respectively. The pH changes over the column leaching experiment are plotted as dotted lines on the secondary y-axis.

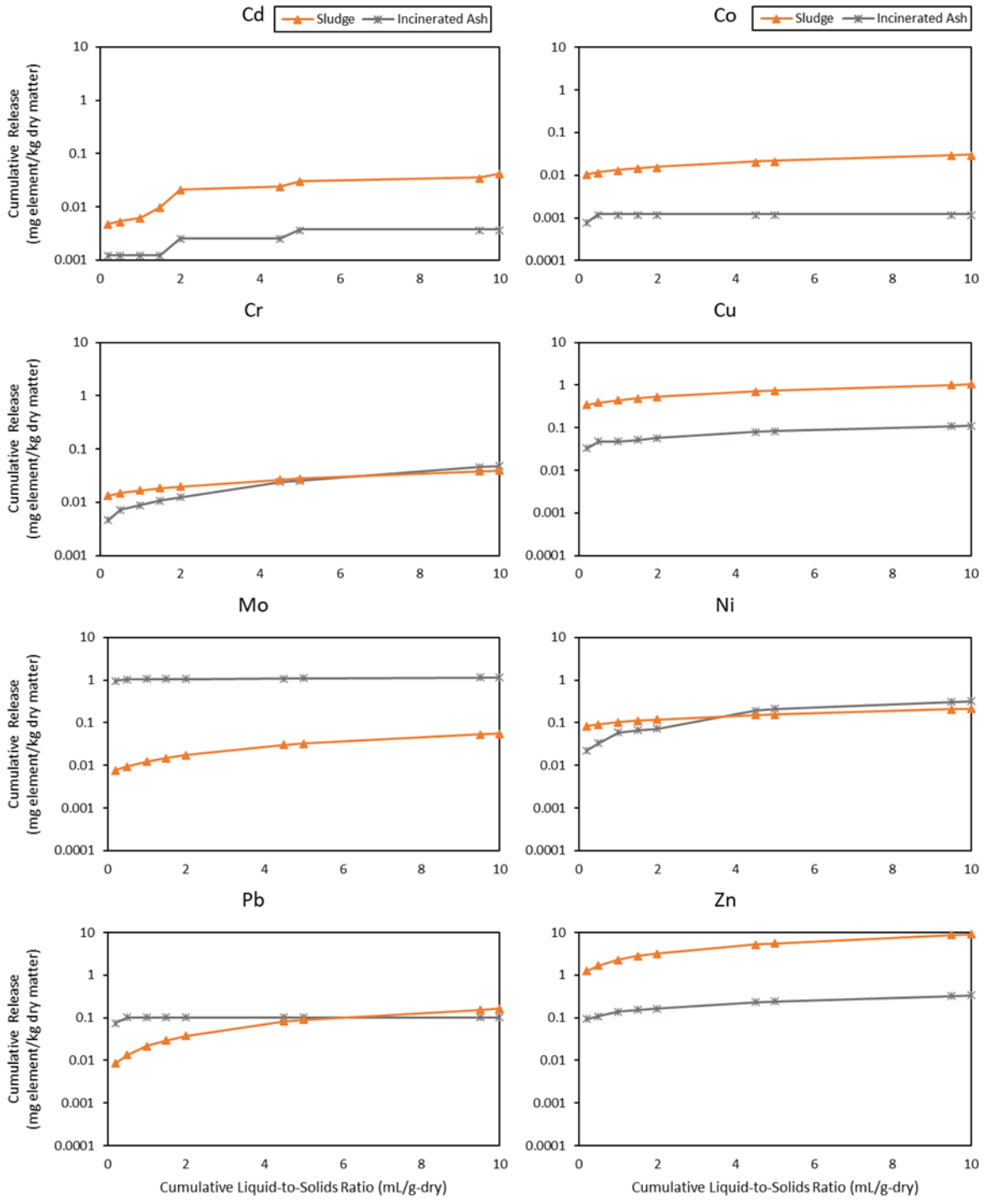

Figure A.3- 4: USEPA Method 1314 cumulative release of 8 PTEs of concern from O. Reg. 338 CM1 NASM for both sludge and incinerated ash.

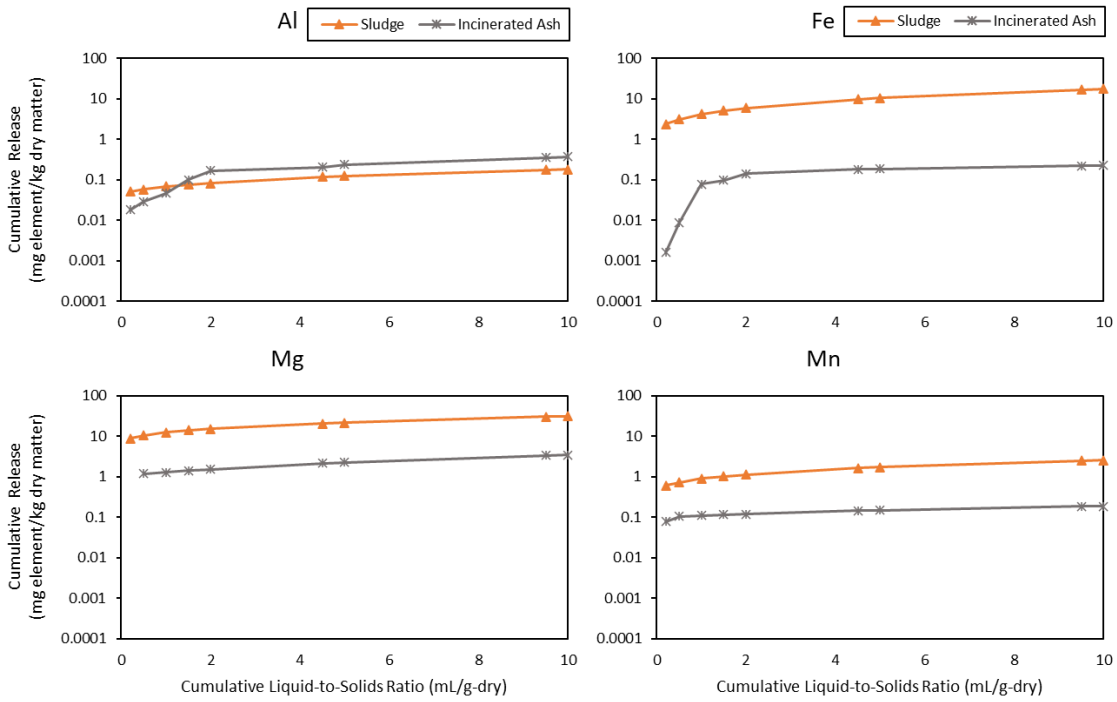

Figure A.3- 5: USEPA Method 1314 cumulative release of Al, Fe, Mg, and Mn per kg dry matter.

Appendix B: Supplementary Material for “Phosphorus Recovery and Reuse Potential from Smouldered Sewage Sludge Ash”

B.1: Supplementary Information on Drum Reactor Experiments

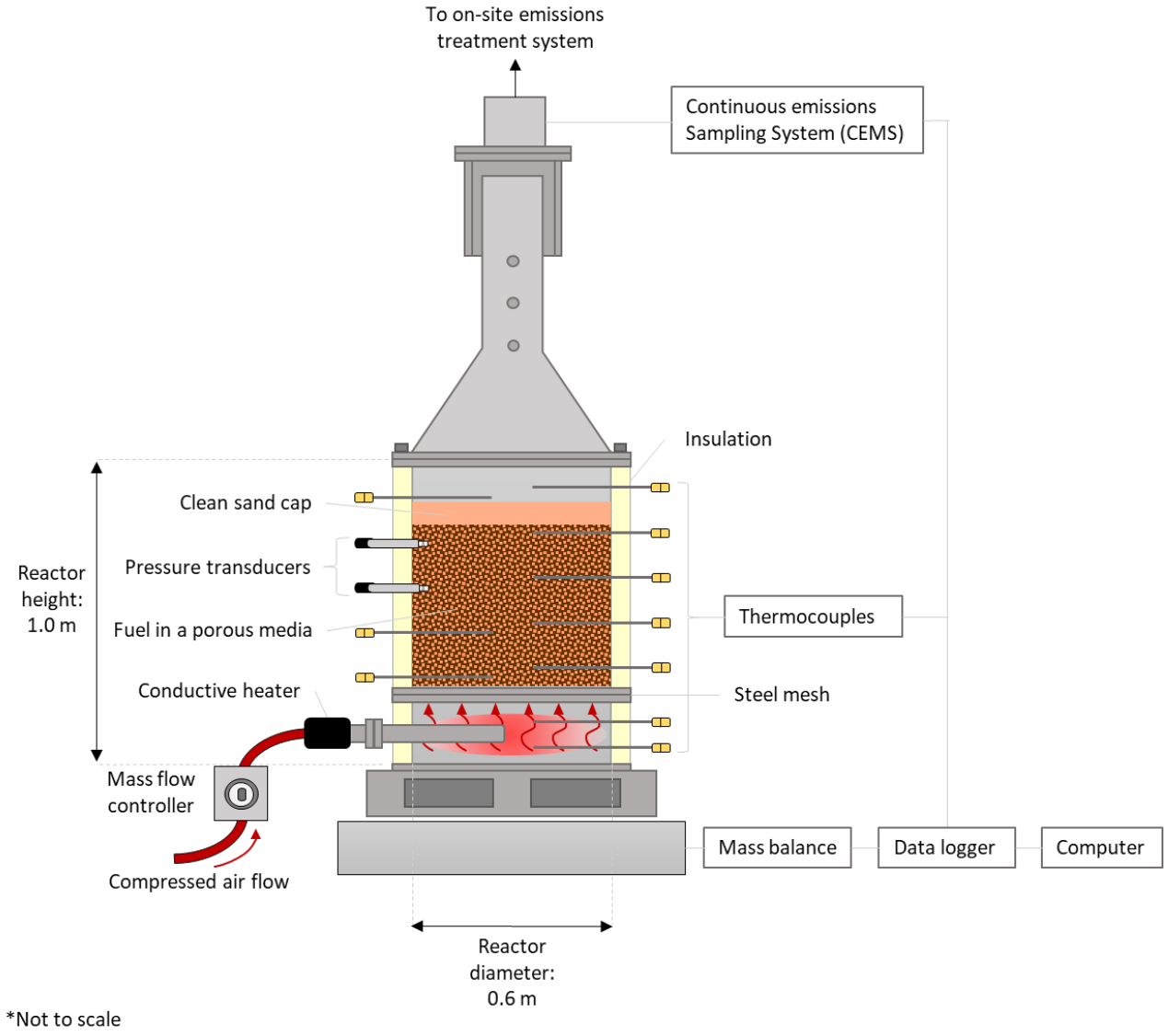

Figure B.1- 1: Schematic of smouldering reactor set-up.

Loading Procedure

The sludge/sand tests consisted of sludge as the fuel embedded in coarse silica sand as the porous media. The co-smouldering tests had a fuel mixture of sludge and woodchips, where the woodchips dually acted as the porous media. The experimental set-ups followed the same procedures for both tests, except for two minor differences for the co-smouldering test. An additional layer of coarse silica sand was added to the base of the reactor, 0.6-2.5 cm thick, to provide insulation between the hot smouldering mixture and the supporting screen. A subsequent layer of woodchips, 1-2 cm thick, was added above the clean sand layer to assist with ignition. Moreover, a clean sand cap was added on top of the sludge/sand pack to lower the exiting temperature for safety purposes.

The sludge mixture was loaded in small batches that were gently lowered to the base of the reactor. Furthermore, to achieve a more uniform density of mixture, while still ensuring material homogeneity, the surface was leveled instead of tamped.

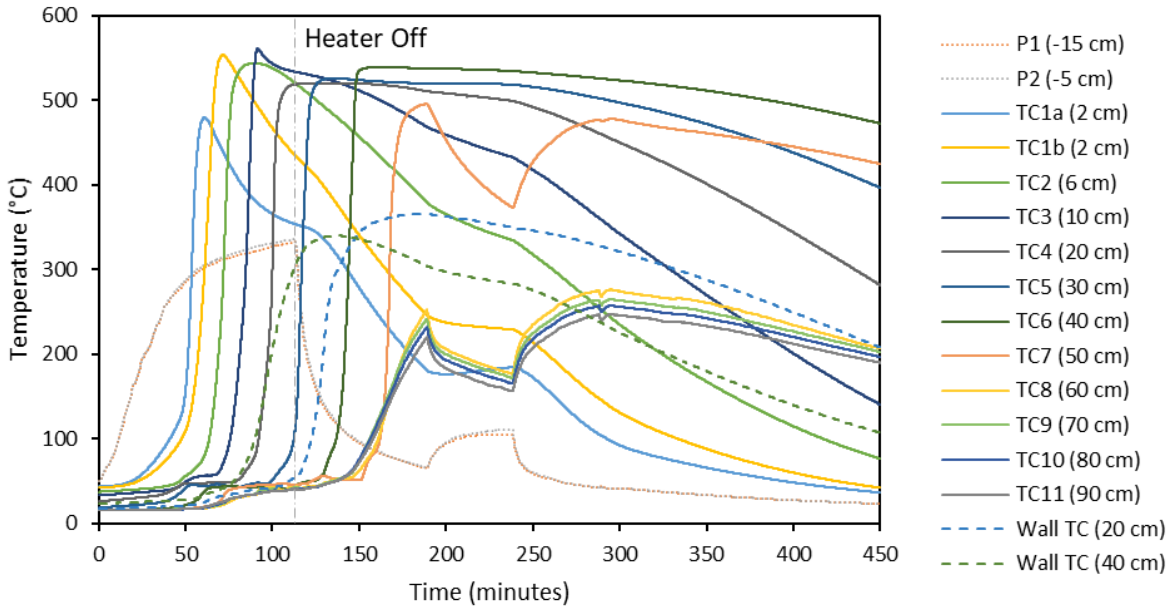

Figure B.1- 2: Temperature profile for the sludge-sand experiment, a self-sustaining smouldering experiment with a 3.81% moisture content sludge in a fixed bed with 25.5 g/g sand/sludge mass ratio. Plenum, centreline, and wall thermocouples are presented. Note the air flux was changed at 190, 238, 288, 290, and 296 minutes.

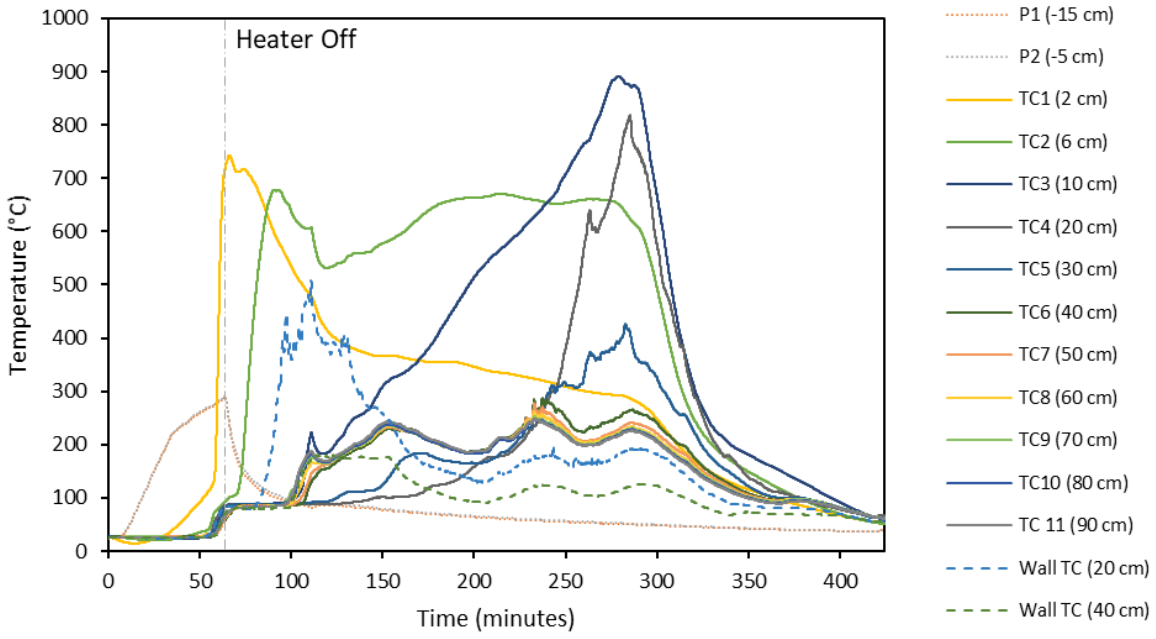

Figure B.1- 3: Temperature profile for the sludge-woodchips experiment, a self-sustaining smouldering experiment with a 75% moisture content sludge in a fixed bed with 0.4/0.3/1 g/g/g woodchips/extra water/sludge mass ratio. Plenum, centreline, and wall thermocouples are presented. Note the air flux was changed at 112 minutes.

B.2: Supplementary Information on Material Characterization and Mass Balances

Table B.2- 1: Total elemental concentrations

Element	Concentration (mg/kg-dry virgin material) ± SE[a]					
	Sludge	Woodchips	Sludge Ash [b]	Sludge/Woodchip Ash [c]	Woodchip Ash [d]	Sand [e]
Al	5400 ± 300	1100 ± 400	7300 ± 1000	480 ± 90	370 ± 600	8000 ± 100
Cd	2.6 ± 0.2	0.3 ± 0.4	1.1 ± 0.8	0.2 ± 0.1	0.15 ± 0.05	1.6 ± 0.01
Co	3.8 ± 0.3	0.4 ± 0.4	3.2 ± 1	0.55 ± 0.3	0.31 ± 0.3	4 ± 0.01
Cr	120 ± 10	34 ± 2	90 ± 40	11 ± 2	10 ± 10	110 ± 0.7
Cu	480 ± 40	16 ± 4	840 ± 400	57 ± 7	8.7 ± 8	93 ± 2
Fe	53000 ± 5000	2100 ± 600	31000 ± 20000	3600 ± 1000	620 ± 800	16000 ± 200
Mg	4200 ± 400	1600 ± 300	5000 ± 1000	850 ± 90	450 ± 500	980 ± 13
Mn	260 ± 30	200 ± 40	390 ± 50	65 ± 9	76 ± 30	110 ± 1
Mo	22 ± 2	1.4 ± 0.6	15 ± 2	1.2 ± 0.3	0.57 ± 1	50 ± 0.3
Ni	47 ± 6	13 ± 2	49 ± 10	5.1 ± 1	3.1 ± 4	45 ± 0.2
P	26000 ± 3000	480 ± 90	24000 ± 6000	2600 ± 20	150 ± 20	7700 ± 50
Pb	110 ± 10	70 ± 10	62 ± 60	6.1 ± 4	10 ± 4	220 ± 0.2
Zn	630 ± 90	64 ± 30	780 ± 500	70 ± 10	23 ± 7	210 ± 3

[a] Standard error calculated as $\frac{\sigma}{\sqrt{n}}$

[b] The sludge ash is considered all materials from smouldering experiments of sand mixed with sludge finer than 0.250 mm (< #60 sieve)

[c] The post-treatment ash from smouldering experiments consisting of sludge mixed with woodchips

[d] Woodchips ash generated in the lab according to ASTM-D2866-11

[e] The sand is considered all materials from smouldering experiments of sand mixed with sludge coarser than 0.250 mm (> #60 sieve)

Table B.2- 2: Mass balance of sludge and sand experiment

Element	Total Elemental Contents [a] ± SE * (mg)				Total Mass in Fraction [b] ± SE * (%)			
	Sludge	Sand [c]	Ash [d]	Sum Post-Treatment [e]	Sand [c]	Ash [d]	Sum Post-Treatment [e]	Emissions [e]
Al	45000 ± 2500	67000 ± 22000	27000 ± 2200	94000 ± 22000	150 ± 15	62 ± 6	212 ± 16	0 ± 16
Cd	21 ± 1.7	13 ± 2.2	5 ± 2.3	18 ± 3.2	62 ± 27	25 ± 11	87 ± 29	13 ± 29
Co	31 ± 2.5	34 ± 2.2	13 ± 2.3	47 ± 3.2	107 ± 21	42 ± 8	149 ± 22	0 ± 22
Cr	1000 ± 83	930 ± 150	320± 81	1300 ± 170	91 ± 24	31 ± 8	122 ± 26	0 ± 26
Cu	4000 ± 330	780 ± 450	2300 ± 600	3100 ± 750	20 ± 5	58 ± 16	77 ± 17	33 ± 17
Fe	440000 ± 42000	140000 ± 44000	130000 ± 45000	260000 ± 63000	31 ± 12	29 ± 11	60 ± 16	40 ± 16
Mg	35000 ± 3300	8100 ± 2900	18000 ± 2000	26000 ± 3500	23 ± 3	51 ± 8	74 ± 8	26 ± 8
Mn	2200 ± 250	910 ± 220	1300 ± 98	2300 ± 240	42 ± 6	62 ± 9	105 ± 10	0 ± 10
Mo	180 ± 17	41 ± 66	51 ± 3.9	92 ± 66	23 ± 3	29 ± 3	52 ± 4	48 ± 4
Ni	390 ± 50	370 ± 44	170 ± 19	540 ± 48	95 ± 16	43 ± 7	137 ± 18	0 ± 18
P	210000 ± 25000	63000 ± 11000	83000 ± 12000	150000 ± 16000	30 ± 5	39 ± 7	69 ± 9	31 ± 9
Pb	920 ± 83	1900 ± 48	240 ± 130	2100 ± 140	200 ± 109	26 ± 14	226 ± 110	0 ± 110
Zn	5200 ± 740	1700 ± 660	3100 ± 1200	4900 ± 1300	33 ± 13	60 ± 24	93 ± 27	7 ± 27

[a] Calculated as $\left(elemental\ concentration\left[\frac{mg}{kg} - dry\ matter\right]\right) \times (mass\ of\ fraction\ in\ reactor\ [kg - dry\ matter])$

[b] Calculated as $(elemental\ content[mg]) \div (elemental\ content\ in\ virgin\ material\ [mg]) \times 100\%$

[c] The sand is considered all materials from smouldering experiments of sand mixed with sludge coarser than 0.250 mm (> #60 sieve)

[d] The sludge ash is considered all materials from smouldering experiments of sand mixed with sludge finer than 0.250 mm (< #60 sieve)

[e] Calculated as $(elemental\ content[mg])_{sand} + (elemental\ conctent[mg])_{ash}$

* The standard error was calculated from the uncertainties from each calculation added in quadrature

Table B.2- 3: Mass Balance of the Sludge-Woodchips Smouldering Experiment

Element	Total Elemental Contents ± SE (mg) [a]					
	Virgin Materials		Mixed Ashes [b] *		Elemental Retention (%) [c] *	
	Sludge	Woodchips	Theoretical Maximum [d]	Actual [e]	Sludge Only [f]	Mixed Ash [g]
Al	53600 ± 3000	16300 ± 6200	70000 ± 6900	10600 ± 400	20 ± 1.3	15 ± 1.6
Cd	26 ± 2	4.0 ± 3	30 ± 5	4.4 ± 0.5	17 ± 2.2	15 ± 3.1
Co	38 ± 3	5.8 ± 5	44 ± 6	12 ± 2	32 ± 4.7	28 ± 5.1
Cr	1200 ± 100	480 ± 30	1700 ± 100	240 ± 8	19 ± 1.7	14 ± 0.9
Cu	4800 ± 400	220 ± 60	5000 ± 400	1300 ± 30	27 ± 2.3	25 ± 2.1
Fe	527000 ± 50000	30600 ± 8300	557000 ± 50000	80200 ± 4200	15 ± 1.6	14 ± 1.5
Mg	42000 ± 4000	23300 ± 4200	65000 ± 6000	18700 ± 400	45 ± 4.4	29 ± 2.6
Mn	2600 ± 300	2900 ± 500	5400 ± 600	1400 ± 40	56 ± 6.6	27 ± 3.0
Mo	220 ± 20	20 ± 20	240 ± 50	27 ± 1	12 ± 1.3	11 ± 2.7
Ni	470 ± 60	180 ± 30	650 ± 70	110 ± 3	24 ± 3.1	17 ± 1.8
P	258000 ± 30000	6900 ± 1300	265000 ± 30000	57300 ± 100	22 ± 2.6	22 ± 2.4
Pb	1100 ± 100	990 ± 140	2100 ± 200	140 ± 18	12 ± 2.0	6 ± 1.0
Zn	6300 ± 900	910 ± 340	7200 ± 1000	1600 ± 60	25 ± 3.7	22 ± 3.0

[a] Calculated as $\left(elemental\ concentration\left[\frac{mg}{kg} - dry\ matter\right]\right) \times (mass\ added\ to\ reactor\ [kg - dry\ matter])$

[b] Combined ashes from smouldering treatment of sludge mixed with woodchips

[c] Calculated as $\left((actual\ elemental\ content[mg\ element]) \div (theoretical\ maximum\ elemental\ content\ [mg\ element])\right) \times 100\%$

[d] Assuming no losses, calculated as the sum of the contents in the virgin sludge and woodchips

[e] Calculated as $\left(elemental\ concentration\left[\frac{mg}{kg} - ash\right]\right) \times (mass\ of\ ash\ remaining\ in\ reactor\ [kg - ash])$

[f] Elemental retention considering only contribution of the sludge to the post-treatment ash

[g] Elemental retention considering both the contribution of the woodchips and the sludge

* The standard error was calculated from the uncertainties from each calculation added in quadrature

B.3: Supplementary Information on Leaching Tests and Extraction Potentials

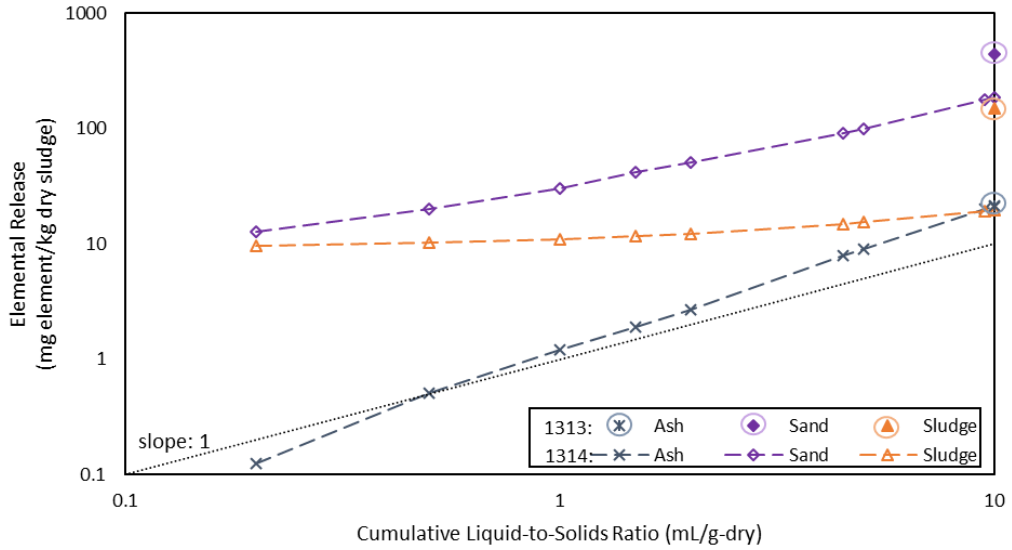

Figure B.3- 1: Total phosphorus release as a function of the log of the cumulative liquid-to-solids ratio with the available content of the materials from USEPA Method 1313 at native pH plotted at an L/S of 10 mL/g-dry. A dotted line with a slope of 1 has been added to each plot.

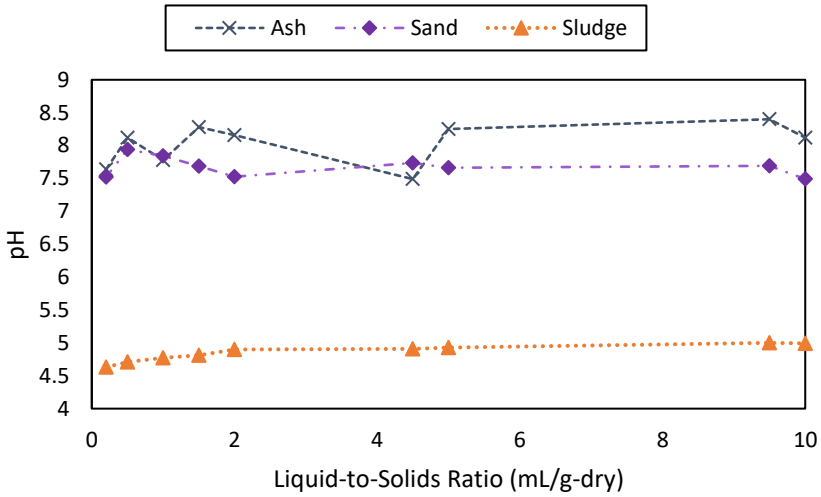

Figure B.3- 2: pH changes observed during the column percolation experimental (following USEPA Method 1314). The results are presented for sludge and post-treatment ash and sand as a function of the liquid-to-solids ratio.

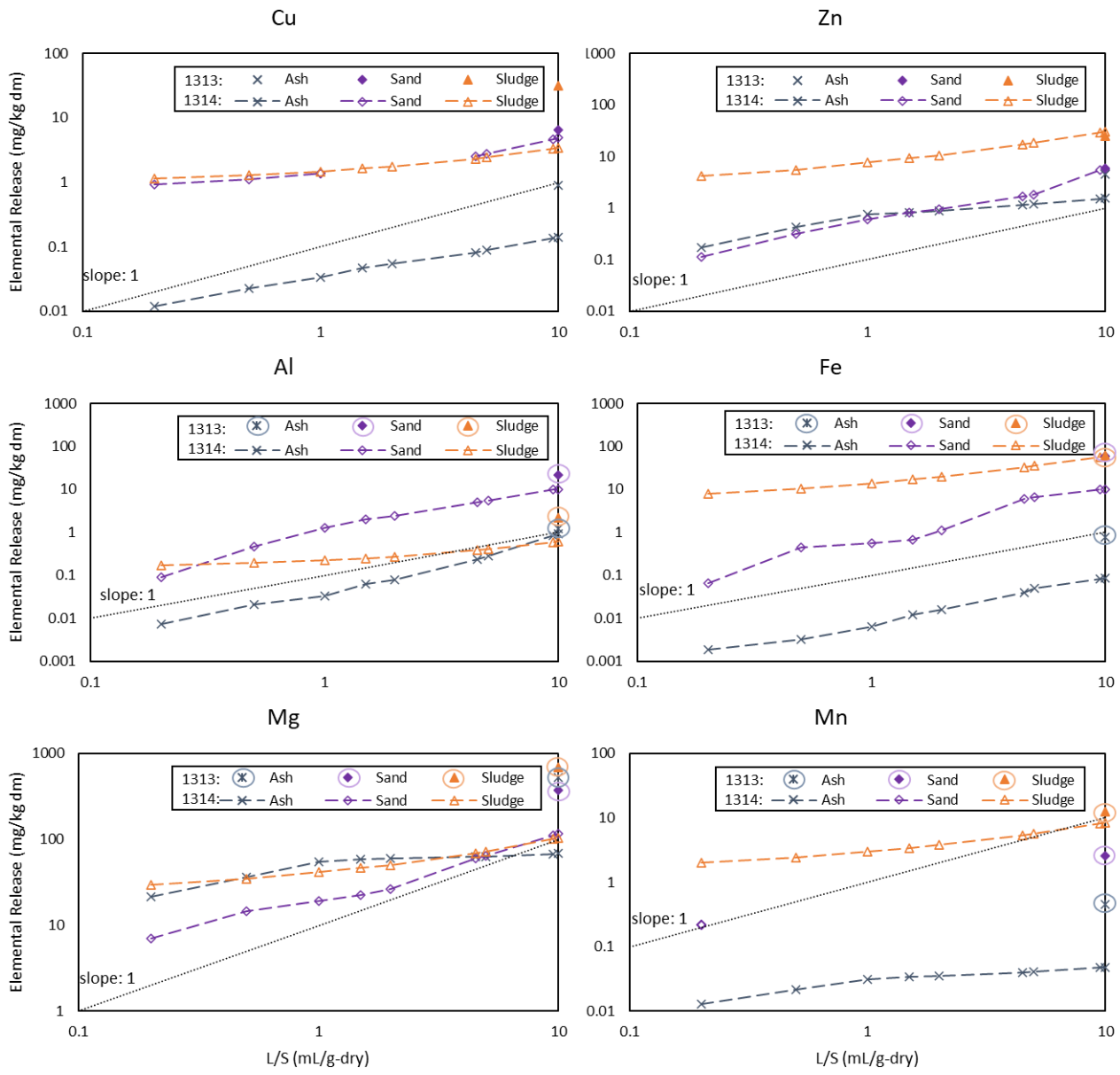

Figure B.3- 3: column percolation experimental results (following USEPA Method 1314) for 6 common potentially toxic elements from the virgin sludge and post-treatment ash and sand. The elemental release is shown as cumulative release as a function of the liquid-to-solid ratio. The values have been normalized to mg of element per kg of dry sludge. The available content of the materials from USEPA Method 1313 at native pH has been plotted at an L/S of 10 mL/g – dry. A dotted line with a slope of 1 has been added to each plot.

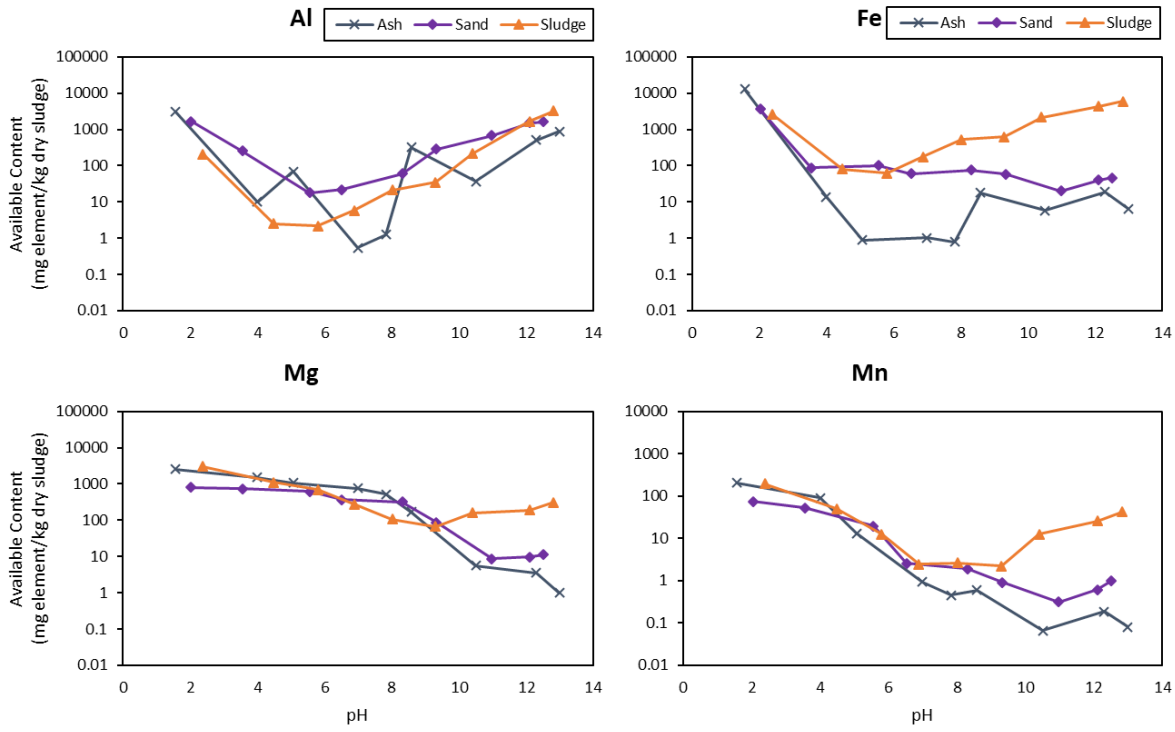

Figure B.3- 4: pH-dependent leaching (following USEPA Method 1313) of 4 other elements of interest from the virgin sludge compared to the post-treatment ash and sand. All values have been normalized to mg of P per kg of dry material.

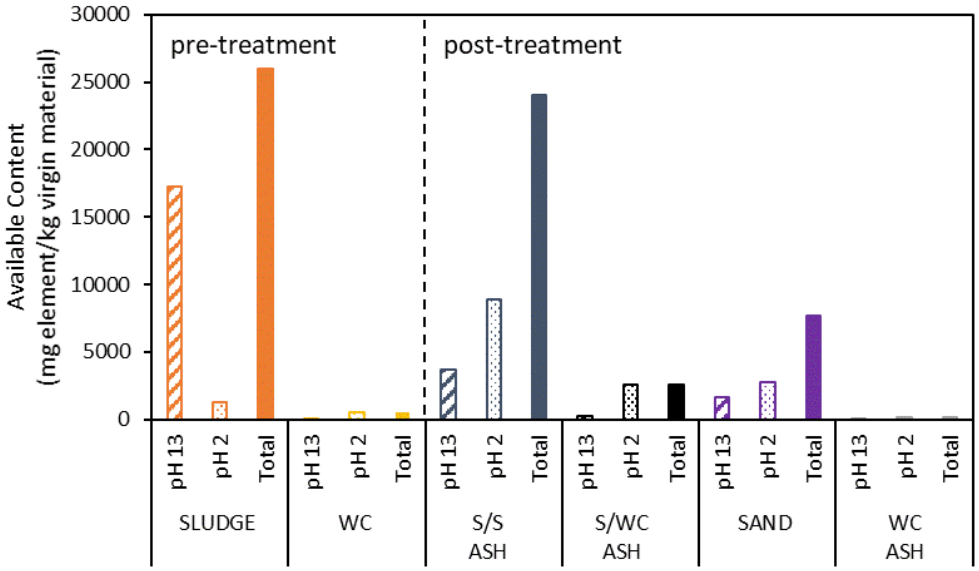

Figure B.3- 5: Available and total phosphorus contents within the pre- and post-treatment materials from sludge-sand and mixed sludge-woodchips smouldering experiments. Virgin woodchips are denoted as 'WC', 'S/S' is sieved ash from sludge-sand smouldering experiments, and 'S/WC' is ash from mixed sludge-woodchips smouldering.

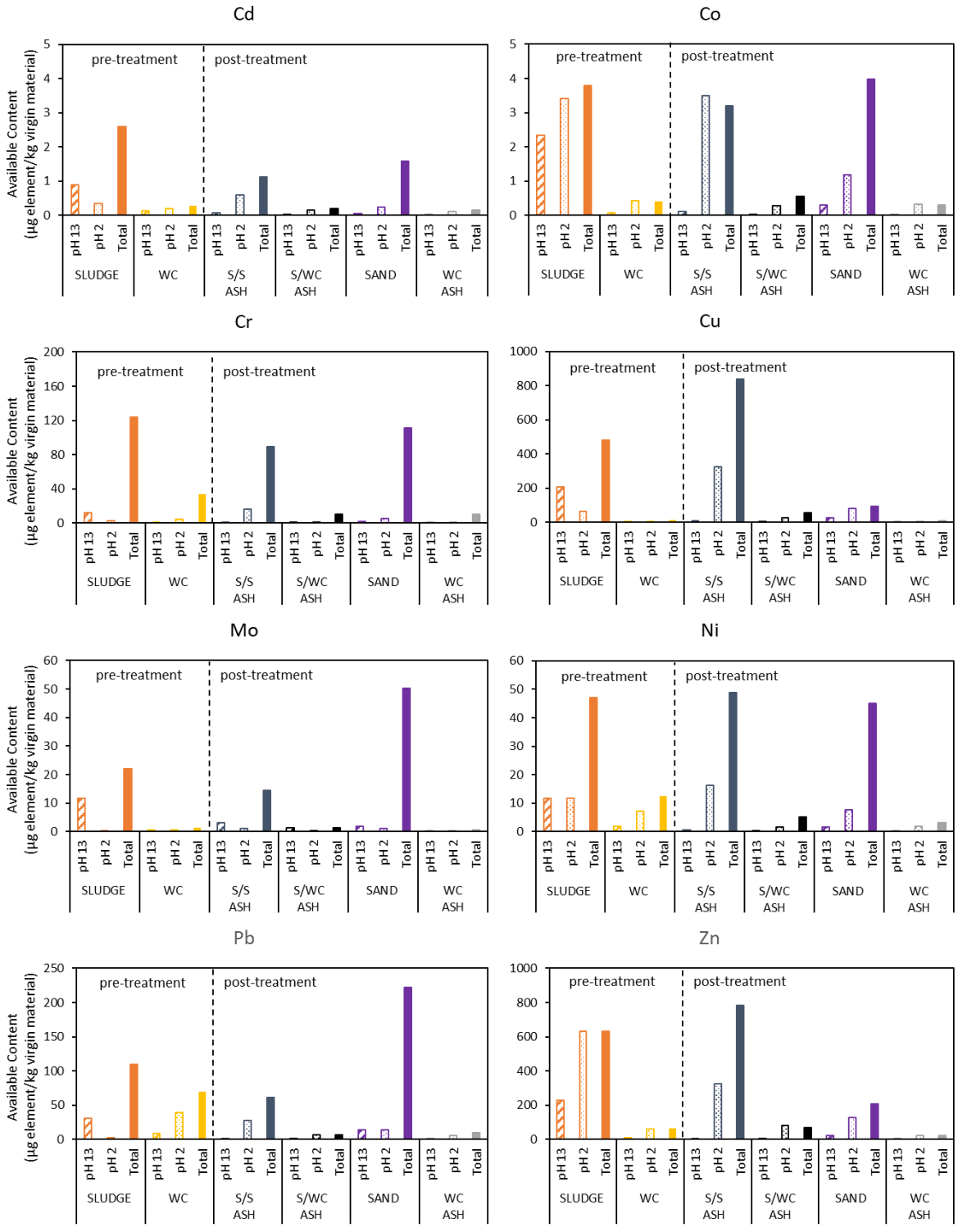

Figure B.3- 6: Available and total contents of 8 potentially toxic elements within the pre- and post-treatment materials from sludge-sand and mixed sludge-woodchips smouldering experiments. Virgin woodchips are denoted as 'WC', 'S/S' is sieved ash from sludge-sand smouldering experiments, and 'S/WC' is ash from mixed sludge-woodchips smouldering.

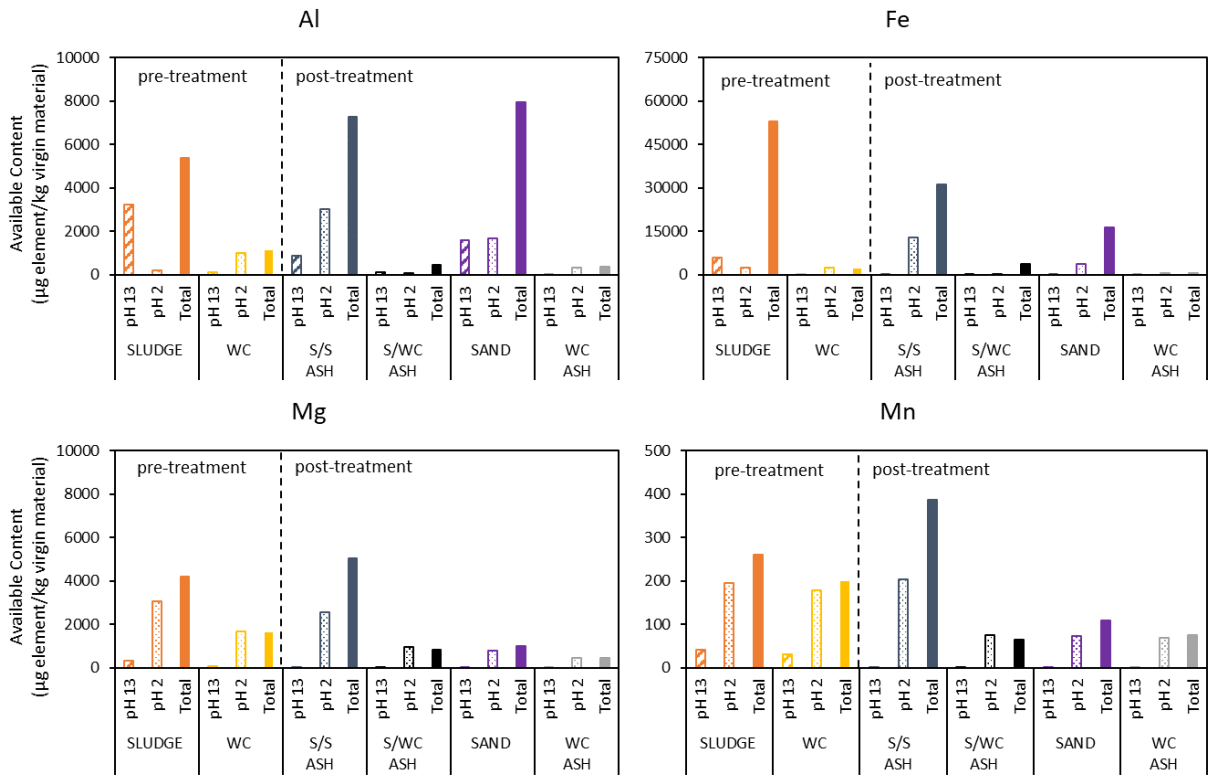

Figure B.3- 7: Available and total contents of aluminum, iron, magnesium, and manganese within the pre- and post-treatment materials from sludge-sand and mixed sludge-woodchips smouldering experiments. Virgin woodchips are denoted as 'WC', 'S/S' is sieved ash from sludge-sand smouldering experiments, and 'S/WC' is ash from mixed sludge-woodchips smouldering.

Table B.3- 1: Extraction Potential Normalized to Sludge Content

Element	Maximum Recoverable Content (mg of element/kg of dry sludge) ± SE[a]					
	Water [b]		pH 2 [c]		pH 13 [c]	
	Sludge	Sand + Ash [d]	Sludge	Sand + Ash [d]	Sludge	Sand + Ash [d]
Al	3 ± 0.3	16 ± 7	320 ± 32	2600 ± 810	4900 ± 490	1600 ± 550
Cd	0.03 ± 0.004	0.1 ± 0.04	0.3 ± 0.04	0.4 ± 0.1	0.7 ± 0.1	0.05 ± 0.01
Co	0.6 ± 0.08	0.04 ± 0.03	2 ± 0.3	1.2 ± 0.3	1.5 ± 0.2	0.06 ± 0.05
Cr	0.3 ± 0.04	2 ± 0.6	1.6 ± 0.2	14 ± 5	7.5 ± 1	2.9 ± 0.8
Cu	10 ± 1	12 ± 9	21 ± 2	270 ± 120	67 ± 8	50 ± 35
Fe	21 ± 3	66 ± 28	900 ± 130	12000 ± 3500	2000 ± 290	57 ± 22
Mg	210 ± 30	870 ± 290	920 ± 130	2800 ± 1100	92 ± 13	16 ± 6
Mn	5 ± 1	2.6 ± 0.8	71 ± 10	180 ± 77	15 ± 2	0.9 ± 0.3
Mo	0.2 ± 0.04	1.4 ± 0.8	0.09 ± 0.02	0.9 ± 0.4	2.4 ± 0.5	3.8 ± 2
Ni	4 ± 1	0.5 ± 0.1	6 ± 1	7.5 ± 4	6 ± 1	1.5 ± 0.5
P	160 ± 25	500 ± 97	1400 ± 210	12000 ± 2800	19000 ± 2900	5500 ± 1100
Pb	0.2 ± 0.07	0.8 ± 0.4	0.8 ± 0.2	19 ± 9	9.4 ± 3	0.5 ± 0.1
Zn	13 ± 3	2.7 ± 0.7	330 ± 63	150 ± 50	120 ± 23	5 ± 1

[a] Standard error calculated as $\frac{\sigma}{\sqrt{n}}$

[b] Recovery at native pH where samples were mixed with only deionized water (pH 6 for sludge, 7 for sand, and 8 for post-treatment ash)

[c] The actual sample pH values are within ± 0.5 pH units of the specified value

[d] Combined post-treatment materials (i.e., coarse-grained quartz sand and smouldered ash)

Table B.3- 2: Extraction Potential from Sand Mixed with Post-Treatment Ash

Element	Percentage of total content in dry material ± SE[a]		
	Water [b]	pH 2 [c]	pH 13 [c]
Al	0.2 ± 0.1%	29 ± 11%	18 ± 7%
Cd	6.9 ± 2.1%	18 ± 5%	2.7 ± 0.7%
Co	1.1 ± 0.9%	34 ± 9%	1.7 ± 1.3%
Cr	1.8 ± 0.6%	13 ± 4%	2.6 ± 0.8%
Cu	2.4 ± 1.8%	54 ± 25%	10 ± 7%
Fe	0.2 ± 0.1%	35 ± 11%	0.2 ± 0.1%
Mg	22 ± 8%	71 ± 28%	0.4 ± 0.2%
Mn	1.1 ± 0.4%	72 ± 33%	0.4 ± 0.1%
Mo	13 ± 7%	7.9 ± 4%	34 ± 21%
Ni	1.3 ± 0.3%	27 ± 11%	3.5 ± 1.4%
P	0.1 ± 0.01%	55 ± 14%	25 ± 6%
Pb	1.3 ± 0.5%	35 ± 16%	4.1 ± 0.5%
Zn	0.4 ± 0.1%	20 ± 7%	0.6 ± 0.2%

[a] Standard error calculated as $\frac{\sigma}{\sqrt{n}}$

[b] Recovery at native pH where samples were mixed with only deionized water (pH 6 for sludge, 7 for sand, and 8 for post-treatment ash)

[c] The actual sample pH values are within ± 0.5 pH units of the specified value

Table B.3- 3: Recovery Potential from Mixed Sludge-Woodchips Ash

Element	Elemental Retention [a] ± SE * (%)		Maximum Recoverable Content [b] ± SE * (mg/kg – dry starting material)		Recovery Potential [c] ± SE * (%)	
	Mixed Ash [d]	Emissions [e]	pH 2	pH 13	pH 2	pH 13
Al	15 ± 1.6	85 ± 1.6	82 ± 7.4	110 ± 8.5	2.5 ± 2.3	3.3 ± 0.4
Cd	15 ± 3.1	85 ± 3.1	0.2 ± 0.04	0.01 ± 0.0	12 ± 3.0	0.9 ±0.1
Co	28 ± 5.1	72 ± 5.1	0.3 ± 0.02	0.03 ± 0.0	14 ± 2.2	1.6 ±0.2
Cr	14 ± 0.9	86 ± 0.9	1.1 ± 0.82	0.19 ± 0.0	1.3 ± 1.0	0.2 ± 0.0
Cu	25 ± 2.1	75 ± 2.1	28 ± 9.8	0.09 ± 0.06	12± 4.2	0.0 ± 0.0
Fe	14 ± 1.5	86 ± 1.5	220 ± 220	0.32 ± 0.04	0.8 ± 0.8	0.0 ± 0.0
Mg	29 ± 2.6	71 ± 2.6	980 ± 170	0.02 ± 0.00	32 ± 6.2	0.0 ± 0.0
Mn	27 ± 3.0	73 ± 3.0	79 ± 19	0.01 ± 0.00	31 ± 8.1	0.0 ± 0.0
Mo	11 ± 2.7	89 ± 2.7	0.4 ± 0.34	1.40 ± 0.14	3.9 ± 3.1	12 ± 2.2
Ni	17 ± 1.8	83 ± 1.8	1.7 ± 0.36	0.04 ± 0.01	5.5 ± 1.3	0.1 ± 0.0
P	22 ± 2.4	78 ± 2.4	2700 ± 1800	240 ± 15	21 ± 14.3	1.9 ± 0.2
Pb	6 ± 1.0	94 ± 1.0	6.6 ± 1.1	0.2 ± 0.06	6.6 ± 1.2	0.2 ± 0.1
Zn	22 ± 3.0	78 ± 3.0	83 ± 34	1.4 ± 0.30	24 ± 10.5	0.4 ± 0.1

[a] Elemental retention of the mixed sludge and woodchips ash determined in Table S2-3

[b] Available elemental content determined from USEPA Method 1313

[c] Calculated as $\left((elemental\ content[mg\ element]) \div (total\ elemental\ content\ in\ starting\ material\ [mg\ element])\right) \times 100\%$

[d] Combined ashes from smouldering treatment of sludge mixed with woodchips

[e] Calculated as $100\% - (elemental\ retention\ in\ mixed\ ash[\%])$

* The standard error was calculated from the uncertainties from each calculation added in quadrature

Appendix C: Supplementary Material for “Behaviour of PCDD/Fs and potentially toxic elements in sewage sludge during smouldering treatment”

C.1: Supplementary Information on LAB Reactor Experiments

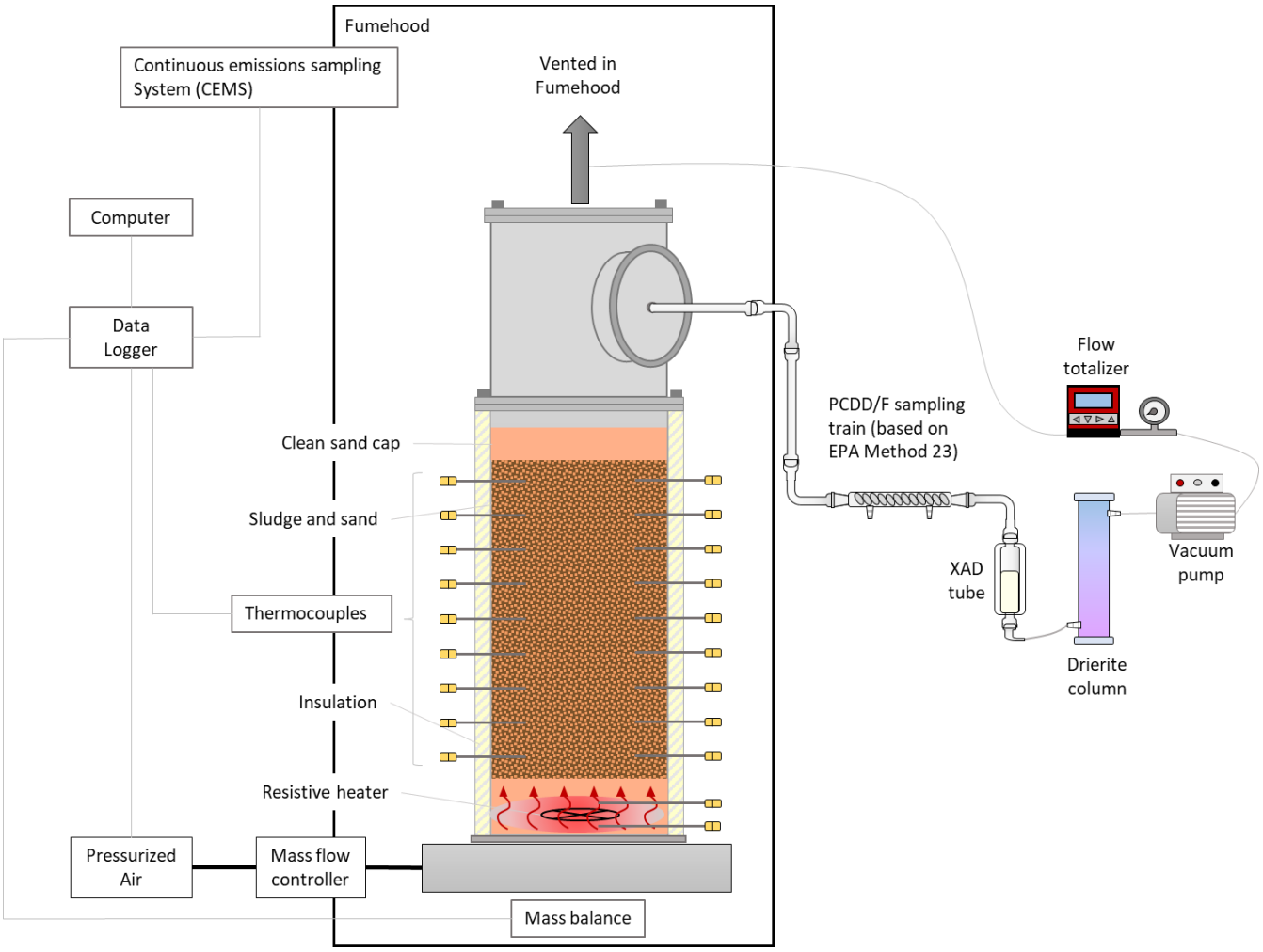

Figure C.1- 1: Experimental set-up and sampling locations for LAB tests.

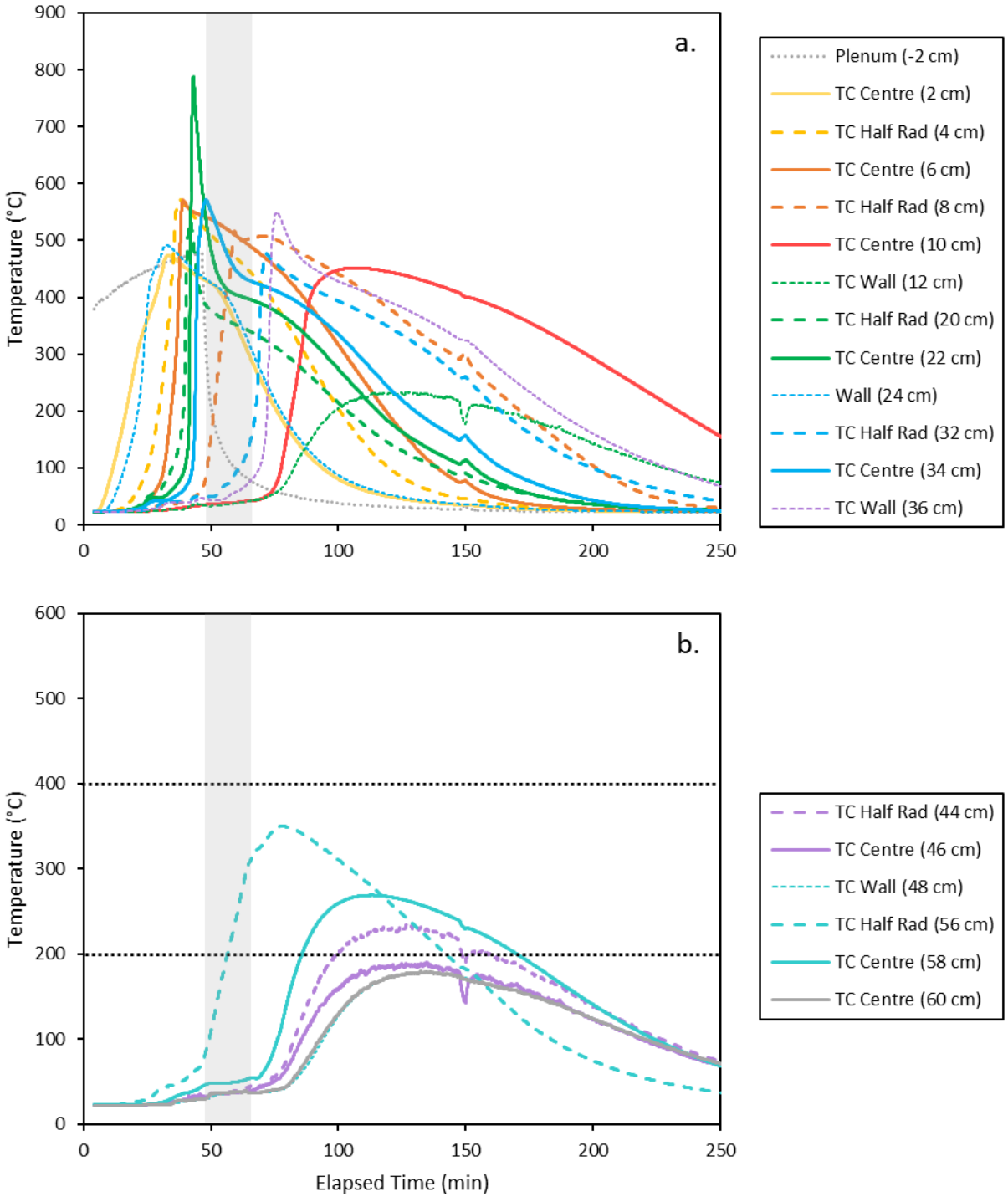

Figure C.1- 2: Temperature profiles for LAB 1a, a. presents the centreline (solid lines) and wall (broken line) temperatures within the fuel bed, and b. shows the emissions temperatures above the fuel bed. The sampling timing and duration is shown as a grey block.

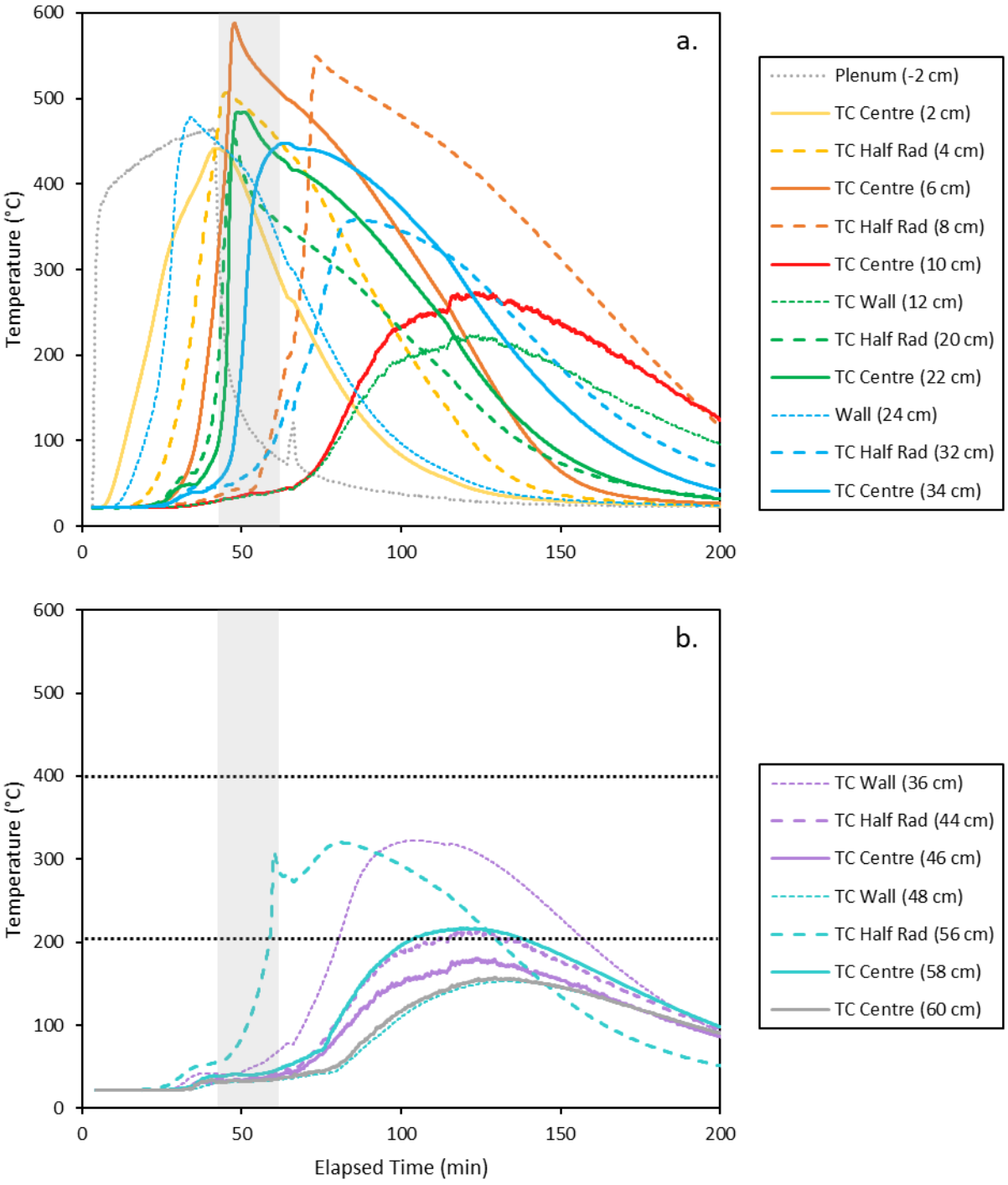

Figure C.1- 3: Temperature profiles for LAB 1b, a. presents the centreline (solid lines) and wall (broken line) temperatures within the fuel bed, and b. shows the emissions temperatures above the fuel bed. The sampling timing and duration is shown as a grey block.

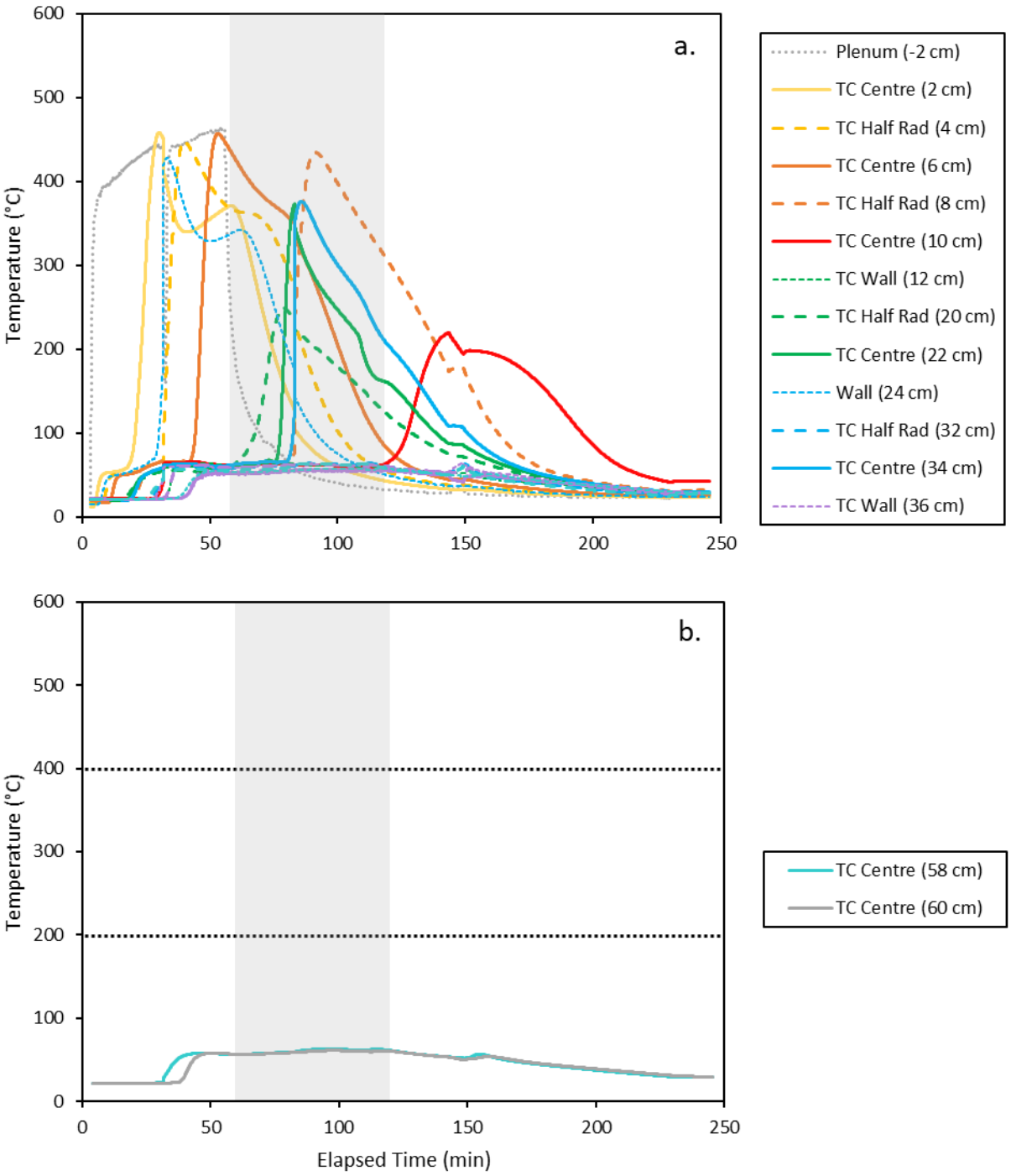

Figure C.1- 4: Temperature profiles for LAB 2, a. presents the centreline (solid lines) and wall (broken line) temperatures within the fuel bed, and b. shows the emissions temperatures above the fuel bed. The sampling timing and duration is shown as a grey block.

C.2: Supplementary Information on DRUM Reactor Experiments

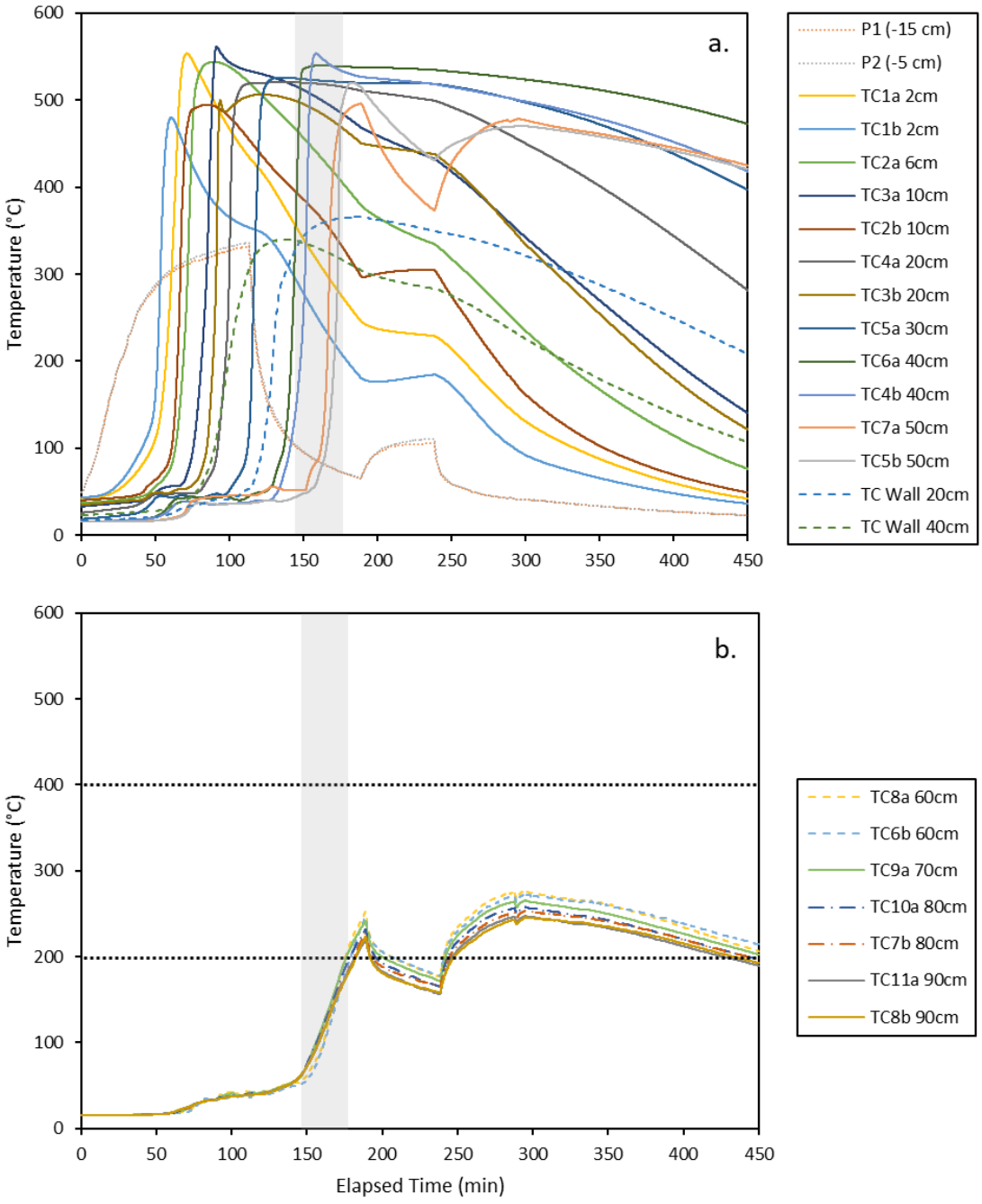

Figure C.2- 1: Temperature profiles for DRUM 1, a. presents the centreline (solid lines) and wall (broken line) temperatures within the fuel bed, and b. shows the emissions temperatures above the fuel bed. The sampling timing and duration is shown as a grey block.

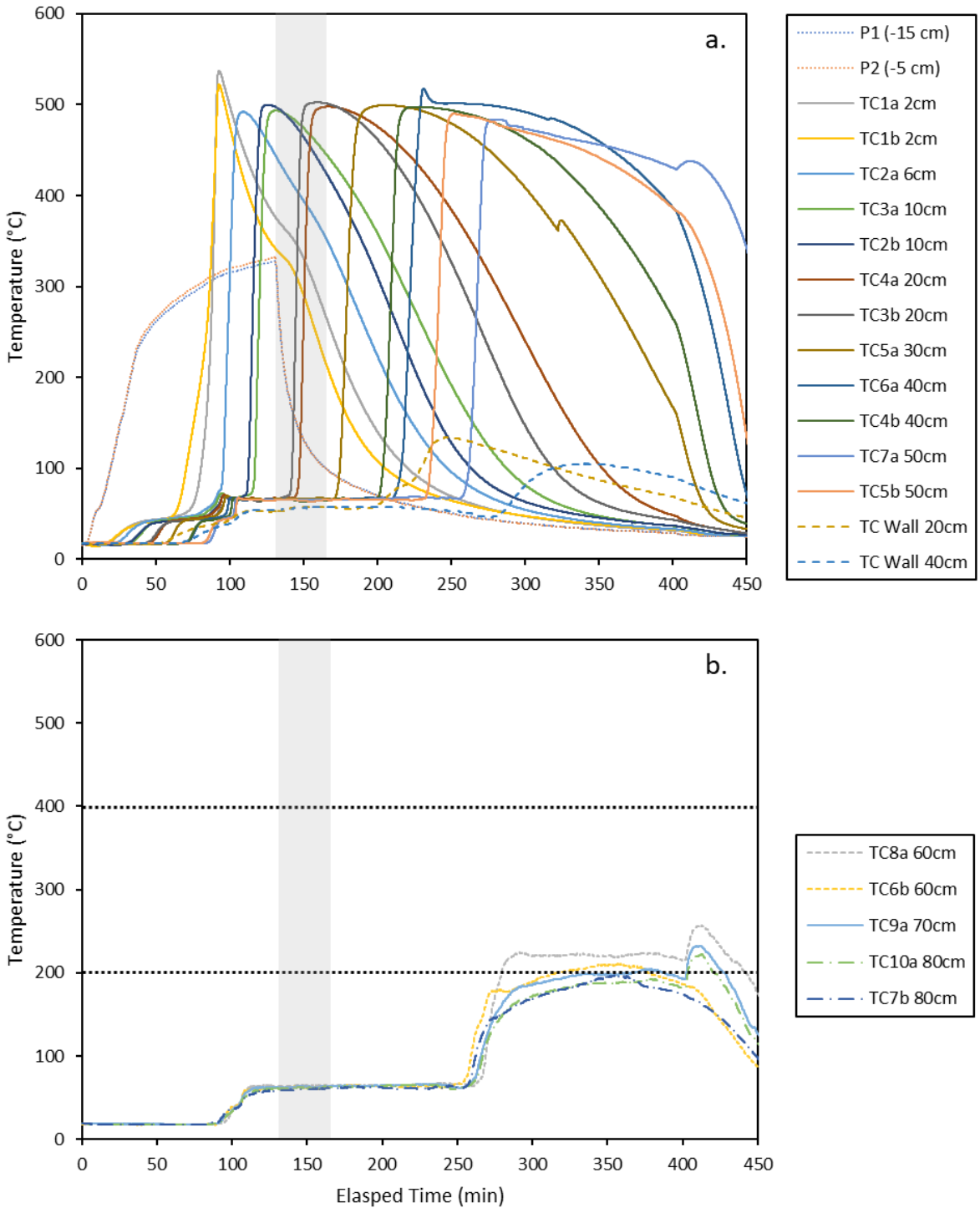

Figure C.2- 2: Temperature profiles for DRUM 2, a. presents the centreline (solid lines) and wall (broken line) temperatures within the fuel bed, and b. shows the emissions temperatures above the fuel bed. The sampling timing and duration is shown as a grey block.

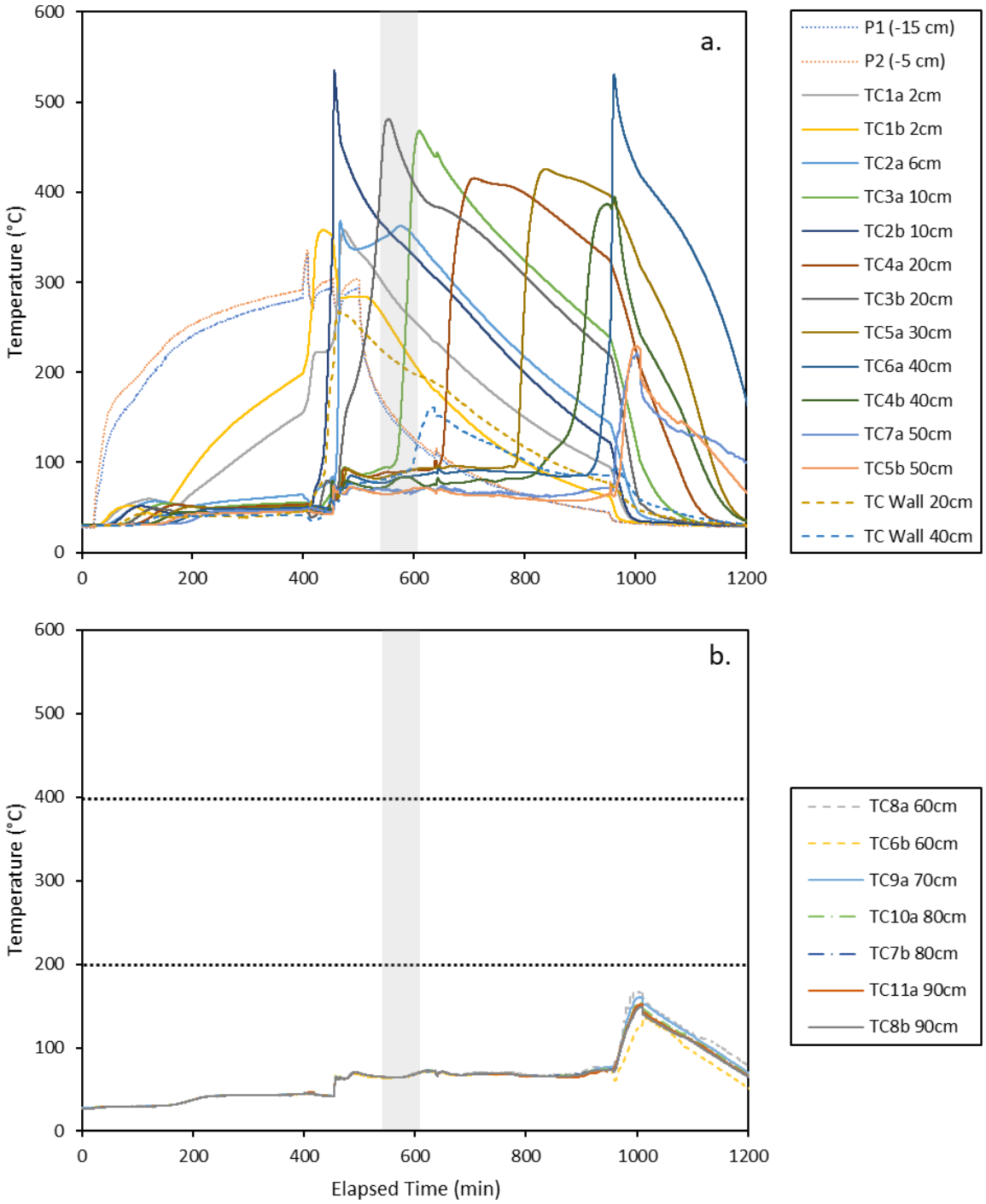

Figure C.2- 3: Temperature profiles for DRUM 3, a. presents the centreline (solid lines) and wall (broken line) temperatures within the fuel bed, and b. shows the emissions temperatures above the fuel bed. The sampling timing and duration is shown as a grey block. Air flux changes occurred at 397 (1.00 – 2.00 cm/s), 406 (2.00 – 3.00 cm/s), 415 (3.00 – 1.00 cm/s), 640 (1.00 – 0.00 cm/s), 642 (0.00 – 1.00 cm/s), 951 (1.00 – 3.00 cm/s), 1009 (3.00 – 5.01 cm/s) minutes.

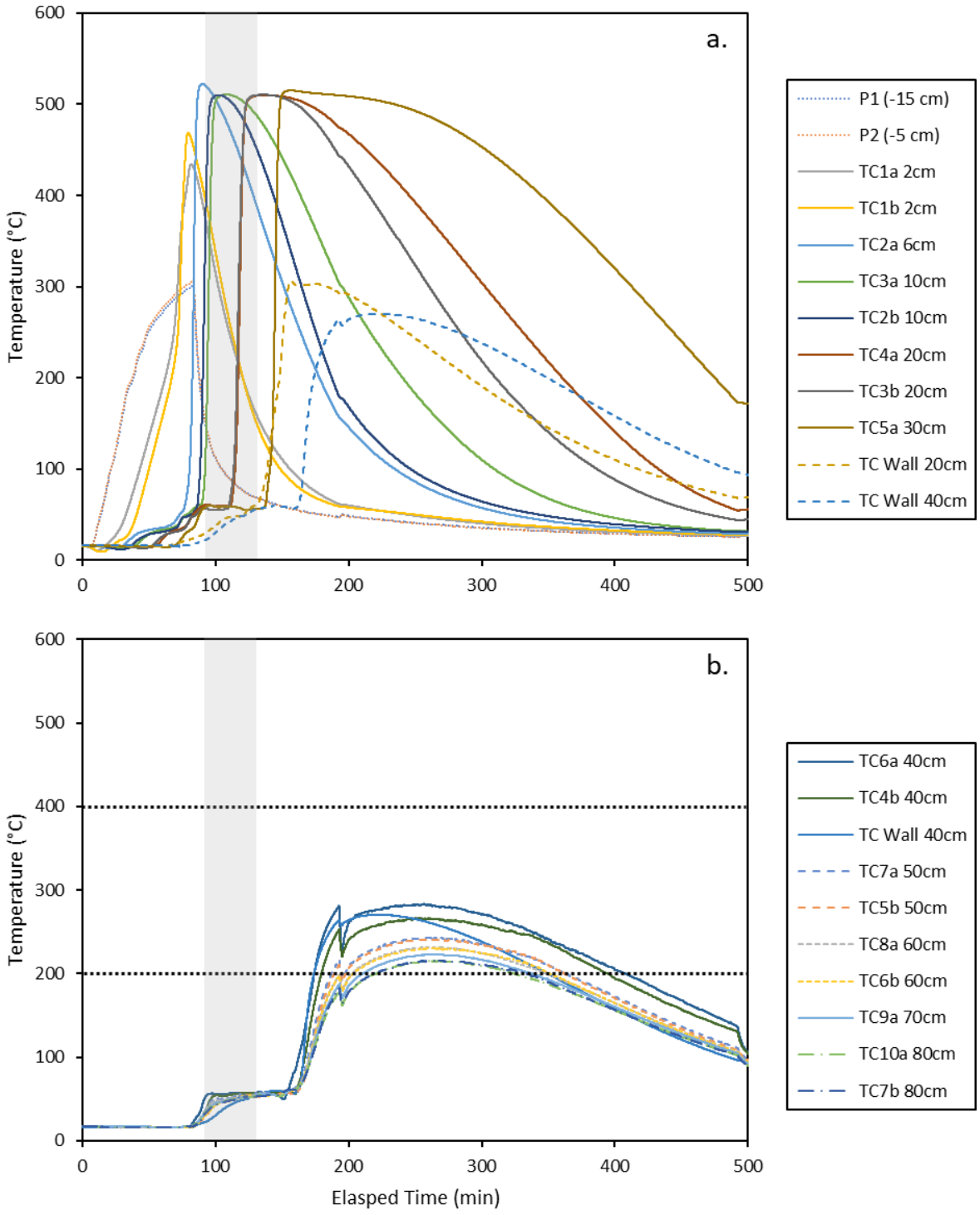

Figure C.2- 4: Temperature profiles for DRUM 4, a. presents the centreline (solid lines) and wall (broken line) temperatures within the fuel bed, and b. shows the emissions temperatures above the fuel bed. The sampling timing and duration is shown as a grey block.

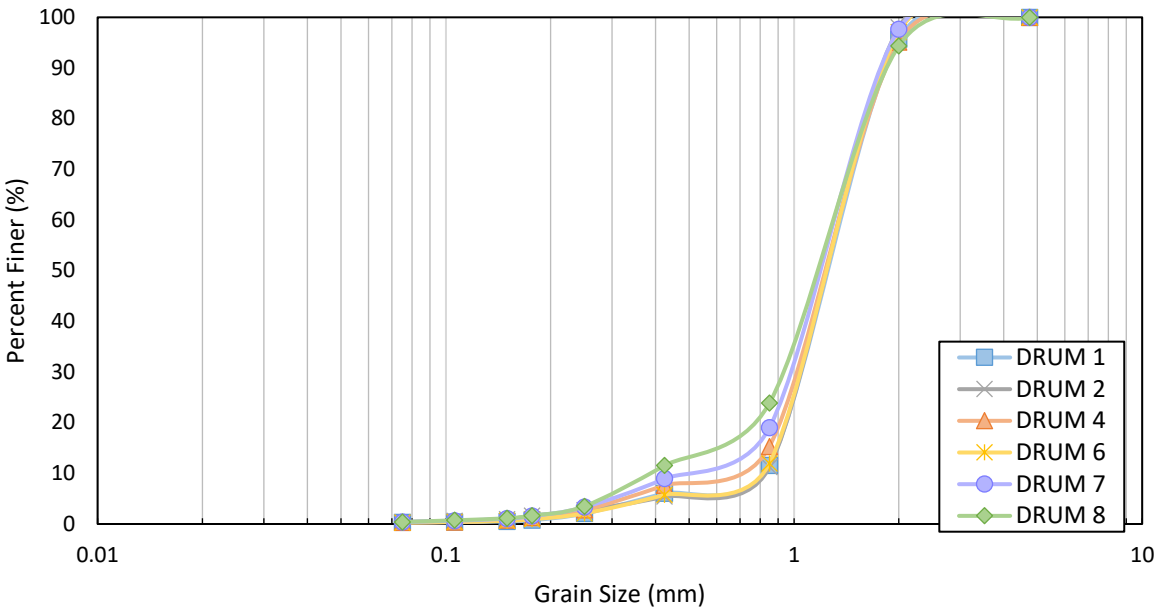

Figure C.2- 5: Sieve analysis of post-treatment ash and sand.

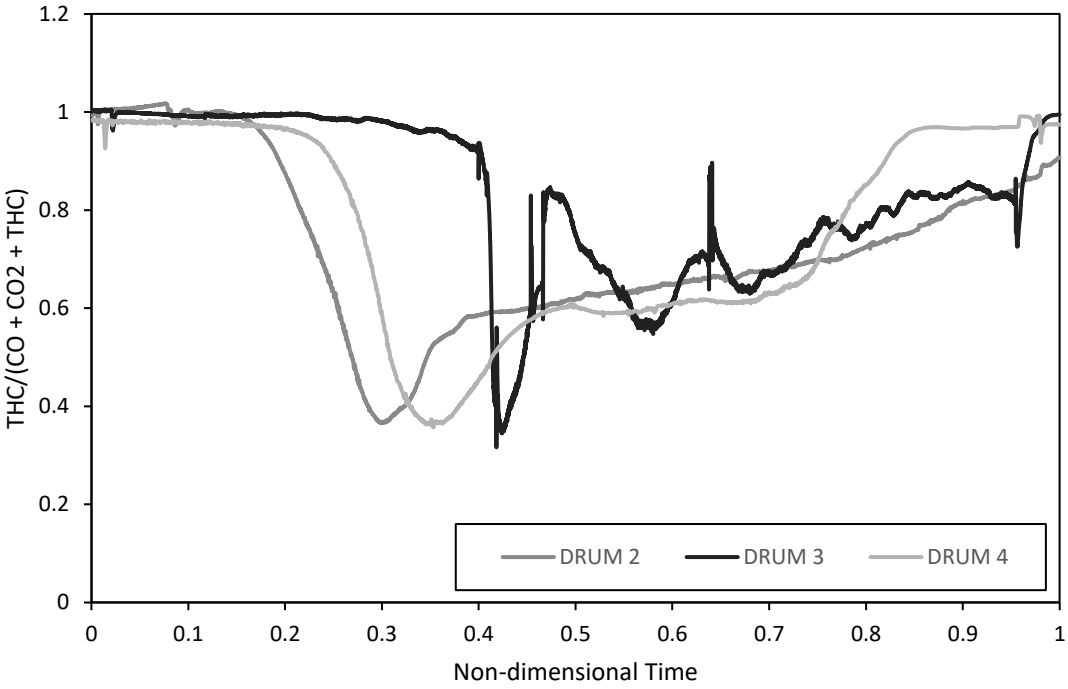

Figure C.2- 6: Total hydrocarbon release from the smouldering reactor during DRUM test 2, 3, and 4 which quantified PCDD/Fs in emissions. The total hydrocarbons were normalized to the sum of the combustion gases (i.e., carbon monoxide and carbon dioxide) and the total hydrocarbons and plotted against the test duration presented as non-dimensional time (defined in (Rashwan et al., 2021a)).

C.3: Supplementary Information on PCDD/F Results

The toxic equivalency quantities (TEQs) of the 17 most toxic PCDD/F congeners (i.e., the PCDD/Fs containing chlorine atoms in the 2,3,7,8 positions on the benzene rings) (Reiner, 2016) were approximated by multiplying the mass (in pg) by their toxic equivalency factors (TEFs) as outlined by WHO (2005) (see Table C.3-2). The sum of the congeners (in pg TEQ (ET)) was divided by the total emissions sample volume to provide an approximation of the absolute PCDD/F concentration per emissions volume (i.e., pg TEQ/m^3). Finally, to compare the emissions concentrations of PCDD/Fs to regulatory standards, the values were corrected to 11% oxygen content according to guidance from the Canadian Council of Ministers of the Environment (1989).

Table C.3- 1: PCDD/F sampling conditions from DRUM and LAB tests

Parameter	Units	Test						
		LAB			DRUM			
		1a	1b	2	1	2	3	4
Sampling Time [1]	min	18	21	61	31	33	58	34
Flow Rate [2]	m^3/min	0.0021	0.0020	0.0020	0.0019	0.0020	0.0026	0.0021
Sample Volume [3]	m^3	0.038	0.040	0.13	0.059	0.066	0.15	0.071
Oxygen content [4]	%	16.0	16.8	18.8	17.8	15.8	16.4	17
Oxygen correction factor [5]	-	2.0	2.4	4.7	3.2	1.9	2.2	2.5

[1] Measured from the time the pump was turned on, diverting air flow from the column through the PCDD/F sampling train, to the time the pump was turned off.
[2] Measured using a flow totalizer incorporated into the PCDD/F sampling train.
[3] Calculated as $(sampling\ time\ [min]) \times (flow\ rate\ [m^3/min])$
[4] Measured using a continuous gas analyzer for LAB tests and Landtec GEM2000 portable gas analyzer immediately after the sampling train for DRUM tests
[5] Calculated according to the Canadian Council of Ministers of the Environment (1989) equation: $Concentration\ (at\ 11\%\ O_2) = Concentration \times [(20.9 - 11.0)/(20.9 - (O_2)_{reference}$

Table C.3- 2: Summary of PCDD/F release in combustion gases from DRUM and LAB tests

Congener	TEF[1]	Mass of PCDD/F in combustion gases (pg)						
		LAB			DRUM			
		1a	1b	2	1	2	3	4
2378-TCDD	1	4	7	3	20	*BDL*[2]	*BDL*	17
12378-PeCDD	1	*BDL*	*BDL*	*BDL*	*BDL*	*BDL*	*BDL*	*BDL*
23478-PeCDF	0.3	*BDL*	*BDL*	*BDL*	*BDL*	*BDL*	*BDL*	*BDL*
123478-HxCDF	0.1	*BDL*	*BDL*	*BDL*	*BDL*	*BDL*	*BDL*	*BDL*
123678-HxCDF	0.1	*BDL*	*BDL*	*BDL*	*BDL*	*BDL*	*BDL*	*BDL*
234678-HxCDF	0.1	*BDL*	*BDL*	*BDL*	*BDL*	*BDL*	*BDL*	*BDL*
123789-HxCDF	0.1	*BDL*	*BDL*	*BDL*	*BDL*	*BDL*	*BDL*	*BDL*
2378-TCDF	0.1	*BDL*	*BDL*	*BDL*	*BDL*	*BDL*	*BDL*	11
123478-HxCDD	0.1	*BDL*	*BDL*	*BDL*	*BDL*	*BDL*	*BDL*	*BDL*
123678-HxCDD	0.1	*BDL*	*BDL*	*BDL*	*BDL*	*BDL*	*BDL*	41
123789-HxCDD	0.1	*BDL*	*BDL*	*BDL*	*BDL*	*BDL*	*BDL*	*BDL*
12378-PeCDF	0.03	*BDL*	*BDL*	*BDL*	*BDL*	*BDL*	*BDL*	*BDL*
1234678-HpCDF	0.01	*BDL*	*BDL*	*BDL*	*BDL*	*BDL*	*BDL*	2
1234789-HpCDF	0.01	7	*BDL*	*BDL*	*BDL*	*BDL*	*BDL*	25
1234678-HpCDD	0.01	*BDL*	*BDL*	*BDL*	*BDL*	*BDL*	*BDL*	13
OCDF	0.0003	28	34	19	64	*BDL*	*BDL*	120
OCDD	0.0003	85	90	183	116	*BDL*	*BDL*	281
Total Mass	pg	3101	3452	1605	3396	0	0	3384

[1] Toxic equivalency factors (USEPA, 2010)

[2] BDL is below the detection limit, detection limits are summarized in Table S3-3

Table C.3- 3: Summary of PCDD/F release in smouldering exhaust stack

Congener	TEF[1]	MDL [2] (pg/g)	QA/QC (pg)	Method spike (% rec)	Concentration of PCDD/F in exhaust stack (pg/m^3)			
					DRUM 3	DRUM 5	DRUM 9	DRUM 10
2378-TCDD	1	0.5	ND	102	*BDL* [3]	*BDL*	*BDL*	*BDL*
12378-PeCDD	1	2	0.8	107	*BDL*	*BDL*	*BDL*	*BDL*
23478-PeCDF	0.3	2	0.5	104	*BDL*	8	*BDL*	*BDL*
2378-TCDF	0.1	0.6	0.3	107	*BDL*	11	*BDL*	*BDL*
123478-HxCDF	0.1	3	0.4	110	*BDL*	*BDL*	*BDL*	*BDL*
123678-HxCDF	0.1	2	0.5	114	*BDL*	*BDL*	*BDL*	*BDL*
234678-HxCDF	0.1	3	0.7	113	*BDL*	*BDL*	*BDL*	*BDL*
123789-HxCDF	0.1	3	0.8	117	*BDL*	*BDL*	*BDL*	*BDL*
123478-HxCDD	0.1	2	0.5	104	*BDL*	*BDL*	*BDL*	*BDL*
123678-HxCDD	0.1	4	0.3	98	*BDL*	27	*BDL*	*BDL*
123789-HxCDD	0.1	3	0.2	102	*BDL*	*BDL*	*BDL*	*BDL*
12378-PeCDF	0.03	2	1.1	116	*BDL*	11	*BDL*	*BDL*
1234678-HpCDF	0.01	3	1.8	113	*BDL*	*BDL*	*BDL*	*BDL*
1234789-HpCDF	0.01	2	ND	118	*BDL*	14	*BDL*	*BDL*
1234678-HpCDD	0.01	2	0.8	110	*BDL*	15	*BDL*	*BDL*
OCDF	0.0003	5	0.8	113	*BDL*	10	*BDL*	*BDL*
OCDD	0.0003	5	2	103	*BDL*	30	*BDL*	*BDL*
Total Mass Concentration	pg / m³				0	125	0	0
Total TEQ Concentration	pg TEQ / m³				0	14.9	0	0
Oxygen content	%				--	19.8	--	--
Oxygen correction factor	-				--	9	--	--
TEQ Concentration (corrected to O_2)	pg TEQ / m³				0	61.1	0	0

[1] Toxic equivalency factors (USEPA, 2010)
[2] Method detection limits
[3] BDL is below the method detection limit

Table C.3- 4: PCDD/F concentrations in post-treatment smouldered ash from DRUM 1

Congener	TEF[1]	PCDD/F Concentration in Post-Treatment Ash from DRUM 1				
		Repeat (1)		Repeat (2)		Average
		Concentration[2] (pg/g)	Qualifier[3]	Concentration[2] (pg/g)	Qualifier[3]	Concentration[2] (pg/g)
2378-TCDD	1	<0.47	[U]	<0.58	[U]	*BDL*
12378-PeCDD	1	<0.68	[U]	<0.87	[U]	*BDL*
23478-PeCDF	0.3	<0.45	[U]	<0.74	[U]	*BDL*
2378-TCDF	0.1	<0.45	[U]	<0.63	[U]	*BDL*
123478-HxCDF	0.1	<0.49	[M,U]	<0.59	[U]	*BDL*
123678-HxCDF	0.1	<0.56	[U]	<0.67	[U]	*BDL*
234678-HxCDF	0.1	<0.42	[U]	<0.58	[U]	*BDL*
123789-HxCDF	0.1	<0.59	[M,U]	<0.82	[M,U]	*BDL*
123478-HxCDD	0.1	<0.35	[U]	<0.55	[U]	*BDL*
123678-HxCDD	0.1	<0.36	[U]	<0.53	[U]	*BDL*
123789-HxCDD	0.1	<0.36	[U]	<0.56	[U]	*BDL*
12378-PeCDF	0.03	<0.55	[M,U]	<1.0	[U]	*BDL*
1234678-HpCDF	0.01	<0.31	[M,J,R]	<0.49	[U]	*BDL*
1234789-HpCDF	0.01	<0.27	[U]	<0.61	[U]	*BDL*
1234678-HpCDD	0.01	1.28	[M,J]	1.26	[M,J]	1.27
OCDF	0.0003	0.474	[M,J]	<1.2	[U]	0.237
OCDD	0.0003	6.02	[J]	4.16	[M,J]	5.09

[1] Toxic equivalency factors (USEPA, 2010)
[2] Ash samples were analyzed externally by ALS Life Sciences lab in London, ON
[3] Qualifiers identified by ALS Life Sciences
[U] The analyte was not detected above the EDL.
[M] A peak has been manually integrated.
[J] The analyte was detected below the calibrated range but above the EDL.
[R] The ion abundance ratio(s) did not meet the acceptance criteria. Value is an estimated maximum.

C.4: Normalization Derivation

Nomenclature

Latin Letters

A_C	Cross sectional area, m^2
Ash	Ash content, %
m/m	Mass ratio, -
$\dot{m}$	Mass flux, kg s^{-1}
m_{em}	Mass of emissions sample, pg
M_{air}	Molar mass of air, kg mol^{-1}
MC	Moisture content, %
P	Pressure, Pa
R	Universal gas constant, m^3 Pa mol^{-1} K^{-1}
T	Temperature, K
$\vec{v}$	Air flow velocity, m s^{-1}
$\vec{v}_{oxid}$	Smouldering propagation velocity, m s^{-1}
$\dot{V}$	Volumetric air flux, m^3 s^{-1}
V_{em}	Volume of emissions sample, m^3

Greek Symbols

ρ	Density, kg m^{-3}

Subscripts

$bulk$	Volume averaged
des	Destroyed fuel
dry	Dry fuel
$fuel$	Fuel
in	Into the reactor
NTP	Conditions at normal temperature and pressure
out	Out of the reactor

Mass Out:

The mass flux out of the reactor is calculated to be a conservatively high estimate of the PCDD/Fs leaving the system. If all sewage sludge is destroyed during smouldering, we assume a high amount of PCDD/Fs leaving the system. Therefore, the mass flux out of the system is assumed to be the sum of the mass flux into the reactor and the dry mass destroyed during smouldering, given in Equation (C.4-1):

$$\dot{m}_{out}\left[\frac{kg}{s}\right] = \dot{m}_{in}\left[\frac{kg}{s}\right] + \dot{m}_{des}\left[\frac{kg}{s}\right] \qquad (C.4-1)$$

Airflow Volume Flux:

The airflow volume flux of the system is the product of the air flux and the reactor area. The size of the reactor varies from a radius of 0.3 m at the DRUM scale, to 0.15 m at the LAB scale. For the volume flux into the reactor, the air flux is based on the air flow rate into the base of the column, given in Equation (C.4-2):

$$\dot{V}_{in}\left[\frac{m^3}{s}\right] = \vec{v}\left[\frac{m}{s}\right] \cdot A_C[m^2] \qquad (C.4-2)$$

The mass destroyed is related to the total mass lost per time. Therefore, the airflow volume flux is a function of the smouldering front propagation velocity upwards through the reactor, given in Equation (C.4-3):

$$\dot{V}_{des}\left[\frac{m^3}{s}\right] = \vec{v}_{oxid}\left[\frac{m}{s}\right] \cdot A_C[m^2] \qquad (C.4-3)$$

Mass In:

The ideal gas law was used to determine the mass flux into the system, given in Equation (C.4-4):

$$\dot{m}_{in}\left[\frac{kg}{s}\right] = \frac{\dot{V}_{in}\left[\frac{m^3}{s}\right] P_{NTP}[Pa]}{R\left[\frac{m^3 \cdot Pa}{mol \cdot K}\right] \cdot T_{NTP}[K]} \cdot \left(M_{air}\left[\frac{kg}{mol}\right]\right) \qquad (C.4-4)$$

The airflow into the reactor was assumed to be at normal temperature and pressure conditions. The molar mass of air was used to convert the ideal gas law constant from a molarity to a mass.

Substituting Equation (C.4-2) into Equation (C.4-4) gives an equation for the mass flux into the reactor in terms of the airflow rate into the reactor and the area of the column, given by Equation (C.4-5):

$$\dot{m}_{in}\left[\frac{kg}{s}\right] = \frac{\vec{v}\left[\frac{m}{s}\right] \cdot A_C[m^2] \cdot P_{NTP}[Pa]}{R\left[\frac{m^3 \cdot Pa}{mol \cdot K}\right] \cdot T_{NTP}[K]} \cdot \left(M_{air}\left[\frac{kg}{mol}\right]\right) \qquad (C.4-5)$$

Dry Bulk Density:

The bulk density of each fuel mixture was determined for each test. Since the moisture content of the sewage sludge varied for each test, the bulk density was converted to dry bulk density to account for the difference and is given in Equation (C.4-6):

$$\rho_{dry\ bulk}\left[\frac{kg}{m^3}\right] = \frac{\rho_{bulk}\left[\frac{kg}{m^3}\right]}{\left(1 + \frac{m_w}{m_s}\right)} = \frac{\rho_{bulk}\left[\frac{kg}{m^3}\right]}{\left(1 + \frac{MC_{fuel}\,[\%]}{100\%}\right)} \qquad (C.4-6)$$

Dry Mass Destroyed:

The dry mass destroyed is a function of the rate that the smouldering front moves up the column and the dry bulk density of the fuel, given in Equation (C.4-7):

$$\dot{m}_{des}\left[\frac{kg}{s}\right] = \dot{V}_{des}\left[\frac{m^3}{s}\right] \cdot \rho_{dry\ bulk}\left[\frac{kg}{m^3}\right] \qquad (C.4-7)$$

Substituting Equation (C.4-3) and Equation (C.4-7) into Equation (C.4-8) gives an equation for the dry mass destroyed in terms of the smouldering velocity, area of the reactor, bulk density and moisture content of the fuel, given by Equation (C.4-8):

$$\dot{m}_{des}\left[\frac{kg}{s}\right] = \vec{v}_{oxid}\left[\frac{m}{s}\right] \cdot A_C[m^2] \cdot \frac{\rho_{bulk}\left[\frac{kg}{m^3}\right]}{\left(1 + \frac{MC_{fuel}\,[\%]}{100\%}\right)} \qquad (C.4-8)$$

Considering Sand-to-Sludge Ratio and Ash Content:

The dry bulk density of the fuel considers the mixture of silica sand with sewage sludge. Since only the sewage sludge is destroyed during smouldering, the mass destroyed should be normalized to the sewage sludge content by considering the sand-to-sludge ratio (on a dry mass basis) for each test. Furthermore, since not all the sewage sludge is destroyed during smouldering, i.e., some amount of ash remains, the dry mass destroyed should also be normalized to the ash content of the sewage sludge. Equation (C.4-8) can therefore be rewritten to include the sand-to-sludge ratio, and the ash content of the sewage sludge, given in Equation (C.4-9):

$$\dot{m}_{des}\left[\frac{kg}{s}\right] = \vec{v}_{oxid}\left[\frac{m}{s}\right] \cdot (A_C)[m^2] \cdot \frac{\rho_{bulk}\left[\frac{kg}{m^3}\right]}{\left(1 + \frac{MC_{Fuel}\ [\%]}{100\%}\right)} \cdot \left(m/m\left[\frac{kg}{kg}\right]\right)_{dry} \cdot \left(\frac{Ash_{fuel}[\%]}{100\%}\right) (C.4-9)$$

Volume Out of Reactor:

The air volume flux out of the reactor can be determined by rearranging the ideal gas law, given by Equation (C.4-10):

$$\dot{V}_{out}\left[\frac{m^3}{s}\right] = \frac{\dot{m}_{out}\left[\frac{kg}{s}\right] \cdot R\ \left[\frac{m^3 \cdot Pa}{mol \cdot K}\right] \cdot T_{out}\ [K]}{P_{out}[Pa]} \cdot \left(\frac{1}{M_{air}}\left[\frac{mol}{kg}\right]\right) \qquad (C.4-10)$$

The temperature of emissions leaving the column is taken from the highest thermocouple measurement within the column, above the fuel pack i.e., the closest thermocouple to the PCDD/F sampling train. An average temperature is used. The pressure of the emissions is corrected to the temperature leaving the column. Again, the molar mass of air is used to convert the ideal gas constant from a molarity to mass.

Normalized Dioxin and Furan Measurement:

Finally, the PCDD/F sample collected from the emissions leaving the reactor can be scaled to approximate the total mass of PCDD/Fs released from smouldering sewage sludge. The mass quantity of PCDD/Fs in the emissions, $m_{PCDD/F}$ [pg], were quantified per volume of emissions sample, $V_{PCDD/F}$ [m^3], for each test. Multiplying this concentration by the volume flux out of the reactor provides an approximation of the PCDD/Fs released from the system, given by Equation (C.4-11):

$$\dot{m}_{em,Total}\left[\frac{pg}{s}\right] = \frac{m_{em}\,[pg]}{\dot{V}_{em}\,[m^3]} \cdot \dot{V}_{out}\left[\frac{m^3}{s}\right] \qquad (C.4-11)$$

The PCDD/F flux can then be normalized to the dry mass destroyed during smouldering to approximate the mass of PCDD/Fs leaving the system per mass of dry sludge, given in Equation (C.4-12):

$$m_{em,Total}\left[\frac{pg}{kg_{dry\ fuel}}\right] = \frac{m_{em}\,[pg]}{\dot{V}_{em}\,[m^3]} \cdot \frac{\dot{V}_{out}\left[\frac{m^3}{s}\right]}{\dot{m}_{des}\left[\frac{kg}{s}\right]} \qquad (C.4-12)$$

C.5: Supplementary Information on Greenway Pollution Control Plant, London, ON

Table C.5- 1: Summary of element releases in emissions from Greenway's incinerator stack

Annual sludge processing [1]	(tonnes) [2]	67734		
		Element		
	Units	Cd	Pb	Zn
Average elemental concentration [3]	(mg element/ kg sludge)	1.1	103	579
Annual Elemental Loading [3]	(kg / year)	75	6977	39218
Incinerator stack releases [4]	(kg / year)	9	76	2700
Post-treatment ash disposals [4]	(kg / year)	19	346	6000
Total element in emissions [4]	(kg / year)	28	422	8700
Percent Elemental Release in Emissions [5]	(%)	**38%**	**6%**	**22%**

[1] Greenway WWTP Annual 2018 Report (London, 2019a)
[2] On a wet mass basis
[3] Calculated as the product of the average elemental concentration and annual sludge processed
[4] NPRI 2018 Report (London, 2019b), note that these quantities are all below the CCME ECA requirements for releases from the incinerator exhaust stack
[5] Calculated as the quotient of the annual elemental loading and total elemental content in emissions

Table C.5- 2: Sample qualifiers and descriptions (ALS Greenway Report, 2018)

Qualifier	Description
J, R	The analyte was detected below the calibrated range but above the EDL, and the ion abundance ratio(s) did not meet the acceptance criteria. Value is an estimated maximum.
M	A peak has been manually integrated.
M, J	A peak has been manually integrated, and the analyte was detected below the calibrated range but above the EDL.
M, J, R	A peak has been manually integrated, and the analyte was detected below the calibrated range but above the EDL, and the ion abundance ratio(s) did not meet the acceptance criteria. Value is an estimated maximum.
R	The ion abundance ratio(s) did not meet the acceptance criteria. Value is an estimated maximum.
[J]	The analyte was detected below the calibrated range but above the EDL.
[U]	The analyte was not detected above the EDL.

Table C.5- 3: Summary of PCDD/Fs at Greenway Pollution Control Plant, London, ON

Congener	TEF[1]	Cake Sludge		Incinerator Ash		Stack Emissions	
		Concentration [2] (pg/g)	Qualifier [3]	Concentration [4] (pg/g)	Qualifier [3]	Concentration [5] (pg TEQ/m^3)	Qualifier [3]
2378-TCDD	1	<1.1	[U]	<0.24	[U]	<0.062	[U]
12378-PeCDD	1	1.1	M, J, R	<0.14	[U]	<0.071	[U]
23478-PeCDF	0.3	0.94	[J]	<0.061	[U]	0.028	--
2378-TCDF	0.1	1.4	M, J	<0.20	[U]	<0.19	[U]
123478-HxCDF	0.1	<0.82	[U]	0.094	M, J, R	<0.040	[U]
123678-HxCDF	0.1	1.2	J, R	0.082	M, J	<0.037	[U]
234678-HxCDF	0.1	<1.0	[U]	0.201	M, J, B	0.045	--
123789-HxCDF	0.1	1.3	M, J, R	<0.064	[U]	0.0041	--
123478-HxCDD	0.1	0.46	J, R	<0.10	[U]	<0.11	[U]
123678-HxCDD	0.1	1.6	J, R	<0.10	[U]	<0.044	[U]
123789-HxCDD	0.1	1	M, J, R	<0.10	[U]	0.025	--
12378-PeCDF	0.03	0.86	[J]	<0.069	[U]	<0.23	[U]
1234678-HpCDF	0.01	9.7	R	0.26	M, J, R	<0.072	[U]
1234789-HpCDF	0.01	<1.9	[U]	<0.10	[U]	<0.023	[U]
1234678-HpCDD	0.01	46.5	M	0.37	M, J	<0.0054	[U]
OCDF	0.0003	27.3	--	0.621	[J]	<0.23	[U]
OCDD	0.0003	555	--	1.47	[J]	<0.00063	[U]

[1] Toxic equivalency factors (USEPA, 2010)
[2] ALS Greenway Report (2013)
[3] For qualifier descriptions see Table S5
[4] ALS Greenway Report (2018)
[5] Greenway Ortech Report (2018), note that these values are averages from 3 exhaust stack emissions samples, and the sum is well below the Canadian Council of Ministers of the Environment (CCME) ECA requirement of 80 pg TEQ/m^3 (corrected to 11% O_2).

Appendix D: Supplementary Material for “Smouldering to Treat PFAS in Sewage Sludge”

D.1: Preliminary PFAS Analysis

Table D.1- 1: Preliminary PFAS Analysis on Sewage Sludge Collected between 2018-2019

PFAS Concentration (ng/g)	Test			
	1 [a]	2 [a, b]	3 [c]	4 [d]
PFBA	1580 ± 862	553 ± 37.1	1060 ± 641	1940 ± 160
PFPeA	3320 ± 282	2390 ± 507	1720 ± 578	2310 ± 5.43
PFBS	*B.Q.L.*	*B.Q.L.*	*B.Q.L.*	*B.Q.L.*
PFHxA	1110 ± 73.1	657 ± 14.0	882 ± 429	863 ± 60.0
PFHpA	6190 ± 1580	3450 ± 1140	3420 ± 568	5720 ± 234
PFOA	*B.D.L.*	*B.D.L.*	*B.D.L.*	*B.D.L.*
PFHxS	*B.D.L.*	*B.D.L.*	*B.D.L.*	*B.D.L.*
PFNA	*B.D.L.*	*B.D.L.*	*B.D.L.*	*B.D.L.*
PFDA	*B.D.L.*	*B.D.L.*	*B.D.L.*	*B.D.L.*
PFOS	1590 ± 638	449 ± 224	458 ± 229	*B.D.L.*
PFUnA	*B.D.L.*	*B.D.L.*	*B.D.L.*	*B.D.L.*
PFDoA	*B.D.L.*	*B.D.L.*	*B.D.L.*	*B.D.L.*
PFOSA	*B.D.L.*	*B.D.L.*	*B.D.L.*	*B.D.L.*

[a] Sludge had a MC of 3.23%, ash content of 26.7%, and was collected in February, 2018
[b] Secondary batch of sludge
[c] Sludge had a MC of 72.3%, ash content of 26.9%, and was collected in May, 2018
[d] Sludge had a MC of 74.4%, ash content of 24.8%, and was collected in June, 2018

D.2: Supplemental Information on Smouldering Experiments

Table D.2- 1: Additional experimental data and results from LAB scale Phase I & II

	Experimental Conditions					Results			
	Moisture Content					Average Peak Temperature			
Experiment	After drying (%)	After rehydrating (%)	Sand/ Sludge (g/g)	GAC Concentration (g GAC/ kg sand)	CaO Added (g CaO/ kg sand)	Centreline (°C)	Half Radius (°C)	Sand Cap (°C)	Air Phase (°C)
PHASE I: LAB Base case									
I-1	<1	-	6.5 [a]	-	-	856 ± 34	805 ± 67	499 ± 63	186 ± 10
I-2	<1	-	6.5 [a]	-	-	737 ± 37	818 ± 34	- [c]	175 ± 10
I-3	<1	-	6.5 [a]	-	-	831 ± 41	877 ± 37	562 ± 60	181 ± 17
PHASE II: LAB High MC and Amendments									
II-1-1	<1	75	4.5 [b]	20	-	746 ± 21	573 ± 89	434 ± 13	151 ± 13
II-1-2	<1	75	4.5 [b]	30	-	905 ± 21	749 ± 89	521 ± 24	210 ± 3
II-2-1	<1	-	6.5 [a]	-	5	818 ± 57	721 ± 48	550 ± 6	235 ± 36
II-2-2	<1	-	6.5 [a]	-	10	824 ± 54	741 ± 72	661 ± 62	263 ± 55

[a] Measured on a dry-mass basis

[b] Measured on a wet-mass basis

[c] No thermocouples were present in the sand cap during this test

Emissions Sampling Train: Leak Test Procedure

Both the PFAS and HF emissions sampling trains were leak tested prior to each experiment and contribution of ambient air to the system was minimized to <5%. To do this, nitrogen was injected through one sampling train at a time and the emissions exiting were analyzed using a CEMS. A vacuum pump (DOA-P704-AA, Gast) pulled nitrogen through the system at ~3 L/min. The system ran for several minutes to allow the emissions reading to stabilize. An oxygen measurement of <1% is ideal, however, due to complexities of the emissions sampling train, a measurement of <5% was deemed acceptable and the test would proceed as planned. If a measurement >5% was obtained, each joint of the sampling train would be cleaned, greased, and resecured and the leak test would be repeated.

Temperature Profiles

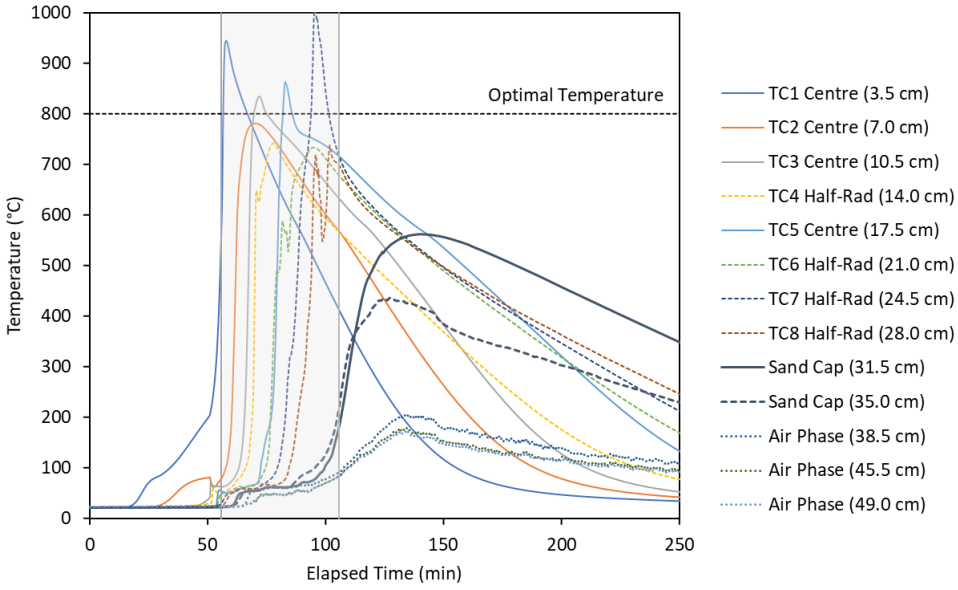

Figure D.2- 1: Test I-1, the first of 3 base case tests where dried sludge was mixed with sand at a ratio of 6.5:1 sand:dried sludge. The sampling period from 56 – 106 min is shaded in grey. The lower temperature range for significant PFAS degradation is shown as a dotted line.

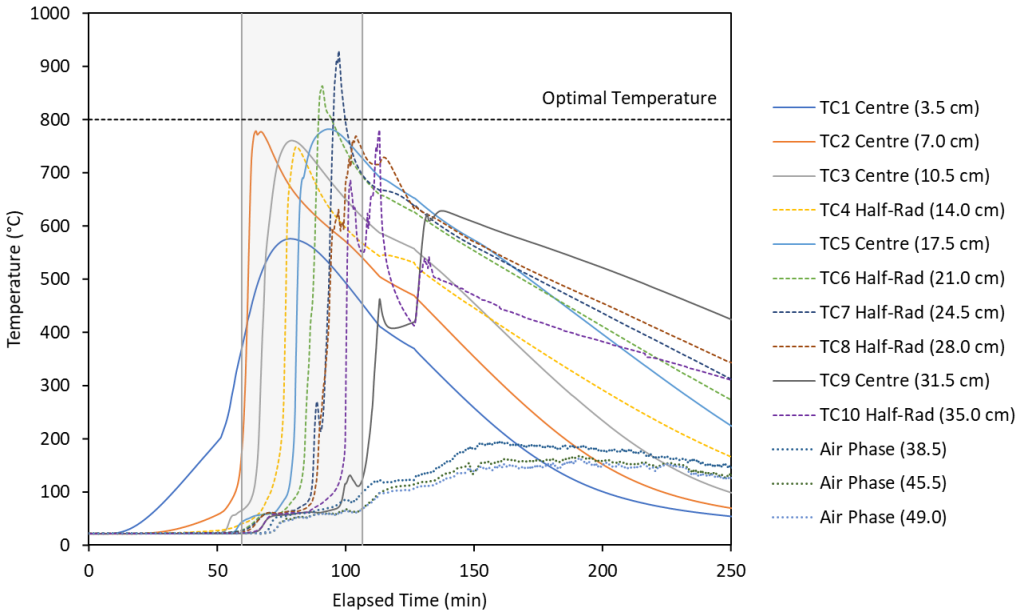

Figure D.2- 2: Test I-2, the second of 3 base case tests where dried sludge was mixed with sand at a ratio of 6.5:1 sand:dried sludge. The sampling period from 60 – 107 min is shaded in grey. The lower temperature range for significant PFAS degradation is shown as a dotted line.

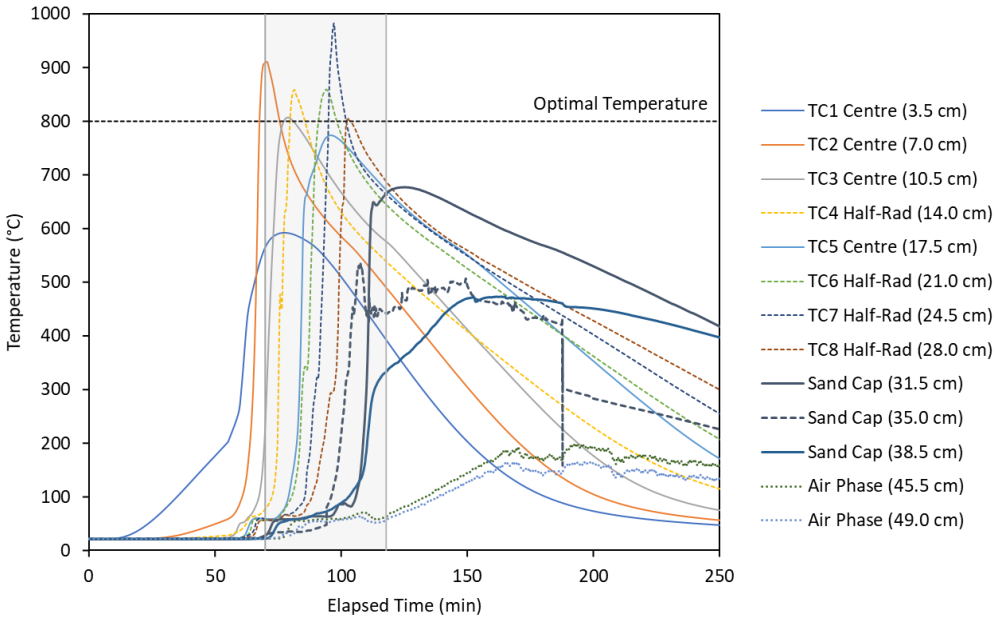

Figure D.2- 3: Test I-3, the third of 3 base case tests where dried sludge was mixed with sand at a ratio of 6.5:1 sand:dried sludge. The sampling period from 70 – 118 min is shaded in grey. The lower temperature range for significant PFAS degradation is shown as a dotted line.

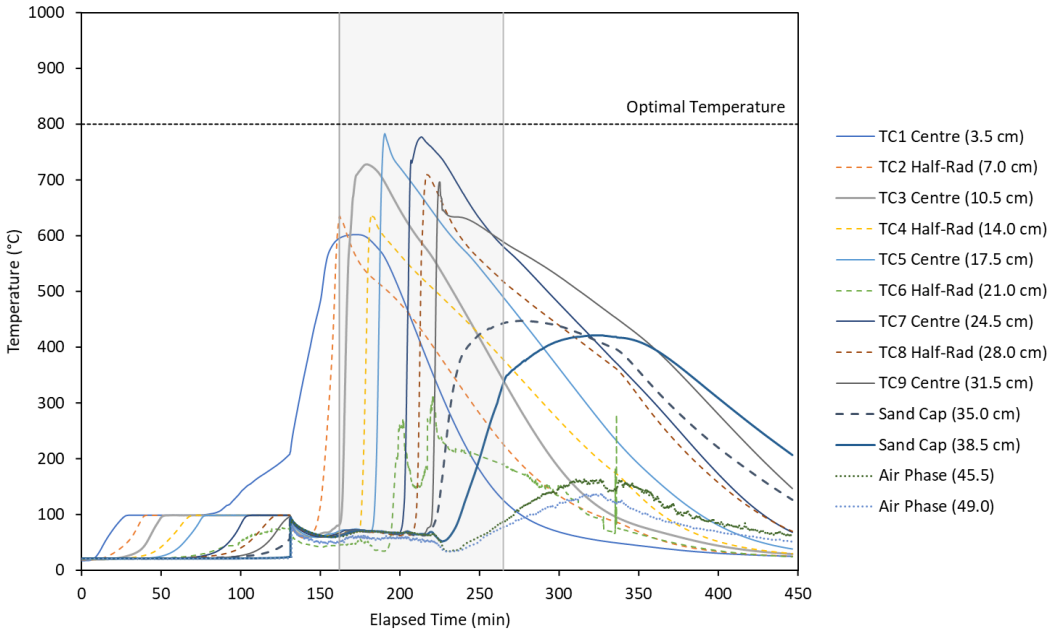

Figure D.2- 4: Test II-1-1, the first high MC content (75%) smouldering test where 20 g GAC / kg sand was added to supplement the fuel. The sampling period from 162 – 265 min is shaded in grey. The lower temperature range for significant PFAS degradation is shown as a dotted line.

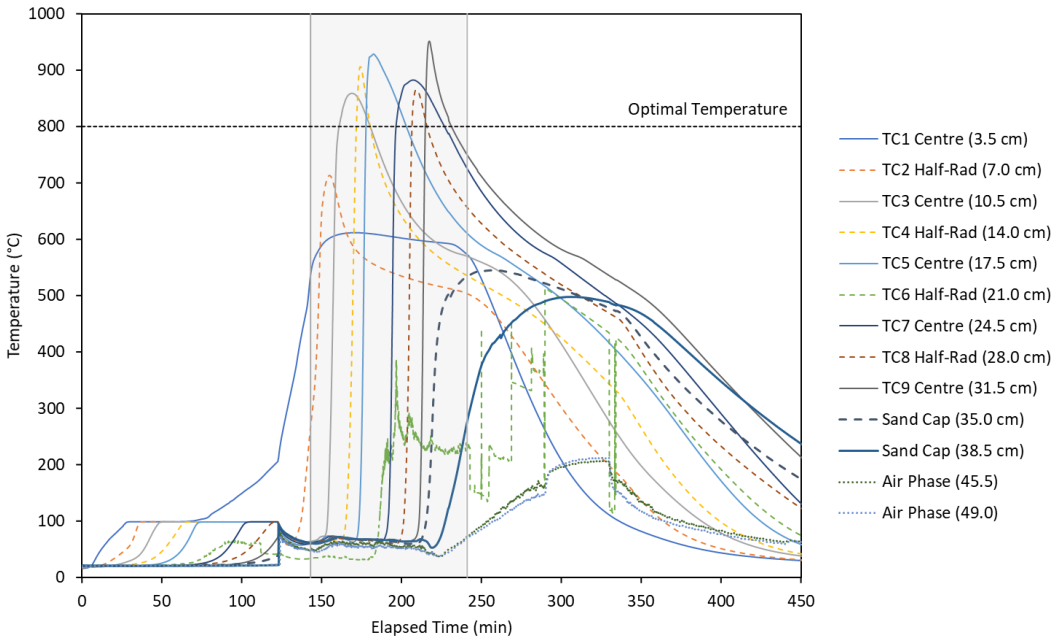

Figure D.2- 5: Test II-1-2, the second high MC content (75%) smouldering test where 30 g GAC / kg sand was added to supplement the fuel. The sampling period from 143 – 241 min is shaded in grey. The lower temperature range for significant PFAS degradation is shown as a dotted line.

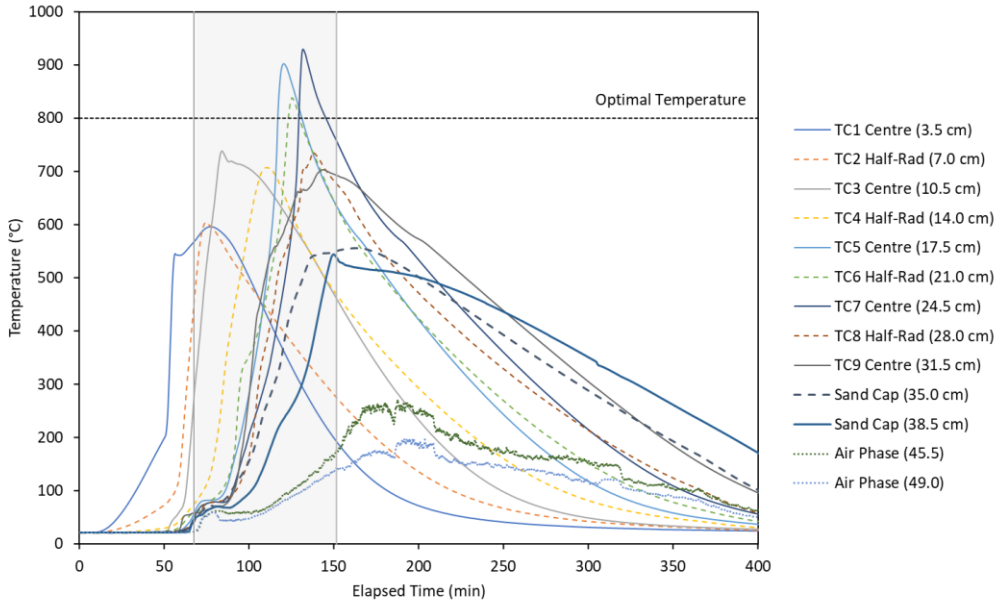

Figure D.2- 6: Test II-2-1, the first CaO test where 5 g CaO / kg sand was combined with dried sludge and sand at a ratio of 6.5:1 sand:dried sludge. The sampling period from 68 – 152 min is shaded in grey. The lower temperature range for significant PFAS degradation is shown as a dotted line.

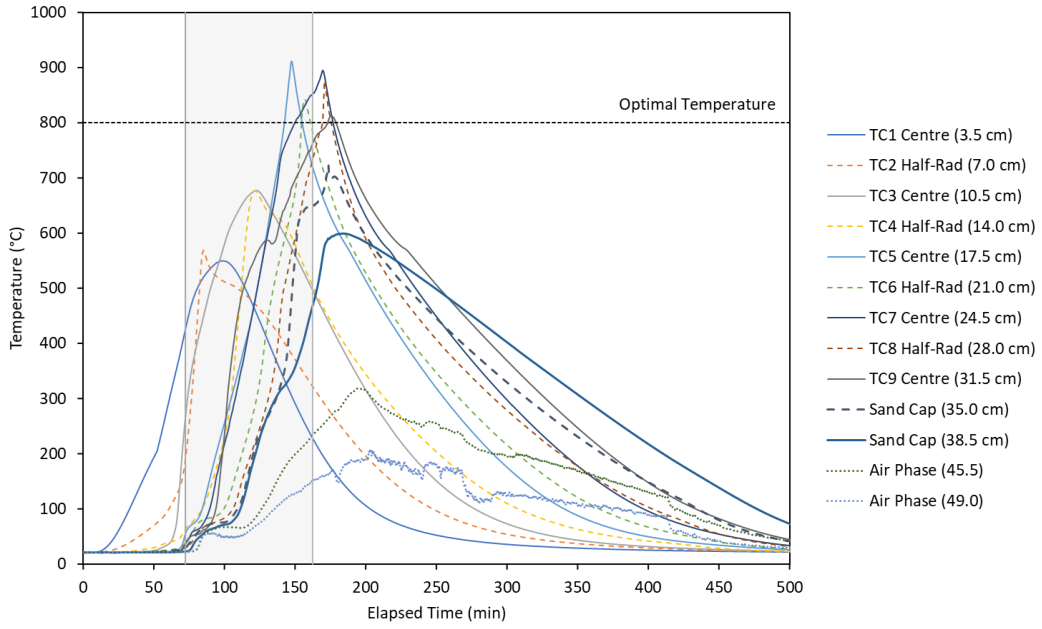

Figure D.2- 7: Test II-2-2, the second CaO test where 10 g CaO / kg sand was combined with dried sludge and sand at a ratio of 6.5:1 sand:dried sludge. The sampling period from 72 – 162 min is shaded in grey. The lower temperature range for significant PFAS degradation is shown as a dotted line.

Heating Rates

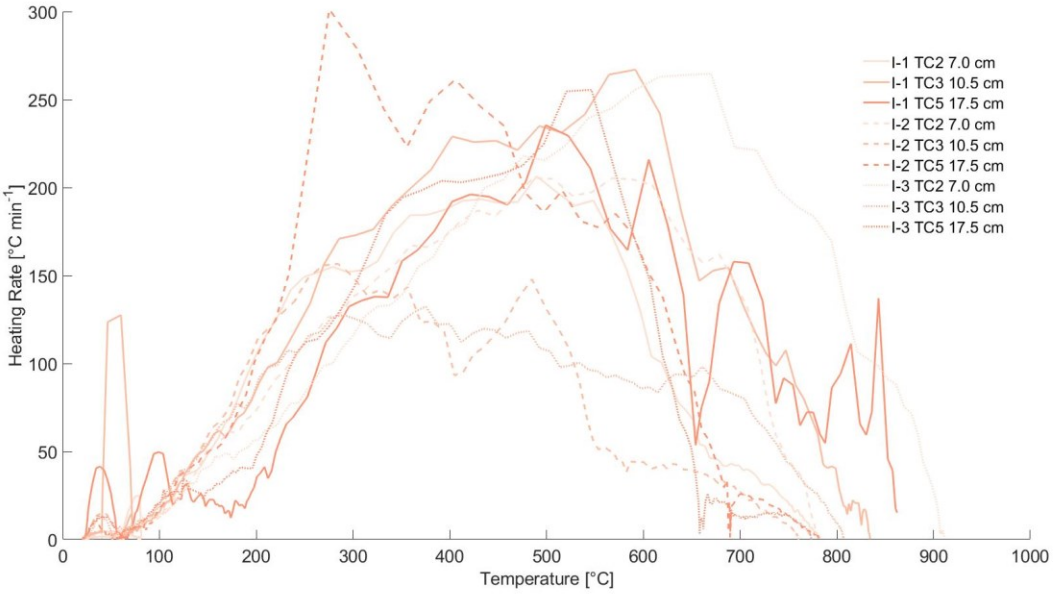

Figure D.2- 8: Heating rates as a function of temperature for the base case tests. I-1 is presented as a solid line, I-2 as a dashed line, and I-3 as a dotted line. Only the centreline thermocouples within the fuel bed have been included.

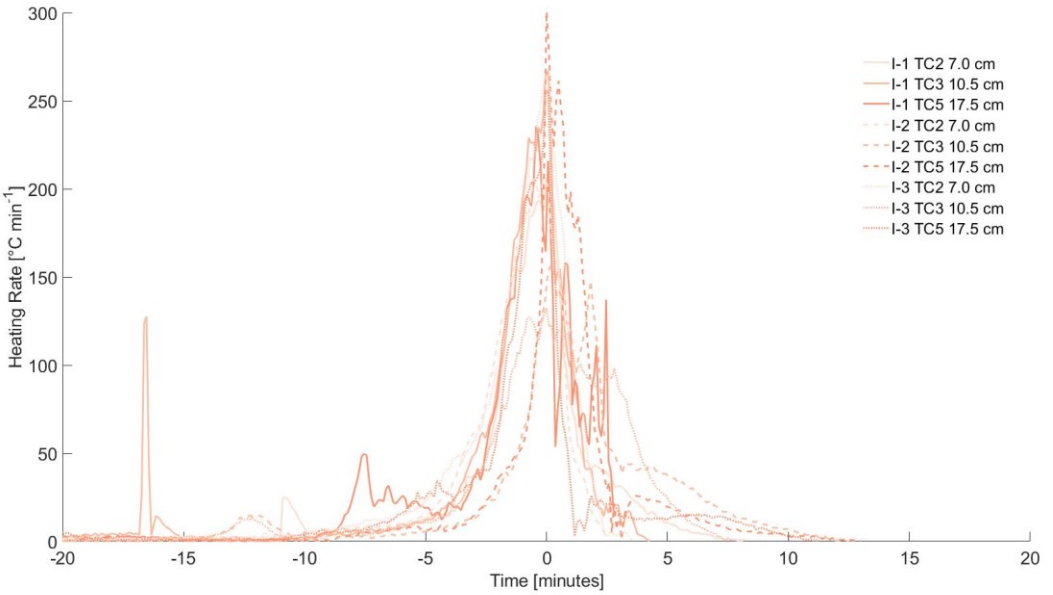

Figure D.2- 9: Heating rates as a function of normalized time for the base case tests. I-1 is presented as a solid line, I-2 as a dashed line, and I-3 as a dotted line. Only the centreline thermocouples within the fuel bed have been included.

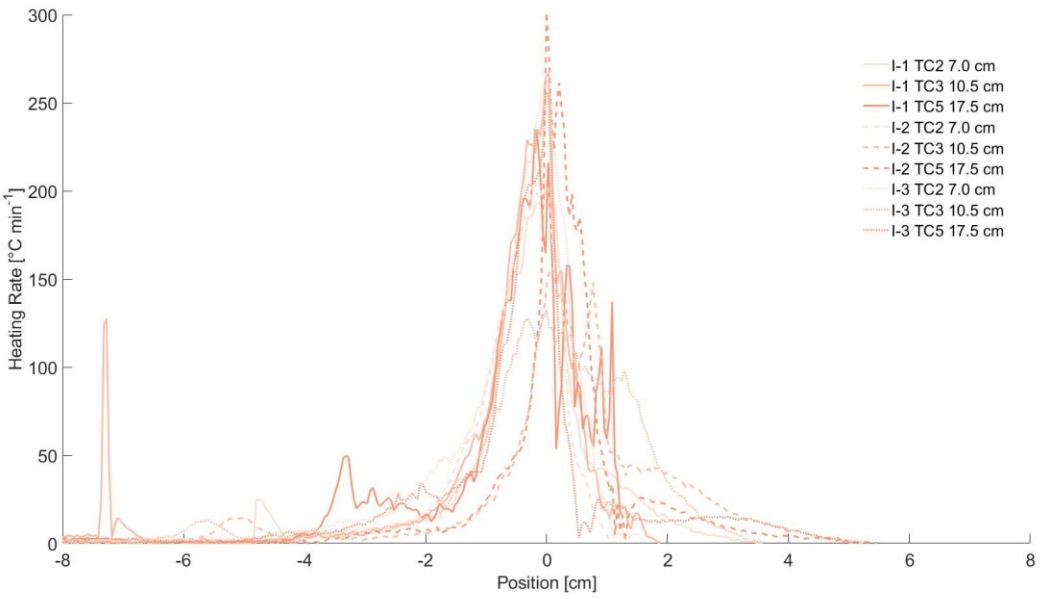

Figure D.2- 10: Heating rates as a function of normalized position in the reactor for the base case tests. I-1 is presented as a solid line, I-2 as a dashed line, and I-3 as a dotted line. Only the centreline thermocouples within the fuel bed have been included.

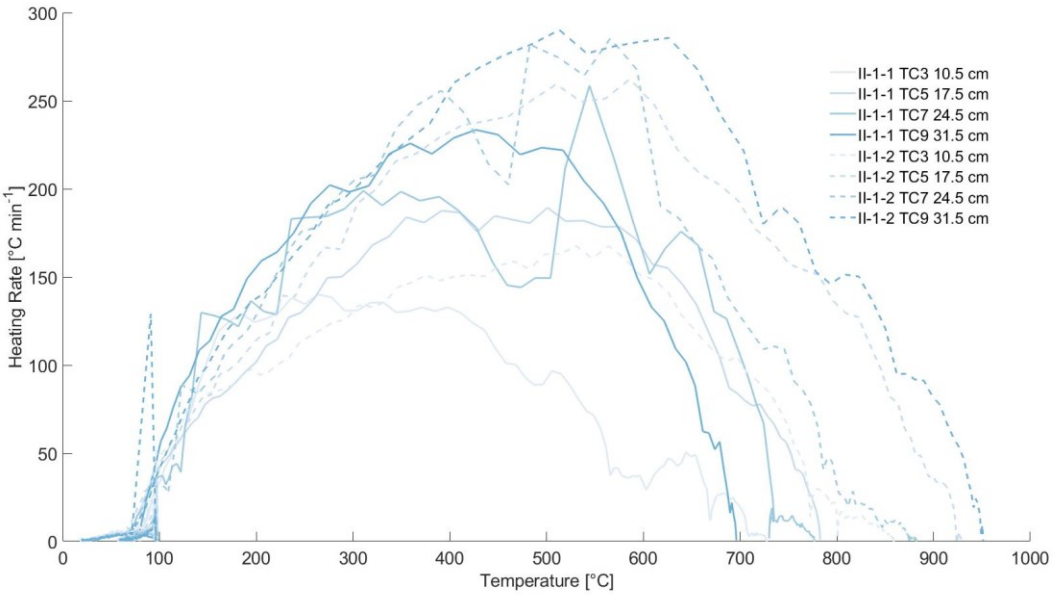

Figure D.2- 11: Heating rates as a function of temperature for the high MC (75%) and GAC tests. II-1-1 (20 g GAC/kg sand) is presented as a solid line, and II-1-2 (30 g GAC/kg sand) as a dashed line. Only the centreline thermocouples within the fuel bed have been included.

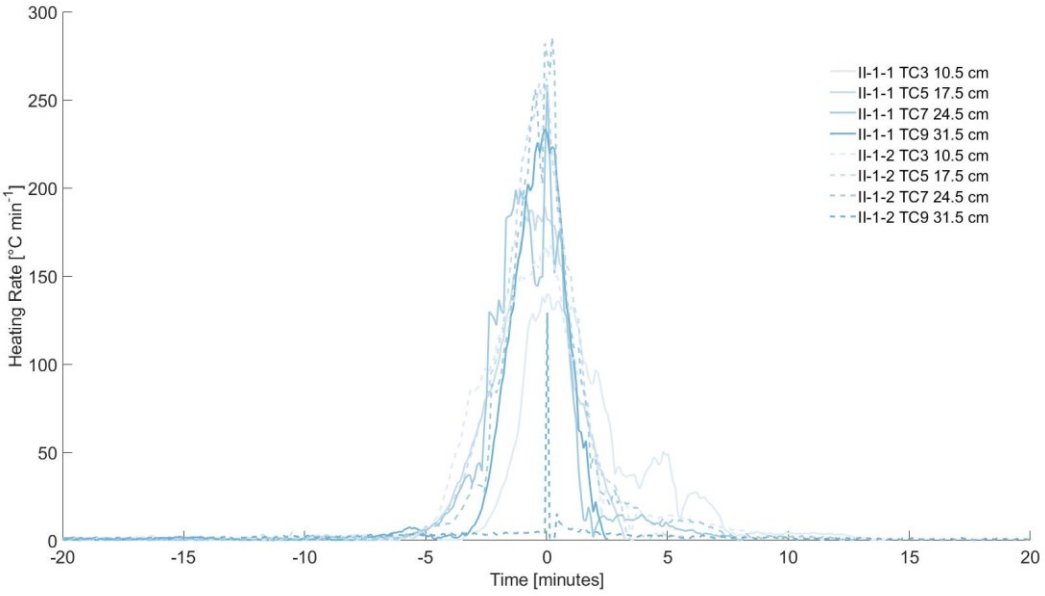

Figure D.2- 12: Heating rates as a function of normalized time for the high MC (75%) and GAC tests. II-1-1 (20 g GAC/kg sand) is presented as a solid line, and II-1-2 (30 g GAC/kg sand) as a dashed line. Only the centreline thermocouples within the fuel bed have been included.

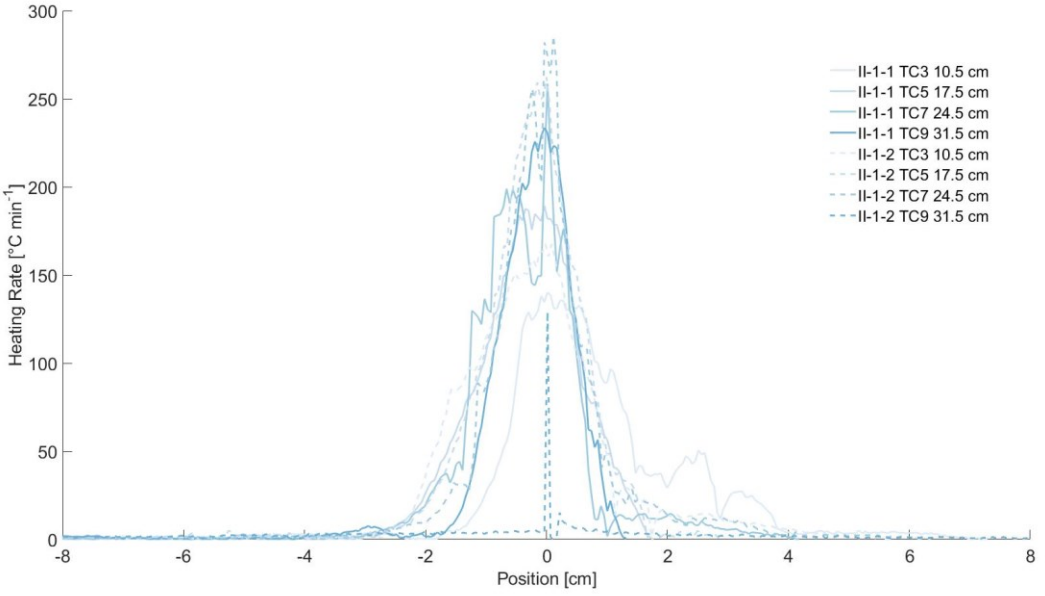

Figure D.2- 13: Heating rates as a function of normalized position in the reactor for the high MC (75%) and GAC tests. II-1-1 (20 g GAC/kg sand) is presented as a solid line, and II-1-2 (30 g GAC/kg sand) as a dashed line. Only the centreline thermocouples within the fuel bed have been included.

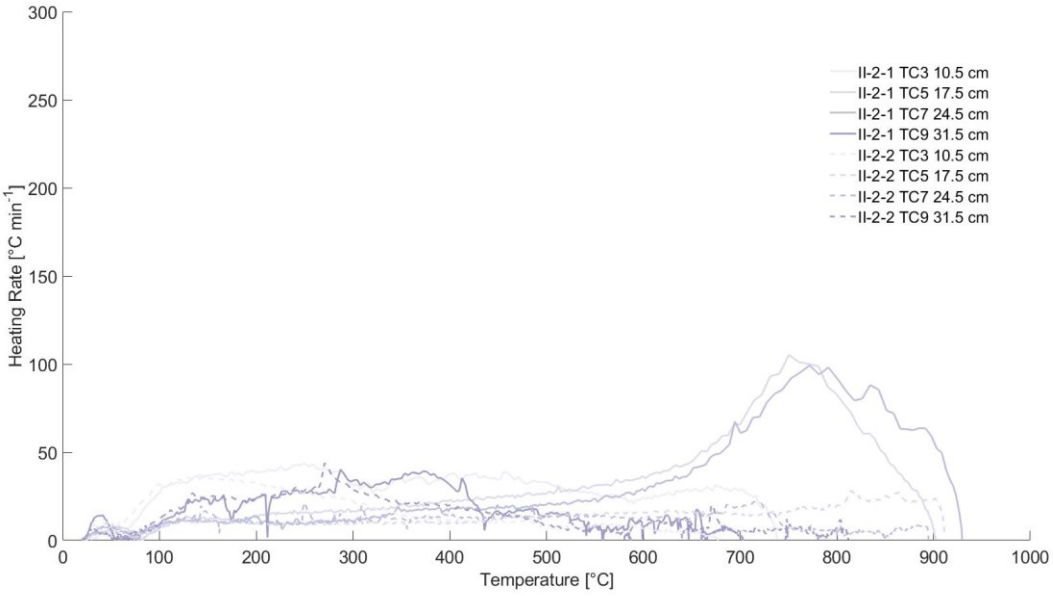

Figure D.2- 14: Heating rates as a function of temperature for the CaO tests. II-2-1 (5 g CaO/kg sand) is presented as a solid line, and II-2-2 (10 g CaO/kg sand) as a dashed line. Only the centreline thermocouples within the fuel bed have been included.

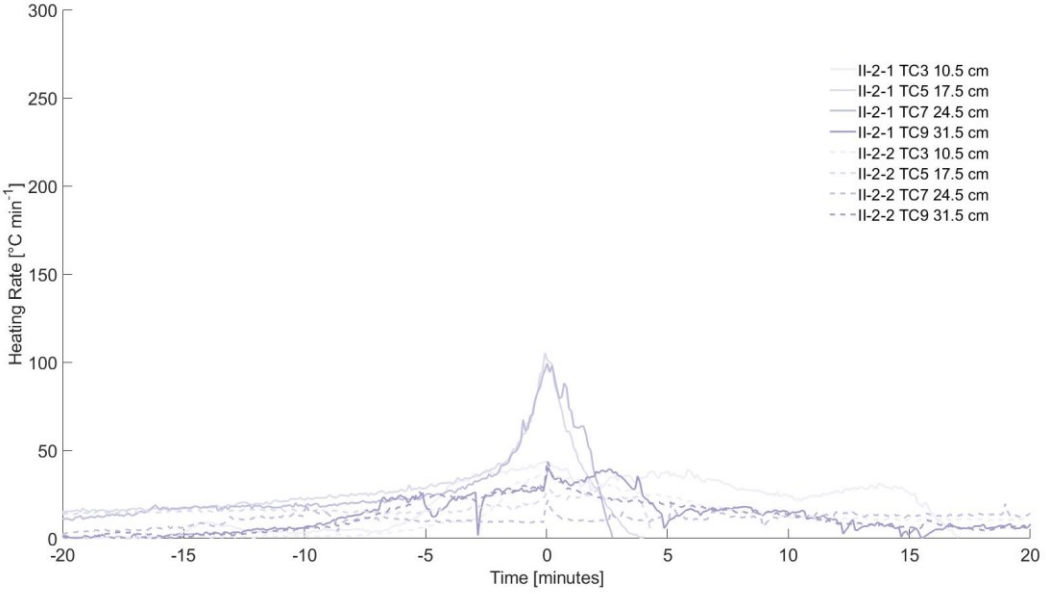

Figure D.2- 15: Heating rates as a function of normalized time for the CaO tests. II-2-1 (5 g CaO/kg sand) is presented as a solid line, and II-2-2 (10 g CaO/kg sand) as a dashed line. Only the centreline thermocouples within the fuel bed have been included.

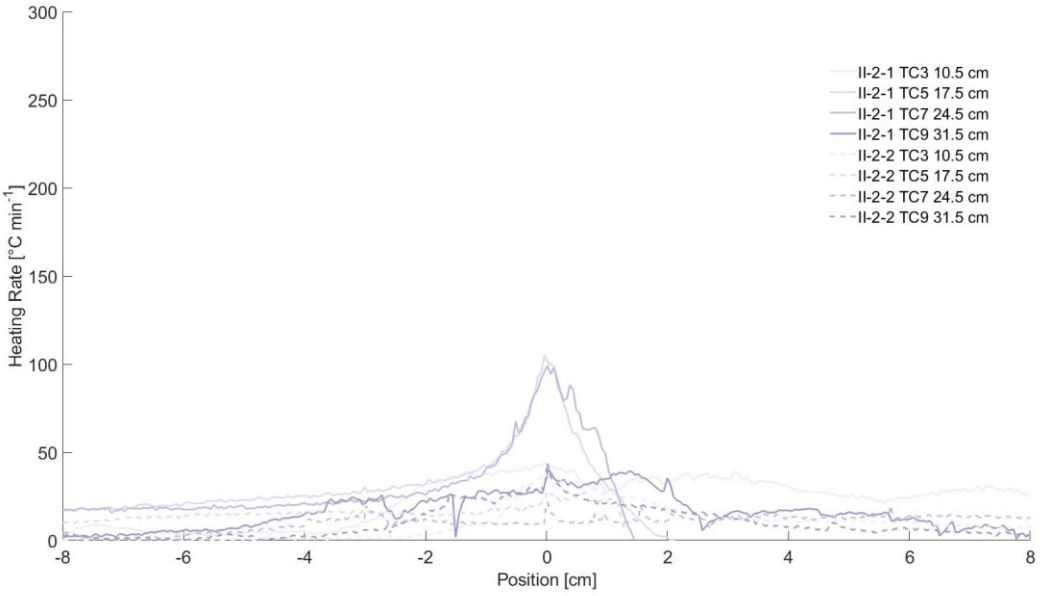

Figure D.2- 16: Heating rates as a function of normalized position in the reactor for the CaO tests. II-2-1 (5 g CaO/kg sand) is presented as a solid line, and II-2-2 (10 g CaO/kg sand) as a dashed line. Only the centreline thermocouples within the fuel bed have been included.

Post-Treatment Ash and Sand

Figure D.2-17 shows the post-treatment samples from following the smouldering treatment of sewage sludge. The top sand cap (~38 – 48 cm from reactor base) was initially clean sand added to lower the temperature of the emissions exiting the column. During sludge smouldering, bio-oil volatilized during sludge heating and recondensed in the top sand cap. As the smouldering front exited the column, the bio-oil was pyrolyzed (Figure D.2-17a.). The post-treatment materials in the top of the fuel bed (~27 – 31 cm from reactor base), and the bottom of the fuel bed (~13 – 20 cm from reactor base) were very similar with sewage sludge ash (~20% ash content) surrounded by silica sand (Figure D.2-17a./b.). The silica sand used in all tests was conserved during smouldering.

Figure D.2- 17: Experimental photos of the post-treatment ash and sand from base case I-1 from three locations within the reactor, a. the top sand cap, b. the middle of the fuel bed, and c. the bottom of the fuel bed.

D.3: Supplementary Information on Drum Reactor Experiments

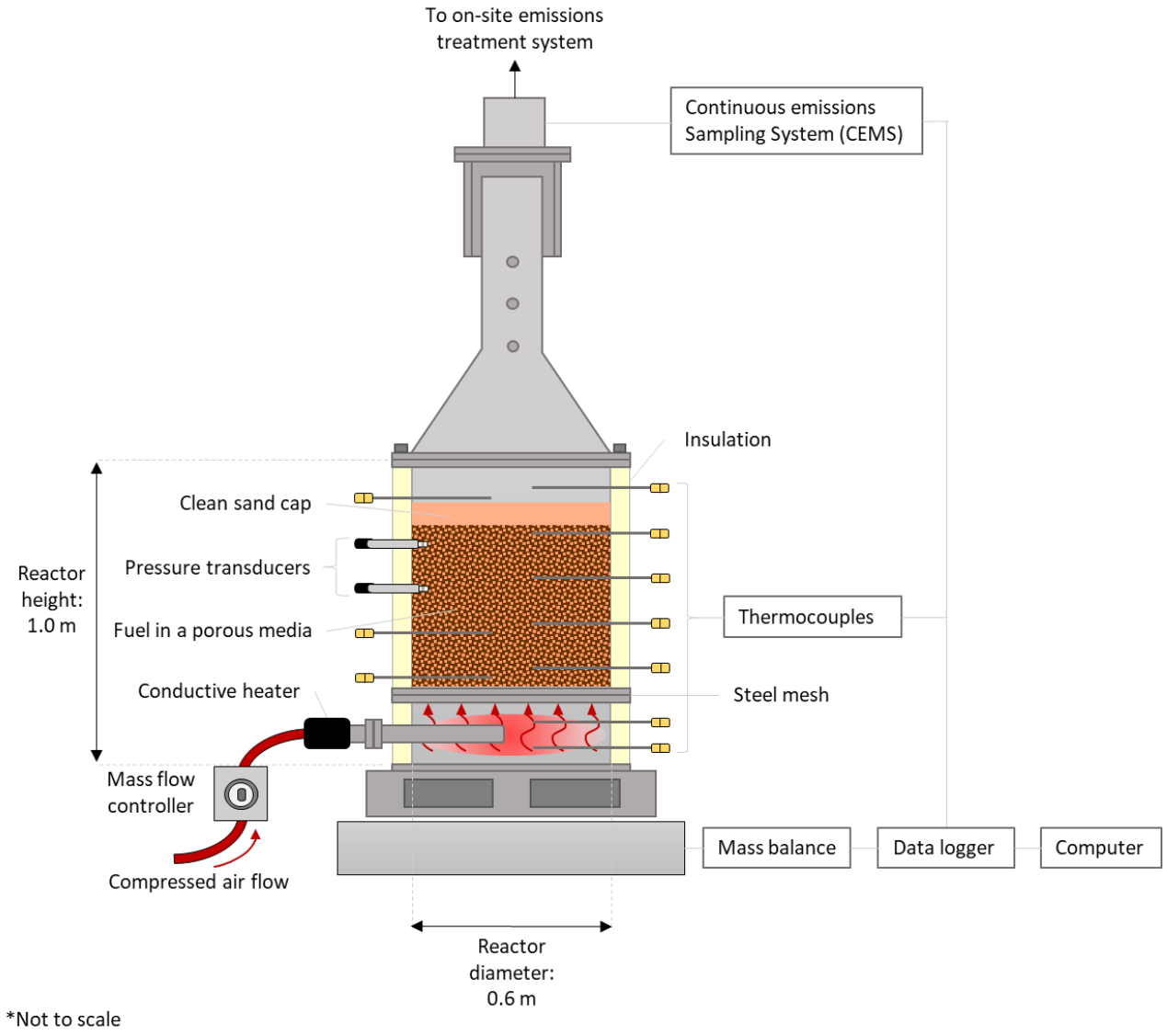

Figure D.3- 1: Schematic of smouldering reactor set-up.

Experimental Set-up and Procedure: DRUM Reactor

The experimental set-up for the DRUM tests is shown in Figure D.3-1. The ignition procedure is described below. Air – operated using a mass flux controller (8290B045PDB67 ASCO Numatics) – was injected into the base of the DRUM reactor from the beginning of the test. With the air on, the base of the reactor was then heated via a convective heater (F074736 36 kW SureHeat® MAX, Osram Sylvania) until ignition occurred. Ignition was confirmed the first thermocouple in the contaminant pack peaked (i.e., 0.06 m up the column in the DRUM experiments). Following ignition, the heater was turned off and the air flow was maintained to support self-sustaining smouldering. The end of each experiment was identified when the smouldering front reached the end of the contaminant pack in the reactor. Continuous emissions monitoring systems (CEMS) measured methane, carbon dioxide, carbon monoxide, and total hydrocarbons from the DRUM tests every five seconds (ABB Ltd.).

The emissions exiting the DRUM reactors were passed through an onsite treatment system prior to release from a stack. The custom treatment system (Newterra Ltd.) consisted of two granular activated carbon vessels (with 820 and 75 kg of material in each vessel), followed by an impregnated potassium permanganate vessel (with 150 kg of material).

Representative samples, ~19 – 100L per DRUM test, of the post-treatment material (i.e., ash mixed with silica sand) were collected in 19 L buckets. These large sample volumes aimed to capture the heterogeneities throughout the reactor.

Temperature Profiles

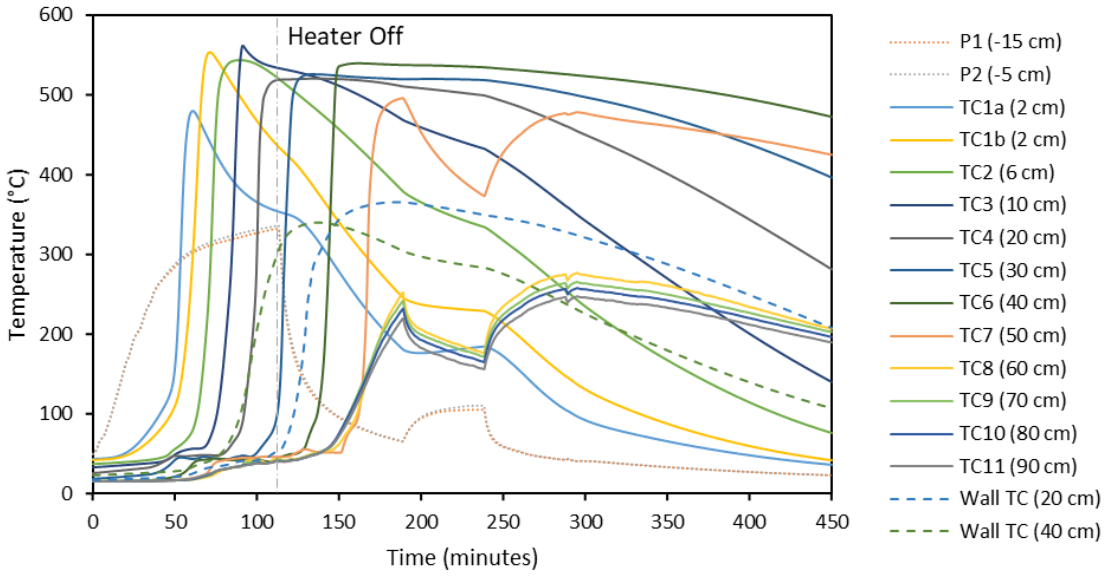

Figure D.3- 2: Temperature profile for Test III-1, a self-sustaining smouldering experiment with a 3.81% moisture content sludge in a fixed bed with 25.5 g/g sand/sludge mass ratio. Plenum, centreline, and wall thermocouples are presented. Note the air flux was changed at 190, 238, 288, 290, and 296 minutes.

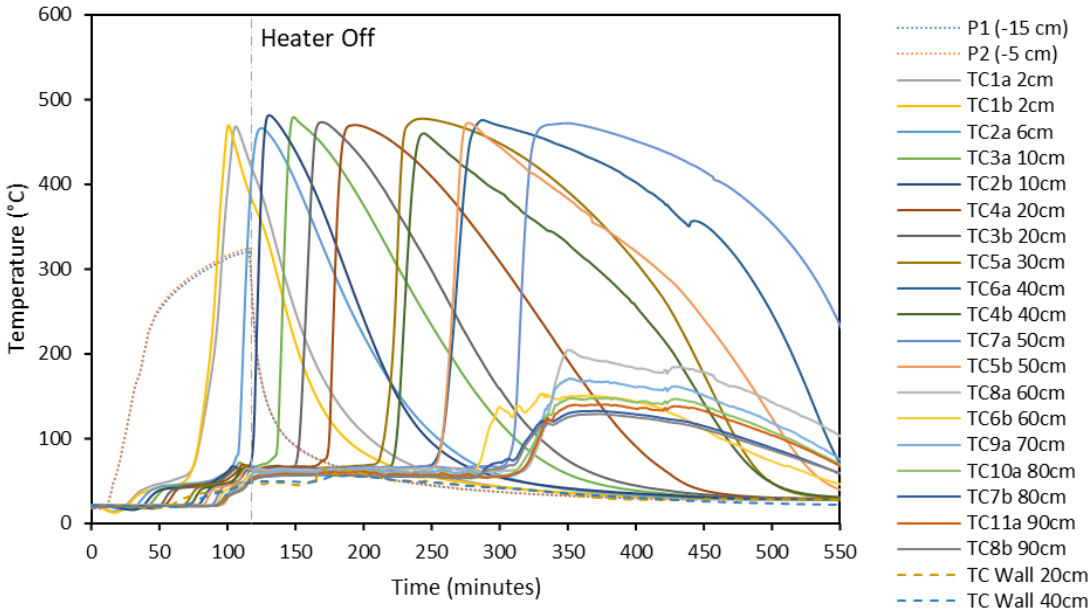

Figure D.3- 3: Temperature profile for Test III-2, a self-sustaining smouldering experiment with a 72.3% moisture content sludge in a fixed bed with 4.5 g/g sand/sludge mass ratio. Plenum, centreline, and wall thermocouples are presented.

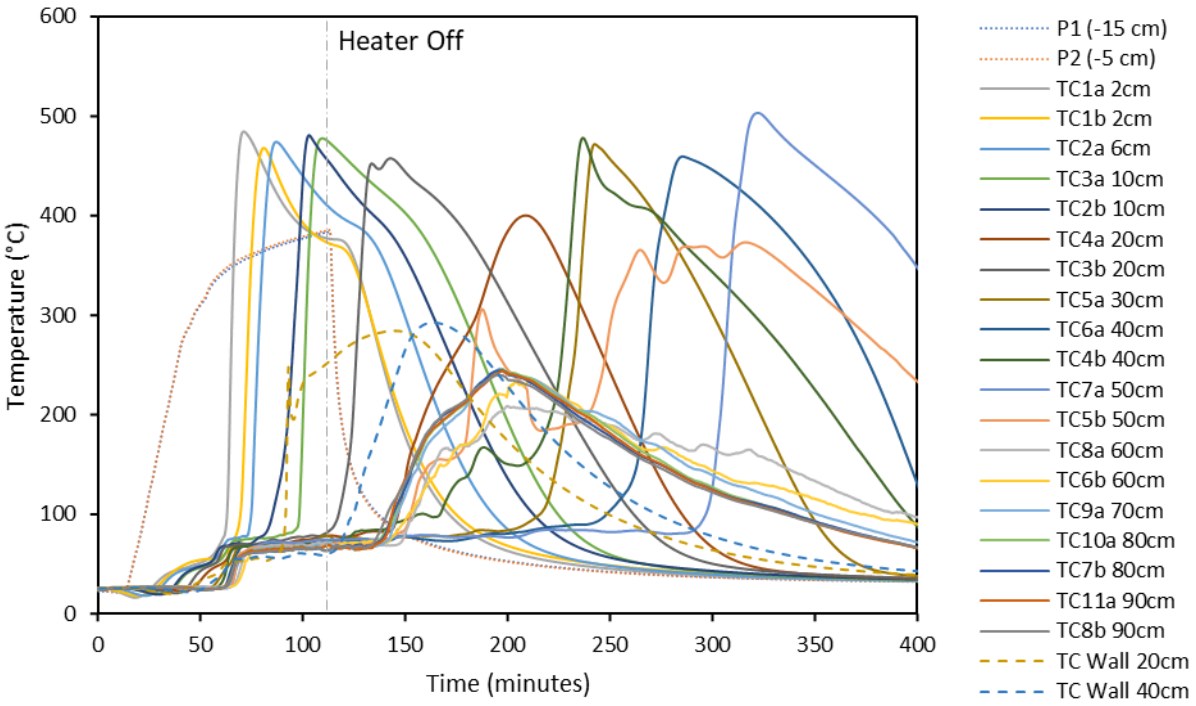

Figure D.3- 4: Temperature profile for Test III-3, a self-sustaining smouldering experiment with a 74.4% moisture content sludge in a fixed bed with 4.5 g/g sand/sludge mass ratio. Plenum, centreline, and wall thermocouples are presented.

D.4: PFAS in virgin sludge and post-treatment ash

Base Case Tests

Smouldering resulted in 92 – 100% reduction in total PFAS in the post-treatment materials. The highest concentrations of PFAS in the post-treatment materials during base case tests tended to be in the top sand cap (Figure D.4-1). TFA (2C) was the primary compound measured in the ash (1.1 ng/g-DS of PFPA was measured in the ash from I-2). PFPA (3C) was primarily measured in the top ash. Since neither TFA nor PFPA were measured in the dried sludge, their presence in the post-treatment materials could be from breakdown products of larger PFAS. PFOS retained in top sand cap from I-1 is 68% less than present in the dried sludge. With 100% removal of PFOS and PFOA from the ash from I-1, the presence of PFOS in the sand cap is evidence of the compound recondensing. This was also observed during test I-3 where the sand cap retained 1% of the PFOS originally present in the sludge but none was measured in the ash. The sand cap from I-2 had no PFOS or PFOA. This could be due to the flaming that occurred at the end of this test. A combination of an insufficient sand cap (required to reduce exiting temperatures), and bio-oil accumulation in the sand cap resulted in flaming occurring as the smouldering front exited the contaminant pack. The flaming significantly increased the temperatures in the sand cap, removing any PFOS or PFOA that may have recondensed there during smouldering.

High MC/GAC Tests

For both high MC/GAC tests, only TFA (2C) was measured in the ash following smouldering treatment. TFA was also the only compound measured in the sand cap from II-1-2. In comparison, the sand cap from II-1-1 also contained PFPA (3C) and PFHpS (7C) (Figure D.4-2). The concentration of the three compounds were similar with 54 ng/g-DS TFA, 69 ng/g-DS PFPA, and 63 ng/g-DS PFHpS (Figure D.4-1). Since neither TFA nor PFPA were measured in the virgin sludge, the presence of these compounds in the top sand cap are evidence of the breakdown of larger PFAS. Similar to the base case tests, the presence of PFAS in the sand cap demonstrate recondensation occurring.

CaO Tests

For both CaO tests, only TFA (2C) was measured in the ash and additionally PFPA (3C) in the sand cap (Figure D.4-2). The concentration of TFA was higher in the sand cap than ash for both tests. The lower CaO test had a higher fraction of PFCA in the sand cap (II-2-1: 42% TFA, 58% PFCA) than the higher CaO test (II-2-2: 68% TFA, 22% PFCA). Overall, smouldering resulted in a 99% reduction in PFAS in the ash from both II-2-1 and II-2-2. Similar to the base cases and high MC/GAC tests, recondensation of PFAS occurred in the sand cap.

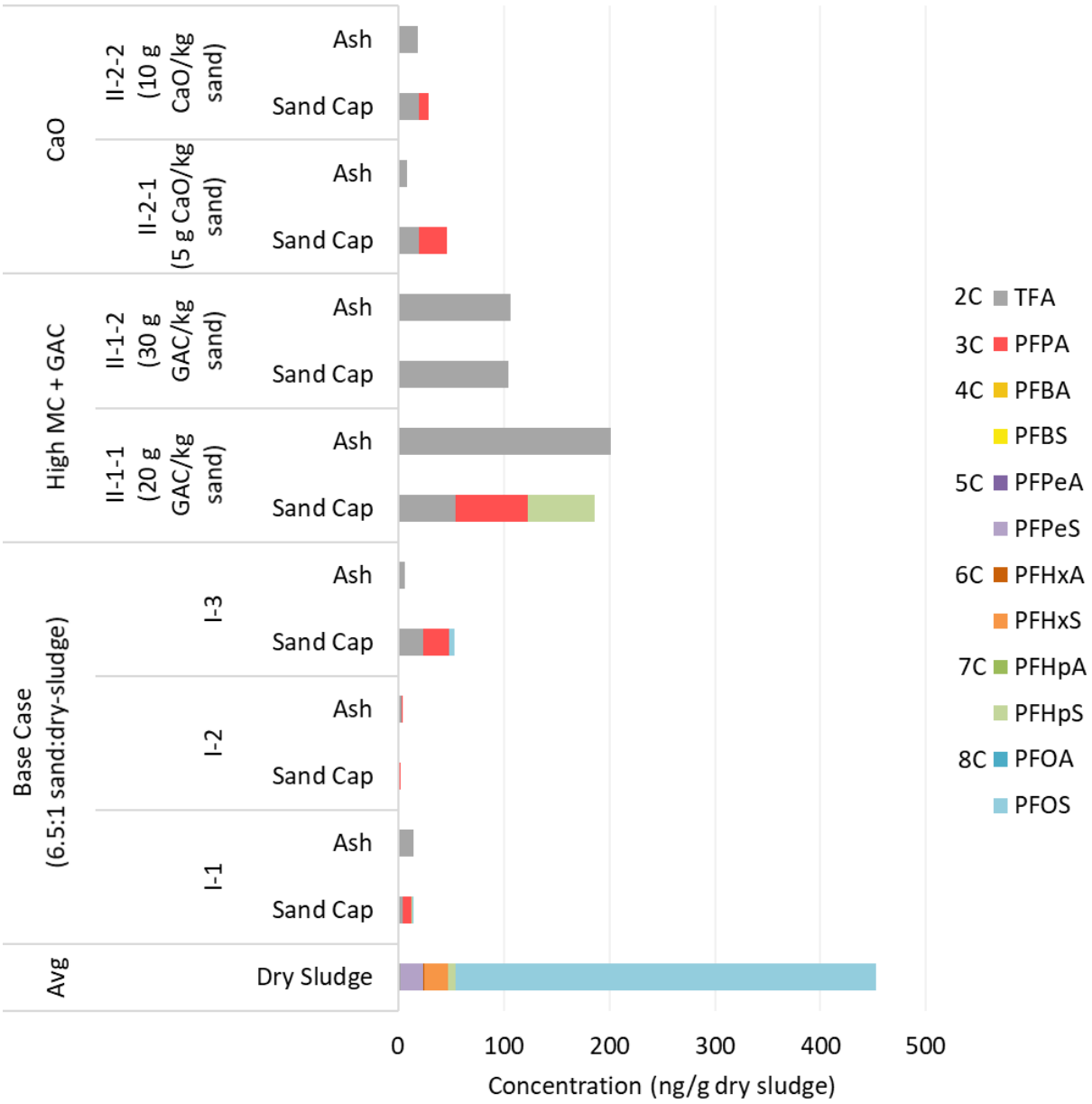

Figure D.4- 1: Content of 12 PFAS originally present in the dried sludge utilized for the LAB smouldering tests and the post-treatment ashes normalized per mass of dried sludge. The content in the top sand cap have been presented with the content in the post-treatment ash. All base cases have been presented separately.

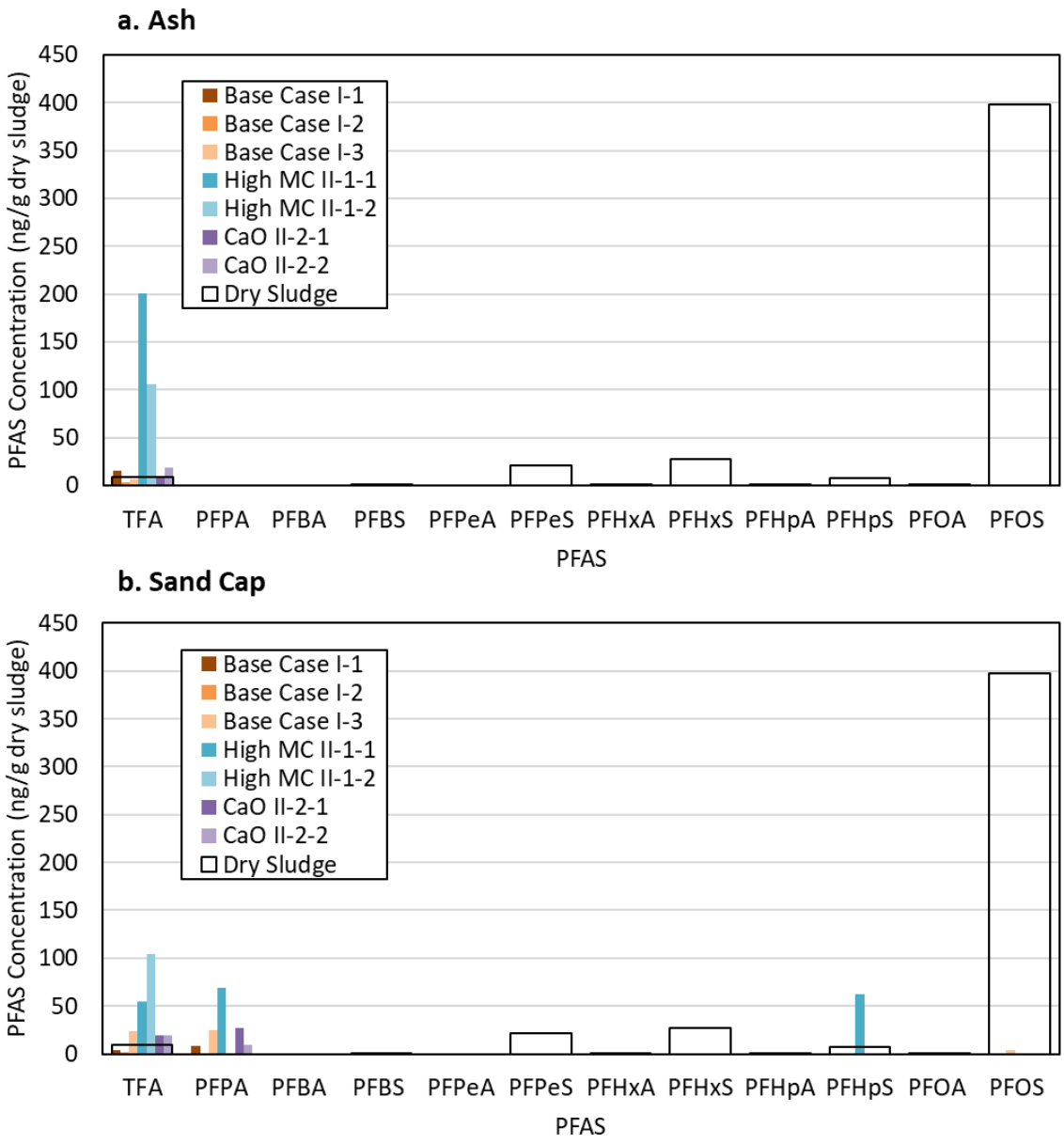

Figure D.4- 2: The content of 12 PFAS originally present in the sludge are compared to the content in a. the post-treatment ash, and b. the top sand cap. The solid columns present the PFAS content observed during each LAB test and the outlined columns show the original content in the sludge. All values have been normalized per mass of dried sludge.

D.5: PFAS in emissions

The GAC in the second absorbent tube (XAD 2) often contained more PFAS than the first absorbent tube (XAD 1), likely due to breakthrough (Figure D.5-1). Bio-oil/condensate breakthrough from XAD 1 to XAD 2 was observed during every test. This is an argument for designing a different emissions capture system especially for high MC/condensable fuels. Comparatively, the PFAS content from XAD 1 rinse was consistently higher than XAD 2. Since XAD 1 tended to capture most of the bio-oil/condensate from the tests, the rinse procedure recovered more PFAS from this absorbent tube.

The emissions from the base case tests contain the highest quantities (by mass) of PFOS and PFOA (Figure S5-3). PFOA makes up the largest mass fraction in the emissions from I-1 (68%) and I-2 (65%), while PFOS makes up the largest mass fraction in I-3 (87%) (Figure D.5-2).

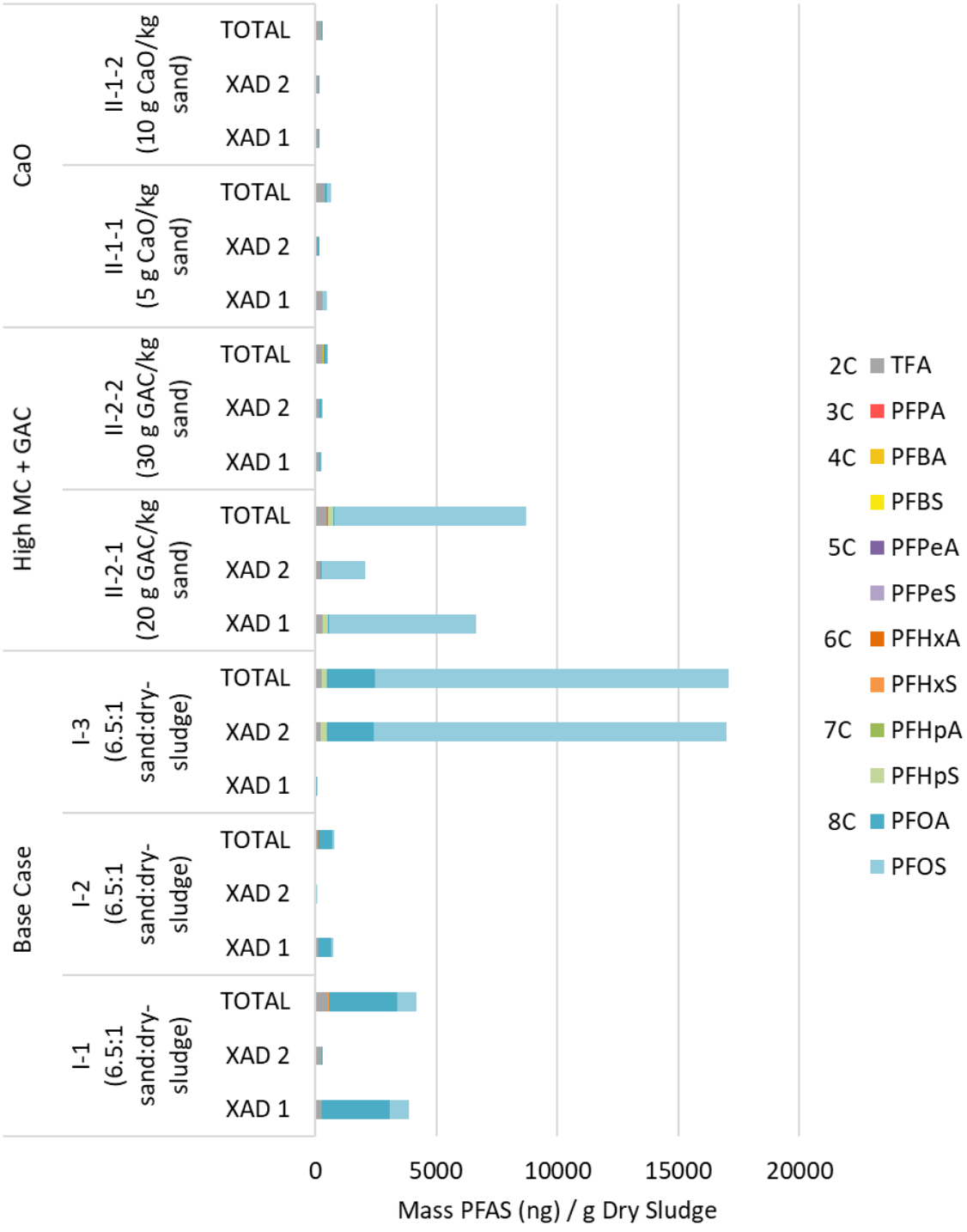

Figure D.5- 1: Content of 12 PFAS in the emissions during smouldering compared to the content originally present in the dried sludge. The PFAS content in the two XAD tubes which collected the emissions are presented in addition to the total content. The results from the base case tests are presented separately. The contents in the emissions have been normalized to account for differences between the experiments.

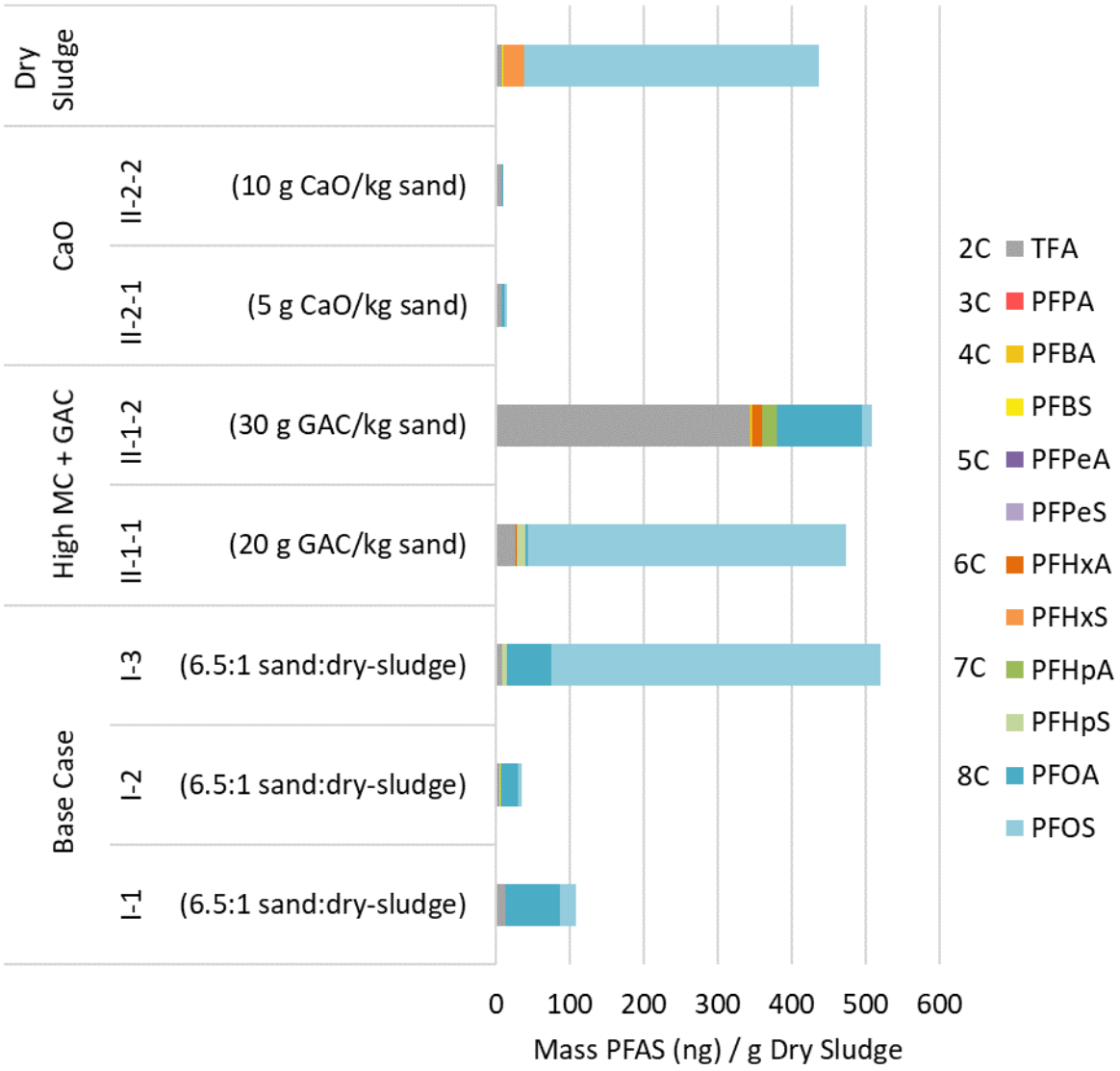

Figure D.5- 2: Content of 12 PFAS in the emissions during smouldering compared to the content originally present in the dried sludge. The contents in the emissions have been normalized to account for differences between the experiments. Results from each base case test are presented separately.

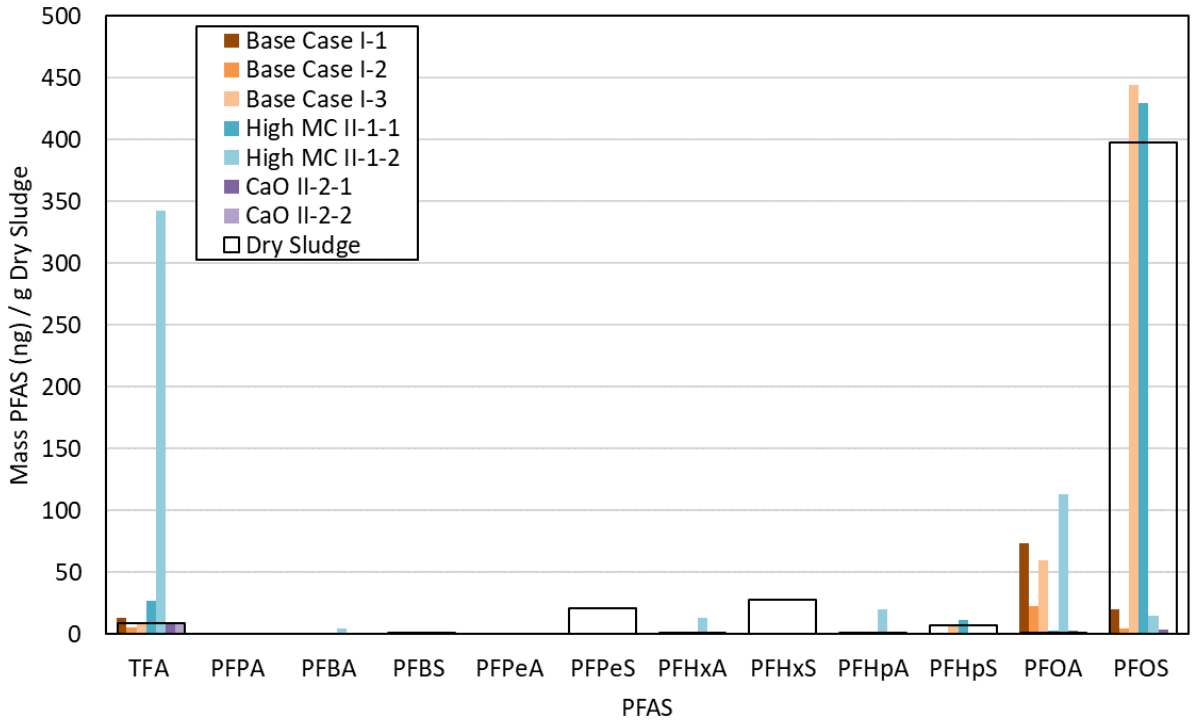

Figure D.5- 3: The content of 12 PFAS originally present in the sludge are compared to the content in the emissions. The solid columns present the PFAS content observed during each LAB test and the outlined columns show the original content in the sludge. The contents in the emissions have been normalized to account for differences between the experiments. Results from each base case test are shown.

D.6: Defluorination

Impingers 1 and 2 contained the highest quantity of HF collected from the emissions. There was still breakthrough and measurable amounts in impingers 3 and 4, as well as residual on the glassware (exceeding quantities in impingers 3 and 4) that was recovered by rinsing.

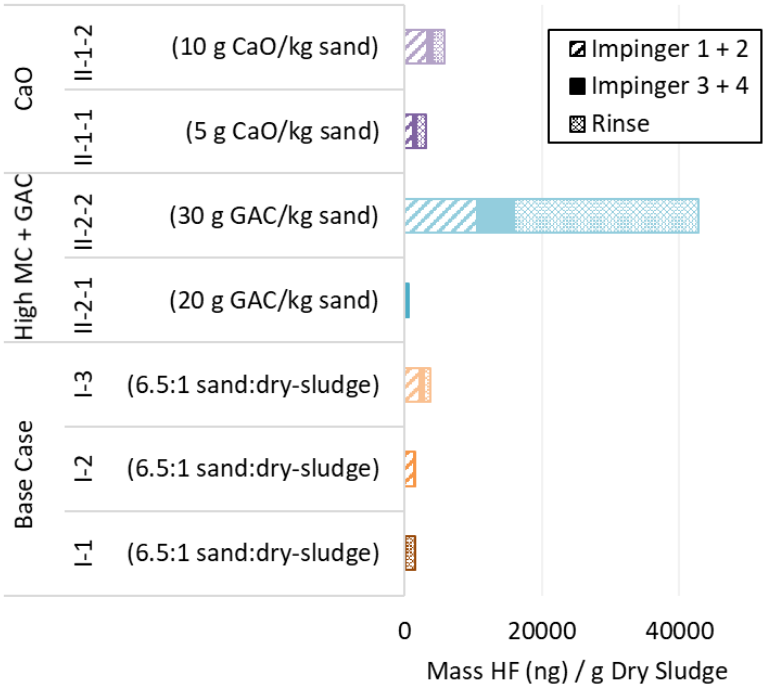

Figure D.6- 1: HF content measured in the emissions from each laboratory smouldering experiment. The content collected from two sections of the glassware sampling train and additionally the glassware rinse have been presented separately. The results from each base case have also been presented. The contents in the emissions have been normalized to account for differences between the experiments.

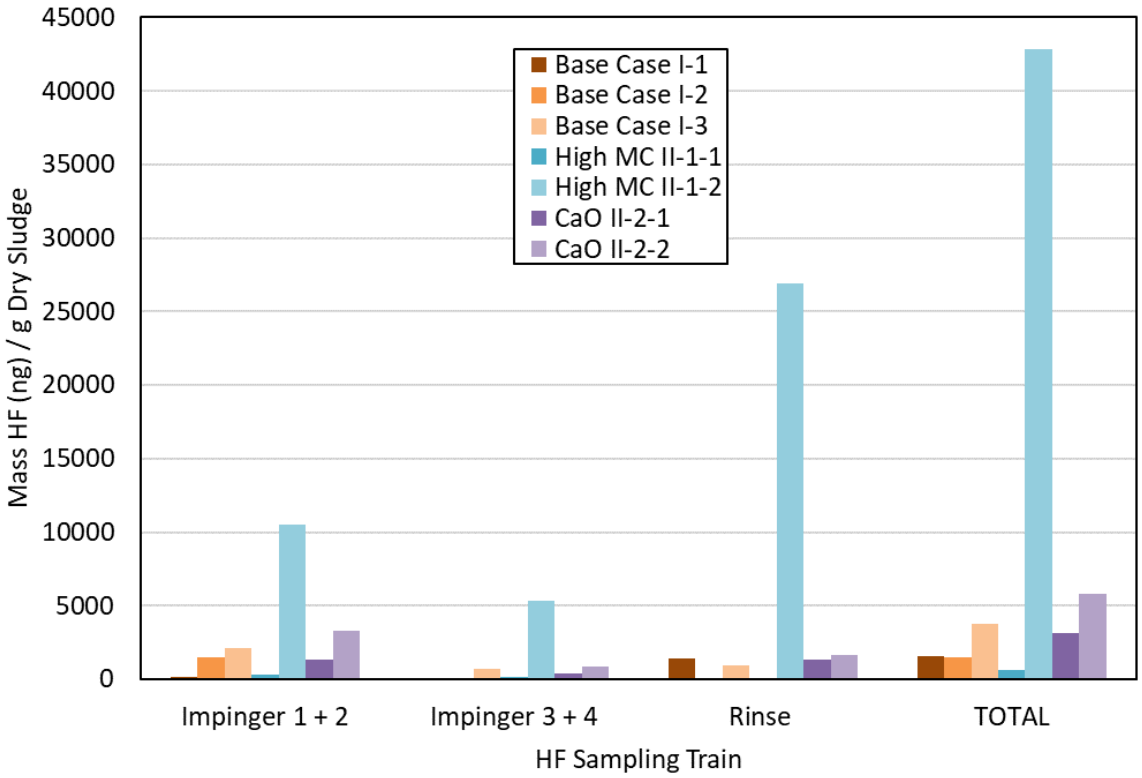

Figure D.6- 2: HF content measured in the emissions from each laboratory smouldering experiment. The content collected from two sections of the glassware sampling train and the glassware rinse have been presented separately. In addition, the total content is shown. The results from each base case have also been presented. The contents in the emissions have been normalized to account for differences between the experiments.

D.7: Normalization Derivation

Nomenclature

Latin Letters

A_C	Cross sectional area, m^2
Ash	Ash content, %
m/m	Mass ratio, -
$\dot{m}$	Mass flux, kg s^{-1}
m_{em}	Mass of emissions sample, ng
M_{air}	Molar mass of air, kg mol^{-1}
MC	Moisture content, %
P	Pressure, Pa
R	Universal gas constant, m^3 Pa mol^{-1} K^{-1}
T	Temperature, K
$\vec{v}$	Air flow velocity, m s^{-1}
$\vec{v}_{oxid}$	Smouldering propagation velocity, m s^{-1}
$\dot{V}$	Volumetric air flux, m^3 s^{-1}
V_{em}	Volume of emissions sample, m^3

Greek Symbols

ρ	Density, kg m^{-3}

Subscripts

$bulk$	Volume averaged
des	Destroyed fuel
dry	Dry fuel
$fuel$	Fuel
in	Into the reactor
NTP	Conditions at normal temperature and pressure
out	Out of the reactor

Mass Out:

The mass flux out of the reactor is calculated to be a conservatively high estimate of the PFAS leaving the system. The following equations assume that all sewage sludge is destroyed during smouldering, i.e., only inorganic ash and sand remains in the reactor post-treatment. The mass flux out of the system is assumed to be the sum of the mass flux into the reactor and the dry mass destroyed during smouldering, given in Equation (D.7-1):

$$\dot{m}_{out}\left[\frac{kg}{s}\right] = \dot{m}_{in}\left[\frac{kg}{s}\right] + \dot{m}_{des}\left[\frac{kg}{s}\right] \qquad (D.7-1)$$

Airflow Volume Flux:

The airflow volume flux of the system is the product of the air flux and the reactor area. The size of the reactor varies from a radius of 0.3 m at the DRUM scale, to 0.075 m at the LAB scale. For the volume flux into the reactor, the air flux is based on the air flow rate into the base of the column, given in Equation (D.7-2):

$$\dot{V}_{in}\left[\frac{m^3}{s}\right] = \vec{v}\left[\frac{m}{s}\right] \cdot A_C[m^2] \qquad (D.7-2)$$

The mass destroyed is related to the total mass lost per time. Therefore, the airflow volume flux is a function of the smouldering front propagation velocity upwards through the reactor, given in Equation (D.7-3):

$$\dot{V}_{des}\left[\frac{m^3}{s}\right] = \vec{v}_{oxid}\left[\frac{m}{s}\right] \cdot A_C[m^2] \qquad (D.7-3)$$

Mass In:

The ideal gas law was used to determine the mass flux into the system, given in Equation (D.7-4):

$$\dot{m}_{in}\left[\frac{kg}{s}\right] = \frac{\dot{V}_{in}\left[\frac{m^3}{s}\right] P_{NTP}[Pa]}{R\left[\frac{m^3 \cdot Pa}{mol \cdot K}\right] \cdot T_{NTP}[K]} \cdot \left(M_{air}\left[\frac{kg}{mol}\right]\right) \qquad (D.7-4)$$

The airflow into the reactor was assumed to be at normal temperature and pressure conditions. The molar mass of air was used to convert the ideal gas law constant from a molarity to a mass.

Substituting Equation (D.7-2) into Equation (D.7-4) gives an equation for the mass flux into the reactor in terms of the airflow rate into the reactor and the area of the column, given by Equation (D.7-5):

$$\dot{m}_{in}\left[\frac{kg}{s}\right] = \frac{\vec{v}\left[\frac{m}{s}\right] \cdot A_C[m^2] \cdot P_{NTP}[Pa]}{R\left[\frac{m^3 \cdot Pa}{mol \cdot K}\right] \cdot T_{NTP}[K]} \cdot \left(M_{air}\left[\frac{kg}{mol}\right]\right) \qquad (D.7-5)$$

Dry Bulk Density:

The bulk density of each fuel mixture was determined for each test. Since the moisture content of the sewage sludge varied for each test, the bulk density was converted to dry bulk density to account for the difference and is given in Equation (D.7-6):

$$\rho_{dry\ bulk}\left[\frac{kg}{m^3}\right] = \frac{\rho_{bulk}\left[\frac{kg}{m^3}\right]}{\left(1 + \frac{m_w}{m_s}\right)} = \frac{\rho_{bulk}\left[\frac{kg}{m^3}\right]}{\left(1 + \frac{MC_{fuel}\,[\%]}{100\%}\right)} \qquad (D.7-6)$$

Dry Mass Destroyed:

The dry mass destroyed is a function of the rate that the smouldering front moves up the column and the dry bulk density of the fuel, given in Equation (D.7-7):

$$\dot{m}_{des}\left[\frac{kg}{s}\right] = \dot{V}_{des}\left[\frac{m^3}{s}\right] \cdot \rho_{dry\ bulk}\left[\frac{kg}{m^3}\right] \qquad (D.7-7)$$

Substituting Equation (D.7-3) and Equation (D.7-7) into Equation (D.7-8) gives an equation for the dry mass destroyed in terms of the smouldering velocity, area of the reactor, bulk density and moisture content of the fuel, given by Equation (D.7-8):

$$\dot{m}_{des}\left[\frac{kg}{s}\right] = \vec{v}_{oxid}\left[\frac{m}{s}\right] \cdot A_C[m^2] \cdot \frac{\rho_{bulk}\left[\frac{kg}{m^3}\right]}{\left(1 + \frac{MC_{fuel}\,[\%]}{100\%}\right)} \qquad (D.7-8)$$

Considering Sand-to-Sludge Ratio and Ash Content:

The dry bulk density of the fuel considers the mixture of silica sand with sewage sludge. Since only the sewage sludge is destroyed during smouldering, the mass destroyed should be normalized to the sewage sludge content by considering the sand-to-sludge ratio (on a dry mass basis) for each test. Furthermore, since not all the sewage sludge is destroyed during smouldering, i.e., some amount of ash remains, the dry mass destroyed should also be normalized to the ash content of the sewage sludge. Equation (D.7-8) can therefore be rewritten to include the sand-to-sludge ratio, and the ash content of the sewage sludge, given in Equation (D.7-9):

$$\dot{m}_{des}\left[\frac{kg}{s}\right] = \vec{v}_{oxid}\left[\frac{m}{s}\right] \cdot (A_C)[m^2] \cdot \frac{\rho_{bulk}\left[\frac{kg}{m^3}\right]}{\left(1 + \frac{MC_{Fuel}\ [\%]}{100\%}\right)} \cdot \left(m/m\left[\frac{kg}{kg}\right]\right)_{dry} \cdot \left(\frac{Ash_{fuel}[\%]}{100\%}\right) (D.7-9)$$

Volume Out of Reactor:

The air volume flux out of the reactor can be determined by rearranging the ideal gas law, given by Equation (D.7-10):

$$\dot{V}_{out}\left[\frac{m^3}{s}\right] = \frac{\dot{m}_{out}\left[\frac{kg}{s}\right] \cdot R\ \left[\frac{m^3 \cdot Pa}{mol \cdot K}\right] \cdot T_{out}\ [K]}{P_{out}[Pa]} \cdot \left(\frac{1}{M_{air}}\left[\frac{mol}{kg}\right]\right) \qquad (D.7-10)$$

The temperature of emissions leaving the column is taken from the highest thermocouple measurement within the column, above the fuel pack i.e., the closest thermocouple to the PFAS and HF sampling trains. An average temperature is used. The pressure of the emissions is corrected to the temperature leaving the column. Again, the molar mass of air is used to convert the ideal gas constant from a molarity to mass.

Normalized Dioxin and Furan Measurement:

Finally, the PFAS and HF samples collected from the emissions leaving the reactor can be scaled to approximate the total mass of PFAS and HF released from smouldering sewage sludge. The mass quantity of both PFAS and HF in the emissions, m_{PFAS} [ng] and m_{HF} [ng], respectively, were quantified per volume of emissions sample, V_{PFAS} [m^3] and V_{HF} [m^3], for each test. Multiplying this concentration by the volume flux out of the reactor provides an approximation of the PFAS and HF released from the system, given by Equation (D.7-11):

$$\dot{m}_{PFAS,Total}\left[\frac{ng}{s}\right] = \frac{m_{PFAS}\,[pg]}{\dot{V}_{em}\,[m^3]} \cdot \dot{V}_{out}\left[\frac{m^3}{s}\right] \qquad (D.7-11)$$

The PFAS and HF flux can then be normalized to the dry mass destroyed during smouldering to approximate the mass of both PFAS and HF leaving the system per mass of dry sludge, given in Equation (D.7-12):

$$m_{em,Total}\left[\frac{ng}{g_{dry\ fuel}}\right] = \frac{m_{em}\,[pg]}{\dot{V}_{em}\,[m^3]} \cdot \frac{\dot{V}_{out}\left[\frac{m^3}{s}\right]}{\dot{m}_{des}\left[\frac{kg}{s}\right]} \frac{[kg]}{1000\,[g]} \qquad (D.7-12)$$

D.8: Mineral Analyses

X-ray diffractometer (XRD) analysis was performed on the post-treatment ash from I-1, II-2-1, II-2-2, and III-1 tests to evaluate the use of calcium to mineralize fluorine from the sludge. A powder XRD technique was utilized. Scanning Electron Microscopy coupled with Energy Dispersive X-ray (SEM/EDX) Spectroscopy was performed in addition to XRD analysis, to assist in results interpretation. This analysis was performed by Surface Science Western using The Rigaku SmartLab.

X-ray diffractometer (XRD)

Table D.7- 1: Instrument Specifications and Operating Conditions for XRD Analysis

Instrumentation	
X-ray Diffractometer (XRD)	Rigaku SmartLab
X-ray Detector	2D HyPix-3000 (Horizontal)
X-ray Tube	2.2 kW long-fine focus Cu- X-ray
Goniometer	Inplane Goniometer
Attachment	Standard Attachment Head
Filter	Kβ Filter for Cu
Operating Conditions	
X-Ray Generator	40 kV 40 mA
Scan Speed	4.00° /min
Step Width	0.02°
Scan Axis	θ/2θ
Scan Range	8° to 90°
Incident Slit Box	2/3°
Length-Limiting Slit	10 mm
Analysis Tools	
Analysis Software	Crystallinity determination module
Databases	1) PDF-4+ Database 2) Crystallography Open Database (COD) 3) FIZ/NIST Inorganic Crystal Structure Database (ICSD)

Scanning Electron Microscopy Coupled with Energy Dispersive X-ray (SEM/EDX) Spectroscopy

Table D.7- 2: Instrument Specifications and Operating Conditions for SEM/EDX Analysis

Hitachi SU8230 Regulus Ultra High-Resolution Field Emission SEM	
Resolution	3 nm at 30 kV (high vacuum mode) 4 nm at 30 kV (low vacuum mode)
Pressure	Variable (~6 – 650 Pa)
Imaging Modes	1) secondary electron (SE) detector 2) multi-segment solid-state backscattered electron (BSE) detector 3) SE equivalent variable pressure (UVD) detector
Drift Detector	X-Max 50mm2 Silicon Drift Detector with 127 eV resolution (Peltier cooling)
Analysis Software	AZtecFeature Automated Analysis
Detection Limit	~0.5 weight % (*for most elements)
Bruker X-Flash FQ5060 Annular Quad EDX detector	
Solid Angle	1.1 sr
Detector	Annular four channel detector with 60 mm^2 active area
Energy Resolution	127 eV
Analysis Software	ESPRIT
Bruker X-Flash 6160 EDX detector	
Active Area	60 mm^2
Energy Resolution	125 eV
Analysis Software	ESPRIT

XRD Results: I-1

Table D.7- 3: XRD Peak List for Test I-1 showing only major phases detected.

No.	2θ, °	d, Å	Height, counts	FWHM, °	Int. I., counts°	Int. W., °	Asymmetry	Decay(ηL/mL)	Decay(ηH/mH)	Size, Å
1	10.92(2)	8.093(15)	255(3)	0.15(3)	57(6)	0.23(3)	1.6(11)	1.3(4)	0.0(8)	561(106)
2	13.717(15)	6.450(7)	413(5)	0.96(6)	714(23)	1.73(8)	0.50(10)	0.2(2)	1.55(7)	87(5)
3	17.126(19)	5.173(6)	457(5)	0.64(5)	619(24)	1.35(7)	3.0(5)	1.55(10)	1.5(2)	132(11)
4	19.41(17)	4.57(4)	200(3)	3.61(16)	771(48)	3.9(3)	1.4(3)	0.0(3)	0.0(3)	23.3(10)
5	20.270(12)	4.377(3)	609(7)	0.46(3)	377(22)	0.62(4)	1.48(15)	0.70(5)	0.51(12)	181(10)

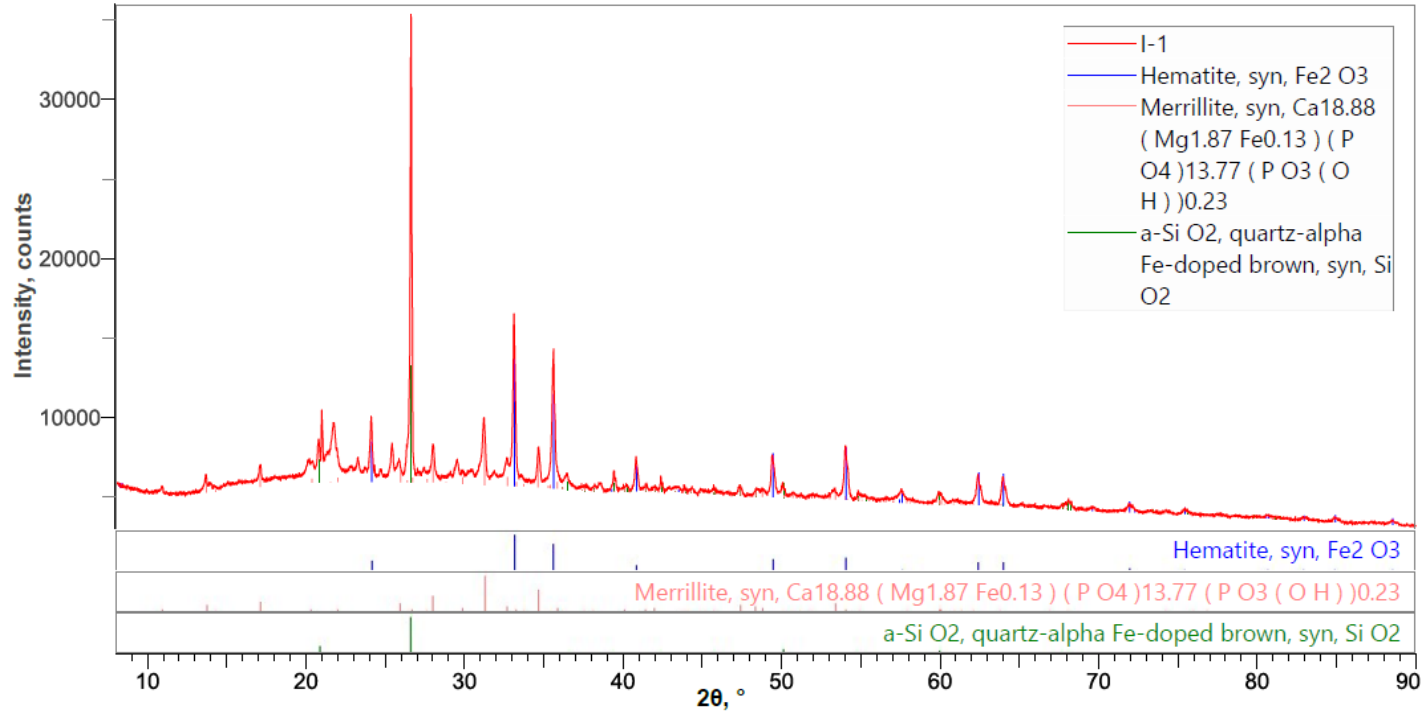

Figure D.7- 1: XRD Phase Data View for Test I-1 showing only major phases detected.

XRD Results: II-2-1

Table D.7- 4: XRD Peak List for Test II-2-1 showing only major phases detected.

No.	2θ, °	d, Å	Height, counts	FWHM, °	Int. I., counts°	Int. W., °	Asymmetry	Decay(ηL/mL)	Decay(ηH/mH)	Size, Å
1	13.66(4)	6.480(18)	318(5)	0.66(7)	413(18)	1.30(8)	0.6(2)	1.54(19)	1.34(19)	126(14)
2	17.111(8)	5.178(3)	270(4)	0.14(3)	49(8)	0.18(3)	1.13(2)	0.66(2)	0.559(16)	609(121)
3	17.950(3)	4.9376(8)	8120(66)	0.563(3)	6066(22)	0.747(9)	1.13(2)	0.66(2)	0.559(16)	149.3(7)
4	20.32(2)	4.367(4)	168(3)	0.19(5)	53(9)	0.31(6)	0.9(2)	1.55(15)	0.4(2)	445(112)
5	20.822(5)	4.2626(9)	1705(24)	0.086(7)	244(8)	0.143(7)	0.9(2)	1.55(15)	0.4(2)	976(77)

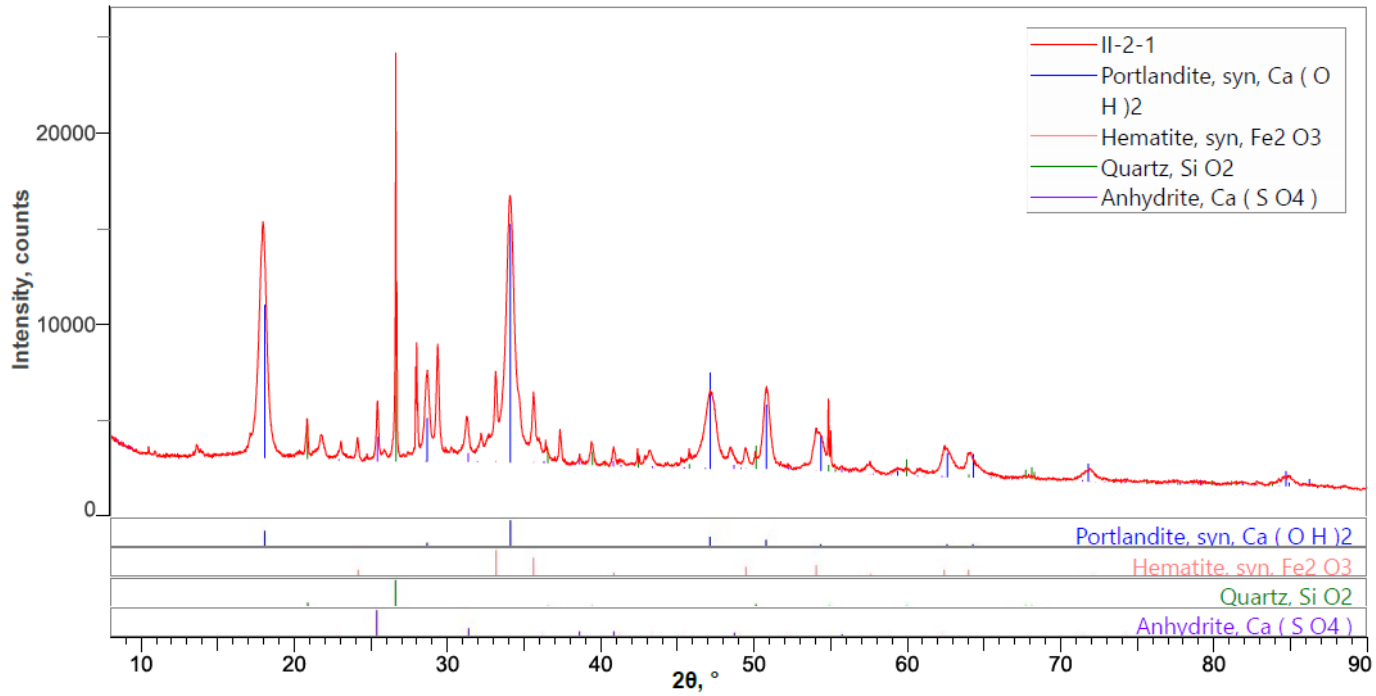

Figure D.7- 2: XRD Phase Data View for Test II-2-1 showing only major phases detected.

XRD Results: II-2-2

Table D.7- 5: XRD Peak List for Test II-2-2 showing only major phases detected.

No.	2θ, °	d, Å	Height, counts	FWHM, °	Int. I., counts°	Int. W., °	Asymmetry	Decay(ηL/mL)	Decay(ηH/mH)	Size, Å
1	15.60(5)	5.68(2)	104(3)	0.63(11)	138(11)	1.33(14)	1.5(8)	1.5(2)	1.5(3)	133(24)
2	17.946(2)	4.9387(6)	5728(58)	0.574(2)	4427(10)	0.773(10)	1.083(17)	0.726(11)	0.564(11)	146.4(5)
3	20.825(17)	4.262(3)	127(3)	0.111(18)	17(2)	0.13(2)	2.6(18)	0.5(5)	0.0(10)	758(123)
4	21.79(2)	4.076(4)	218(6)	0.356(19)	110(4)	0.50(3)	1.4(4)	0.72(18)	0.8(2)	237(13)
5	23.032(10)	3.8585(16)	435(11)	0.210(11)	135(3)	0.312(14)	1.9(5)	0.73(11)	1.1(2)	404(21)

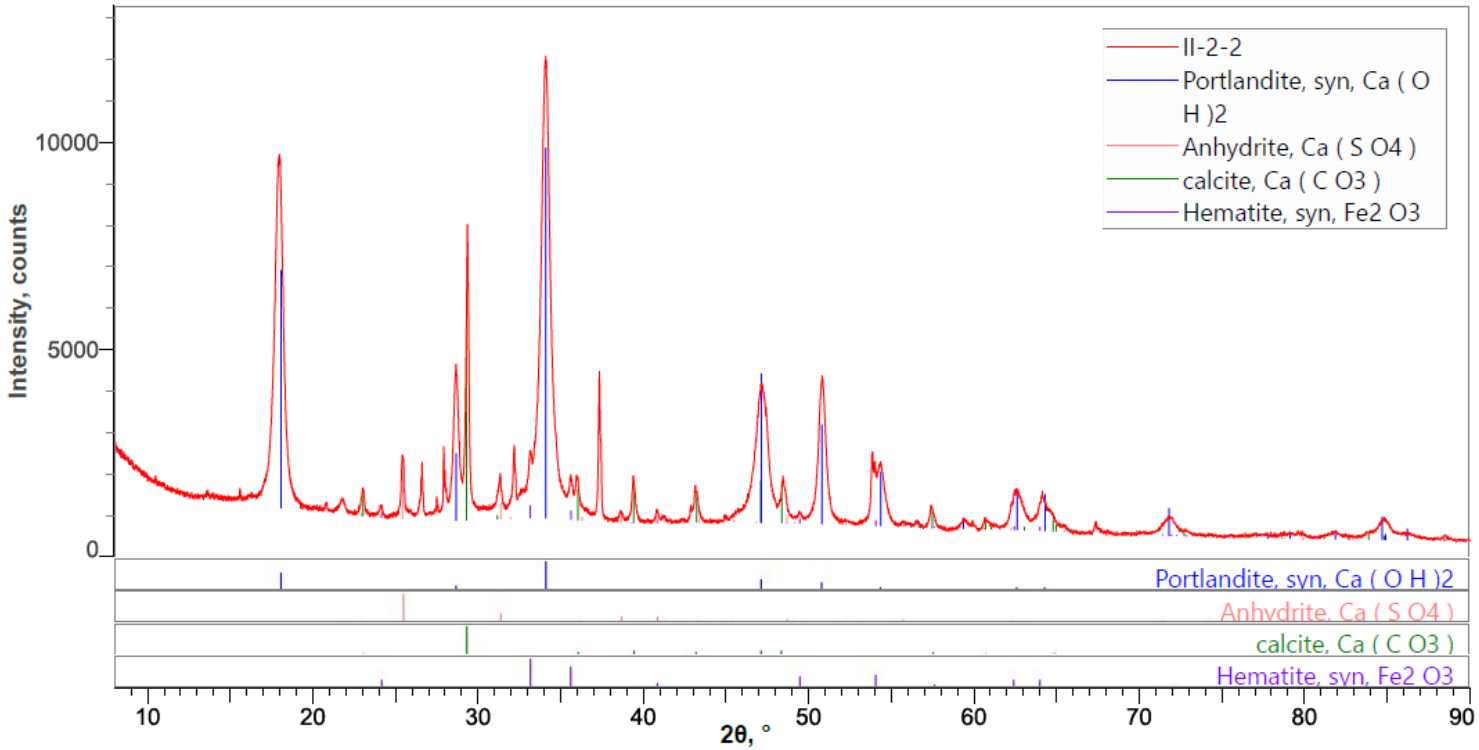

Figure D.7-3: XRD Phase Data View for Test II-2-2 showing only major phases detected.

XRD Results: III-1

Table D.7- 6: XRD Peak List for Test III-1 showing only major phases detected.

No.	2θ, °	d, Å	Height, counts	FWHM, °	Int. I., counts°	Int. W., °	Asymmetry	Decay(ηL/mL)	Decay(ηH/mH)	Size, Å
1	9.415(19)	9.386(19)	430(6)	0.17(3)	115(10)	0.27(3)	4(3)	1.1(3)	0.1(9)	487(80)
2	18.775(12)	4.723(3)	177(3)	0.12(4)	43(6)	0.24(4)	1.3(17)	1.3(4)	1.5(6)	675(192)
3	20.6288(9)	4.30215(18)	3592(37)	0.046(2)	227(10)	0.063(3)	2.05(10)	0.68(3)	0.74(4)	1837(99)
4	20.7995(8)	4.26722(17)	30544(148)	0.0854(9)	3587(19)	0.1174(12)	2.05(10)	0.68(3)	0.74(4)	988(10)
5	21.82(2)	4.070(4)	256(4)	0.82(7)	288(18)	1.12(9)	2.05(10)	0.68(3)	0.74(4)	104(9)

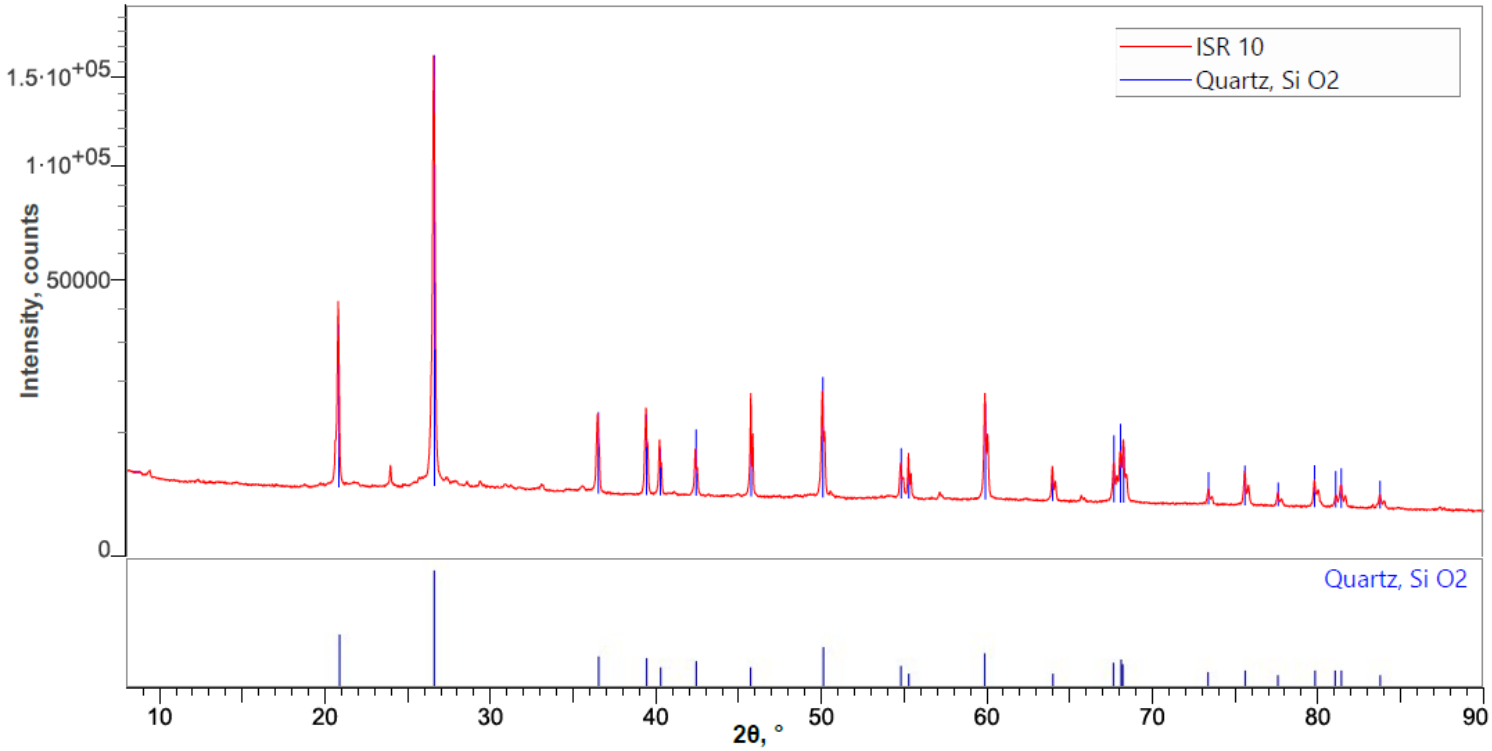

Figure D.7- 3: XRD Phase Data View for Test III-1 showing only major phases detected.

SEM/EDX Results

Table D.7- 7: SEM/EDX Results

Sample	Elemental Concentration (weight %)															
	C	O	Na	Mg	Al	Si	P	S	Cl	K	Ca	Ti	Mn	Fe	Cu	F
I-1																
1	11.7	44.2	0.6	0.8	1.7	9.0	7.0	0.5	*B.D.L.*	0.6	7.1	0.5	*B.D.L.*	16.3	0.2	*B.D.L.*
2	7.9	39.4	*B.D.L.*[1]	1.2	1.7	4.8	5.7	*B.D.L.*	*B.D.L.*	0.7	5.5	0.9	*B.D.L.*	32.3	*B.D.L.*	*B.D.L.*
3	8.3	43.7	0.5	1.1	1.9	6.3	7.7	0.5	*B.D.L.*	0.7	6.8	0.5	*B.D.L.*	22.0	*B.D.L.*	*B.D.L.*
4	11.5	54.3	0.3	0.2	0.8	26.0	1.3	*B.D.L.*	*B.D.L.*	0.4	1.5	0.1	*B.D.L.*	3.6	*B.D.L.*	*B.D.L.*
5	10.6	53.3	0.2	0.3	0.5	24.9	1.7	*B.D.L.*	*B.D.L.*	0.3	1.9	0.1	*B.D.L.*	6.3	*B.D.L.*	*B.D.L.*
6	7.2	31.5	*B.D.L.*	0.5	0.9	4.0	7.8	*B.D.L.*	*B.D.L.*	1.1	6.7	0.3	*B.D.L.*	40.0	*B.D.L.*	*B.D.L.*
7	10.4	43.7	0.9	1.1	3.0	8.6	6.6	0.6	*B.D.L.*	0.9	7.9	0.7	*B.D.L.*	15.6	*B.D.L.*	*B.D.L.*
II-2-1																
1	7.4	48.8	*B.D.L.*	0.4	0.3	0.6	0.4	0.2	*B.D.L.*	*B.D.L.*	40.7	*B.D.L.*	*B.D.L.*	1.2	*B.D.L.*	*B.D.L.*
2	6.7	30.6	0.4	1.1	1.5	5.0	6.5	*B.D.L.*	*B.D.L.*	1.2	17.4	0.9	0.4	28.5	*B.D.L.*	*B.D.L.*
3	11.4	42.6	*B.D.L.*	*B.D.L.*	*B.D.L.*	39.0	*B.D.L.*	0.5	*B.D.L.*	*B.D.L.*	5.2	*B.D.L.*	*B.D.L.*	1.3	*B.D.L.*	*B.D.L.*
4	7.5	42.7	*B.D.L.*	0.7	1.1	3.1	2.3	0.6	0.1	0.4	29.8	0.3	*B.D.L.*	11.4	*B.D.L.*	*B.D.L.*
II-2-2																
1	5.9	44.4	*B.D.L.*	0.2	0.1	0.2	0.3	0.8	0.2	*B.D.L.*	47.4	*B.D.L.*	*B.D.L.*	0.6	*B.D.L.*	*B.D.L.*
2	13.6	44.6	0.6	0.7	1.5	8.1	5.6	1.1	0.1	1.0	9.1	0.5	*B.D.L.*	13.5	*B.D.L.*	*B.D.L.*
3	7.4	49.7	*B.D.L.*	0.5	0.2	0.3	0.3	0.3	0.1	*B.D.L.*	40.6	*B.D.L.*	*B.D.L.*	0.8	*B.D.L.*	*B.D.L.*
4	7.7	44.8	*B.D.L.*	0.4	0.4	1.0	1.0	0.6	0.1	0.2	41.4	*B.D.L.*	*B.D.L.*	2.5	*B.D.L.*	*B.D.L.*
III-1																
1	10.5	52.6	0.1	0.3	1.0	32.7	0.4	0.2	*B.D.L.*	0.3	0.5	*B.D.L.*	*B.D.L.*	1.4	*B.D.L.*	*B.D.L.*
2	11.7	53.5	*B.D.L.*	0.3	1.7	30.5	0.2	0.2	*B.D.L.*	0.4	0.4	0.2	*B.D.L.*	1.0	*B.D.L.*	*B.D.L.*
3	10.2	46.2	0.4	1.0	2.0	19.4	3.3	1.2	0.2	0.8	4.9	0.2	*B.D.L.*	10.2	*B.D.L.*	*B.D.L.*
4	10.9	46.7	0.3	0.9	2.1	17.9	3.2	0.9	0.2	0.9	4.3	0.3	*B.D.L.*	11.2	*B.D.L.*	*B.D.L.*
5	10.7	44.7	0.4	0.9	2.3	17.2	3.8	1.0	0.2	1.0	5.3	0.3	*B.D.L.*	12.3	*B.D.L.*	*B.D.L.*
6	20.8	44.8	0.4	0.8	1.8	15.8	2.9	0.6	*B.D.L.*	0.9	3.5	0.1	*B.D.L.*	7.6	*B.D.L.*	*B.D.L.*

[1] Below instrument detection limit

Curriculum Vitae

Name: Taryn Ashley Fournie

Post-secondary Education and Degrees:

The University of Western Ontario
London, Ontario, Canada
2013-2017 BESc., Civil and Environmental Engineering
Specialization in International Development

The University of Western Ontario
London, Ontario, Canada
2017-Current Ph.D., Civil and Environmental Engineering, Water Resources Management

Honours and Awards:

Government of Ontario Graduate Scholarship
2018

L.G. Soderman Award
2018

Douglas W. Muzyka International Graduate Student Research Fellowship
2019

NSERC Post Graduate Scholarship - Doctoral
2019-2022

Related Work Experience

Research Assistant
The University of Western Ontario
2014-2017

Teaching Assistant
The University of Western Ontario
2017-2022

Publications:

Fournie, T., Switzer, C., & Gerhard, J. I. (2021). USEPA LEAF methods for characterizing phosphorus and potentially toxic elements in raw and thermally treated sewage sludge. *Chemosphere*, *275*, 130081.

Fournie, T., Rashwan, T. L., Switzer, C., & Gerhard, J. I. (2022). Phosphorus recovery and reuse potential from smouldered sewage sludge ash. *Waste Management*, *137*, 241-252.